GENE EXPRESSION ANALYSIS DURING WEST NILE VIRUS DISEASE, INFECTION, AND RECOVERY

By

MELISSA ANN BOURGEOIS, DVM

A DISSERTATION PRESENTED TO THE GRADUATE SCHOOL
OF THE UNIVERSITY OF FLORIDA IN PARTIAL FULFILLMENT
OF THE REQUIREMENTS FOR THE DEGREE OF
DOCTOR OF PHILOSOPHY

UNIVERSITY OF FLORIDA

2010

To my parents and my sister, for their unfailing support and unconditional love throughout the years

ACKNOWLEDGMENTS

I thank the members of the Long lab at the University of Florida, including Maureen Long, Sally Beachboard, Katie Maldonado, Kathy Seino, and Deanne Fanta for their invaluable assistance over the entire course of this project. I also thank the members of my committee, Maureen Long, Nancy Denslow, Paul Gibbs, David Allred, David Bloom, and James Maruniak for their wonderful insight and contributions to the evolution and progression of this project. I thank the members of the UF Interdisciplinary Centers for Biotechnology and Research, Gigi Ostrow, Li Liu, and Savita Shanker for their help in accomplishing different portions of this project. And finally, I thank my wonderful family and friends for their unfailing support throughout the entire course of my graduate degree. This project was funded with a grant from the USF Centers for Biological Defense.

TABLE OF CONTENTS

page

LIST OF TABLES

LIST OF FIGURES

LIST OF ABBREVIATIONS

BLAST	Basic Local Alignment of Sequences
CNS	Central nervous system
DNA	Deoxyribonucleic acid
EST	Expressed sequence tag
GO	Gene ontology
IPA	Ingenuity Pathways Analysis
NCBI	National Center for Biotechnology Information
PFU	Plaque forming unit
RNA	Ribonucleic acid
WNV	West Nile virus

Abstract of Dissertation Presented to the Graduate School
of the University of Florida in Partial Fulfillment of the
Requirements for the Degree of Doctor of Philosophy

GENE EXPRESSION ANALYSIS DURING WEST NILE VIRUS DISEASE, INFECTION, AND RECOVERY

By

Melissa Bourgeois

May 2010

Chair: Maureen T. Long
Major: Veterinary Medical Sciences

It was the goal of this project to profile gene expression during West Nile virus (WNV) infection in the central nervous system (CNS) of horses. It was hypothesized that there are gene pathways whose expression changes in a significant and consistent manner due to WNV as a result of exposure status, survival/immune status, and CNS location. To test this hypothesis, the equine CNS transcriptome was sequenced, these sequences were used to create a custom microarray, and this array was used to analyze gene expression in the thalamus and cerebrum of three different groups of horses (naïve/WNV exposed, vaccinated/WNV exposed, and normal). Statistical and pathway analysis was performed on this data to identify genes and gene pathways of interest.

In total, 41,040 genes and contigs were sequenced and annotated from the transcriptome- 1,280 of which were novel to the equine genome project. Significant differences ($p<0.05$) in gene expression were seen due to exposure in 9,020 genes, survival in 7,395 genes, and location in 7,649 genes. Pathways analysis revealed that many genes mapped to neurological and immunological categories, which were found

to be downregulated in WNV infection. Detailed analysis of the immunological pathways revealed that both innate and adaptive components of the immune response were involved in the response to WNV infection, and that higher levels of expression of these pathways were correlated with survival. PTX3 (pattern recognition response to viruses), interleukin-15 production, and the JAK/STAT pathway were found be be upregulated by WNV infection. Infection with WNV also led to an increase in the expression of SOCS3, a negative feedback inhibitor of the JAK/STAT pathway, possibly reflecting evasion of innate immunity by the virus. Apoptosis was found to be upregulated due to WNV infection, providing expression level evidence of neuropathology due to viral infection. Transcriptional genes also demonstrated changes in expression levels due to WNV infection. Detailed analysis of neurological pathways revealed that transcripts in both the glutamate and dopamine signaling pathways were decreased in expression in the WNV infected brain, providing evidence of glutamate excitotoxicity and pathology associated with a lack of dopamine. In addition, many of the transcripts mapped to non-infectious neurological disease functions, including mental disorders and degenerative neuropathies, suggesting a correlate between the neuropathology induced by viral infection of the CNS and the neuropathology seen in non-infectious neurological disease. This project provided novel insights into global gene expression during WNV infection, and led to a better understanding of how the CNS responds to viral infection. Confirmation studies looking at individual transcripts of interest will be performed. This data will be used to contribute to potential therapeutics and diagnostic options for WNV and other viral encephalitides.

CHAPTER 1
INTRODUCTION

West Nile virus (WNV) is one of the leading causes of arboviral encephalitis in the United States in both horses and humans. Like other encephalitic flaviviruses, WNV can be devastating in its ability to cause long term neurological deficits and even death. Since the introduction of WNV to New York in 1999, the virus has spread rapidly throughout both North and South America. In the United States alone, 25,748 clinical cases of disease have been confirmed in horses[1], and 29,624 cases of clinical disease have been reported in humans with 1,161 human deaths.[2]

A number of vaccines are currently available for horses and have been shown to be efficacious in preventing clinical disease. The availability of these vaccines has been one of the major reasons for the decline in equine cases. Vaccines are in clinical trials for humans, but are not yet available for use. However, despite the presence of these vaccines, further research into WNV is necessary as future outbreaks of this disease may still occur in naïve environments and/or due to mutation. West Nile virus can be used as a model to understand the ecology, epidemiology, and pathophysiology of many arboviral and encephalitic diseases, and this knowledge can be used to improve our response to arbovirus epidemics and epizootics. In addition, there is a need for ante mortem tissue specific diagnostics that can rapidly differentiate previous exposure from current infection in animals and humans. There is also a lack of knowledge with regard to pathophysiology and immunopathology, especially involving host-pathogen interactions during WNV infection. Specifically, there is a large gap of knowledge regarding how the central nervous system (CNS) responds to viral infection and in understanding which gene pathways are dysregulated due to viral encephalitis. This is

especially evident regarding neuroinvasion, neurovirulence, and the neurological immune response. Finally, and likely most important in the naïve host, there are few, if any, effective therapeutic interventions for any viral encephalitis, leading to lifelong disease, disability, and even death in animals and humans.

Gene expression analysis on a global scale can provide detailed information on host-pathogen interactions and can lay a scientific foundation for future diagnostic tests and therapeutic options that are necessary to address deficiencies in knowledge of infectious disease. Deep sequencing for the construction of microarrays is one such methodology and tool through which new knowledge can be rapidly generated. Tissue specific, validation microarrays can then be used to investigate the levels of gene expression within and between hosts. These data can provide detailed information on the host response to infection and on a pathogen's specific manipulation of the host response by global analysis of gene expression. Analysis of gene dysregulation can then be targeted toward the analysis of pathways of genes changed due to viral encephalitis. The enhanced understanding this will provide can be used to increase our understanding of and ability to combat viral encephalitis.

The long term goal of this research was to develop methods and generate host expression data at the level of brain and spinal cord to develop more rapid diagnostic tests and interventional strategies for viral encephalitis. The short term goal of this project was to sequence the equine brain transcriptome and use tissues from a model of WNV infection and encephalitis in horses to create a custom equine high density microarray for profiling of gene expression during WNV infection. It was hypothesized that there are genes that change in a consistent manner during WNV disease, infection,

and recovery. Specifically, there should be a difference in gene expression between exposure to WNV, survival from WNV infection, and location in the brain.

This hypothesis was explored in four specific aims. In the first aim, the transcriptome from the central nervous system of the horse was sequenced, annotated, and analyzed. In the second aim, samples from horses experimentally infected with WNV (vaccinated and non-vaccinated) and horses not exposed to WNV (negative controls) were hybridized to 4x44,000 spotted microarrays based upon the afore-mentioned sequences. These data were then subjected to statistical analysis for the third specific aim to determine whether there were differences in gene expression between: 1. the cerebrum and thalamus of horses infected with WNV (not vaccinated), 2. between vaccinated and non-vaccinated horses infected with WNV, and 3. between non-vaccinated horses infected with WNV and untreated horses not exposed to WNV. The gene expression levels of the array were validated with relative quantitation reverse transcription real time PCR on six genes that were shown to be significantly differentially regulated between naïve and non-naïve horses exposed to WNV. The probes on the array were validated by BLASTing the array probe sequences against the EqCab2 genome. Finally, in the fourth specific aim, these data were used in pathway analysis and gene ontology enrichment to determine the common pathways of genes that were changed between and amongst analyses due to viral infection.

This exploration of gene expression during WNV infection in the horse is the first step in the development of new therapies, diagnostics, and new preventative strategies. This information will eventually be combined with other components of a systems biology approach, combining interdisciplinary scientific fields to gain a better

understanding of host pathogen interactions (such as proteomics and cell biology) to verify the global analysis conducted herein. This information could eventually be used to combat not only outbreaks of WNV, but also as a model to understand and reduce the impact of viral encephalitis in general.

CHAPTER 2
LITERATURE REVIEW

West Nile virus

Epidemiology

West Nile virus (WNV) was first discovered in 1937 in the West Nile province of Uganda. Before 1999, the virus was considered enzootic in Africa, the Middle East, the Mediterranean, and West/central Asia with periodic incursions into Europe. Few cases of WNV actually resulted in neurological disease or death. Exceptions included an outbreak in the 1960s in France, a 1996-1997 outbreak in Romania, a 1996 outbreak in southern Russia, and a 1998 outbreak in Israel, all of which resulted in neurological disease and death in either horses, humans, or birds.[3, 4]

In 1999, a single point introduction of WNV occurred in North America in New York City.[5, 6] Because this occurred into a naïve environment, it provided a unique opportunity to monitor how an arbovirus interacts with and adapts to a new environment. By 2001, the virus had been documented in 21 states, the Cayman Islands, and Canada. By 2002, WNV had reached California on the western coast of the US, 5 Canadian provinces, Hispaniola, Guadeloupe, and Mexico. In 2003, the virus was isolated in 22 Mexican states, Central America (Belize, Guatemala, and El Salvador), Cuba, Puerto Rico, and the Bahamas. By 2004, the virus had spread to South America with documentation in Trinidad and Columbia. And in 2006, WNV had reached as far south as Argentina. WNV is now the most widely distributed Flavivirus, present on all continents except Antarctica.[7-9]

Ecology and Host Range

West Nile virus is a seasonal disease, with case occurrence corresponding with peak mosquito vector activity. In northern, temperate climates, peak activity occurs in the summer months. In tropical and subtropical climates, disease activity is high year-round, although it may fluctuate slightly dependent upon rainfall.[10] One of the major questions in the epidemiology of WNV is how the virus overwinters, especially in Northern latitudes. Previous studies have isolated WNV from overwintering female *Culex pipiens* mosquitoes.[3, 11] In addition, as noted above, the virus undergoes year-round transmission in warmer climates, and may be transported back to temperate locations by migratory birds. And finally, either chronic infections in birds or non-traditional reservoir hosts may incubate the virus during warmer months. It should be noted that for viral transmission to occur, a minimal threshold temperature of 14.7^{o}C is required with higher temperatures increasing amplification of virus linearily.[12]

The Flaviviridae are traditionally thought to be maintained in nature in a bird-mosquito-bird cycle. In North America, over 60 species of mosquito have been found to be capable of transmitting WNV. Based on host feeding and vector competency studies, it appears that *Culex* species are the main vector species responsible for the transmission. The primary Culex species varies according to geographic region with *Cx. pipens*, the Northeastern vector, the *Cx.tarsalis* the western vector, and, putatively, *Cx. quinquefasciatus* and *nigripalpus,* the Southern vectors.[10, 13-18] Early feeding studies and blood meal analysis on *Culex* species demonstrate that these mosquitoes preferentially feed on birds and only occasionally feed on mammals, except where many mammalian hosts are available (Rios L, unpublished data). So while *Culex* species may play a role as a bridge vector for WNV, other mosquito species are likely to

be involved in the life-cycle involving mammalian disease.[19] The species that appear to be capable of functioning as bridge vectors include *Aedes spp, Anopheles spp,* and *Coquillettidia spp*.[10, 13, 19, 20] Once the virus enters the mosquito, it replicates in the fat and endothelial cells of the posterior midgut. At around the fourth day post infection (PI), the virus enters the hemocoele and spreads to other parts of the body including the head and salivary glands. Thus the virus is incubated by the mosquito for approximately seven days PI before it can be transmitted.[4] During this time, the virus undergoes a variety of interactions with the mosquito and the environment dependent on temperature, seasonality, and climate conditions. The virus has also been shown to be capable of trans-ovarial transmission, albeit at a low rate.[21]

Birds serve as the main reservoir host for WNV and develop high levels of viremia at $>10^7$ PFU/mL post-infection. Between 74 and 100% of mosquitoes become infected when feeding on hosts with viral titers $>10^7$, while only 0-36% of mosquitoes become infected when feeding on hosts with viral titers $>10^5$.[22] It was originally thought that Corvidae (i.e. crows, blue jays, ravens) served as the major reservoir for the virus. However, while these birds develop high viremias, they quickly succumb to clinical disease. Laboratory infection of Corvidae with the NY99 strain of WNV resulted in the clinical signs of lethargy, reluctance to fly, depression, anorexia, and sporadic neurological signs (i.e. ataxia) four days post-infection (pi). By day five PI, all birds either spontaneously died or were euthanized. Viral titers in all birds measured $>10^7$ PFU/mL.[23] In another study in which birds were infected via mosquito bite, oral ingestion, or contact, the Corvidae were highly susceptible to disease. The birds demonstrated clinical signs of lethargy, ruffled feathers, and unusual posture with a high

viremia and death 24 hours after the onset of clinical disease.[24] Therefore while Corvidae function as excellent sentinels for monitoring the introduction of WNV into an area, they do not survive long enough to function as effective reservoirs. A recent study on blood meal analysis of trapped mosquito species demonstrated that *Culex* mosquito species do not preferentially feed on the Corvidae. Instead, blood meal analysis on *Culex* mosquito species revealed that these mosquitoes preferentially feed on passerines including the American robin, the Northern cardinal, the common grackle, and the house finch.[19, 25] Yet minimal mortality due to WNV has been noted in these birds during these surveillance studies. In another study, robins, house finches, and sparrows were infected with WNV orally, via mosquito bite, and by direct contact with other infected birds. These birds developed a high viremia ($10^{5.4}$-$10^{8.9}$ PFU/mL) with few clinical signs and minimal mortality.[24] Thus, these particular passerine birds have been designated the major potential reservoir for WNV, rather than corvids. These findings are consistent with the sister North American flavivirus, St. Louis encephalitis (SLE),.[26, 27]

Other arboviruses have been shown to be maintained in non-avian reservoirs (i.e. Venezuelan equine encephalitis). Experimental peripheral infections with WNV in 'nontraditional' (i.e. not avian, equine, or murine) species have been performed to investigate the possibility of unknown reservoir and incidental hosts. Infections of bats, pigs, and dogs have resulted in low levels of virus (10^{1}-10^{3} PFU/mL) and the absence of clinical signs and it is unlikely that these hosts function in nature as effective reservoirs [28-30] Alternatively, experimental infection of cats resulted in mild, non-neurological signs of disease with moderate viremias of 10^{3}-10^{4} PFU/mL, demonstrating that cats

may be capable of viral amplification and transmission.[28] The possibility of rodents as a reservoir is of particular concern due to the role of wild rodents in VEE. Experimental peripheral inoculation of fox squirrels with WNV resulted in clinical signs in only 1 of 11 subjects with levels of viremia ranging from $10^{1.7}$-$10^{6.1}$ PFU/mL.[31] Similar results were obtained in chipmunks, with peripheral inoculation resulting in no clinical signs with virus titers of $10^{3.9}$-$10^{6.7}$.[32] Reptiles may also serve as a reservoir for WNV infection. In laboratory infection of 24 juvenile alligators, all became infected and were able to sustain this viremia for up to 8 days with 88% developing WNV titers >10^5 PFU/mL. In addition, there was evidence of oral and cloacal shedding of WNV with contact transmission.[33] In a naturally occurring outbreak in Florida, neurological disease in farmed alligators was noted, with serum viral titers ranging from $10^{3.6}$-$10^{6.5}$ PFU/mL.[34] Therefore there is evidence that wild rodents and reptiles may serve as WNV reservoirs in nature, altering the traditional view of a bird-mosquito-bird maintenance cycle (see Figure 2-1).

Molecular Epidemiology

West Nile virus is classified as a Flavivirus within the genus Flaviviridae. The genera Flaviviridae encompasses a wide range of viruses, most of which are spread through mosquitoes and ticks (arthropod-borne diseases). Other, related viruses of veterinary import within this genera include Pestiviruses (bovine viral diarrhea and classical swine fever), as well other Flaviviruses including Japaneses encephalitis virus (JEV) and Kunjin virus (KJ). Closely related flavivirus primarily of human importance include SLE and tick-borne encephalitis (TBE).

There are two distinct phylogenetic lineages of West Nile virus (lineage 1 and lineage 2). The virus that was introduced into North America was of lineage 1

genotype, and is generally considered to be more pathogenic than lineage 2 viruses (primarily restricted to Africa). Although both lineage 1 and 2 viruses can result in neuroinvasive disease, lineage 2 viruses are responsible for outbreaks of flu-like disease.[8] Genetic mutations within the viruses are responsible for the differences in virulence and phylogenetic classification, and include alterations in the envelope (E) protein and nonstructural (NS) proteins.[7, 8, 35, 36] This can be seen in North America, where limited evolution of WNV has occurred during the spread of the virus to the west.[37-40]

Viral Structure and Life Cycle

WNV is an enveloped, single-stranded positive sense RNA virus, approximately 50 nm in size. The genome of WNV is approximately 11,000 base-pairs in length and codes for 10 viral proteins, including 3 structural proteins and 7 non-structural proteins in the order 5'-Capsid-preMembrane-Envelope-NS1-NS2A-NS2B-NS3-NS4A-NS4B-NS5-3' (see Figure 2-2).[41] The NS proteins are largely involved in viral replication, while the structural proteins mainly function in maintenance of the virion and are responsible for the majority of host immunogenicity.

The first step in viral infection occurs when domain III of the E protein binds to as-yet-uncharacterized host cell receptors, although some host proteins have been demonstrated to assist movement of the virus in host tissues.[42] Receptor mediated endocytosis occurs, and the virus enters the host cell within a low pH vesicle. The virus is then released from the vesicle into the cellular cytoplasm as a single strand of positive sense RNA. Translation occurs first, since viral proteins are required for subsequent RNA replication steps. Host cell elongation initiation factors (eIF) bind to the 5' untranslated region (UTR) of the viral genome. Then the traditional initiation,

elongation, and termination steps of translation occur forming a viral polyprotein coding for 10 proteins (5'-Capsid-preMembrane-Envelope-NS1-NS2A-NS2B-NS3-NS4A-NS4B-NS5-3'). Host cell proteases then cleave the polyprotein, allowing replication to occur. In subsequent translational events, the viral NS2B/NS3 protease carries out the cleavage of the polyprotein.[43, 44]

Replication of viral RNA starts at the 3' UTR of the genome. The viral NS4B/NS5 RNA-dependent-RNA-polymerase (RdRp) binds to conserved stem loop structures of the 3'UTR along with a variety of host cell proteins in an incompletely characterized event.[45, 46] Other viral proteins involved in this replication complex include NS1 and NS4A. The viral NS3 helicase acts to unwind/stabilize the RNA genome.[47] Replication of a negative-sense RNA strand then occurs in a 5' to 3' direction. These negative sense strands serve as the template for the creation of positive-sense viral RNA genomes. Replication of positive-sense RNA strands occurs when the same viral and host replication complex binds to the 3' end of the negative-sense RNA (5' UTR of the viral genome).[48-50] There is evidence that only a few negative strands are created, and that multiple replication events occur simultaneously on one of these strands to produce a large amount of positive sense RNA viral genomes. These positive-sense RNA strands have two functions which include serving as a translational template for the creation of more polyproteins and as the viral genome that is released from the cell. There is no polyA tail on the viral RNA genome, but a 5' cap is added by the NS5 viral protein.[51]

Viral packaging occurs once enough viral proteins and genomes have been created in the golgi apparatus. The capsid (C) protein is arranged in an icosahedral

symmetry around the positive-sense RNA with the assistance of NS2A.[52] The preMembrane (prM) and E proteins are then arranged around the viral capsid. The prM conformation of the M protein protects the low pH mediated membrane fusion domain of the E protein during transit in a vesicle from the cell. Once released by exocytosis, the prM protein is cleaved to the M (membrane) form.[41, 53] The virus is then ready to bind to and infect new host cells.

Experimental Models of Infection

Controlled studies of WNV infection are difficult due to a lack of well-defined models and difficulty in reproducing infection in the mammalian host. Horses and other incidental hosts, including humans, have a high rate of subclinical disease (or exposure) with only a small proportion developing clinical signs of infection.[24, 28-32, 54-56] Conversely, some small mammal models demonstrate extreme susceptibility to disease with high mortality rates and short survival times.[23, 24, 57] Both of these scenarios make studying the pathogenesis of WNV difficult as a low rate of clinical signs requires a large number of subjects and the small mammal models may have very different immunopathological mechanisms of disease. Thus many experimental protocols have limited proven translational applicability and questionable extrapolation to disease in naturally affected hosts.

Mosquito or peripheral experimental challenge of the horse is one example of a model in which there is limited reproduction of clinical disease with a symptomatic:asymptomatic ratio of 1:12.[54] Yet experimental inoculation of the horse should be an ideal model for studying WNV, since equines develop clinical disease and pathology during WNV infection similar to humans. In response to this problem, an intrathecal model for WNV laboratory infection in horses has been developed. This

method uses a sterile technique to directly inject the virus (~10^5PFU) into the subarachnoid space of the CNS at the atlanto-occipital junction of the horse while under anesthesia, resulting in clinical disease in 100% of naïve subjects.[58, 59] Peripheral inoculation with vaccines developed against WNV has been successful in protecting against clinical disease induced by direct inoculation of the CNS and serves as the basis for studying the pathogenesis of WNV in this current research.

Currently accepted methods of viral infection include intradermal, intramuscular, intraperitoneal, intravenous, and intrathecal needle injection, as well as mosquito infection. Each of these methods has problems associated with their use. Needle injection is meant to mimic mosquito bite infection. However, needles cannot simulate the biological factors associated with mosquito bite infection that may influence disease, including differing bite locations, mosquito-associated factors (vector capacity, salivary proteins and enzymes, incubation temperature), and locale-specific host response. Work aimed at understanding mosquito/virus interactions traced the path of WNV through the mosquito. As previously described, the virus undergoes initial viral replication, spreading to the hemocoele, head, and salivary glands in a 7 day cycle. [4] During this time, the virus may undergo as-yet-uncharacterized interactions with the vector that cannot be replicated in a mechanical infection model and may affect how the virus affects the laboratory model.

Yet the mosquito infection model is not ideal either. The amount of virus inoculated into the host will vary depending on the number of mosquitoes that bite the host and the stage of viral replication within the vector, thus confounding the results of experiments which require known infectious doses. This is supported by different

arbovirus experiments involving LaCrosse virus in deer and in another involving WNV in chickens where unexpectedly higher viremias were induced with mosquito infection compared to needle inoculation.[57, 60] There are also a variety of environmental factors that influence viral replicative ability in the mosquito host that it may be difficult to control in the laboratory, including ambient temperature, seasonality, and climate conditions..[12] Other studies have demonstrated a lack of correlation in the pathological lesions of WNV between mosquito, needle, and oral routes of infection.[55] Therefore, while a lack of biological factors is problematic with mechanical methods of WNV infection, the lack of ability to control these biological factors confounds even the most 'naturally simulated' laboratory infection.

Birds are an example of a laboratory model that demonstrates both low rates of infection/subclinical disease and high rates of infection/mortality. This is dependent upon the species of bird affected. The family of birds Corvidae (crows, blue jays, ravens, etc.) appear to be the most severely affected clinically with high viral titers, a short incubation period, and a high mortality rate. Clinical signs of lethargy, reluctance to fly, depression, anorexia, and sporadic neurological signs (i.e. ataxia) by four days post-infection (PI) during laboratory infection intravenously with 10^3 PFU/mL of the NY99 strain of WNV was seen in crows and blue jays. By day five PI, all birds either spontaneously died or were euthanized. Viral titers in the blood of all birds measured $>10^7$ PFU/mL consistent with field infection levels.[23] In another study in which birds were infected via mosquito bite, oral ingestion, or contact, the Corvidae were highly susceptible to disease. The birds demonstrated clinical signs of lethargy, ruffled feathers, and unusual posture with a high viremia and death 24 hours post onset of

clinical disease.[24] Thus laboratory infection of Corvidae appears to simulate natural infection based on clinical signs and viral titers, but these birds make a poor laboratory model due to their extreme susceptibility to disease. Young chickens appear to be susceptible to WNV, and are easier to obtain, thus they make a better substitute model for understanding mechanisms of pathogenesis in the avian host. Adult chickens are exceptionally resistant allowing for understanding successful innate responses to WNV.[57, 61, 62]

Laboratory investigations into the use of raptors as laboratory models have not been consistent. In the wild, raptors appear to be highly susceptible to WNV. In a surveillance study, 61 out of 149 (66%) total raptors submitted to a clinic tested positive for WNV through real time PCR. Clinical signs in these birds depended on the species of raptor. Great horned owls presented with neurological signs of head tremors, head incoordination, and ataxia, while red-tailed hawks presented with the more general signs of emaciation, dehydration, depression, and variable mild neurological abnormalities.[63] This is in contrast to one study which compared mosquito, needle, and oral infection of kestrels, hawks, and owls. No clinical signs were noted in any species yet high viral titers (>10^5 PFU/mL) were obtained with pathological lesions that varied according to species and route of infection.[55]

Passerines appear to maintain a subclinical disease with high viral titers for an extended period of time in the wild and in the laboratory setting. Blood meal analysis of mosquito species has demonstrated that *Culex* mosquito species (the main species responsible for WNV transmission among birds[13, 15]) preferentially feed on passerines including the American robin, the Northern cardinal, the common grackle, and the house

finch.[19, 25] Yet minimal mortality has been noted in these birds due to WNV in surveillance studies and laboratory studies support this finding. In one study, robins, house finches, and sparrows were infected with WNV orally, through mosquito bite, and through contact. These birds developed a high viremia ($10^{5.4}$-$10^{8.9}$ PFU/mL) with few clinical signs and minimal mortality.[24]

Experimental peripheral infection of both nontraditional and traditional laboratory mammal species has been performed to investigate their effectiveness as laboratory models of WNV. Infections of bats, pigs, and dogs have resulted in low levels of virus (10^{1}-10^{3} PFU/mL) and the absence of clinical signs.[28-30] Therefore, it is unlikely that these hosts will serve as effective laboratory models. This is in contrast to laboratory mice and cats which develop both a moderate to high viremia and clinical signs. Needle inoculation of cats results in mild, non-neurological signs of disease with viremias of 10^{3}-10^{4} PFU/mL.[28]. Peripheral inoculation of WNV in the laboratory murine host (C57BL and BALBc) results in a high viremia and clinical signs of encephalitis, anorexia, depression, and death.[64] The susceptibility of laboratory mice to WNV is in distinct contrast to wild mice that are genetically resistant. Laboratory mice contain a point mutation in the 2'5'oligoadenylate synthetase gene in the *flv* locus on chromosome 5 which makes them susceptible to WNV infection.[64-66]

Therefore the mouse, due to its small size and the ease with which genetic manipulations can be performed, remains one of the main models for studying WNV infection. However, the applicability of the mouse model to other species is controversial due to inbreeding to obtain genetic mutants which may have deleterious effects on such factors as the immune response. In addition, the infection itself results

in CNS infection that is distinct from that of humans and horses in terms of pathology and virus localization. Other rodent models have been explored as an effective laboratory model. To date, all have demonstrated subclinical signs with high levels of viremia, providing evidence of their possible role as effective reservoir hosts but questionable role as an accurate laboratory representation of WN encephalitis in the outbred host. Experimental peripheral inoculation of fox squirrels with WNV resulted in clinical signs in only 1 of 11 subjects with levels of viremia ranging from $10^{1.7}$-$10^{6.1}$ PFU/mL.[31] Similar results were obtained in chipmunks, with peripheral inoculation resulting in no clinical signs and virus titers of $10^{3.9}$-$10^{6.7}$.[32] Finally, experimental infection of the golden hamster induces high viral titers up to $10^{4.7}$ and fatality but no clear indication of infection through clinical disease. Also this model is pathologically different in that hamsters develop a high degree of tissue necrosis in the CNS, which is minimal in natural infection of horses and humans.[56]

Clinical Signs in Horses

In the horse, the majority of WNV infections are subclinical. It is estimated, based on experimental mosquito challenge and epidemiological analysis, that about 10% of horses naturally exposed to WNV actually develop clinical disease.[67] Clinical signs usually begin between nine and eleven days of infection.[58, 67, 68] Initially, these include the general systemic signs of fever (38.3^{o}C-39.4^{o}C), anorexia, and depression. The onset of neurological disease is usually abrupt and there are changes in behavior or mentation with an insidious onset of motor deficits.[69, 70] Horses exhibit signs consistent with an encephalomyelitis (diffuse inflammation of the brain and spinal cord disease) exhibited by a combination of mentation and spinal cord abnormalities and defects in cranial nerves. Spinal cord abnormalities include a stiff stilted gait (which can

be mistaken for lameness but is likely bradykinesia), ataxia (involving two or more limbs, symmetric or asymmetric), flaccid paralysis (lower motor neuron disease), paresis, and recumbency. Several hours or days of muscle fasciculations (most notable around the muzzle but can involve the entire body) are often noted. Cranial nerve abnormalities include weakness of the tongue (CNXII- hypoglossal), muzzle deviation (CNVII- facial), head tilt and/or difficulty balancing (CN-VIII- vestibulocochlear), and difficulty swallowing (CNIX- glossopharyngeal). Changes in mentation include a change in sensorium defined as “a change in animal’s normal habits, personality, attitude, reaction to environment” and hyperesthesia with intense reactions to environmental sounds and motion.[71] In addition, changes in behavior including severe aggression, somnolence, and coma may be seen.

Approximately 30% of horses with clinical signs of disease die spontaneously or are humanely euthanized (this number increases to 100% if the horse is recumbent). The remaining 70% of horses with clinical disease recover between three and seven days after the onset of clinical signs. However, approximately 30% of the horses that recover will recrudesce within two weeks and can go through a short or prolonged bout of the the previously described clinical signs. Of the horses that completely recover, 10% will retain long-term complications, including weakness, ataxia, and fatigue.[10, 54, 58] In these studies, many owners indicated that horses also seemed to have evidence of personality change. All the former may have led to loss of use of the animal for the owner.

Clinical Signs in Humans

Natural infection in humans has been documented from mosquito bites, transfusions, breast feeding, intrauterine transmission, and organ transplants.[72] Most

infections with WNV in humans are subclinical, with clinical signs developing in about 20-40% of people infected and an average incubation period of two to 14 days. The most common clinical presentation consists of flu-like complaints of illness, oftenaccompanied by skin rash, increased body temperature, headache, myalgia, vomiting, diarrhea, and fatigue. Approximately 1% of people progress to neurological signs which can be divided into brain-like symptoms of encephalitis/meningitis (including disorientation, seizures, tremors, ataxia, photophobia, stiff neck, Parkinson-like syndrome, etc.) and/or acute flaccid paralysis (loss of use of breathing, limbs, paresis, and complete paralysis). Movement disorders are consistent with bradykinesia with the lesion of paralysis consistent with anterior horn syndrome. Recovery among these patients is variable, ranging from complete recovery to chronic long-term deficits. The case-fatality rate is approximately 8% in neurologically affected patients. Other complications, though rare, include chorioretinitis, rhabdomyolysis, myositis, autonomic involvement, hepatitis, pancreatitis, myocarditis, orchitis, uveitis, and vitritis.[73]

Immune Response

After the bite of an infected mosquito, WNV is inoculated peripherally into the skin and muscle. Dendritic cells and other antigen presenting cells (APCs) take up the virus through recognition of the viral envelope proteins with conserved pattern recognition receptors and induce an innate immune response. Toll-like receptor (TLR)-3 has been shown to play an important role in this regard, although the question of whether the receptor is protective or increases neuroinvasion of the virus has yet to be resolved.[74, 75]

Type I interferons (IFN-α and IFN-β) that are produced by the APCs in response to activation of the pattern recognition receptors (PRRs) induce transcription of 2'5' oligoadenylate synthetase (OAS) and protein kinase R (PKR), Eukaryotic translation initiation factor 2-alpha kinase 2 (human gene)]. The 2'5'-OAS enzyme transforms the RNaseL protein to an active form that degrades viral RNA and prevents viral replication. Protein kinase R is also activated by the type I interferons. This protein acts to phosphorylate eukaryotic initiation factor 2 (eIF-2) and prevent translation initiation. The APCs also produce IFN-γ which functions to upregulate MHC-I expression and enhance natural killer (NK) cell activity. The virus is transported by the APCs to the regional lymph nodes to initiate an adaptive immune response. This is largely driven by the cytokine expression pattern of the macrophages and dendritic cells, as well as by NK T lymphocytes.

Expression of IL-12 in association with IFN-γ secretion by macrophages and dendritic cells induces the differentiation and proliferation of of T-helper type 1 (Th1) lymphocytes. These cells secrete interleukin (IL)-2 and IFN-γ which, along with NK T-cell production of IFN-γ, activates and enhances the activity of CD8+ T lymphocytes. Once activated, CD8+ T lymphocytes undergo positive feedback through the self secretion and stimulation of IFN-γ and IL-2. Activated CD8+ T lymphocytes kill virally infected cells by inducing apoptosis in target cells expressing the proper MHC-I/ PAMP combination. Apoptosis can be induced by T lymphocytes through two pathways: the perforin/granzyme pathway and the Fas/FasL pathway (TNF-α and TGF-β secreted by microglia can also induce the Fas/FasL pathway). The perforin/granzyme pathway is a direct pathway wherein the perforin acts to create membrane pores which allow the

granzymes to enter the target and start cellular degradation. This pathway has been shown to be essential in the WNV immune response.[76] The Fas/FasL pathway induces apoptosis by initiating an intracellular caspase cascade (cytoplasmic or mitochondrial) which activates proteins that degrade cellular nucleic acids. Both mechanisms of apoptosis result in the death of an infected cell. Laboratory studies have demonstrated increased mortality and viral loads in CD8+ T lymphocyte deficient mice. In addition, CD8+ T lymphocyte deficient mice that did survive had long-term, low levels of persistent viremia.[77]

Expression of IL-4/5/10 by macrophages and dendritic cells drives the differentiation and proliferation of T lymphocytes cells into a Th2 phenotype. These cells function to stimulate the B lymphocyte response (including B lymphocyte phagocytic activity, antibody isotype switching and somatic hypermutation) and also may inhibit the Th1 cell response depending on species. In addition, B lymphocytes initially produce IgM antibodies to WNV and then undergo a class switch to produce IgG.[78-81] Antibodies are important in fighting viral infection through multiple mechanisms, the most important of which include virus neutralization (binding to the virus to prevent binding to cell receptors and uptake of virus), antibody-dependent cell-mediated cytotoxicity (binding to the virus to enhance Fc receptor recognition from NK cells and phagocytosis of the virus), and complement activation. Numerous studies have shown that antibody production against WNV is essential in protecting against disease. Mice deficient in IgM production (C57BL/J6 IgM-/-) were unable to combat WNV infection and succumbed to disease even at low viral titers. Subsequent passive transfer of WNV specific antibodies was able to protect against disease in susceptible

mice.[82] In another study, polyclonal antibody was passively transferred to wild type, B lymphocyte deficient (μMT), and B lymphocyte and T lymphocyte deficient (RAG) naïve mice. Wild type mice were protected compared to controls and were able to clear viral infection. However, while administration of the antibodies to μMT and RAG1 mice did reduce morbidity and mortality, these mice were unable to completely clear viral infection.[83] Thus, vaccination leads to a specific antibody response that is essential to protect against viral infection. The onset of this host immune response corresponds with the viremia that occurs between two and four days post-infection.

If the host is unable to neutralize the virus, the virus may gain access to the CNS by breaching the blood brain barrier. Several ways in which this might occur have been postulated. The first includes disruption of the barrier when endothelial cells are exposed to pro-inflammatory cytokines released by macrophages and dendritic cells of the innate immune system. These cytokines, including tumor necrosis factor (TNF)-α, IL-6, and IL-12, induce blood vessel dilation and the endothelial cell expression of cellular receptors such as E-Selection and ICAM-1 for leukocyte migration.[80] The second hypothesis involves the infection of circulating peripheral mononuclear cells that migrate across the blood brain barrier.[80, 81] This is supported by research demonstrating that mice deficient in TLR-3 cell receptors found on immune cells have decreased neurological disease compared to wild type mice.[80, 81] A third hypothesis involves the use of peripheral nerves such as the olfactory nerve to travel to the CNS.[80]

Once the virus gains access to the CNS, a combination of the neuronal cell response, innate and adaptive immunity, and the virus life cycle likely produce the neuropathological change responsible for clinical disease in the host. Most of the

mechanisms have been solely derived from murine models of WNV that heavily rely on genetically modified strains. The virus initially binds to host T lymphocyte receptors on microglia including TLR-3, RIG-1, MDA-5, and integrins which begins the immunological cascade. It has been demonstrated that T lymphocytes lacking in TLR-3, RIG-1, and MDA-5 receptors have diminished cytokine and antiviral responses compared to cells that have these receptors.[84-86] Binding to the cell receptors activates a signaling cascade involving transcription factors such as interferon regulatory factor (IRF)-3, NFκB, and MAPK, which lead to the production of type I interferons (IFN-α and IFN-β). Lack of the IRF-3 signaling pathway *in vitro* leads to a more virulent WNV phenotype.[85] These IFNs then bind to cell receptors and induce an antiviral response through secondary signaling, including the JAK/STAT pathway. Mice that completely lack both IFN-α and IFN-β exhibit increased mortality (100%) with a decreased time to death compared to WT mice (mortality 62%). In addition, IFN α/β-/- mice had higher viral loads in a greater number of tissues compared to WT mice.[87] The type 1 IFNs induce the transcription of 2'5-Oligoadenylate synthetase which leads to RNAseL production and the degradation of viral RNA, as well as the transcription of PKR kinase which leads to the production of eIF-2 and inhibition of viral transcription. Mice that are PKR-/- and RL-/- demonstrate increased mortality (90%) compared to WT mice (30%) as well as increased viral loads in multiple tissues.[80] *In vitro*, RNaseL-/- cells produced 5-10 times higher viral loads than RNaseL +/+ cells.[88]

The majority of the time, the antiviral response by microglial cells is beneficial to the host. However, microglial cells also produce a variety of inflammatory mediators that lead to host cell damage. These include nitric oxide synthetase (NOS), reactive

oxygen species (ROS), IL-6, IL-12, TNF-α, TGF-β, phospholipase A, and matrix metalloproteins. These inflammatory mediators produce damage both directly and indirectly through signaling cascades. Nitric oxide synthetase induces the production of peroxynitrite which damages cell lipids and proteins, and potentiates glutamate excitotoxicity. The ROS molecules, hydrogen peroxide and hydroxyl radicals, and matrix metalloproteinases (MMPs) also lead to generalized cellular damage. Interleukin-6, IL-12, and TNF-α induce inflammation and the migration of CD8+ T lymphocytes which can lead to cell damage. Tumor necrosis factor-α and transforming growth factor (TGF)-β can lead to apoptosis. Phospholipase A increases the production of arachadonic acid, eventually leading to prostaglandin, thromboxane, prostacyclin, and leukotriene production with subsequent inflammation. The production of these detrimental mediators by microglial cells has been studied in JEV infection of mice.[89] Thus microglial cells, while essential for the innate immune response, can also lead to neuropathology in the host.

Neuronal infection by WNV also leads to host cell damage, both directly through the actions of the virus, and indirectly through the host immune response. During infection, neurons express the chemokines, CXCL10 and CCR5, which drive the recruitment of CD8+ T lymphocytes.[90] Lack of CXCL10 has been shown to decrease CD8+ T lymphocytes recruitment, increase viral titers in the brain, and increase morbidity and mortality in experiments involving mice.[90] This, combined with IFN-γ secreted by NK T lymphocytes and IFN-γ and IL-2 secreted by Th1 cells, functions to recruit CD8+ T lymphocytes to sites of viral replication and upregulate MHC-I expression. CD8+ T lymphocytes, once activated, undergo positive feedback through

the self secretion and stimulation of IFN-γ and IL-2. As previously mentioned, CD8+ T lymphocytes kill virally infected cells[76, 77] However, CD8+ T lymphocyte activity in the CNS may be detrimental to the host. In one study, mice infected with a high viral load of WNV (10^8 PFU/mL) suffered 100% mortality with a six day mean survival time. This was in comparison to mice that were infected with a low viral load (10^3 PFU/mL) which suffered 27% mortality, with a mean survival time of 11 days. Histopathology of the brains revealed neuronal degeneration and inflammation consisting predominantly of CD8+ T lymphocytes. When β2 microglobulin mice (β2M) mice lacking MHCI and incapable of recruiting CD8+ T lymphocytes were infected in the same study with high titers (10^8 PFU/mL) of virus, mean survival time was increased. But when these same mice were infected with low titers of virus (10^3 PFU/mL), increased mortality but prolonged mean survival time was noted.[91] Thus CD8+ T lymphocytes appear to function in both the recovery from and pathology of WNV infection. Since WNV preferentially infects the neuronal cell bodies of the thalamus, midbrain, hindbrain, and spinal cord, the gray matter of these regions is most affected, leading to virus and immune-induced neuropathology.

Another mechanism of neuronal cell death, partially contributed to by T lymphocyte-mediated apoptosis, may be neuronal excitotoxicity.[92-96] This mechanism is suspected to be involved in WNV pathology, since there can be extensive apoptosis and necrosis with limited virus load. This phenomenon has been extensively studied in neuronal HIV infection[92-95] and Sinbis virus infection.[96] Briefly, glutamate is the primary excitatory neurotransmitter in the nervous system. Upon release (exocytosis) from the presynaptic cleft, glutamate binds to ionotropic (NMDA, AMPA) and

metabotropic (G protein coupled) cell receptors on the post-synaptic cleft. This binding results in the opening of calcium channels (ionotropic) as well as the activation of the PIP_2/IP_3/DAG pathway (metabotropic), both of which result in a net increase in intracellular calcium. This increase in calcium leads to an action potential and the propagation of neuronal signals. When too much glutamate is present, excessive calcium accumulates in the neuron and leads to the production of toxic substances such as phospholipase A and NOS. Excessive levels of glutamate in the synaptic cleft can be due to apoptosis of neighboring neurons (i.e. due to CD8+ T-cell mediated killing), lack of energy and/or oxygen (leading to failure of glutamate re-uptake with energy dependent glutamate transporters), and loss of GLUT-1 receptors (function in glutamate reuptake).[97] This has been investigated in a study looking at the expression of the principle excitatory amino acid transporter (EAAT) in the spinal cord during WNV infection. This study found decreased EAAT expression with increased astrocyte expression during WNV infection, providing indirect evidence for glutamate excitotoxicity.[98]

Neurological Response

In contrast to the immune response to viral infection, few studies have been performed to increase our understanding of the response of the CNS to WNV infection. The majority of work in this area has involved an examination of the clinical signs and pathological distribution of lesions during WNV infection and the subsequent histopathology associated with these lesions.[99-101] Limited work has been performed looking at the neurological response of the host at the molecular/genetic level. This has mainly consisted of the afore-mentioned study examining the expression of glutamate transporters in the spinal cord during WNV infection.[98] Another study focused on the

detection of biomarkers in CSF fluid.[102] However, little or no work has been performed to look at the response of the nervous system on the level of gene expression and the downstream effects of these changes. This includes changes in neurotransmitters, receptors, and structural components of the nervous system. Work in this area could lead to a greater understanding of how the CNS responds to infection with WNV and other viral encephalitides, and measures that may be taken to combat these affects.

Pathology

Clinicopathologically, WNV causes a polioencephalomyelitis mainly involving the midbrain, hindbrain, and spinal cord. This is characterized grossly by an increasing number of lesions progressing from the diencephalon through the hindbrain and down to the spinal cord. Spinal cord lesions become progressively worse caudally. Congestion of the meninges and hemorrhagic foci may be seen. Histopathologically, inflammatory lesions characterized by layer of monocellular perivascular cuffing are present. These layers of monocellular cells may also be present in the gray matter (gliosis). These lesions are the most severe in the basal ganglia, thalamus, pons, and medulla (midbrain and hindbrain). Gliosis and monocellular perivascular cuffing are also present in the spinal cord and become worse caudally. Few, if any, lesions are seen in the cerebrum and cerebellum of the outbred hosts, horses and humans, further emphasizing the predilection of this virus for cell body enriched tissues of the midbrain, hindbrain, and spinal cord.[10]

Diagnostics

Since no clinical signs are pathognomonic for WNV infection, all horses that are suspected of being infected with WNV should undergo ancillary diagnostic testing to rule out other diseases. This should include a complete blood count (CBC) and serum

biochemistry as well as a cerebrospinal fluid analysis (CSF). Blood analysis is usually normal, although there may be a lymphopenia, elevated muscle enzymes secondary to trauma, and hyponatremia. Cell and protein counts in the CSF may be elevated, usually consisting of an elevated mononuclear cell population, protein concentration of N<70mg/dL, and mild xanthochromia.[103-106]

Differentials for neurological disease in the horse suspected of WNV infection should include hepatoencephalopathy, rabies, alphavirus infection (EEE, WEE), equine protozoal myeloencephalitis (EPM), leukoencephalomalacia, tremorigenic toxicities, equine herpesvirus-1 (EHV-1), botulism, hypocalcemia, and verminous meningoencephalmyelitis.[10] These diseases and metabolic conditions may be ruled out with the pertinent testing but the similarity of these conditions can make accurate antemortem diagnosis difficult.

The preferred test developed by the National Veterinary Services Laboratory for the detection of WNV in the horse is the IgM capture enzyme-linked immunosorbent assay (MAC-ELISA). This test detects whether the horse has had *recent* exposure to WNV by testing for the presence of IgM antibodies. High levels of IgM antibodies are usually present post-exposure to WNV, at the time of clinical disease in the horse and last for approximately 6 weeks. After this time, circulating levels of IgM WNV antibodies decline and are replaced by IgG antibodies. The sensitivity and specificity of this test is 81% and 100%. Briefly, the test works by coating the wells of a charged plate with some type of anti-horse IgM antibody (i.e. goat). The sample of interest is placed on the plate, and the antibodies present in the sample bind to the anti-horse antibodies. WNV antigen is then added, which binds only to the IgM WNV antibodies present that are

themselves bound to the anti-horse antibody. Finally, an anti-WNV monoclonal antibody linked to some type of identifier is added to the well, binds the WNV antigen, and a color change is induced. Those animals that contain WNV IgM antibodies thus have a color change, while animals negative for WNV IgM antibodies do not. The test takes approximately 24-48 hours to run and relies upon the presence of clinical disease. The quantity of this response has no correlation to severity of disease and does not predict survival.[10, 107]

In the unvaccinated horse, the plaque reduction neutralization test (PRNT) can be utilized. This test can be used to diagnose WNV infection if there is a four-fold rise in paired neutralizing antibody titers. Briefly, cells are grown to confluent monolayers on plates. Samples of interest containing dilutions of the serum sample to be tested are mixed with known concentrations of virus. The mixed samples are cultured on the plates under agar to prevent spread of viral plaques. The wells are stained and the number of plaques per well, per dilution are counted. Horses with high levels of neutralizing antibody will have no plaques even at high dilutions of the serum (i.e. 1:64 or lower) due to the antibody binding to and preventing the virus from infecting the cells. Horses with little or no neutralizing antibodies will have wells demonstrating a cytopathic effect (plaques) even at low dilutions (i.e. 1:2). In this manner, the titer of the antibody can be determined (the lowest dilution at which there are no viral plaques). If this test is run sequentially (i.e. at 1 and 4 weeks) and there is a four-fold rise in the antibody titers, then the horse has been recently exposed to WNV. This test has fallen out of favor for diagnosis of WNV infection due to the fact that vaccination produces antibodies which confound the results and the length of time that it takes to complete (1-2 weeks). This

test is now mainly used to determine the titer of antibodies to WNV in the subject of interest.[10, 107, 108]

Other accepted methods of testing for the virus post-mortem include real-time PCR to detect viral antigen, viral culture to isolate the virus, and immunohistochemistry to detect viral antigens. All of these tests are used post-mortem, since it is very difficult to detect the virus in the live animal- this is only possible during the viremic phase- at approximately 2-4 days after the onset of clinical signs. If these forms of testing are desired, whole brains (especially the midbrain and hindbrain) and/or spinal cord should be submitted to a testing laboratory, chilled and in proper containers for biocontainment.[10, 109]

Treatment

Currently, there is no effective anti-viral treatment for WNV and treatment can only be focused on providing supportive care. Horses that present with clinical signs of WNV should be placed on flunixin meglumine (1.1mg/kg every 12 hours intravenously). This appears to reduce the muscle tremors and fasciculations associated with WNV. There is controversy in the use of corticosteroids in horses affected with WNV due to the possibility of enhancing the viral load both peripherally and in the CNS. Recumbent horses generally require more aggressive therapy, due to the high mortality associated with recumbency. For the short term relief of anxiety, acepromazine can be used (0.02 mg/kg IV or 0.05 mg/kg IM). For long-term tranquilization, detomidine hydrochloride (0.02-0.04 mg/kg IV or IM) can be used. Therapies that have yet to be tested and proven efficacious include the use of IFN-α and WNV-specific IV immunoglobulin.[10]

Vaccination

Inactivated Whole Virion/Subunit Vaccines. Killed and subunit vaccines are often used in veterinary medicine for their safety record (will not revert to live virus) and for their potential in over-the-counter marketing. The first licensed vaccine (Innovator, Fort Dodge Animal Health, Overland Park, KS), available since 2001, is a killed West Nile vaccine consisting of a formalin-inactivated whole virion. The adjuvant present in this vaccine is MetaStim™- a proprietary oil, non-aluminum, dual phase adjuvant.[110, 111] This vaccine is currently labeled for the control of viremia of WNV infection in the horse. Efficacy and duration of immunity studies using this vaccine demonstrated that 18 out of 19 vaccinated horses did not develop a detectable viremia. It should be noted that the duration of protection against WNV clinical disease has yet to be tested in the clinical challenge model.[112] Initial field studies indicate that there is a limited antibody response in 30% of horses with a rapid decrease in the level of antibodies by 5 to 7 months after vaccination.[113] No subunit vaccines are currently licensed for use in the horse. Inactivated whole virion vaccines do not actively replicate once administered in the host. Thus, multiple vaccinations are required for the naïve equine. However, the earliest vaccine series within foals should not begin before 3 months of age due to possible interference with maternal antibodies.

Foals born to vaccinated mares should receive a 3-dose series of this vaccine. The first dose should be administered at 4-6 months of age with the second dose following 4-6 weeks after the first. The third dose should be given at 10-12 months of age before the major vector season. In foals residing in areas with high vector activity (i.e. the Southeast), the initial dose should be administered at 3 months of age. In foals

born to unvaccinated mares, the 3-dose series of vaccines should start at 3-4 months of age (extra first dose at 3 months of age in foals living in areas with high vector activity) with a second dose 4 weeks after the initial dose. The third dose should be given at 10-12 months of age; again, before the onset of the peak vector season. For adults with an unknown vaccination history and/or no history of vaccination, a 2-dose series of vaccines should be given with the second dose given 4-6 weeks after the first. These horses should be given a booster before the onset of the vector season. In adult horses with a known history of vaccination, one vaccination is required prior to the onset on the vector season (usually in the spring) each year. However, if the horse lives in an area with vector activity year-round (i.e. the Southeast), two doses of vaccine are recommended each year- one before the onset of peak vector activity in the spring and a booster in the late summer/fall.[114]

Modified Live Vaccines. Modified live virus vaccines are considered more desirable due to their ability to mimic natural infection without causing clinical disease, thus inducing long-term immunity to viral pathogens. Two recombinant live vector preparations are licensed for commercial use in horses. The canarypoxvirus vector vCP2017 (CP-WN; Recombitek™, Merial, Duluth, GA) was the first licensed in 2004. This vaccine expresses the WNV membrane (prM) and envelope (E) genes under control of and packaged with a carbopol adjuvant which is a proprietary cross-linking polymer adjuvant that has a depot effect to slow release of antigen. This adjuvant is considered superior to the aluminum-based adjuvants as it is proposed to induce both humoral and T cell responses. After a single dose of CP-WN, 90% of horses demonstrated protection against viremia.[115]

In foals born to both vaccinated and unvaccinated mares, a 3-dose series of vaccines should start with the initial dose at 5-6 months of age (in areas with high vector activity, an extra dose at 3 months of age for foals born to unvaccinated mares, and the first dose at 3 months of age in foals born to vaccinated mares should be given). The second dose should be given 4 weeks after the first and the third dose at 10-12 months prior to the onset of peak vector activity. In adult horses with an unknown vaccination history, a 2-dose series of vaccines should be given 4-6 weeks apart with a booster prior to the onset of peak vector activity. In horses with a history of vaccination, annual boosters should be given before peak vector activity. If living in areas with high mosquito activity year round (endemic for WNV), two vaccines should be given- one in the spring and one in the late summer/early fall.[114]

A nonadjuvanted, single-dose attenuated WNV, live flavivirus chimera (WN-FV) vaccine (PreveNile®, Intervet, DeSoto, KS) became available in 2006.[116] This vaccine expresses the envelope (E) and membrane (prM) of WNV in the yellow fever vaccine 17D (YF17D). The safety, efficacy and duration of immunity of the veterinary chimera (YF-WN) were investigated.[58, 117] This vaccine, given at 20X and 100X immunogenicity dosages did not revert to virulence or have a detectable viremia despite the development of neutralizing antibody after vaccination.

In foals born to both vaccinated and unvaccinated mares, a 2-dose series of vaccines starting at 5-6 months of age with a second dose administered at 10-12 months of age before the onset of peak vector activity should be given. In areas of high vector activity, an extra dose should be given to foals born to unvaccinated mares at 3 months of age and the primary vaccination given at 3 months of age for foals born to

vaccinated mares. For adult horses with an unknown vaccination history, one dose should be given initially and then a booster dose administered every year before the onset of peak vector activity. In horses with a known vaccination history, vaccination should occur yearly before the onset of peak vector activity.[114]

High Throughput Pyrosequencing

Pyrosequencing is a high-throughput sequencing methodology that can generate reads (sequenced transcripts) of 250 base-pairs with greater than 100 million base-pairs per run. Briefly, the nucleic acids contained in a library of interest are randomly fragmented by nebulization. Linkers (A and B) are attached to each end of the fragments. Avidin-biotin purification is used to select only the fragments containing both A and B linkers. The ssDNA containing the linkers are attached to DNA capture beads and immersed in water-in-oil microreactors. Clonal amplification is performed in each microreactor such that each DNA capture bead contains multiple copies of a specific ssDNA fragment. The DNA beads containing the libraries are placed into individual 44 mm wells. The sequencing reactions then occur, in which each base is cycled individually. A chemiluminescent signal is emitted with the correct basepair matching. Specifically, ATP is generated when added sulfurylase reacts with the pyrophosphate released from the reaction extension. The ATP then reacts with added luciferase and luciferin to generate light plus oxyluciferin, which is read by the computer as correct incorporation.

The use of high-throughput sequencing technologies, including pyrosequencing, is becomingly increasingly common as a method to sequence eukaryotic and prokaryotic genomes.[118, 119] Recently pyrosequencing has also gained popularity as an analysis tool in other genetic methodologies, involving both disease and non-diseased

states. These include the identification and analysis of epigenetic changes in cancer,[120-124] the discovery of disease-causing mutations,[125-127] and the identification and analysis of small-interfering and micro- RNAs.[128-131] Applications have also demonstrated the usefulness of pyrosequencing as a means of analyzing the transcriptome for expression profiling and new gene discovery in both plants and animals.[132-135] This is especially useful in newly assembled genomes where annotation of the information, as well as the prediction of new genes, may be incomplete.

Thus the information gathered from pyrosequencing experiments can be used in a variety of applications. One such example of where high-throughput pyrosequencing would be useful in a newly assembled genome is the horse genome project. Assembly of the horse genome was completed in 2007 with 6.8X coverage of the approximately 2.7 billion base-pair genome.[136] However, while the sequencing of the genome is complete, work on the annotation and identification of the sequences is still in progress. Sequencing the genome does not provide information on which genes are expressed and at what frequency. Analysis of the transcriptome of newly sequenced organisms can provide invaluable information that will help to develop a comprehensive picture of an organism's biology and genetics.

Microarray Analysis

Microarrays are useful tools to analyze the nucleic acid components of organisms. The number of applications for arrays has increased in recent years, and has included such diverse functions as pathogen identification [137, 138], microRNA/siRNA discovery[139, 140], and exon analysis[141-143]. One of the more common applications of microarrays is in the analysis of gene expression for a systems biology appoach, especially in regards to diseased states.[144, 145] This is particularly useful when

analyzing gene expression on a global scale, as interactions between pathways of interest can be targeted to understand how pathogens affect the host and defined as an integrated model.

Microarrays have facilitated the study of the Flaviviridae in multiple applications including detection of variants of Dengue virus (DV) in human samples[146], differentiation between different flaviviral and other viral infections[147, 148], and mutations in the structural regions of the WNV genome[149]. Microarrays have also been applied to analyze gene expression at both the cell culture and organism level for DV, JEV, and yellow fever virus (YFV) infection.[150-155] However, the analysis of gene expression during WNV infection has been limited. The only study involving whole organism gene expression analysis was performed in mice, an animal that is not naturally susceptible to WNV infection. The study consisted of analyzing the differences in gene expression between mice infected with strains of WNV differing in neurovirulence, and thus did not incorporate gene ontologies into an integrated model. As expected, genes involved in immunological, neurological, and apoptotic functions were differentially regulated. Forty-seven genes were shown to be upregulated in highly neuroinvasive strains.[156] Thus there is still a lack of knowledge in how infection with WNV causes global changes in gene expression in naturally affect hosts. This information could be used to gain a better understanding of host-pathogen interactions.

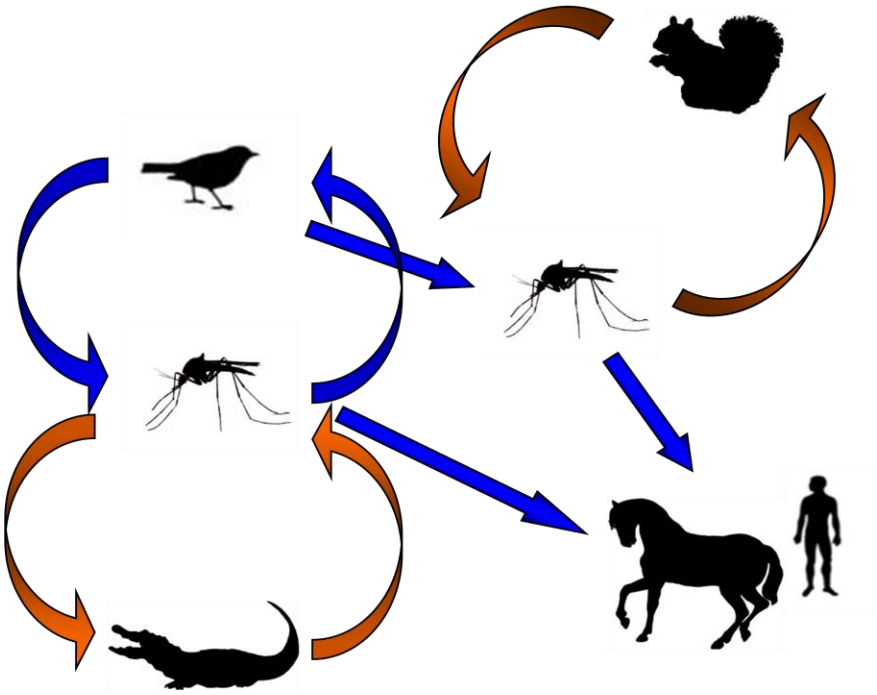

Figure 2-1. Life cycle of West Nile virus. Blue arrows represent how the virus is known to be maintained in nature, in a bird-mosquito-bird cycle, with periodic infections of dead-end hosts (horses and humans). Orange arrows represent other, recently discovered methods of transmission through which the virus may be maintained in nature.

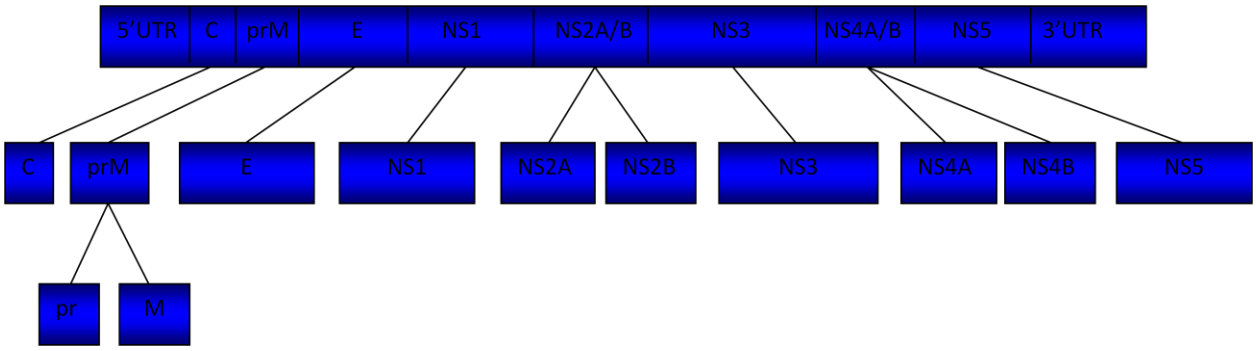

Figure 2-2. Structure of West Nile virus genome. The genome codes for 10 proteins. These include 3 structural proteins (capsid, premembrane, and envelope) and 7 non-structural proteins (NS1, NS2A/B, NS3, NS4A/B and NS5). The protein coding region is flanked by two untranslated regions- one on the 5' end and one on the 3' end.

CHAPTER 3
DEEP SEQUENCING, ANNOTATION, AND ANALYSIS OF THE EQUINE CENTRAL NERVOUS SYSTEM TRANSCRIPTOME

Methodology

Sample Collection

Tissues to create the cDNA library were obtained from the archived tissues samples of three groups of two horses each (total of 6 individuals) and consisted of 1) naïve horses infected intrathecally with 1 X 10^5 WNV, 2) non naïve horses vaccinated utilizing a modified live attenuated Yellow Fever (YF) chimera vaccine for protection against WNV (Prevenile, Intervet-Schering-Plough) and infected intrathecally with 1 X 10^5 WNV , and 3) horses that were not infected or vaccinated (see Table 3-1). Experimental infection and vaccination of horses occurred according to previously published data.[58] Horses from groups 1 and 2 were euthanized (University of Florida IACUC protocols #F077, #F093, #D163) if demonstrating clinical signs or at the end of the study (day 21) if not demonstrating clinical signs. Horses from group 3 were normal healthy horses, not infected with WNV and were euthanized due to other causes. All horses were necropsied immediately upon euthanasia. Tissues were snap frozen in dry ice and ethanol and stored at -80^{o}C until RNA extraction was performed. Eight tissues were collected from each horse and included cerebrum, cerebellum, thalamus, midbrain (rostral and caudal colliculus, tectum, and tegmentum), hindbrain (pons and medulla oblongata), cervical spinal cord, lumbar spinal cord, and spleen.

RNA Extraction and Quality Analysis

Total RNA was extracted from the tissues listed in Table 3-1 (48 total samples). A 30 mg piece of tissue was weighed out for each sample on dry ice. The tissues were homogenized using manual disruption and placed in 1 mL of guanidium thiocyanate

(Trizol ®, Invitrogen, Carlsbad, CA). The samples were vortexed and allowed to remain at room temperature for 5 minutes to allow complete dissociation of the nucleoprotein complexes. Two hundred μL of molecular grade chloroform (Fisher Scientific ®) was added to each sample. The samples were placed at room temperature for 2 minutes, then centrifuged at 12,000 x *g* at 4°C for 15 minutes. The chloroform and centrifugation step were repeated to ensure complete removal of the lipids. A 0.5 mL aliquot of isopropanol alcohol was added to each sample and incubated at room temperature for 5 minutes. The samples were centrifuged at 12,000 x *g* at 4°C for 10 minutes to precipitate the RNA. One mL of 75% ethanol was added to each pellet, mixed, and centrifuged at 7,500 x *g*, for 5 minutes at 4°C. The ethanol was poured off and the pellets air dried for 5 minutes. RNAsecure® (Ambion, Austin, TX), diluted to a 1X concentration, was heated on a heat block at 60°C for 5 minutes and 75 μL added to each pellet to inactivate any residual RNases. The pellets were incubated at 60°C for 10 minutes in RNAsecure and cooled to room temperature. For DNase treatment, 7.5 μL of 10X DNase buffer and 1 μL of rDNase (Ambion®, Austin, TX) was added to each sample. Samples were incubated at 37°C for 1 hour. After incubation, 7.5 μL of DNase inactivating reagent® (Ambion, Austin, TX) were added to each sample and the samples were incubated at room temperature for 2 minutes. The samples were centrifuged at 10,000 rpm for 2 minutes, removed from the inactivating reagent, and placed at -80°C until quality assessment.

RNA quality assessment was performed using a microfluidics platform. One μL of each RNA sample was placed on a nano-drop machine (ND-1000, Nanodrop Technologies, Wilmington, DE). The concentration and 260:280 ratio of each sample

was assessed. One μL of each RNA sample was then run on the Agilent 2100 Bio-analyzer (Santa Clara, CA) to assess the degree of RNA degradation. Briefly, the sample was incubated with fluorescent dyes, run on a gel, and excited with a laser to generate an electropherogram. From this electropherogram, the ratio of the 28S and 18S ribosomal peaks was obtained and software extraction performed. A RNA integrity number (RIN) was generated with high values (6-10) corresponding with tall 28S and 18S rRNA peaks and a low baseline, indicating minimal degradation of the RNA and a high quality sample. Low values (1-5) corresponding with a shift in the height of the 28S and 18S rRNA peaks and an increasing baseline, indicating a large amount of RNA degradation and low quality samples. Only samples with a RIN >6 were used for the study. An analysis of all techniques to determine the best technique for the isolation of high quality RNA can be seen in Appendix A.

First Strand cDNA Synthesis and Amplification- cDNA Library Construction

The RNA isolated from the tissue samples from each horse were pooled to create 5 samples total. The RNA was converted to full-length, double-stranded cDNA using the SMART PCR cDNA synthesis kit, the Advantage® 2 PCR kit, and the PowerScript Reverse Transcriptase (Clontech, Mountainview, CA). To create the first strand of cDNA, 1 μg of RNA sample was mixed with 1μL 3'SMART CDS Primer II A, 1μL SMART II A Oligonucleotide mix and DI Water for a total volume of 5 μL. The contents of the tube were mixed, centrifuged briefly, and incubated in a thermocycler at 70^{o}C for 2 minutes. Two μLs 5X first-strand buffer, 1μL DTT, 1μL dNTP mix, and 1μL MMLV Reverse Transcriptase were added to each tube. The tubes were mixed, centrifuged briefly, and incubated at 42^{o}C for 1 hr in an air incubator. Tris EDTA buffer

(10mM Tris, 1mM EDTA) at a volume of 40μL was added to each tube and the tubes were heated at 72^{o}C for 7 minutes. One μL of cDNA was added to 9 μL of deionized water to amplify the cDNA. Seventy four μL DI water, 10μL 10X Advantage 2 PCR Buffer, 2μL 50X dNTP, 2μL 5'PCR Primer II A, and 2μL 50X Advantage 2 Polymerase Mix was added for a total volume of 90μL. The tubes were vortexed and centrifuged. The tubes were held at 95°C for 1 minute, then cycled 17 times with the following parameters: 95°C for 15 seconds, 65°C for 30 seconds, and 68°C for 6 minutes. The amplified cDNA was then analyzed using a micro-fluidics platform to determine concentration and purity.

The cDNA was purified using a proprietary PCR purification kit (QIAquick PCR Purification Kit®, Qiagen, Valencia, CA). Proprietary binding buffer (PB1) at a volume of 450 μL was added to the 90 μL cDNA sample from SMART PCR cDNA Synthesis kit and placed in a QIAquick spin column. The samples were centrifuged at 13,000 rpm for 30–60 s. The flow-through was discarded, and 0.75 mL of proprietary cleansing buffer (PE) was added to the columns and centrifuged at 13,000 rpm for 60 s. The flow-through was discarded and the column centrifuged 13,000 rpm for an additional 1 minute. The DNA was then eluted by adding 50 μL water (pH 7.0–8.5) to the center of the membrane and centrifuging the column at 13,000 rpm for 1 min. A micro-fluidics platform was used to check the concentration and purity of the sample.

Normalization of the cDNA Library

The purified cDNA sample was normalized to ensure equal expression of all transcripts (cDNA Normalization Trimmer Kit®, Evrogen, Moscow, Russia). All tubes containing the cDNA samples (5 total) were combined and 1000 ng of purified cDNA

was placed into a 2 mL Sarstedt tube. Three Molar sodium acetate (0.1 volumes), pH 4.8 was added, then 2.5 volumes of 98% ethanol was added and the tube vortexed. The sample was centrifuged for 15 min at 13,000 rpm and the supernatant removed. One hundred μL of 80% ethanol was laid over the pellet. The tubes were centrifuged at 13,000 rpm for 5 minutes. The supernatant was removed and the ethanol wash repeated. The pellet was air dried for 15 min at room temperature, then dissolved in sterile water to the final cDNA concentration of 100-150 ng/μL.

Eight μLs of ds cDNA were combined with 4 μL 4X hybridization buffer and 4 μL sterile water to begin hybridization. The contents were mixed and 4 μL aliquoted into each of four tubes. The tubes were centrifuged at 14,000 rpm for 2 min, incubated in a thermal cycler at 98^{o}C for 2 min, and incubated at 68^{o}C for 5 hours. Proprietary duplex specific endonuclease (DSN) treatment was performed. Two tubes were created- one with a 1:1 ratio of DSN storage buffer to 1 μL of DSN solution, the other with a 3:1 ratio of 3 μL of DSN storage buffer to 1 μL of DSN solution. The DSN master buffer was preheated at 68^{o}C and 5 μL was added to each tube containing hybridized cDNA. The tubes were centrifuged and incubated at 68^{o}C for 10 min. The DSN enzyme was added to each tube as specified in Table 3-2. DSN functions to degrade double-stranded cDNA which should only be present after denaturing and reannealing with the abundant transcripts. The tubes were incubated in the thermal cycler at 68^{o}C for 25 min. Ten μLs of DSN stop solution was added to each tube, and the tubes were mixed and centrifuged. The tubes were incubated in the thermal cycler at 68^{o}C for 5 min, then placed on ice. Twenty μLs of sterile water was added to each tube.

The amplification steps of the normalized cDNA were performed. A master mix was prepared (40.5 μL Sterile water, 5 μL 10X PCR Buffer, 1 μL 50X dNTP mix, 1.5 μL Evrogen PCR primer M1, and 1 μL 50X Polymerase Mix) and 49 μL added to 1 μL of each diluted cDNA sample (from DSN treatment, see above). The tubes were mixed and centrifuged briefly. Amplification was performed by cycling 18 times at 95^{o}C for 7s, 66^{o}C for 30 s, and 72^{o}C for 6 min. The samples were run on a gel and the wells containing normalized samples were combined. A second amplification step was then performed. Two μLs of normalized cDNA was combined with 20 μL of sterile water. The tube was mixed and centrifuged briefly. For a control, 2 μL of control cDNA was aliquoted into another tube and combined with 20 μL of sterile water. The tube was mixed and centrifuged briefly. Two μL of each of these diluted samples (control and normalized) were then mixed with a master mix consisting of 80 μL Sterile water, 10μL 10X PCR Buffer, 2 μL 50X dNTP mix, 4 μL Evrogen PCR primer M2, and 2 μL 50X Polymerase Mix. PCR was performed on both tubes cycling 12 times at 95^{o}C for 7s, 64^{o}C for 10s, and 72^{o}C for 6 min. The concentration and purity of the normalized equine WNV library was determined using a micro-fluidics platform and run on a gel to assess concentration and purity.

High-throughput Pyrosequencing of the Normalized cDNA Library

The library was sequenced using the high-throughput sequencing system, Gene Sequence 20 (454 Life Sciences, Branford, CT), located in the UF Interdisciplinary Centers for Biotechnology Research High-Throughput DNA sequencing core lab. An initial titration run was performed to ensure transcript normalization followed by two full sequencing runs. Briefly, the cDNA library was randomly enzymatically digested,

adaptors added, and the pieces immobilized on streptavidin-coated Sepharose beads. The beads were immersed in water-in-oil microreactors and subjected to theromocycling parameters for clonal amplification. The beads were added to microwells. Reaction beads containing sulfurylase and luciferase and primers corresponding to the adaptor sequences were added to each microwell. The primer sequences used for the sequencing runs were as follows:

A- 5'-CCA TCT CAT CCC TGC GTG TCC CAT CTG TTC CCT CCC TGT CTC AG-3'

B- 5'-CCT ATC CCC TGT GTG CCT TGC CTA TCC CCT GTT GCG TGT CTC AG-3'

Each dNTP was added in a flow through sequence to the microwells, and luminescence reactions captured by camera and the Peak Height Determination Software (Pyrosequencing AB).

Library Annotation and Analysis

The sequence data was initially assembled using sequence assembly software (Newbler 454 Life Sciences, Roche Applied Science, Indianapolis, IN) and the EqCab2 and Ensembl databases. Singlets and contiguous, non-redundant sequences (contigs) were identified. A second sequence assembly software program was used for final assembly of data (Paracel Transcript Assembler, Paracell Inc, Pasadena, CA). PTA was used to perform additional sequence cleaning, sequence clustering (including seed clustering –matching to known mRNA sequences-, clustering –matching to similar sequences-, and pairwise comparisons –evaluation based on both polarities of 5’ to 3’ and 3’ to 5’-), and assembly for the final development of a set of nonredundant sequences (contigs) and the identification of genes. Annotation of these sequences was performed with the Basic Local Alignment Search Tool (BLAST) quest algorithm for storage, management, and analysis of expressed sequence tag (EST) sequences. This

consisted of a homology search using BLASTX (protein) and BLASTN (nucleotide) against the NCBI databases (NT Nucleotide Database, NR Protein Database), and equine databases (Horse draft genome database, predicted proteins in the horse genomes, and EST collection for the horse). Only genes that were positively identified by BLAST with Expect Values (E-value) below 10^{-4} were used to compile the results.

BLAST results were further cleaned and stored in BlastQuest, a database developed by the ICBR (UF, Gainesville, FL) that facilitates management of BLAST results and the Rare Ontology Consortium (GO) term browsing. A query for the top 100 BLAST hits for each contig against the NCBI Gene database was performed (Assembly Filter, UF ICBR, Gainesville, FL). This provided annotation information, gene function, and metabolic pathway associations based on GenMAPP and KEGG pathway database maps. The GO terms and pathway information associated with the lowest e-value and consistent with the NCBI databases were assigned to the query assembly process. Contigs with the highest agreement were maintained and the least similar sequences were eliminated. Sequence orientations were determined by software instruments, AssemblyFilter and ESTscan (EMBnet, Switzerland). Sequences were analyzed and grouped according to GO function. Sequences were further analyzed for species composition. The complete sequenced transcriptome was run against the human expressed sequence tag database (Fisher cluster, UF, Gainesville, FL) to determine sequence homology between the human and horse. An E-value of $< 10^{-4}$ was set and only one match per sequence generated.

Results

Nucleic Acid Quality Assessment and Normalized cDNA Library Titration

The tissues from which RNA was isolated to create the cDNA library were obtained from three groups of two horses each (total of 6 individuals) (Table 3-1). The quality and purity of the RNA sample was determined using the RNA Integrity Number and 260:280 ratio, respectively. Only samples with a RIN > 6 and 260:280 ratio > 1.75 were used to create the cDNA library. The average RIN for all RNA samples was 7.37, and the average 260:280 ratio was 1.97 (Table 3-3, Figure 3-1).

cDNA Library Quality Assessment

The concentrations and the purities of the individual cDNA libraries were also measured. For the naïve/non-exposed cDNA sample, the concentration was measured at 512.24 ng/uL with a 260:280 ratio of 1.82. The non-naïve/exposed cDNA samples had concentrations of 474.31 ng/uL and 644.69 ng/uL with 260:280 ratios of 1.84. The naïve/exposed sample had concentrations of 452.86 ng/uL and 640.41 ng/uL with 260:280 ratios of 1.85 and 1.83, respectively.

Successful normalization was confirmed via a titration sequencing run in which five to ten percent of the library was sequenced and 6,197 reads were assembled from 226,271 total bases analyzed. Vector filtration resulted in a total of 1,474 reads (23.8% contamination) for a total of 386,740 (31.5%) bases. From this clean-up, 4,723 reads were assembled, comprised of 839,531 bases. After grouping according to occurrence, there were 273 completely assembled reads, 678 partially assembled reads, 3,113 singletons, 460 repeats, and 199 outliers. All of the sequences were then analyzed for overlap to establish the presence of contigs. 308 contigs were identified with an

average length of 208.1 base pairs. Only 4 large contigs were identified (average length 634.8 base pairs), confirming that normalization was effective (Table 3-4).

Normalized cDNA Library Sequencing Results

Newbler assembly software analysis resulted in the assembly of 514,462 sequences from a total of 49,857,586 bases after linker contamination was removed. In total, 70,828 sequences were classified as fully assembled reads, while 64,823 sequences were classified as partially assembled reads. There were 276,760 sequences defined as singletons with 93,504 sequences defined as repeats and 8,497 sequences classified as 'outliers'. From these data, 16,895 contigs (sets of overlapping DNA sequences) comprised of 4,720,747 bases were assembled. These contigs ranged in size from 93 to 2,827 base pairs with an average length of 279.4 base pairs. Large contigs (1,902) were also assembled with an average length of 818 base pairs (Table 3-5).

Sequences from three input sequence sets (16,895 contigs obtained from the Newbler assembly, 443,584 sequence sets left from the 454 sequencing run – partially assembled reads, singletons, outliers, and repeats-, and 22,748 sequences from the Equus Caballus 2 genome database) were fed into the Paracel Transcript Assembler (PTA) for a total of 483,227 sequences (Table 3-6). A total of 188,885 final sequences were clustered after cleaning. Clusters were determined by the amount of overlap between similar sequences (100 bp minimum) and 61,499 sequences matching with 'seed' sequences (i.e. well known/studied mRNA sequences) were placed in seed clusters. Sequences that were not identified as 'seed' sequences (127,386) were clustered in three steps via partitioning (arranging the sequences in a 3'-5' direction based on annotation), pairwise comparison (comparing every sequence with every

other sequence in both orientations (i.e. 3' and 5'), and clustering (determining similarity based on sequence overlap). Pairwise comparisons resulted in 75,413 of these being classified as 'singlets', while 51,919 were identified as 'sequences'. A total of 21,421 seed clusters and 11,634 clusters were formed. From these clusters, 11,621 cluster contigs and 8,058 seed cluster contigs were identified. In addition, 2,098 cluster singlets and 37,654 seed cluster singlets were identified. Using PTA, 19,670 contigs and 75,413 singlets were identified.

Combining the results from Newbler and PTA analyses and utilizing known sequences from the equine genome databases, 19,987 contigs and 21,053 genes were assembled. Unassembled sequences were not considered for further analysis. Thus in total, 41,040 sequences were used in the BLAST analysis [19,679 PTA contigs (=11,621 non-seeded contigs + 8,058 seeded contigs), 308 newbler contigs and 21,053 unassembled EquCabv2 genes]. These sequences have been submitted to GenBank[157] for public access (study # SRP000619).

BLAST and GO Analysis

A BLAST search was run against five separate databases including the NR database, NT database, EquCab2 chromosomes database, EquCab2 predicted genes database, and EquCab2 ab initio predicted genes by GenScan. The e-value was set at 10^{-4} for the 41,040 sequences searched and 31,357 good sequence hits were obtained with this criterion (Table 3-7). Approximately 73.7% of the sequences identified in this project were matched in the equine chromosome database and at least one of the equine predicted genes databases, while 23.1% of the sequences recognized in this project were only identified in the equine chromosome database. Completely novel

genes that have as yet to be identified by the equine genome project were represented by 3.1% (1,278) of the sequences identified.

The average HspScores indicated a high degree of alignment of the sequences with those in the equine databases, at 492.3956, 1326.042, and 643.1346 (Table 3-8). The average hit length for the databases was 501.524, 1,328.69, and 647.97 base pairs respectively, indicating that the sequences identified were of a significant length. The majority of sequences for all databases demonstrated positive identity greater than 95%. For the EqCab2 Chromosomes database, 40,145 of the 40,973 sequences had a positive identity of >95% (Figure 3-2a,b). In the EqCab2 Predicted Genes database, 40,264 of the 40,999 sequences had a >95% identity. And finally, for the EqCab2 ab initio Predicted Genes database, 39,650 of the 40,977 sequences had a percent positive identity >95%.

The genes were then grouped into Gene Ontology categories with particular interest in the genes involved in the immune system, the CNS, and programmed cell death (apoptosis). For the three major GO categories, 27,355 genes grouped in molecular function, 25,582 genes grouped in cellular component, and 24,351 genes grouped in biological process. In the GO category of cell death under biological process, 1,119 genes were identified, with 1,046 (93.5%) of these involved in apoptosis (Figure 3-3). In the GO category of organismal physiological processes, 5,278 genes were classified, including 1,920 (36.4%) in neurophysiological processes and 1,272 (24.1%) in the immune response (Figure 3-4). In addition, 569 sequences were classified as having neurotransmitter receptor activity (including dopamine, neuropeptides, benzodiazepines, and acetylcholine) while 571 sequences were

classified as having neurotransmitter binding activity. These results demonstrate that this library successfully identified genes in the horse that are involved in the immune response and genes that are neurologically specific.

Comparison of Species- NR/NT NCBI Database

Top species counts for the NCBI databases were compared against all sequence hits. With an e-value $\leq 10^{-4}$ for all databases, there were 39,257/41,040 accurate hits for both the NR and NT NCBI databases. For the NR database alone, there were 30,011 accurate hits with 26,955 'perfect' (e-value= 0) hits, while for the NT database, there were 39,217 accurate hits with 32,825 'perfect' hits. For both databases, matches to horses comprised the greatest number of hits (18,927 NR and 25,887 NT) with the species groups humans, primates, canines, and bovines containing the next greatest number of hits (see Figures 3-5a,b). Some discrepancy was noted between the different databases, and is likely explained by the database program which selects only the top hits in the results list.

Novel Genes Analysis

Further analysis was performed on the 1,280 (3.1%) sequences not recognized by any of the equine databases. Of these novel sequences, 709 (55.4%) were classified into gene ontology databases. With overlap, 579 could be classified into biological processes, 592 into cellular component, and 619 into molecular function. The average length of all these sequences was 595 base pairs with a range of 50-8,802 base pairs (Figure 3-6).

In order to eliminate redundancy of genes, the genes were grouped into 16 categories based on their GO function wherein multiple overlapping GO functions were grouped within each category (Figure 3-7). Many of the novel genes were associated

with the CNS and included transport (97), signal transduction (91), neurological genes with structural and physiological functions (86), protein modification (82), and transcription (77).

Biomarker Discovery

Using Ingenuity Pathways Analysis software, biomarker discovery analysis was performed on the 41,040 sequences. This analysis searches for transcripts that may correlate with molecules present in clinical samples that can be used to detect certain diseased or physiological states. For all biomarker categories, 3,227 potential biomarkers were discovered (Table 3-9). For specific disease processes, most biomarkers were in the categories of neurological disease (496), although categories such as inflammatory disease, organismal injury and abnormalities, hematological disease, immunological disease, and inflammatory disease also had large numbers of possible biomarkers. This analysis provided a prediction of clinical samples which would likely contain biomarkers with 1,319 detectable in blood or serum samples.

Of the 1,280 novel genes, 11 (0.94%) were found to be potentially useful biomarkers (Table 3-10). The majority of these biomarkers are found in nervous tissue (9/11) with 4, Tet oncogene 1 (TET1), structural maintenance of chromosomes 1A (SMCA1), embryonic ectoderm development (EED), and adenine phosphoribosyltransferase (APRT), predicted in blood and urine. Two of the genes are known to be associated with neurological disease (glutamate receptor, ionotrophic, AMPA 4- GRIA4 and neurofilament, medium polypeptide- NEFM) and one of the genes with inflammatory disease/organismal damage (adenine phosphoribosyltransferase-APRT).

Analysis Against the Human EST Database

Sequences were run against the human expressed sequence tag database. With an E-value cut-off $\leq 10^{-4}$, 31,473 equine transcriptomic sequences matched against the human EST sequence database (8,050 contigs, 6,296 seed contigs, and 17,127 singlets). This represented a percentage match of the equine transcriptome to the human transcriptome at 69.27% (contigs), 78.13% (seed contigs), and 80.17% (singlets), indicating a high degree of sequence homology between the human and equine transcriptome. Equine sequences demonstrated good match to the human EST database with an average percent identity of 90.17%, an average bit score of 512.91, and an average alignment length of 424.85 (see Table 3-11).

Discussion

This is the first project to sequence the neurological transcriptome of the equine. These data will be invaluable for future studies involving a variety of applications for both pathological and nonpathological studies in the equine and other hosts. For this project, 41,040 sequences were identified by BLAST analysis in 5 sequence databases. There was overall consensus amongst the NCBI databases as to the hits on species, with the vast majority of sequences matching to the horse. Dogs, primates, humans, and cattle also had a large number of hits. Further analysis of the sequenced transcriptome revealed that 9,504 of the identified sequences were missed by equine predicted databases, and 1,280 of the identified sequences have yet to be discovered in the equine genome project. This is most likely due to the incomplete annotation of the equine genome. Since other species' genomes have undergone more comprehensive annotation and analysis, transcriptomic sequences that should be recognized by the equine databases may be recognized in other organisms. Another possibility for the

discrepancy could be differences between the equine genome and transcriptome (i.e. splice variants). These issues are likely to improve with time and increasing annotation of the equine genome project.

Over 27,000 of the identified sequences grouped under Gene Ontology classifications. Identification is dependent upon the GO database classifications, which at this point are incomplete. Continued study of genes will lead to improvements within the GO database and more comprehensive identifications. Not surprisingly, for this project, GO classifications were enriched for neurological sequences. Biomarker analysis performance will be important in the future to target comprehensive systems biology approaches. For this project, 3,227 potential biomarkers were identified with 496 of these involved in neurological disease. These biomarkers will be useful in the future once confirmed, as many of the biomarkers for the genes that were identified are accessible in submitted clinical samples (urine, blood, plasma, CSF). Future work will need to be conducted to ensure the presence of these biomarkers. This portion of the project also demonstrated high sequence homology between the equine and human EST database, showing that the horse may be useful in the study of the human organism.

Future Work and Issues to be Addressed

Some of the major limitations of this portion of the project involved the process of annotation. Because the horse genome sequencing project is relatively new, correctly identifying transcripts can be a challenge. This project highlighted this complication, as novel sequences were identified in the transcripts sequenced that should have been present in the equine genome project. Another major issue is the identification of transcript variants. Because of the software programs used to annotate the data, and

because the databases containing the reference sequences are limited in their scope, it is not possible to identify every possible SNP or alternatively spliced transcript. In addition, it is difficult to map transcripts that originate in repetitive regions due to the short read length of the sequences and the non-unique regions of DNA to which they are being mapped. Finally, because of the short reads generated by pyrosequencing (250 base pairs or less), aligning the sequences correctly and not discarding transcripts with similar sequences can be an issue. These problems demonstrate that pyrosequencing is a powerful tool for transcriptomic analysis, but it is only as good as the databases against which it can be referenced.

The major problems that were encountered during this project were in preserving the RNA and cDNA library quality. RNA quality was preserved by immediately freezing the tissues at -80^{o}C upon harvesting, storing the samples at -80^{o}C until use, working quickly with the samples in an RNase free environment, storing the samples in RNAsecure, and analyzing the quality of the samples with the Agilent 2100 bioanalyzer. For the cDNA library quality, there was a problem with linker contamination. This appears to be a problem with the kits used to create the library, and was solved with software removal of the linker sequences.

Future work for this portion of the project will involve continued analysis of the annotated library. This will include data mining on the sequences to identify transcripts of interest. Of particular interest are microRNA sequences and transcript variants. PCR and Sanger sequencing will also be performed on the identified biomarkers to validate the results. It would also be of interest to attempt to identify the biomarkers in stored

serum samples. The annotation and analysis of the equine brain transcriptome provided a wealth of data that will continue to provide valuable data.

Conclusions

This portion of the project used pyrosequencing technology to sequence the transcriptome of the central nervous system of horses (naïve and non-naïve) challenged with West Nile virus and untreated, normal controls. In total, 41,040 sequences were identified by BLAST analysis in 5 sequence databases (NR database, NT database, EquCab2 chromosomes database, EquCab2 predicted genes database, and EquCab2 ab initio predicted genes by GenScan). There was overall consensus amongst the NCBI databases as to the hits on species, with the vast majority of sequences matching to the horse. Dogs, primates, humans, and cattle also had a large number of hits. Over 27,000 of these sequences grouped under Gene Ontology classifications. These sequences were enriched for those genes involved with the nervous system. Of these sequences, 9,504 sequences were identified that were missed by equine predicted databases, and 1,280 genes were identified that have yet to be discovered in the equine genome project. Biomarker analysis was performed on all of the sequences and 3,227 recognized potential biomarkers were identified with 496 of these involved in neurological disease. These will be important targets for system biology strategies utilizing genomic and proteomic techniques. Biomarker analysis performed on the novel sequences identified 11 potential biomarkers. Many of the biomarkers for all genes and novel genes that were identified are accessible in submitted clinical samples (urine, blood, plasma, CSF). Thus this project identified many genes that are specific to the neurological system, are completely novel to the horse, and have potential applications as biomarkers. Finally, the comparison of the equine transcriptome sequenced in this

project to the human EST project demonstrates high sequence homology between the ESTs of the two species, and provides evidence that data generated from equine studies can be directly applicable to human studies. This project demonstrates the importance of gene expression studies to supplement the limitations of current sequence databases. This is the first report of the use of pyrosequencing to analyze the transcriptome of the equine with contribution of genes novel to the equine genome project. Thus it appears that next generation sequencing, including pyrosequencing, is an effective tool to annotate the transcriptome of organisms. In addition, pyrosequencing is a useful tool to identify novel sequences and possible biomarkers for disease in the analysis of the transcriptome of organisms, even those with annotated genomes.

Table 3-1. Experimental tissues used to create the normalized cDNA library

Sample category (n)	Sample type (#)	Experiment specifics
Vaccinates/Immune + exposed (n = 2)	Cerebrum (2), cerebellum (2), thalamus (2), midbrain (1), hindbrain (2), cervical spinal cord (2), lumbar spinal cord (2)	Day 0- non control horses vaccinated[A] Day 365- challenged with WNV[B] intrathecally Day 365-386- monitored for clinical signs Day 386 (21 days PI)- euthanasia, necropsy, tissue collection
Unvaccinated/Non-immune + exposed (n = 2)	Cerebrum (2), cerebellum (2), thalamus (2), midbrain (2), hindbrain (2), cervical spinal cord (2), lumbar spinal cord (2)	Day 0- mock vaccination Day 365- challenged with WNV[B] intrathecally Day 365-374- monitored for clinical signs Day 372-374 (7-9 days PI)- euthanasia, necropsy, tissue collection
Unvaccinated + non-exposed (n = 2)	Cerebrum (1), cerebellum (1), midbrain (1), hindbrain (1), cervical spinal cord (2), lumbar spinal cord (1)	Normal horse

[A]Live-chimera WNV vaccine containing the prM and E proteins of WNV expressed in a YF17D vector

[B]WNV NY99 strain 10^5 pfu/mL

Note: This table describes the experiments conducted on the horses whose tissues were used to create the normalized cDNA library. There were three groups of two horses each (column 1). Neurological tissue and spleen were collected from each horse and used for RNA isolation (column 2). Column 3 describes the experiment details, including dates of vaccination, infection, and euthanasia/necropsy where applicable.

Table 3-2. Dilutions of duplex specific endonuclease used to normalize the cDNA library

Component	Tube 1 S1 DSN1	Tube 2 S1 DSN1/2	Tube 3 S1 DSN1/4	Tube 4 S1 Control
DSN Enzyme in Storage Buffer	1 uL	-	-	-
½ DSN Dilution	-	1 uL	-	-
¼ DSN Dilution	-	-	1 uL	-
DSN Storage Buffer	-	-	-	1 uL

Table 3-3. Average RNA quality data for samples

Sample	Number of Tissues	Concentration (ng/uL)	RIN	260:280 Ratio
Naïve + Non-exposed	8	411.63 (152-652.53)	7.1 (6-7.8)	1.96 (1.8-2.08)
Non-naïve + Exposed	16	829.55 (122-1551)	7.4 (6.7-8.4)	1.99 (1.87-2.06)
Naïve + Exposed	16	439.02 (182-968)	7.6 (6.7-8.4)	1.95 (1.75-2.04)
Total Average			7.37	1.97

Note: The average RNA quality data for the sample groups is illustrated. The RNA Integrity Number (RIN) was used to assess the degree of RNA degradation. The average 260:280 ratio was used to determine the purity of the sample.

Table 3-4. Data from 454 sequencing titration run

Reads	Number
Total reads	6,197
Total bases	1,226,271
Average length	197.8
Min. length	45
Max. length	379
Vector filtered reads	1,474 (23.8%)
Vector filtered bases	386,740 (31.5%)
Reads to be assembled	4,723
Bases to be assembled	839,531
Completely assembled reads	273
Partial assembled reads	678
Singletons	3,113
Repeats	460
Outliers	199
Total contigs	308
Total bases	67,174
Average length	218.1
Min. length	101
Max. length	901
Total large contigs	4
Total bases	2,539
Average length	634.8
Min. length	529
Max. length	901

Note: Successful normalization of the cDNA library was confirmed with a titration run in which five to ten percent of the library was sequenced. Software was used to filter the vectors (linkers added by the cDNA library construction kits) to clean up the sequences for BLAST analysis. From this clean-up, 4,723 reads were assembled comprised of 839,531 bases. The 4,723 reads were grouped according to occurrence as completely assembled reads, partially assembled reads, singletons, repeats, and outliers. All of the sequences were analyzed for overlap to establish the presence of contigs. 308 contigs were identified with only 4 large contigs identified, confirming that normalization was effective.

Table 3-5. Data from 454 sequencing runs Newbler Assembler

Reads	Number
Total # of reads	826,176
Total # of clean reads	514,412 (62.3%)
Total # of bases	95,486,897
Total # of clean bases	49,857,586 (52.2%)
# of fully assembled reads	70,828
# of partially assembled reads	64,823
# of singletons	276,760
# of repeat reads	93,504
# of outlier reads	8,497
# of all contigs	16,895
# of bases covered	4,720,747
Avg. contig size	279.4
Min. contig size	93
Max contig size	2,827
# of large contigs	1,902
# of bases covered	1,557,286
Avg. large contig size	818
Min. large contig size	500
Max. large contig size	2,827

Note: Newbler assembly software was first used to assemble the sequences. 514,462 sequences were assembled from a total of 49,857,586 bases after linker contamination was removed. Sequences that could be linked from beginning to end were classified as ‘fully assembled reads’, sequences that were shown to have some association were classified as ‘partially assembled reads’, standalone sequences coding once for areas of individual genes were classified as ‘singletons’, standalone sequences coding for areas of individual genes at a frequency of greater than 5% were classified as ‘repeats’, and standalone sequences coding for areas of individual genes at a frequency of less than 5% were classified as ‘outliers’. From this data, 16,895 contigs (sets of overlapping DNA sequences) composed of 4,720,747 bases were assembled.

Table 3-6. Data from 454 sequencing runs Paracel Transcript Assembler

Reads	Number
No. of current input sequences	483,227
No. of sequences removed during cleanup	294,342 (609 were EquCabv2 genes)
No. of sequences kept after cleanup	188,885 (22,139 were EquCabv2 genes)
No. of sequences in seed clusters	61,499
No. of sequences pairwise compared	127,386
No. of singlets after pairwise compared	75,413
No. of problem sequences	54
No. sequences in clusters	51,919
No. of seed clusters	21,421
No. of clusters	11,634
Largest cluster	cl.007 (2,998)
2nd largest cluster	cl.015 (2,721)
Largest seed cluster	sd.17584 (112)
2nd largest seed cluster	sd.3613 (105)
No. final assemblies	134,844
No. of cluster.contigs	11,621
No. of cluster singlets	2,098 (4 genes + 19 newbler contig + 2,075 reads)
No. of seed cluster.contigs	8,058
No. of seed cluster singlets	37,654 (*21,021 genes + 29 newbler contig + 2,498 reads)
No. of PTA contigs	19,679 (11,621 + 8,058)
No. of singlet	75,413 (28 genes + 260 newbler contig + 75,125 reads)
No. of contigs	19,987 (=11,621 + 8,058 + 19 + 29 + 260)
No. of genes	21,053 (=4 + 21,021 + 28)

Note: Data from the sequencing runs using Paracel Transcript Assembly software. After clean-up, 188,885 sequences were used for assembly. Sequences were placed into seed clusters where applicable (61,499). Sequences that were not identified as 'seed' sequences (127,386) underwent clustering including partitioning, pairwise comparison, and clustering. In total, there were 134,844 final assemblies. These were identified as 19,987 contigs and 21,053 genes for a total of 41,040 sequences submitted for BLAST analysis.

Table 3-7. Summary of BLAST results for five separate databases

Count	%	NR/NT	EquCab 2 Chr.	EquCab2 Predicted Genes	EquCab2 GeneScan	Newbler contigs	Cluster contigs	Seeded cluster contigs	EquCab2 genes
28,789	70.1%		√	√	√	58	412	7,760	20,559
817	2.0%		√	√	×	37	360	219	201
652	1.6%		√	×	√	11	641	0	0
5,391	13.1%	e-value*	√	×	×	65	5,326	0	0
2,462	6.0%	e-value**	√	×	×	61	2,401	0	0
1,651	4.0%		√	×	×	50	1,601	0	0
677	1.6%	e-value*	×	×	×	13	299	79	286
287	0.7%	e-value**	×	×	×	9	273	0	5
314	0.8%		×	×	×	4	308	0	2
41,040						308	11621	8058	21053

* = e-value < $1e^{-20}$

** = e-value < $1e^{-4}$

Note: The BLAST search was run against five separate databases. The e-value (likelihood that the hit would happen due to chance) was set at 10^{-4} for the 41,040 sequences searched. 73.7% (30,258) of the sequences identified in this project had been previously identified by the equine chromosome database and one or both of the equine predicted genes databases; 23.1% (9,504) of the sequences recognized in this project were missed by both of the EqCab2 predicted genes databases but were identified in the equine chromosome database; and 3.1% (1,278) of the sequences identified in this project were missed by all equine databases. Therefore, 26.2% of the sequences annotated in this project are novel to at least one equine database, while 3.1% of the sequences identified in this project are completely novel to the horse.

Table 3-8. Average scores for equine databases

	EqCab2 Chromosomes	EqCab2 Predicted Genes	EqCab2 ab initio Predicted Genes by GeneScan
Average HspScore	492.3956 (17-11,585)	1326.042 (14-23,780)	643.1346 (15-11,553)
Average BitScore	976.5968 (34.193-22,966.1)	2629.181 (508-47,141)	1275.415 (30.2282-22,902.7)
Average Hit Length	501.524	1328.69	647.97

Note: The average scores for the equine databases indicate a high degree of sequence alignment with the sequences that matched. [HspScore (high-scoring segment pair)- measures degree of local alignments with no gaps. Higher scores indicate better alignment. BitScore- statistical accounting of the raw alignment score which is the sum of the substitution and gap scores. Higher scores indicate better alignment. Average hit length- the length of the sequences that align.]

Table 3-9. Recognized biomarkers for disease

Biomarker Category	Number of Biomarkers	Percent of Genes
All biomarkers	3,227	7.9%
Neurological disease	496	1.2%
Infectious disease	71	0.17%
Inflammatory disease	159	0.39%
Organismal injury and abnormalities	155	0.38%
Metabolic disease	87	0.21%
Infection mechanism	70	0.17%
Immunological disease	163	0.40%
Antimicrobial response	17	0.04%
Antigen presentation	133	0.32%
Inflammatory response	151	0.37%
Hematological disease	216	0.53%
Uncategorized disease	1817	4.43%

Note: Using Ingenuity Pathways Analysis software, biomarker discovery analysis was performed on the 41,040 sequences. For all biomarker categories, 3,227 (7.9%) potential biomarkers were discovered. This table demonstrates the disease categories or biological responses that the biomarkers are associated with.

Table 3-10. Biomarkers identified from novel genes

ID	Symbol	Entrez Gene Name	Location	Type	Sample	Disease
EDL92759	APRT	Adenine phosphoribosyltransferase	Cytoplasm	Enzyme	Nervous tissue, urine	Inflammatory response, organismal injury and abnormality
NP_062542	C21ORF62	Chromosome 21 open reading frame 62	Unknown	Other	Nervous tissue	
BAF84809	EED	Embryonic ectoderm development	Nucleus	Transcription regulator	Nervous tissue, blood	
NP_001099300	EME1	Essential meiotic endonuclease 1 homolog 1 (S. pombe)	Nucleus	Other	Nervous tissue	
EDL85231	GRIA4	Glutamate receptor, ionotrophic, AMPA 4	Plasma Membrane	Ion channel	Nervous tissue	Neurological disease, organismal injury and abnormality
XP_001077729	LOC687257	Hypothetical protein LOC687257	Unknown	Other		
EDL00021	MOBKL3	MOB1, Mps One Binder kinase activator-like 3 (yeast)	Cytoplasm	Other	Nervous tissue	
NP_005373	NEFM	Neurofilament, medium polypeptide	Cytoplasm	Other	Nervous tissue	Neurological disease
BAF84610	SMC1A	Structural maintenance of chromosomes 1A	Nucleus	Transporter	Nervous tissue, blood, plasma/serum	
EAW54299	TET1	Tet oncogene 1	Nucleus	Other	Blood, plasma/serum	
XP_001472818	ZFP422-RS1	Zinc finger protein 422, related sequence 1	Unknown	Other	Nervous tissue	

Note: Genes novel to the equine genome were also submitted to IPA for biomarker discovery analysis. Of the 1,280 genes, 11 (0.94%) were found to be potentially useful biomarkers. The majority of the biomarkers are found in neurological tissue (9/11) but 4 can be found in blood and urine samples. In addition, 2 of the genes are known to be associated with neurological disease and 1 of the genes with inflammatory disease/organismal damage.

Table 3-11. Summary of BLAST analysis of sequenced equine transcriptome to the human expressed sequence tag database

	Contigs	Seed Contigs	Singlets
Number of Matches $E \leq 10^{-4}$	8050/11621	6296/8058	17127/21361
Percent Homology Match	69.27%	78.13%	80.17%
Average E value	1.44636E-05	2.38671E-06	8.09623E-06
Average Bit Score	189.0196894	907.9956004	519.9152099
% Identity	89%	91%	90%
Alignment Length	187.9218634	698.33831	435.6858761

Note: Contigs, seed contigs, and singlets from this project were BLASTed against the human EST database. In total, 31,473 sequences matched to the human EST database (row 1) with an e-value $\leq 10^{-4}$.

Electropherogram Summary Continued ...

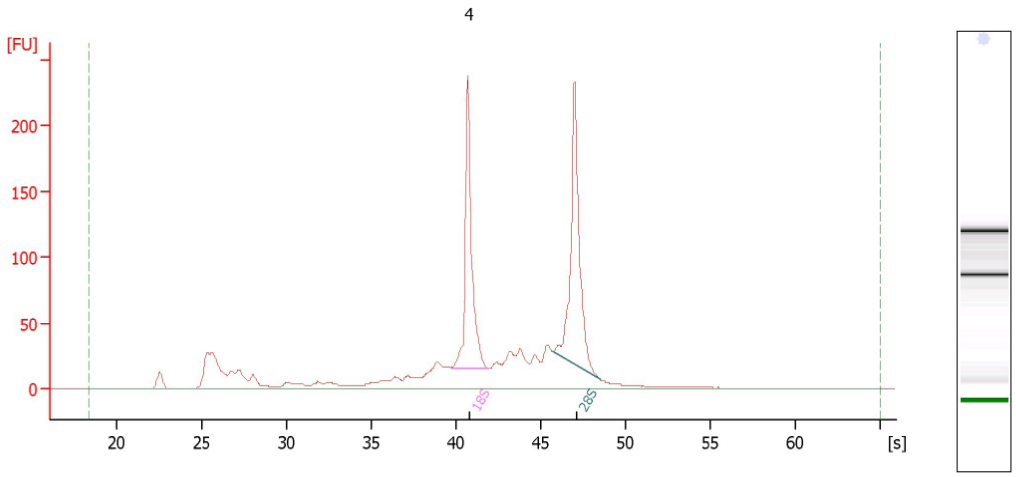

Overall Results for sample 4 : 4

RNA Area:	1,307.5	RNA Integrity Number (RIN):	8.4 (B.02.04)
RNA Concentration:	645 ng/µl	Result Flagging Color:	
rRNA Ratio [28s / 18s]:	1.1	Result Flagging Label:	RIN: 8.40

Fragment table for sample 4 : 4

Name	Start Time [s]	End Time [s]	Area	% of total Area
18S	39.68	41.94	236.8	18.1
28S	45.71	48.48	266.4	20.4

Figure 3-1. Representative electropherogram for RNA samples. RNA samples were assessed for the degree of degradation using the Agilent 2100 Bioanalyzer. Degradation was determined by the ratio of the height of the 28S:18S ribosomal peaks and the height of the baseline by software analysis of the electropherogram. The sample was then assigned an RNA Integrity Number (RIN) with high degrees of degradation corresponding to a RIN<6. Only samples with RIN>6 were used for this study.

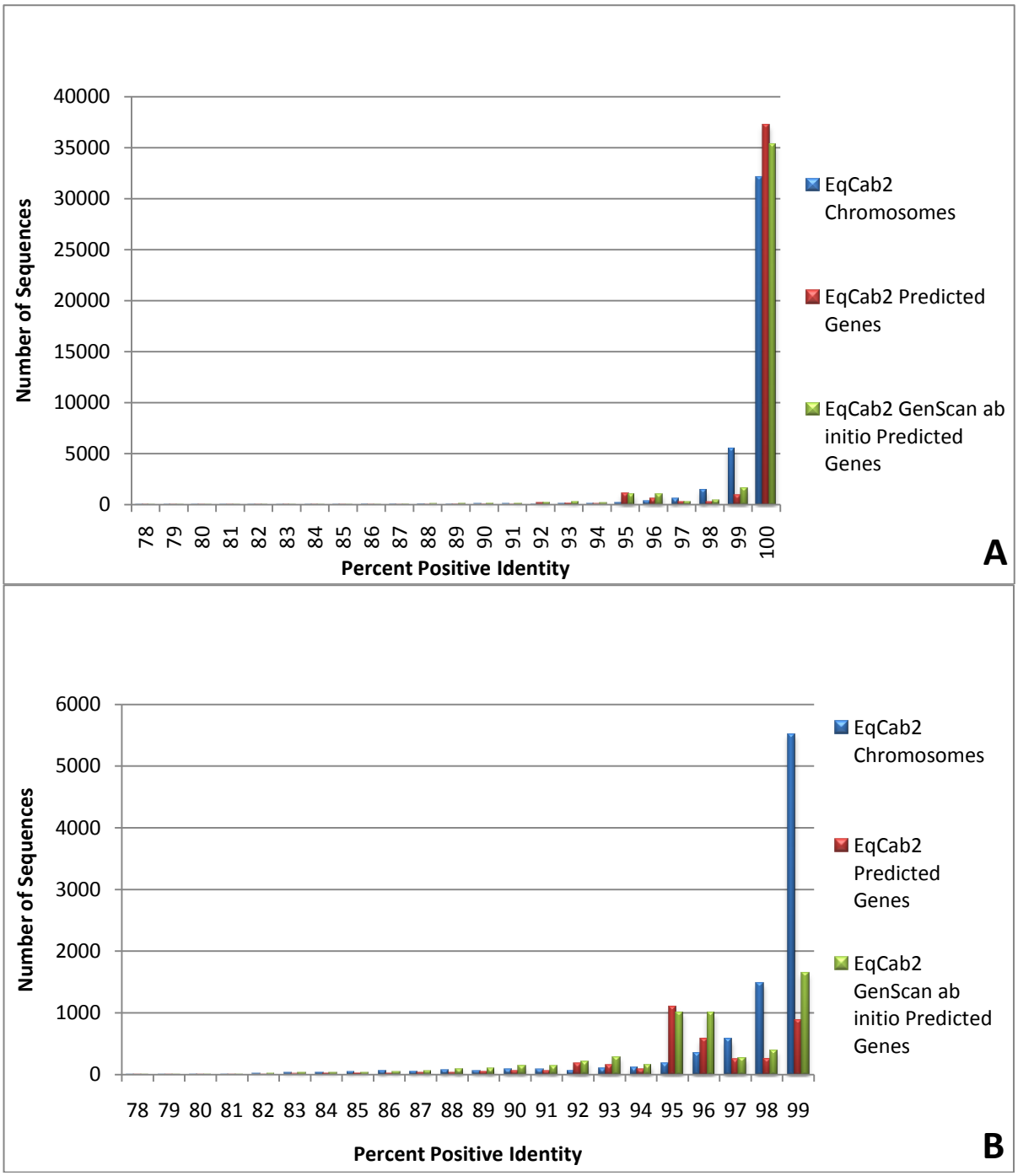

Figure 3-2. Percent positive identity of sequences matching to the equine databases. A) All the percent positive identity scores up through 100%. B) All the percent positive identity scores excluding 100%. The majority of sequences for all databases demonstrated positive identity greater than 95%. EqCab2 Chromosomes database- 40,145/40,973 sequences (97.9%) had a positive identity of >95%. EqCab2 Predicted Genes database- 40,264/ 40,999 sequences (98.2%) had a >95% identity. EqCab2 ab initio Predicted Genes database- 39,650/40,977 sequences (96.7%) had a percent positive identity >95%.

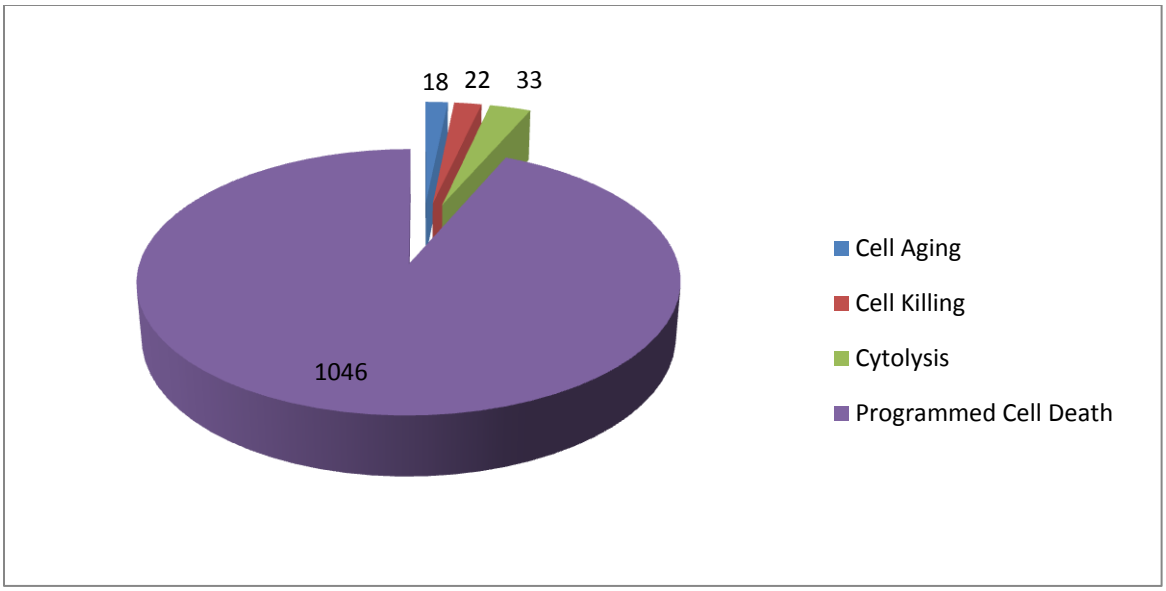

Figure 3-3. Gene ontology classification of cell death. These were categories included under biological processes. The majority of genes involved in cell death were involved with apoptosis (programmed cell death- 1,046 genes).

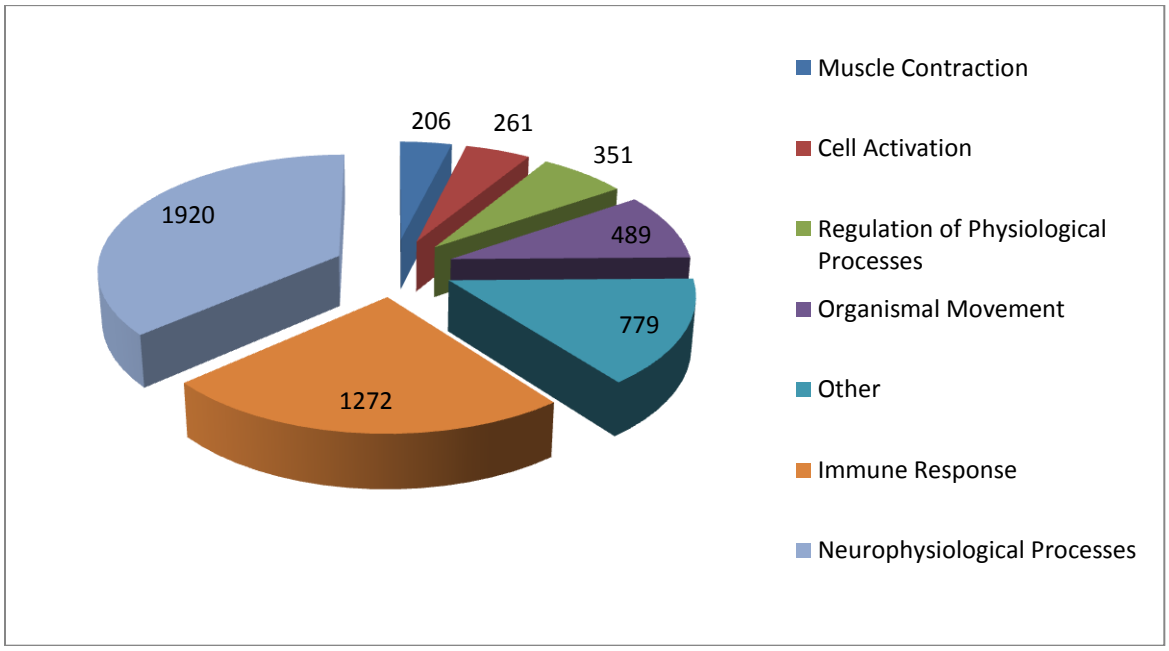

Figure 3-4. Gene ontology classification of physiological processes. These categories were included under biological process. The majority of genes were involved with neurophysiological processes (1,920) and the immune response (1,272).

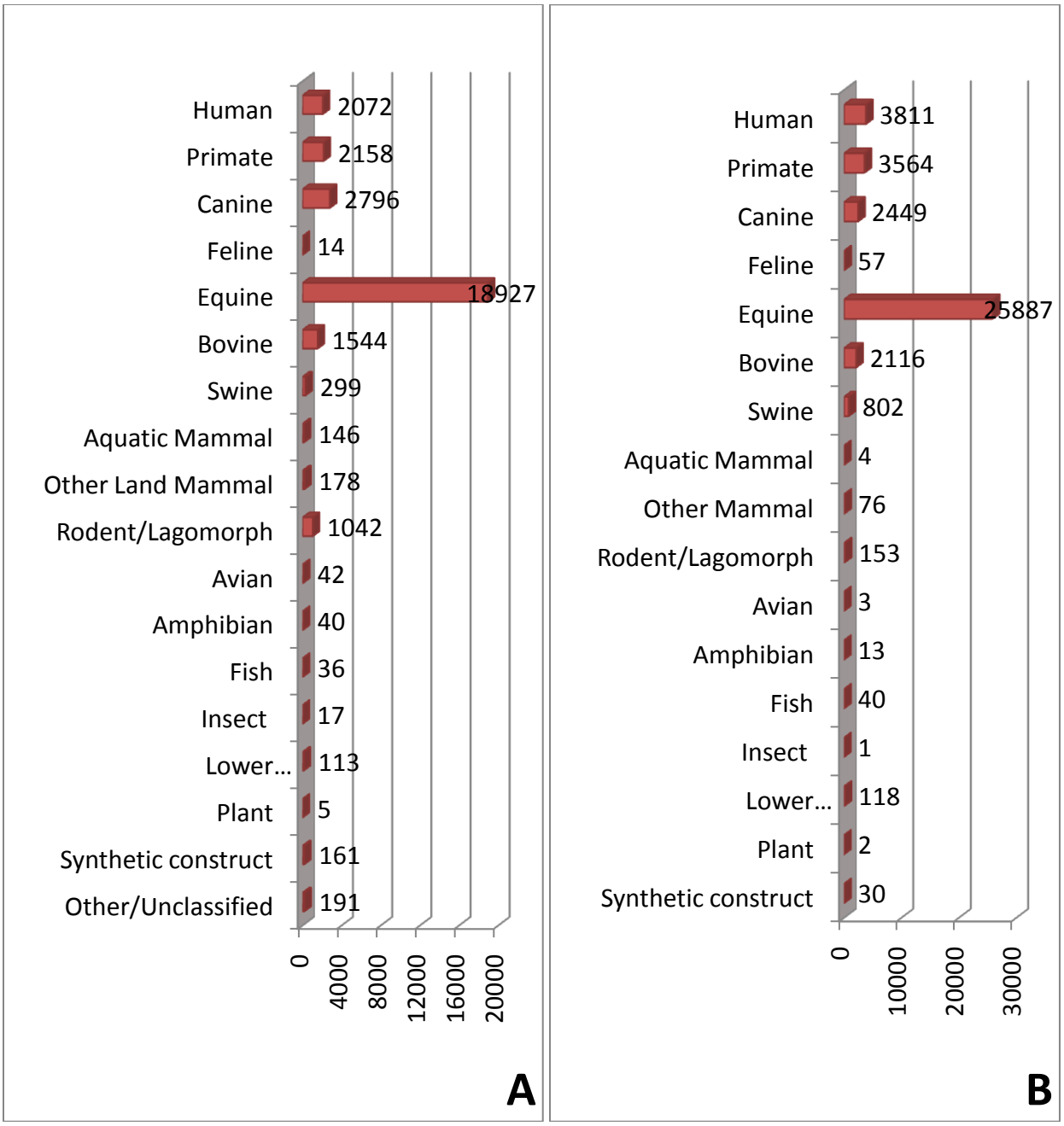

Figure 3-5. Sequence count by species group for the NCBI NR/NT databases. A.) Sequence count for the NR database. The majority of sequences mapped to the horse, with other prominent groups including the human, primate, canine, and bovine. B.) Sequence count for the NT database. The majority of sequences in this database also mapped to the horse, with other prominent groups including the human, primate, canine, and bovine.

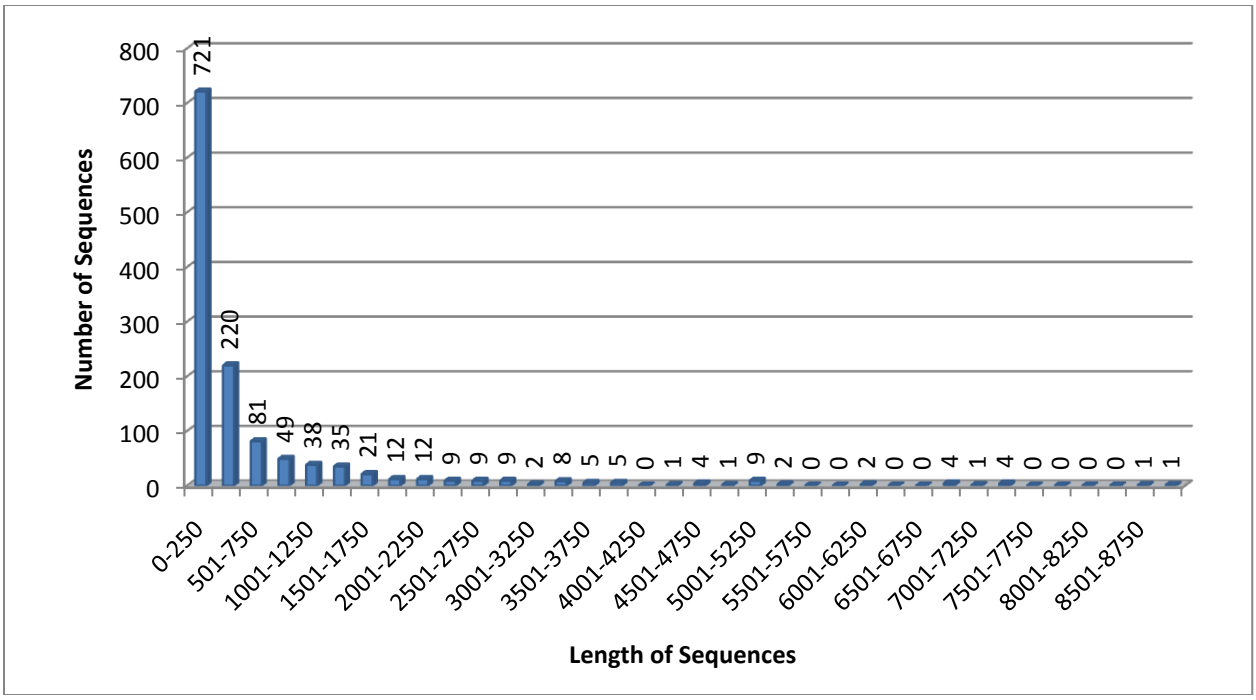

Figure 3-6. Average length of novel sequences. The majority of sequences annotated were less than 1000 base-pairs, with an average length of 595 base-pairs.

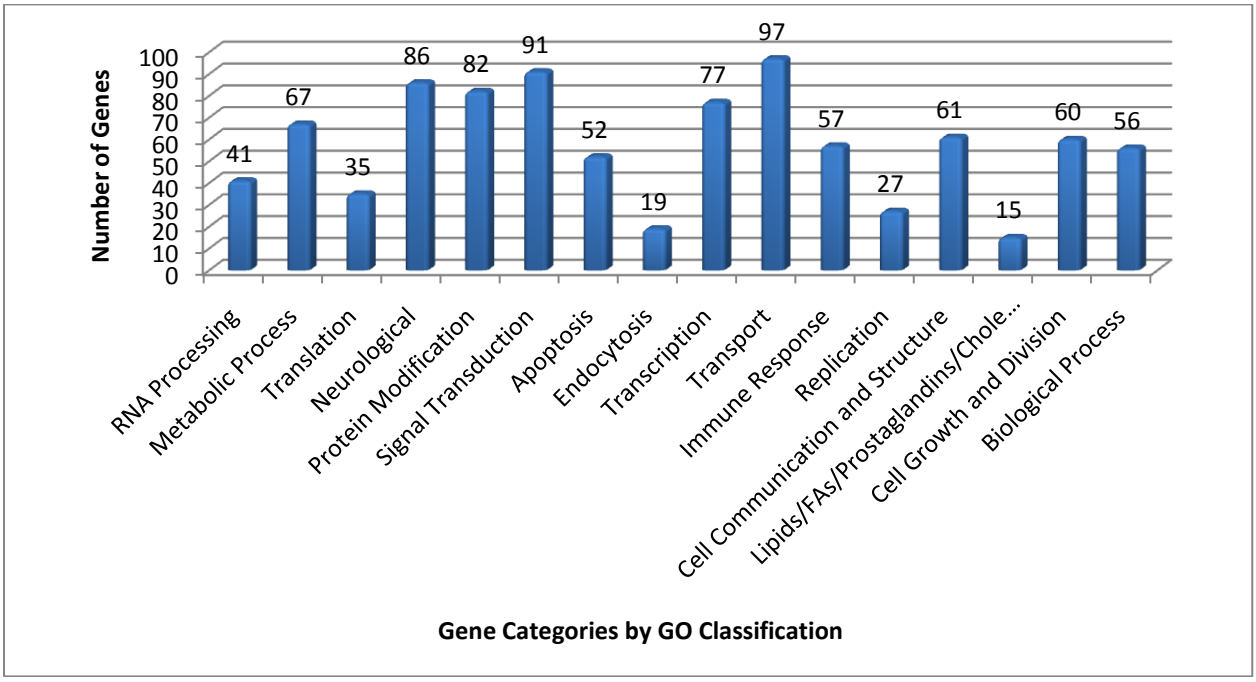

Figure 3-7. Novel gene categories based on gene ontology function. Genes were grouped into general categories based on GO classifications. The categories of transport, signal transduction, neurological, protein modification, and transcription were represented the most.

CHAPTER 4
GENE EXPRESSION ANALYSIS OF THE CENTRAL NERVOUS SYSTEM OF HORSES DURING WNV INFECTION WITH REGARDS TO EXPOSURE, SURVIVAL, AND LOCATION

Methodology

Microarray Probe Design

Probes consisted of oligonucleotides (60-mer) fabricated by a patented algorithm (Agilent Technologies, Santa Clara, CA) based on the annotated equine brain library and a 44,000 gene array (Agilent Technologies, Santa Clara, CA) was constructed. Preference was given to probes with the greatest length, greatest abundance, and lowest e-value (10^{-4}) within a cluster (set of similar sequences). All designed probes were included with one replicate each in 1) annotated, 2) annotated minus orientation, 3) unannotated, and 4) recovered genome categories (see Table 4-1). Several probes consisting of neurological, immunological, and cell death gene ontology categories were considered to be of particular importance and replicates were included on the array. Uniquely designed probes (250) designed by the manufacturer (Agilent) were also included as technological controls on the arrays.

Sample Collection

Tissues for analysis were derived from horses used in an experimental intrathecal challenge model wherein naïve horses developed grave West Nile (WN) encephalitis (100% nonsurvivorship) and all vaccinated horses did not develop clinical disease (100% survivorship). Specifically, brain tissues used to create the cDNA for dye labeling were obtained from these archived samples of three groups of six horses each (total of 18 individuals) and consisted of 1) naïve horses infected intrathecally with 1×10^5 WNV, 2) non naïve horses vaccinated utilizing a modified live attenuated Yellow

Fever (YF) chimera vaccine for protection against WNV (Prevenile, Intervet-Schering-Plough) and infected intrathecally with 1 X 10^5 WNV , and 3) horses that were not infected or vaccinated (Table 4-2). Experimental infection and vaccination of horses occurred according to previously published data.[58] Horses from groups 1 and 2 were euthanized (University of Florida IACUC protocols #F077, #F093, #D163) if demonstrating clinical signs or at the end of the study (day 21) if not demonstrating clinical signs. Horses from group 3 were normal healthy horses, not infected with WNV and were euthanized due to other causes (lameness, age, etc.). All horses were necropsied immediately upon euthanasia. Tissues were snap frozen in dry ice and ethanol and stored at -80^{o}C until RNA extraction was performed. Tissues used in the array included cerebrum and thalamus (one section from each horse for a total of 36 samples).

Three analyses were established to test the hypothesis that there are gene pathways whose expression changes in a significant and consistent manner due to WNV as a result of exposure status, survival/immune status, and CNS location. The analysis and the breakdown of the samples can be seen in Table 4-3. With respect to the experimental analyses, threee subhypotheses were generated to analyze if there was a difference in gene expression between the nonvaccinated/exposed and untreated horses (exposure), the nonvaccinated/exposed and vaccinated/exposed horses (survival), and the nonvaccinated cerebrum and nonvaccinated thalamus (location). In particular, the “survivors” represent the gene expression status of those animals that recover from grave WN encephalitis through induction of vaccine mediated immunity,

and the “non-survivors” represent the gene expression status of naive animals undergoing grave encephalitis.

RNA Extraction

Total RNA was extracted from the tissues listed in Table 4-2 (36 total samples). A 30 mg piece of tissue was weighed out for each sample on dry ice. The tissues were homogenized using manual disruption and placed in 1 mL of guanidium thiocyanate (Trizol®, Invitrogen, Carlsbad, CA). The samples were vortexed and allowed to remain at room temperature (RT) for 5 minutes to allow complete dissociation of the nucleoprotein complexes. Two hundred μL of molecular grade chloroform (Thermo Fisher Scientific ®, Waltham, MA) was added to each sample. The samples were placed at room temperature for 2 minutes, then centrifuged at 12,000 x *g* at 4^{o}C for 15 minutes. The chloroform and centrifugation steps were repeated to ensure complete removal of the lipids. A 0.5 mL aliquot of isopropanol alcohol was added to each sample and incubated at room temperature for 5 minutes. The samples were centrifuged at 12,000 x *g* at 4^{o}C for 10 minutes to precipitate the RNA. One mL of 75% ethanol was added to each pellet, mixed, and repelleted using centrifugation (7,500 x *g*, 4^{o}C, 5 minutes). The ethanol was poured off and the pellets air dried for 5 minutes. RNAsecure (Ambion ®, Austin, TX) diluted to a 1X concentration was heated on a heat block at 60^{o}C for 5 minutes and 75 μL was added to each pellet to inactivate any residual RNases. The pellets were incubated at 60^{o}C for 10 minutes in RNAsecure and cooled to room temperature. For DNase treatment, 7.5 μL of 10X DNase buffer and 1 μL of rDNase (Ambion®, Austin, TX) was added to each sample. Samples were incubated at 37^{o}C for 1 hour. After incubation, 7.5 μL of DNase inactivating reagent

(Ambion®, Austin, TX) were added to each sample and the samples were incubated at room temperature for 2 minutes. The samples were centrifuged at 10,000 rpm for 2 minutes, removed from the inactivating reagent, and placed at -80^{o}C until quality assessment. One μL of each RNA sample was placed on a nano-drop machine (ND-1000, Nanodrop Technologies, Wilmington, DE). The concentration and 260:280 ratio of each sample was assessed.

cDNA Creation and Dye Labeling

Dye-labeled cDNA was created using Cy3 dye (One-Color Microarray-Based Gene Expression Analysis kit, Agilent Technologies). The first strand cDNA was created using 3000 ng of RNA in 9 μL or less was aliquoted into individual tubes. 2.5 μL of T7 promoter primer was added to each tube and the tubes were incubated at 65^{o}C for 10 minutes, then placed on ice for 5 minutes. The proprietary master mix (Agilent Technologies) was added to each tube (8.5 μL) consisting of 4 μL of 5X first strand buffer (pre-warmed at 80^{o}C), 2 μL of 0.1M DTT, 1 μL of 10mM dNTP mix, 1 μL MMLV, and 0.5 μL RNAse inhibitor. The tubes were incubated at 40^{o}C for 2 hours, heated to 65^{o}C for 15 minutes, and incubated on ice for 5 minutes. The amplification mixture for dye incorporation consisting of 30 μL of master mix (15.3mL of nuclease-free water, 20 μL 4X transcription buffer, 6 μL 0.1M DTT, 8 μL NTP, 6.4 μL 50% PEG pre-warmed at 40^{o}C for 1 minute, 0.5 μL RNAse OUT, 0.6 μL inorganic pyrophosphate, 0.8 μL T7 RNA polymerase, and 2.4 μL cyanine 3-CTP dye) was added and each tube was incubated at 40^{o}C for 2 hours.

The dye-labeled cDNA was then extracted using a propriety kit (RNeasy®,Qiagen, Valencia, CA). The samples were brought to a total volume of 100

μL by adding 20 μL of nuclease free water and 350 μL of the kit buffer (RLT) was added to each sample and thoroughly mixed with a pipette. Ethanol (100%, 250 μL) was added to each sample and mixed thoroughly with a pipette. Seven-hundred μLs of each sample were transferred to the kit column,and the columns were centrifuged at 13,000 rpm for 30 seconds at 4^{o}C. The columns were transferred to a new collection tube and 500 μL of buffer (RPE) was added to each column. The columns were centrifuged for 60 seconds at 13,000 rpm at 4^{o}C, and the eluant discarded. The buffer RPE and centrifugation steps were repeated. The columns were transferred to a new collection tube and air dried for 2 minutes. To each column 30 μL of RNase-free water was added. The columns were incubated for 1 minute at room temperature and were then centrifuged for 30 seconds at 13,000 rpm at 40^{o}C and this step was repeated with the same sample.

The specific activity and yield of the samples were determined using a microfluidics platform (Nano-drop Technologies, Thermo Scientific). Both the concentration and the incorporation of the dye were measured. The formula Specific Activity = [(Concentration of Cy3)/(Concentration of cRNA)] * 1000 = pmol Cy3 per μg cRNA was used to determine whether the sample would be used for hybridization to the array. Only samples with a specific activity > 8 were used.

Hybridization and Scanning of Arrays

Hybridization to the microarrays was performed according to the manufacturer's protocol. Individual, non-pooled cDNA samples were hybridized to the arrays. Briefly, the prioprietary blocking agent was prepared to a 10X concentration and incubated at 37^{o}C for 5 minutes. Individual tubes were prepared combining 1.65 mg of dye-labeled

cDNA, 11 mL of 10X blocking agent, nuclease-free water, and 2.2 mL of the proprietary 25X fragmentation buffer for a final volume of 55 mL. The tubes were incubated at 60^{o}C for 30 minutes and then placed on ice for 1 minute. Fifty mL of the proprietary 2X hybridization buffer was added to each tube. The samples were mixed, centrifuged at 13,000 rpm for 1 minute at 25^{o}C, and placed on ice. The gaskets were placed into the chambers and 100 mL of sample added to each chamber. The array slides were placed on top of each gasket. The chambers were closed in the hybridization oven and rotated at 10 rpm for 17 hours at 65^{o}C.

After the hybridization, the arrays were disassembled in wash buffer 1. The slides were washed for 1 minute in proprietary wash buffers at 37^{o}C. The excess liquid was dried off and the slides washed for 30 seconds in the proprietary stabilization and drying solution. The slides were scanned and data collected using the proprietary software (Feature Extraction®, Agilent).

Normalization and Statistical Analysis

JMP Genomics version 4.0 (S.A.S. Institute, Cary, NC) was used to analyze the data. All files were transformed (log_2) and normalized using Loess normalization techniques. Normalization was checked using distribution analysis consisting of box plots, correlation heat maps, and overlayed kernel density elements; and principal component analysis consisting of 2D, 3D, and scree plots. A two-way analysis of variance (ANOVA) was performed (location and treatment were independent variables) and possible interactions between location (cerebrum and thalamus) and treatment (vaccinated, not vaccinated, normal) were tested in the analysis addressing location, exposure, and survival ($p<0.05$). Only thalamus was compared between the two analyses addressing exposure and survival due to differences in gene expression

between the cerebrum and thalamus. Variability was estimated in the software via linear regression and Pearson correlation coeffiecient and the R square and residual variance tables were generated for each array. A significant genes lists was generated and a hierarchical clustering was performed.

Gene Ontology Enrichment

Probes for the analyses of location, exposure, and survival that matched to the gene ontology categories of biological process, cellular component, and molecular function were identified. Gene ontology categories (as derived from the original annotation of the cDNA expression library, Fisher Cluster, University of Florida) that involved the neurological system, immunological system, apoptosis/cell death, and transcription/translation were targeted. The three analyses were analyzed based on the number of significantly different genes that grouped into these GO categories.

Pathway Modeling

Significant genes ($p<0.05$) for all three analyses were fed into Ingenuity Pathways Analysis software (Ingenuity Systems, Redwood, CA). Only genes that were contained in the database were mapped, and fold changes >1 and <-1 considered. Network modeling to determine interactions between significant genes, canonical pathways analysis to determine genes involved in known pathways, and disease/physiological function/location annotation was performed on significant genes. A Fisher's exact test was used and both number of transcripts and p-values considered in ranking of pathways, networks, and functions. This process was performed on all significant genes as well as on the gene ontology enriched datasets.

Microarray Validation

For the purposes of the initial validation of the utility of this microarray, several highly significant genes (six) were selected to 1) verify the accuracy of the probe hybridization, and 2) verify the accuracy of the relative expression values detected by the probe. To verify the relative expression values, only transcripts that were significantly upregulated or downregulated ($p<0.05$, fold change >2, <-2) in the exposure analysis were picked for analysis. A total of six transcripts were targeted to be used as primer sets in the validation experiment and included 2'5' oligoadenylate synthetase (2,5 OAS), complement component 1 (CC1), TNFα receptor ligand (TNFR), interleukin-6 (IL-6) , DEAD Box 60 (DB60), and defensin β4 (DB4), with β-actin (ACT) as the endogenous control. Two sets of primers were designed using primer design software (ABI Primer Express version 3.0, Applied Biosystems). The primers are available upon request. The first set of primers was designed to amplify a larger segment of the gene. Conventional PCR was performed using a proprietary master mix (Readymix Taq PCR Mastermix with $MgCl_2$, Sigma-Aldrich, St.Louis, MO). For each primer reaction, 25μL of the reagent mix, 1 μL each of forward and reverse primer (10mM), 5 μL of sample, and 18 μL of water were added to each respective PCR tube. The samples were held at 94^{o}C for 2 minutes, then cycled 25 times at 94^{o}C for 1 minute, 50^{o}C for 2 minutes, and 72^{o}C for 3 minutes. The samples were then held at 72^{o}C for 5 minutes and cooled at 4^{o}C. The reactions were run in triplicate for each set of primers.

The three tubes from each reaction were combined and purified using a PCR purification kit (QIAquick® PCR purification kit, Qiagen, Valencia, CA). Briefly, 5

volumes of the kit binding buffer (PB1) was added. The samples were mixed and placed on the kit column. The tubes were centrifuged at 13,000 rpm (>10,000g) for 60 seconds. The eluant was discarded and 750 μL of wash buffer (PE) was added. The columns were centrifuged at 13,000 rpm for 60 seconds, the eluant discarded, and the columns centrifuged again at 13,000 rpm for 60 seconds. Thirty μLs of water was added to each column membrane and the columns centrifuged again at 13,000 rpm for 60 seconds. The concentration and purity of the samples were determined using a microfluidics platform. The reactions were resolved utilizing a 0.9% agarose gel and imaged under standard UV conditions. If a band(s) was visualized, the samples were submitted to the UF Interdisciplinary Centers for Biotechnology Research for Sanger sequencing.

Sequencing results were checked against expected gene sequences. Once the correct sequence was validated, amplified samples were run under the thermocycling conditions listed above using a second set of nested primers. The presence of a band of the correct length was verified on a 0.9% agarose gel. For each target, a standard curve was generated using 5 two-fold dilutions and triplicate wells. The slope of the reaction and the R square was calculated via the proprietary software (ABI 7900, Applied Biosystems). The primer efficiency was checked using the equation efficiency = 10^(-1/slope). These primers were then used in real time, relative quantitation PCR in a SYBR green assay (Fast SYBR Green Master Mix, Applied Biosystems) to validate the findings of the level of expression demonstrated via array. Using proprietary conditions, 10 μL of Fast SYBR Green Master Mix, a variable amount of each primer dependent on reaction efficiency, 3000 ng of cDNA, and water up to a volume of 20 μL were added to

each well with replicates of three wells performed on each sample. The plate was centrifuged and the real time PCR reactions (7500 Fast Real-Time PCR System, Applied Biosystems) were performed using the reaction parameters consisting of a hold at 95^{o}C for 20 seconds, followed by 40 cycles consisting of a 40 cycle reaction at 95^{o}C for 3 seconds and a 40 cycle reaction at 60^{o}C for 30 seconds. Relative quantitation analysis was performed using the proprietary software for calculation of the comparative Ct method (Applied Biosystems software for the 7500 Fast machine) wherein $2^{-\Delta\Delta Ct}$ is used for the comparison of relative quantitation between the thalamus of vaccinated/exposed horses and nonvaccinated/exposed horses.

To verify the accuracy of the probe hybridizations, the probe sequences were BLASTed against the equine genome (Fisher Cluster, UF ICBR, Gainesville, FL). Only sequences with e-values <10-4 were generated. Sequences were checked for percent identity and sequence alignment.

Results

Study Design

Three microarray experiments were completed to answer the question of whether there were differences in gene expression in WN encephalitis according to exposure status, vaccination status, and CNS region. The analyses and the breakdown of the samples can be seen in Table 4-3. With respect to the experimental groups, three subhypotheses were generated to analyze if there was a difference in gene expression between the nonvaccinated/exposed and untreated horses (exposure), the nonvaccinated/exposed and vaccinated/exposed horses (nonsurvival), and the nonvaccinated cerebrum and nonvaccinated thalamus (location). In particular, gene expression values from the thalamus (6) of the nonvaccinated/exposed horses was

compared to expression values from the thalamus (6) of the untreated group to determine if there was a difference in gene expression due to exposure to WNV. Gene expression values from the thalamus (6) from the nonvaccinated/exposed horses was compared to gene expression values from the thalamus (6) of the vaccinated/exposed horses to determine if there was a difference in gene expression between naïve horses which succumb to WNV and those that are immune, do not develop significant disease and survive from WNV infection. Since the thalamus undergoes a higher viral load as determined by our previous studies[47,48], gene expression values from the thalamus (6) of nonvaccinated/exposed horses was compared to gene expression values from the cerebrum (6) of the same group to determine if there was a difference in gene expression during exposure to WNV in these two different regions of the brain.

Array Normalization

Loess normalization was performed on all arrays and confirmed by distribution analysis. Figure 4-1 illustrates the normalization of each individual array. For analysis of the distribution and variability of the data itself, correlation and principal components analysis for all groups demonstrated that the majority of variance was accounted for with the first three principal components (x, y, and z) with Eigenvalues (percents of variability) of the each component, 11.09 (30.81%), 4.94 (13.71%, and 3.21 (8.94%), respectively. In addition, the mean of the R^2 was 0.939392 (range 0.8781-0.9871) for all arrays. A heat map and dendrogram was generated between all arrays (see Figure 4-2).

Statistical Analysis

Analysis of mean relative difference in gene expression using an ANOVA with interactions between treatment and location revealed significant differences in gene expression ($p < 0.05$) for all analyses (exposure, nonsurvival, and location). To

determine which tissues should be compared in the exposure and nonsurvival groups (i.e. thalamus only or pooled thalamus and cerebrum), differences in gene expression were analyzed between the thalamus and cerebrum of the normal, nonexposed horses. The degree of fold-change (relative fluorescent intensity) was analyzed for all differentially regulated genes. In total, 7,321 genes were significantly different between the two locations (6,911 after duplicate removal). Therefore, for the exposure and nonsurvival groups, only thalamus was compared. This data is summarized in Table 4-4. The same 3,421 were significantly altered in all three analyses and overall, 4,000 (44%), 3,472 (46%), and 3,811 (49%) genes were expressed at levels > -1.0 and < +1.0 for the exposure, nonsurvival, and location groups.

Exposure Status. For exposure status, significant differences in gene expression in the thalamus were seen between nonvaccinated/exposed and normal, nonexposed horses for 9,020 genes (12,029 without duplicate probe removal). When analyzed solely by fold change, 2,936 genes decreased by < -1.0 (395 < -2.0) and 2,084 increased by > +1.0 (749 > +2.0) in the exposed nonvaccinated horses compared to the nonexposed normal horses.

Immune/Survival Status. For immune/survival status, significant differences in gene expression in the thalamus were seen between nonvaccinated/exposed horses (nonsurvivors) and vaccinated/exposed horses (survivors) in 7,395 genes (9,978 without duplicate probe removal). In the nonvaccinated, nonsurvivors, 2,123 genes were decreased by < -1.0 (225 < -2.0) while 1,800 were increased by > +1.0 (666 > +2.0) compared to the vaccinated, survivors.

CNS Location. Where analyzed by location in the brain, significant differences in gene expression were seen between the cerebrum and thalamus of nonvaccinated horses exposed to WNV (location) for 7,649 individual genes (10,555 without duplicate probe removal). For the location analysis, 2,053 genes were decreased by < -1.0 (609 < -2.0) while 1,827 were increased by > +1.0 (406 > +2.0) (Figure 4-3) when the thalamus was compared to the cerebrum in nonvaccinated, exposed horses.

Gene Ontology and Pathways Analysis Overview

Gene ontologies were mined for all significant genes based on those categorized in public accessed databases provided by NCBI. Because of the sheer diversity of GO in this analysis, neurological, immunological, and apoptosis were GO categories specifically chosen for deeper data analysis by pathways analysis. Ingenuities Pathways Analysis Software (IPA) was used to identify putative physiological interactions between genes that were significantly changed. Canonical pathways, functions, and networks were determined using the Fisher exact test with a $p<0.05$ and fold change <-1.0, >+1.0. Fewer than 25% of significant genes mapped to the IPA database for all groups. Of the genes that did map, identification was based on the NCBI nucleotide database gene IDs. Canonical pathways were identified to demonstrate interactions between significantly changed genes. Functions (disease and physiological) were identified based on the transcripts and pathways identified as significantly changed. Transcripts of significance were also targeted for all analyses to identify those that may be of import in future studies.

Exposure Status

Gene ontology. The first subhypothesis asked whether there was a difference in gene expression due to exposure to WNV between nonvaccinated horses exposed to

WNV and normal horses not exposed to WNV. For this exposure analysis, genes that were found to have significant differences in expression were classified into gene ontology (GO) categories. With overlap, 6,009 genes were classified under biological process, 6,454 genes were classified under cellular component, and 6,646 genes were classified under molecular function (Figure 4-4). The genes that mapped to GO categories were then grouped according to the functions of transcription/RNA processing, neurological genes, immunological genes, and cell death/apoptosis. The most genes mapped to GO processes of transcription/RNA processing (2,022) with the second most genes mapping to neurological categories (1,081). Genes also mapped to immunological categories (983) and cell death/apoptosis (430) (Figure 4-5).

Canonical pathways. Canonical pathways were first examined for interactions between multiple significant transcripts. For the canonical pathways assessment of the exposure analysis, the majority of pathways were involved with some aspect of cell signaling for a variety of locations/functions (Table 4-5, Figure 4-6). Seven of the top 25 pathways (based on the p-value) were classified as neurological pathways (81 transcripts) with 2 of the top 25 pathways classified as immunological pathways (25 transcripts).

The neurological canonical pathways were analyzed for exposure and 17 pathways were identified (Figure 4-7). Specific neurological pathways that demonstrated dysregulation for the exposure analysis included neurotransmitter pathways and signaling pathways. These included glutamate receptor signaling (Figure 4-8), dopamine receptor signaling (Figure 4-9), axonal guidance signaling, CREB signaling in neurons, synaptic long term depression, amytrophic lateral sclerosis,

synaptic long term potentiation, GABA receptor signaling, reelin signaling in neurons, neuropathic pain signaling in dorsal horn neurons, Huntington's disease signaling, semaphorin signaling, agrin interactions at neuromuscular junctions, neurotrophin/TRK signaling, CNTF signaling, serotonin receptor signaling, and circadian rhythm signaling.

The immunological canonical pathways were analyzed for the exposure analysis and 47 pathways were identified (Figure 4-10). When examining all of the CPs identified, pathways involved in the innate and adaptive response were present. The immune pathways that were upregulated in the exposure analysis (i.e. due to WNV) included the IL-15 signaling pathway (Figure 4-11), the IL-22 signaling pathway, the IL-9 signaling pathway, and the Interferon Signaling Pathway (Figure 4-12). Multiple pathways involved in apoptosis were also dysregulated in the exposure analysis. These included the retinoic acid mediated apoptosis signaling, calcium-induced T lymphocyte induced apoptosis, cytotoxic T lymphocyte mediated apoptosis of target cells, induction of apoptosis by HIV1, and April mediated signaling.

Functions. Functions were assessed for the exposure analysis, which links the top transcripts in each pathway to their related disease states and normal function. The functions were distributed amongst many analyses, but of particular note are the number of functions involved with neurological and immunological pathways as well as cell death (Table 4-6). For the exposure analysis, 4 categories were identified involving neurological functions (2,326 transcripts), 10 categories were identified involving immunological functions (1,830 transcripts for exposure), and 1 category was identified as involving cell death (1,153 transcripts exposure).

The functions involving neurological categories were further analyzed. Most genes grouped under neurological disease when compared to nervous system development and function, behavior, and psychological disease (Figure 4-13). When further analyzed by specific disease, genes mapped to mental disorders (including bipolar affective disorder, Alzheimer's, and schizophrenia), as well as degenerative neuropathies (including progressive motor neuropathy, Huntington's disease, Parkinson's disease, amytrophic lateral sclerosis, and multiple sclerosis) (Figure 4-14 a,b).

The functions involving immunological pathways were grouped with cell death/apoptosis for analysis. For the exposure analysis, the most genes were categorized under inflammation (992 transcripts). Both innate (inflammatory response, antigen presentation, immune cell trafficking) and adaptive (humoral immune response, cell-mediated immune response, cytotoxicity, immune cell trafficking) aspects of immunity were identified. Cell death and apoptosis categories were also seen for the exposure analysis, with 1,299 total genes involved with cell death, and 1,006 total genes involved with apoptosis (Figure 4-15).

Transcripts. Significantly upregulated and downregulated transcripts for the exposure analysis were identified. Transcripts that were increased in expression by 1-fold or more or decreased in expression by -1-fold or less and mapped to the IPA database were analyzed for the exposure analysis (Appendix B). In total, for the upregulated transcripts, 37 out of 543 transcripts (6.8%) were transcriptional regulators (Table 4-7, Appendix B). For the downregulated transcripts, 84 out of 1,031transcripts (3.9%) were transcriptional regulators (Table 4-8, Appendix B). Specific transcriptional

transcripts upregulated of note included signal transducer and activator of transcription (STAT1), interferon regulatory factor 2 (IRF2), and interferon regulatory factor 3 (IRF3), ets variant 7 (ETV7), basic leucine zipper transcription factor, ATF-like (BATF), eomesodermin homolog (EOMES), zinc finger, NFX1-type containing 1 (ZNFX1), activating transcription factor 3 (ATF3), and WW domain containing transcription regulator 1 (WWTR1). Transcriptional transcripts of particular note that were downregulated included SUB1 homolog (SUB1), nuclear factor I/A (NFIA), ankyrin repeat and SOCS box-containing 1 (ASB1) (Table 4-7, 4-8).

Specific neurological transcripts were also significantly changed in expression (Table 4-9). For the exposure analysis, a total of 176 transcripts were downregulated and 43 transcripts were upregulated. Transcripts involved with neurotransmitter pathways including glutamate receptor signaling (Figure 4-8, Table 4-10) and dopamine receptor signaling (Figure 4-9, Table 4-11) were of particular note. This included a decrease in the expression of NMDA glutamate receptors (GRIN), metabotropic glutamate receptors (GRM8, HOMER3), kainate glutamate receptors (GRIK1), ionotropic glutamate receptors (GRIA1,4), and glutamate clearance receptors (SLC1A) (glutamate receptor signaling), a decrease in the expression levels of the dopamine receptor D5 (DRD5), adenylate cyclase, protein kinase, protein phosphatase, and tyrosine hydroxylase, and an increase in the expression levels of monoamine oxidase (MAO). Catenin (cadherin-associated protein), delta 2 (neural plakophilin-related arm-repeat protein) (CTNND2) was also highly upregulated. This molecule is specific to the brain, and functions to connect cell junctions and cytoskeletal architecture with signaling pathways (Appendix B).

Transcripts involved in the immune response for the exposure analysis were also significantly dysregulated. In total, 176 immune transcripts were downregulated, while 130 transcripts were upregulated (Table 4-12). The most notable was pentraxin 3 (PTX3), upregulated over 9-fold, which functions in the pathway of pattern recognition receptors in recognition of viruses and bacteria. Other upregulated immunological transcripts included DEAD (Asp-Glu-Ala-Asp) box polypeptide 58 (DDX58), zeta-chain (TCR) associated protein kinase 70kDa (ZAP70), Fc fragment of IgG, low affinity IIIa, receptor (CD16a) (FCGR3A), complement component 1, r subcomponent (C1R), CD8a molecule (CD8A), interleukin 4 induced 1 (IL4I1), interleukin 7 (IL7), CD5 molecule-like (CD5L), CD4, CD3, and interleukin 15 (IL15). Transcripts that mapped to specific immunological pathways of interest that were significantly expressed included those that mapped to the IL-15 pathway (upregulation of IL-15, IRF3, STAT1, and TYK2; downregulation of phosphoinositide-3-kinase, regulatory subunit 1 (alpha) (PIK3R)), and those that mapped to the IL9, IL22, and JAK/STAT pathways (upregulation of SOCS3, STAT1, TYK2; downregulation of PIK3R) (Figures 4-11, 4-12; Tables 4-13, 4-14). Apoptotic transcripts were also upregulated in the exposure analysis, including poly (ADP-ribose) polymerase family member 14 (PARP), caspase 4 (CASP4) retinoid receptor (RXR), and retinoic acid nuclear receptor (RAR) (Appendix B).

Immune/Survivor Status

Gene ontology. The second subhypothesis asked if there was a difference in gene expression in the nonsurvivors which were not vaccinated and exposed to WNV compared to the survivors (100%) that were vaccinated and exposed to WNV.[58, 59, 117] The genes that were found to be significantly different in expression were classified into gene ontology (GO) categories. A total of 5,120 genes were classified under biological

process, 5,462 genes were classified under cellular component, and 7,696 genes were classified under molecular function (Figure 4-4) with overlap. Analysis was then performed to analyse the GO categories according to the functions of transcription/RNA processing, neurological genes, immunological genes, and cell death/apoptosis. The most genes mapped to GO processes of transcription/RNA processing (1,864) with the second most genes mapping to immunological categories (850). Genes also mapped to neurological categories (840) and cell death/apoptosis (338) (Figure 4-5).

Canonical pathways. Similar to the analysis to exposure status, the majority of canonical pathways engaged cell signaling for a variety of cell types, functions and transcripts (Table 4-5, Figure 4-6). Ten of the top 25 pathways (based on the p-value) were classified as neurological pathways (156 transcripts). None of the top 25 pathways were identified as immunological pathways.

The neurological canonical pathways were analyzed for nonsurvivorship and 19 pathways were identified (Figure 4-7). Specific neurological pathways that demonstrated dysregulation for the exposure analysis included neurotransmitter pathways and signaling pathways. Like the analysis for exposure status, these included glutamate receptor signaling (Figure 4-8), dopamine receptor signaling (Figure 4-9), CREB signaling in neurons, synaptic long term depression, amytrophic lateral sclerosis, synaptic long term potentiation, GABA receptor signaling, neuropathic pain signaling in dorsal horn neurons, semaphorin signaling, neurotrophin/TRK signaling, CNTF signaling, serotonin receptor signaling, glutamate metabolism, and circadian rhythm signaling. Other pathways identified in this analysis included axonal guidance signaling,

neuregulin signaling, reelin signaling in neurons, Huntington's disease signaling, and agrin interactions at neuromuscular junctions.

Forty-nine pathways involved in both the innate and adaptive immunity were identified as associated with immune/survivorship status (Figure 4-10). The immune pathways that were upregulated (as in the analysis of exposure status) included the IL-15 (Figure 4-11), IL-22, IL-9, and IFN signaling pathways (Figure 4-12). Multiple pathways involved in apoptosis were also dysregulated and the previous analysis included the retinoic acid mediated apoptosis signaling, calcium-induced T lymphocyte induced apoptosis, and death receptor signaling.

Functions. In the assessment of functions associated with nonsurvivorship, multiple transcripts were identified in functions that were distributed amongst many analyses (Table 4-6). Five categories were identified involving neurological functions (2,246 transcripts), nine categories were identified involving immunological functions (1,542 transcripts), and one category was identified as involving cell death (1,082 transcripts exposure).

In the analysis of specific neurological categories, more genes grouped under neurological disease when compared to nervous system development and function, behavior, and psychological disease (Figure 4-13). When further analyzed by specific disease, genes mapped to the similar mental disorders and degenerative identified by the previous analysis (Figure 4-14 a,b).

For deeper analysis of immunological and apoptosis functions, similar functions were identified as those involved in the exposure analysis. Most genes were categorized under inflammation (832 transcripts), with both innate and adaptive immune

functions identified. Cell death and apoptosis categories were also seen for the nonsurvival analysis, with 476 total genes involved with cell death, and 340 genes involved with apoptosis (Figure 4-15).

Transcripts. Individual, significantly upregulated and downregulated transcripts analyzed for their association with nonsurvivorship. Transcripts that were increased in expression by 1-fold or more or decreased in expression by 1-fold or less and modeled in the IPA database (Appendix B). For transcriptional regulators, 35 of 543 transcripts (6.4%) were upregulated (Table 4-7, Appendix B) while 46 of 1,031transcripts (4.4%) were downregulated (Table 4-8, Appendix B). Specific transcriptional genes of interest that were upregulated include STAT1, IRF2, IRF3, ETV7, BATF, BATF, EOMES, ZNFX1, ATF3, and WWTR1. Transcriptional genes of interest that were downregulated included SUB1, NFIA, and ASB5 (Table 4-7, 4-8).

In the subanalysis of neurological transcripts (Table 4-9), a total of 209 downregulated transcripts and 42 upregulated transcripts were identified, and similar to the analysis of exposure status, were primarily composed of transcripts involved with neurotransmitter pathways including glutamate receptor signaling (Figure 4-8, Table 4-10) and dopamine receptor signaling (Figure 4-9, Table 4-11). This included a decrease in the expression GRIN, HOMER3, GRIK1/2, GRIA1/2/3, SLC1A, AC, PK, and PP, and an increase in the expression levels of MAO and CTNND2.

Further analysis of the transcripts involved in the immune response in the nonsurvivors identified 215 immune transcripts which were downregulated, while 116 transcripts were upregulated (Table 4-12). Upregulated transcripts included PTX3 (7.7-fold increase over vaccinates), DDX58, ZAP70, receptor CD16a, FCGR3A, C1R, CD8A,

IL4I1, IL-7, CD5L, CD4, CD3, and IL15. Transcripts that mapped to separate immunological pathways that were significantly changed in expression included those that mapped to the IL-15 pathway (upregulation of IL-15, IRF3, and STAT1; downregulation of PIK3R, PTK2B, and mitogen activated protein kinase 1 (MAPK1)). The transcripts that mapped to IL-9, IL-22, and JAK/STAT pathways included upregulation of SOCS3, STAT1 with downregulation of PIK3R, MAPK1, and protein inhibitor of activated STAT, 2 (PIAS2)) (Figures 4-11, 4-12; Tables 4-13, 4-14). Apoptotic transcripts were also upregulated for the nonsurvivors and included (PARP) and caspase 4. (Appendix B).

CNS Location

Gene ontology. The third subhypothesis asked whether there was a difference in gene expression due to location in the brain during WNV infection between thalamus and cerebrum of the nonvaccinated exposed horses. With overlap, 5,200 genes were classified under biological process, 5,675 genes were classified under cellular component and 5,715 genes were classified under molecular function (Figure 4-4). The genes that mapped to GO categories were then grouped according to the functions of transcription/RNA processing, neurological genes, immunological genes, and cell death/apoptosis. Most genes mapped to GO processes of transcription/RNA processing (1,664) with the second most genes mapping to immunological categories (798). Genes also mapped to neurological categories (447) and cell death/apoptosis (349) (Figure 4-5).

Canonical pathways. For the canonical pathways assessment of the analysis of significantly different genes depending on CNS location analysis, the majority of pathways were involved with some aspect of cell signaling also (Table 4-5, Figure 4-6).

Seven of the top 25 pathways were identified as neurological (125 transcripts) while two of the top 25 pathways were identified as immunological pathways (40 transcripts).

The deeper analysis of the neurological canonical pathways significant for location sixteen pathways were identified (Figure 4-7). Specific neurological pathways that demonstrated dysregulation also included neurotransmitter pathways and signaling pathways. These included glutamate receptor signaling (Figure 4-8), dopamine receptor signaling (Figure 4-9), axonal guidance signaling, CREB signaling in neurons, synaptic long term depression, amytrophic lateral sclerosis, synaptic long term potentiation, GABA receptor signaling, reelin signaling in neurons, neuropathic pain signaling in dorsal horn neurons, neuregulin signaling, Huntington's disease signaling, semaphorin signaling, agrin interactions at neuromuscular junctions, neurotrophin/TRK signaling, CNTF signaling, serotonin receptor signaling, and circadian rhythm signaling.

Forty-eight immunological canonical pathways (Figure 4-10) involving both the innate and adaptive response were present. The immune pathways that were upregulated in the thalamus compared to the cerebrum (Figures 4-11, 4-12) included the same previously identified signaling pathways (IL-15, IL-22, IL-9 and IFN). Multiple pathways involved in apoptosis were also dysregulated in the location analysis. These included the retinoic acid mediated apoptosis signaling, calcium-induced T lymphocyte induced apoptosis, cytotoxic t lymphocyte mediated apoptosis of target cells, induction of apoptosis by HIV1, and apoptosis signaling, and myc mediated apoptosis signaling.

Functions. Functions were assessed for the location in the CNS, which links the top transcripts in each pathway to their related disease states and normal function (Table 4-6). For the location analysis, five categories were identified involving

neurological functions (3,242 transcripts), ten categories were identified involving immunological functions (1,558 transcripts), and one category was identified as involving cell death (719 transcripts). The further analyses of specific neurological function were similar to that mapped for both the exposure and immune status analyses (Figure 4-13), mental disorders and degenerative neuropathies (Figure 4-14 a and b).

The functions involving immunological pathways were grouped with cell death/apoptosis for analysis. Like the previous analyses, most genes were categorized under inflammation (834 transcripts), with involvement of both innate and adaptive immunity. Cell death and apoptosis categories were also seen for the location analysis, with 210 total genes involved with cell death, and 184 total genes involved with apoptosis (Figure 4-15).

Transcripts. Significantly upregulated and downregulated transcripts dependent upon location in the CNS were identified and modeled (also see Appendix B). In total, for the upregulated transcripts, 38 of 543 transcripts (6.9%) were transcriptional regulators (Table 4-7, Appendix B). For the downregulated transcripts, 40 of 1,031transcripts (3.8%) were transcriptional regulators (Table 4-8, Appendix B). Specific transcriptional transcripts changed of note were similar to that of both the exposure analysis and the immune/survivor analysis (Table 4-7, 4-8). These included STAT1, IRF3, ETV7, BATF, ZNFX1, ATF3, and WWTR1 that were upregulated, and SUB1 and ASB1 that were downregulated.

Specific neurological transcripts were also significantly changed in expression (Table 4-9). For the location analysis, a total of 176 transcripts were downregulated and 43 transcripts were upregulated. Transcripts of note were similar to the previous

analyses (Figure 4-8 and 4-9, Table 4-10 and 4-11). This included a decrease in the glutamate signaling expression of GRIN1/2A/2B/3A, HOMER1, GRIK1, GRIA1/2/3/4, and SLC1A. Similar decreases were seen in the dopamine signaling pathway transcripts AC and PP, with an increase in MAO. The protein CTNND2 was also highly upregulated.

Transcripts involved in the immune response for the location analysis were also significantly dysregulated. In total, 266 immune transcripts were downregulated, while 210 transcripts were upregulated (Table 4-12). In this case PTX3 was upregulated over 4-fold. The other upregulated and downregulated immunological transcripts that were identified were similar to the analyses involving exposure and immune status. These included upregulation of DDX58, ZAP70, FCGR3A, C1R, CD8A, IL4I1, and IL7. Transcripts that mapped to specific immunological pathways of interest that were significantly expressed included those that mapped to the IL-15 pathway (upregulation of IL-15, IRF3, JAK3, and STAT1; downregulation of PIK3R, PTK2B, MAPK1, and MAPK1), and those that mapped to the IL9, IL22, and JAK/STAT pathways (upregulation of JAK1, PIK3R3, and STAT1; downregulation of PIK3R1,2, MAPK1, MAP2K1) (Figures 4-11, 4-12; Tables 4-13, 4-14). Apoptotic transcripts were also upregulated in the location analysis and were similar to that of immune/survivorship status, including poly (ADP-ribose) polymerase family member 14 (PARP), and caspase 4 (CASP4) (Appendix B).

Analysis of Overlap Between Exposure, Survival/Immunity, and Location

Genes common to all pathways (3,423 genes) were analyzed by Fisher exact test (IPA). For canonical pathways analysis, four pathways (23 transcripts) involving the neurological system were identified and nine pathways (61transcripts) involving the

immunological system were identified (Figure 4-16). Significant genes were then analyzed for related functions (Table 4-15). The majority of these transcripts modeled for cell death (646), with genetic disorder containing the second highest number of transcripts (629) and neurological disease the third most modeled (479). The neurological functions were analyzed separately (Figure 4-17). Neurological functions that were common to genes in all analyses substantiated the separate findings of all of the separate factor analyses. These included mental disorders (schizophrenia, bipolar affective disorder) and degenerative neuropathies (progressive motor neuropathy, Huntington's disease, Parkinson's disease, amytrophic lateral sclerosis, and multiple sclerosis). For immunological and cell death functions, many genes were also categorized under inflammatory disorders, cell death, apoptosis, and immunologica disease (Figure 4-18). Other functions of significance included cytotoxicity, infectious disease, humoral immune response, cell-mediated immune response, inflammatory response, immune cell trafficking, and antigen presentation.

Array Validation

The correct sequences (checked against the sequences from the transcriptome) were identified for the primer pairs β-actin, 2'5'OAS, CC1R, IL-6, DEADBox60, Def β 4, and TNFαr. The housekeeping gene β-actin was included as the 'house-keeping gene', and the other genes were significantly up-regulated. Primer efficiencies were established for all primer pairs using standard curves analysis and efficiency calculation, with efficiencies ranging between 85 and 97%. Real time relative quantitation PCR was then run in triplicate on the thalamus from 6 of the vaccinates and 6 of the non-vaccinates, with β actin as the endogenous control. The results of the relative

quantitation can be seen in Table 4-16. As expected, there was a relative increase in expression for all primer pairs when comparing the vaccinates to the nonvaccinates. This correlated with the microarray data, which showed an increase in fold change for all of the transcripts chosen.

Probe sequences were analyzed by comparison to the most recent version of the EqCab2 genome using the basic local alignment search tool (BLAST, Fisher Cluster, University of Florida, Gainesville, FL) to determine the accuracy of each sequence to detect single genes as opposed to gene families. In total, 42,843 oligonucleotide probes were analyzed and 40,113 probes matched to one sequence with 100% identity (93.6%). Of these, 3,700 (9.2%) matched more than once to a genomic sequence implying possible binding to a gene family. The majority of these which matched to multiple sequences were identified as belonging to one chromosome. In addition, 2,687 probes matched at <100% identity (average 97.5% identity). Forty three probes did not match, and were most likely present as controls since the sequences could not be detected in the sequenced library (Table 4-17).

Discussion

This experiment was the first study to analyze global gene expression during WNV disease, infection, and recovery in the CNS of natural, outbred equine hosts. The data generated from this project provides invaluable insight into WN encephalitis in both equine and human hosts, and is a useful platform for future studies. The majority of previous work that has been conducted to understand WN encephalitis has been conducted in murine models. Rodents are not natural hosts for WNV and demonstrate clinical disease and pathology that differs greatly from natural host infection. In

contrast, horses (a natural host) demonstrate similar clinical disease and pathological distribution of lesions that closely mimic natural WNV disease in humans. Thus the equine model is recognized as a highly useful tool to study WN encephalitis for the purpose of gaining insight into both horse and human WN disease.

The main hypothesis, that there are families of genes that are changed in a consistent manner in horses undergoing WN encephalitis was investigated. In the actually analysis of the microarray data, three subhypotheses were investigated to explore whether there was a difference in gene expression based on the state of exposure, immunity/survival, and location in the CNS. All three analyses demonstrated highly similar changes in the canonical pathways, functions, and transcripts. Because there was high amount of overlap in our findings from these analysis, and there were interactions between factors, either these findings support a generalized model of WNV encephalitis based on exposure status, recovery, and CNS pathology or the state of WN infection without regard to immunity and recovery has been primarily modeled.

This is entirely feasible because this model is one of grave overwhelming encephalitis. Thus subtle differences between noninfection and recovered WNV horses may not be appreciated based on the experiment design and analysis. Alternatively, It is possible that immunity from WN encephalitis after exposure is similar to a completely naïve, nonexposed state. Additionally, it is likely that the time of sample collection (21 days for vaccinated/exposed horses, 7-9 days for nonvaccinated/exposed horses) influenced gene expression in immune horses.

However, overall, it appears that horses that are exposed to WNV demonstrate similar changes in gene expression, which are highlighted by the changes in the

thalamus. These data indicate that measurement of changes in gene expression in the thalamus correspond to localization of the virus since the thalamus was a primary focus for viral localization in WN infection in these horses at the time of disease.[58, 59, 117] This allows for development of neuronal cell specific models for further investigations of the transcriptome and proteome of WNV infection.

A total of 17 neurological canonical pathways were identified across the three analyses, the majority of which were involved with signaling within the nervous system. The functions identified from these pathways mapped to mental disorders (bipolar affective disorder, Alzheimer's, schizophrenia, and depression) and degenerative neuropathies (progressive motor neuropathy, Huntington's disease, Parkinson's disease, neurodegeneration, amytrophic lateral sclerosis, and multiple sclerosis). These diseases are also highly associated abnormalities of transmitter and synaptic transmission in the thalamus and hypothalamus.

Neurotransmitter pathways were one of the top dysregulated pathways for all groups, including glutamate pathways. Glutamate is the primary excitatory neurotransmitter in the neurological system. Previous work has demonstrated that an excess of glutamate at the synaptic cleft can lead to apoptosis of neurons through glutamate excitotoxicity.[92-98] This can be caused by release of excessive levels of glutamate from the pre-synaptic neuron, downregulation of glutamate receptors on the post-synaptic neuron, and downregulation of glutamate uptake receptors. In this study, the nonvaccinated group of horses exposed to WNV demonstrated gene expression changes consistent with glutamate excitotoxicity. These included a decrease in the expression levels of NMDA glutamate receptors, metabotropic glutamate receptors,

kainate glutamate receptors, ionotropic glutamate receptors, and glutamate clearance receptors. Thus it appears that infection with WNV leads to a downregulation of glutamate receptors on the post-synaptic neuron as well as glutamate uptake receptors on glial cells. This may lead to an increase in glutamate levels in the synaptic cleft, apoptosis through glutamate excitotoxicity, and contribute to the neuropathology associated with WNV infection. Further study involving the detection and quantification of these transcripts from neuronal cells infected with WNV is necessary before any firm conclusions can be drawn.

Dopamine was another neurotransmitter pathway that was significantly changed in all three groups. Dopamine is a stimulatory neurotransmitter that functions, among other things, in the control of voluntary movement (lack of dopamine leads to the inability to control voluntary movement- Parkinson's-like syndrome with bradykinesia and incoordination).[158] In the nonvaccinated group of horses exposed to WNV, a decrease was seen in the expression levels of the DRD5 as well as the downstream affector transcripts AC, PC, and PP. In addition, tyrosine hydroxylase, which catalyzes the conversion of tyrosine to dopamine, was downregulated. The expression of monoamine oxidase (MAO), which functions to breakdown dopamine, was increased in the nonvaccinated exposed group. Thus exposure to WNV may lead to a decrease in dopaminergic receptors and subsequent downstream signaling, a decrease in enzymes to create dopamine, as well as an increase in MAO. This results in a total decrease in available dopamine, which may explain many of the clinical signs seen in WNV infection that seem to mimic human disorders such as Parkinson's disease. Again, further studies targeting the actual transcripts are necessary.

Clinical neurological disease in horses caused by WNV is characterized by a combination of spinal cord, midbrain/hindbrain, and mentation abnormalities. Specifically, a stiff stilted gate (perhaps similar to bradykinesia), ataxia, flaccid paralysis, paresis, recumbency, muscle fasciculations, cranial nerve abnormalities, changes in personality, and hyperesthesia are often noted. Long term in horses that recover, muscle wasting is often seen along with residual neurological deficits.[10] These clinical signs mimic many of the clinical signs seen in some human neurological disorders, including Parkinson's disease, progressive motor neuropathy, Huntington's disease, neurodegeneration, amytrophic lateral sclerosis, and multiple sclerosis. For this study, it was found that many of the pathways and transcripts previously shown to be dysregulated due to these diseases are also abnormally expressed during WNV infection. Thus neurological infection with WNV in horses appears to mimic many of the seemingly non-infectious neurological disorders seen in man. Why this occurs is not known. Perhaps the non-infectious neurological disorders actually have an origin in viral infection. Or perhaps the brain can only behave and react in a certain manner no matter the stimulus or insult. Regardless of the speculation as to why, this study was the first to demonstrate that infection with WNV leads to dysregulation in known neurological gene pathways, including those involved with neurotransmission and downstream signaling. This corresponds with clinical signs of disease in affected hosts, and also suggests a correlate between the neuropathology induced by viral infection of the CNS and the neuropathology seen in non-infectious neurological disease.

The similarities between the three analyses can also be seen when examining the immunological pathways and functions. Previous work in elucidating the

immunological pathways involved with WNV infection have focused on individual pathways, mainly involving the adaptive response. However, this is limiting in that a comprehensive picture of how the host responds to infection with different branches of the immunological system has not been formed. This study demonstrated that both an innate (inflammatory response, antigen presentation, immune cell trafficking) and adaptive (humoral immune response, cell-mediated immune response, cytotoxicity, immune cell trafficking) immune response are present in all analyses. In general, the majority of immune transcripts and pathways were downregulated in the nonvaccinated horses exposed to WNV. Thus there is evidence that a balanced immune response is downregulated during WNV infection at the peak of clinical disease.

In contrast, certain immune pathways appeared to be upregulated during WNV infection in nonvaccinated horses exposed to WNV. The Interleukin-15 signaling pathway is one of these pathways. IL-15 has been shown to stimulate CD8+ T cell and natural killer cell activation and proliferation; activate memory T cells; prevent apoptosis; and phosphorylate the JAK kinases and STAT3, STAT5, and STAT6.[159-162] IL-15 has been shown to be particularly important in providing a protective immune response to viral infection. This study was the first to provide evidence for the upregulation of the IL-15 pathway during WNV infection. For all three analyses, IL-15 was upregulated over 2-fold, as well as STAT1 (transcription factor) which was upregulated over 2-3 fold. Interestingly, the downstream elements of IL-15 were downregulated in the unvaccinated horses exposed to WNV. There could be many explanations for this. The virus could be blocking the downstream effector elements of the IL-15 pathway to prevent the host immune response to the virus. There could also be other elements in

the IL-15 pathway that are not yet elucidated. It is also possible that this finding is only a reflection of the timing when the naïve horses exposed to WNV were euthanized (at the onset of clinical signs) and a beneficial response from IL-15 to viral infection could not be realized in these horses. Thus it appears that IL-15 is upregulated in response to WNV infection, and while it may play a key role in recovery from viral infection, its dysregulation may be a key component of the immunopathology of this disease. Continued work targeting the quantification of IL-15 levels during viral infection at different time points is necessary for further clarification of this data.

Other pathways that were upregulated in non-vaccinated horses exposed to WNV were the IL-22, the IL-9, and the interferon signaling pathways with IL-22 and IL-9 activating similar transcripts. Both of these pathways activate JAK and TYR transcripts, which in turn phosphorylate and activate STAT (Signal Transducers and Activators of Transcription)- specifically STAT1, STAT3, and STAT5. These STAT transcripts induce the expression of ISGs (interferon stimulated genes) through a variety of mechanisms, and lead to the induction of an innate antiviral response.[163] As expected, expression of these JAK/STAT transcripts is upregulated during WNV infection in the unvaccinated horses exposed to WNV. Of interest as well is the finding that the SOCS3 (suppressor of cytokine signaling 3) is also upregulated in the exposure and survival analyses. SOCS3 functions as a negative feedback inhibitor on the JAK/STAT pathway, thereby inhibiting the innate immune response.[164] This has not been documented previously in WNV, but has been shown in other studies to be upregulated by viral infection[165, 166]. Upregulation of SOCS3 allows the virus to escape the innate immune response and has also been shown to lead to chronic infection and inflammation. Thus it is possible that

while the JAK/STAT pathway is upregulated in response to WNV infection for the activation of innate immunity, WNV may induce the expression of the SOCS3 molecule to suppress this pathway and evade the innate immune response.

Many transcripts identified as having various functions were also significantly dysregulated. One group included transcriptional regulators. Transcriptional regulators with increased expression included STAT1, IRF2, IRF3, ETV7, BATF, EOMES, ZNFX1, ATF3, and WWTR1. Understanding these transcripts is important for understanding how the host responds at the cellular level to WNV infection. The general transcriptional regulator, ETV7 may be involved in the cellular response to WNV, the immune response to WNV, or may be involved with WNV replication. The Th-17 response is regulated by BATF[167] and leads to inflammation and tissue injury, consistent with the clinicopathological findings due to WNV. The EOMES transcription factor has been shown to be stimulated by IL-2 and involved in the differentiation of CD8+ T-cells.[168] This is consistent with upregulation of the cellular immune response to WNV. Again, both ZNFX1 and WWTR1 are general transcription factors, inducing components of the immune system. The molecule ATF3 has been shown to be an early response gene that copes with cell stressors and can induce apoptosis,[169] possibly coinciding with the pathology of WNV in these analyses. And finally, STAT1, IRF2, and IRF3 are transcriptional regulators that are involved in the innate immune response to viral infection.[163] Besides the value of understanding the host response to infection, identifying the transcriptional genes that are upregulated during viral infection is important to understand how the virus itself may undergo transcription. The exact

mechanism of this process has yet to be identified, but recognizing the host transcriptional regulators that are upregulated is an important first step.

Downregulation of transcriptional regulators was also noted for all three analyses. These included ASB1, ASB5, SUB1, and NFIA. The ASBs function to suppress the SOCS (suppressor of cytokine signaling) transcripts. This coincides with the evidence of the upregulation of the SOCS3 transcript mentioned in the previous section to combat the innate immune response of the JAK/STAT pathway by the virus. The general transcriptional factor SUB1 (SUB1 homolog) is implicated in Huntington's disease. Downregulation of the nuclear factor, NFIA, (nuclear factor I/A) is notable in that it contradicts previous findings for upregulation during adenovirus transcription.

Other, nontranscriptional genes were also highly upregulated and downregulated. The most highly upregulated transcript for all analyses (9-fold for exposure, 7.7-fold for survival, and 4.2-fold for location) was PTX3 (pentraxin 3). This molecule has many functions, including an integral role in the pathway of pattern recognition receptors in recognition of viruses and bacteria.[170, 171] This gene is induced by IL-1b, and functions in the phagocytosis and opsonization of antigens, as well as in the inflammatory response. Thus infection with WNV and recovery from disease may be associated with an increase in this molecule that plays an integral role in innate immunity.

Another transcript that was highly upregulated in all analyses was CTNND2 – a brain-specific molecule- which functions to connect cell junctions and cytoskeletal architecture with signaling pathways.[172] This could provide evidence that dysregulation of neurological tissue, such as that induced during WNV infection, leads to re-

arrangement of neuronal architecture and the induction of signaling. This may also be important in viral entry into the cell.

A variety of single transcripts involved in the immune response were also upregulated in all analyses. These included DDX58, ZAP70, FCGR3A, C1R, CD8A, IL4I1, IL7, CD5L, CD4, CD3, and IL15 to name a few. Therefore the immune response appears to play a role in both infection with and recovery from WNV. Apoptotic transcripts were also upregulated in all analyses PARP and CASP4, while some apoptotic transcripts were upregulated in only the exposure analysis and these include RXR and, its receptor, RAR.

Understanding which transcripts are upregulated or downregulated during viral infection is important. This provides a glimpse into the affect of the virus on individual transcripts and, with further studies, could lead to the elucidation of many unanswered questions. Specifically, it may identify transcripts that are used by the virus to bind to and enter the cell. It may also identify the cellular components that the virus uses for transcription and translation. Because this study involved samples from the peak of infection and samples during the recovery phase from infection, transcripts that are universally upregulated are of particular import in identifying candidate biomarkers and important genes.

Future Work and Issues to be Addressed. The main limitation of this project was in the samples used for the study. This is particularly evident for the immune status/ survival analysis. For humane reasons, all horses demonstrating clinical signs of disease had to be euthanized immediately. Therefore samples were collected from non-vaccinated exposed horses at the height of clinical disease approximately 4-7 days

post-exposure. The samples collected from vaccinated horses exposed to WNV were taken 14 days post-exposure. Not only was the collection of the samples from each of these analyses at different points in the disease process, there was no ability to collect samples over time. Therefore, the interpretation of data is somewhat limited. Nonetheless in this model none of the protected horses exhibited clinical disease, virus was not isolated from any of these protected horses, nor was there evidence of significant pathology in these horses.

For the exposure analysis, the major limitation was the untreated horses. In the non-vaccinated, exposed analysis, all horses were age matched (all 1.5 years of age at euthanasia) and breed matched. In addition, the environment was controlled (confined to a research laboratory for the majority of their life). The untreated horses consisted of a more diverse population of individuals not matched for age (ranging from 1 year to geriatric) or for breed. The circumstances under which the individual animals lived were not controlled. Finally, the individuals were all being euthanized for different reasons (limb deformity, age, etc.) and one had a known enlargement of the pituitary gland. Thus there may have been an inherent variability in the horses and this may have introduced enough variability so limited detection of differences between normal horses and recovered horses occurred.

Another major limitation of the study involves the inherent problems with microarrays. There were problems with dye incorporation (likely a result of the chemistry of the manufacturer) such that multiple dye labeling experiments needed to be performed at times for certain samples. The probes on the arrays are only 60 oligonucleotides in length, yet transcripts will bind to the probes if there is a 25 base pair

match. Therefore there may be transcript interference when binding to some of the probes.

The last major limitation to be discussed is in the pathway analysis of the data. The IPA database is an excellent resource for building pathways and networks between transcripts of interest and identifying diseased states. However, the program is only as good as the databases that it references. Fewer than 25% of the significant genes in this study were actually identified by the IPA database. The only way in which to solve this problem would be to use a program with a larger database from which to design pathways and networks- a resource that is not yet available. In addition, the program is biased toward the diseases and pathways that are recognized in the software. For example, there may not actually be a "liver pathway" occurring in the brain, but because some of the transcripts that occur in the brain are recognized as similar or the same as those in the liver pathway, they will be mapped accordingly.

Future work with this project will involve continued analysis of the array expression data. This will include continuing to analyze the pathways, functions, and networks identified by the IPA database, as well as feeding this data into other pathway modeling tools. The array will also need to be validated with parallel experiments. Ideally, this would consist of performing a study with WNV in a different host (i.e. a mouse model of infection) and analyzing the gene expression of those tissues on the array. Other studies that would help to validate the array could include immunohistochemistry on molecules that are shown to be significantly upregulated or downregulated with fixed tissue specimens from the same horses. Finally, there are serum samples at different time points over the course of disease from the same horses

analyzed on the arrays. These samples could be used to identify significant biomarkers and to better understand peripheral gene expression over the time course of the disease.

Conclusions

For this portion of the project, the sequenced and annotated transcriptome of the equine CNS was used to create a 4 x 44,000 custom spotted oligonucleotide microarray. This array was used to analyze gene expression in the CNS to answer whether there was a difference in gene expression due to 1) exposure status to WNV (infected vs noninfected), 2) immune/survival from WNV infection, and 3. location in the brain during WNV infection. Statistical analysis was performed on the data to identify genes that were significantly up- or downregulated. Significant genes were then analyzed statistically utilizing a systems biology approach to detect interactions between genes to generate biological models of WNV infection and disease.

A large number of genes were identified as significant when looking at the three different analyses (9,020 for exposure, 7,395 for survival, and 7,649 for location). Gene ontological analysis was performed on the data from all three analyses. Most genes mapped to transcription/RNA processing (5,550) with the second most genes mapping to neurological categories (3,065) for all analyses. A large number of genes also mapped to immunological categories (2,631) and cell death/apoptosis (1,117).

The GO data was supported by the pathways analysis, which found the most genes modeled within signaling pathways, many of which were involved with transcription. After cell signaling (which was not specified to location) the majority of significant genes were modeled within neurological pathways and disease functions. This analysis indicates that components of both the glutamate and dopamine pathways

were down-regulated in the immunologically susceptible horses undergoing challenge to WNV. This findings provides preliminary evidence that glutamate excitotoxicity and dysregulation of the neurotransmitter, dopamine, likely contribute to the clinicopathological features of WNV. Many of the transcripts for all the analyses consisted of several components of previously characterized mental disorders and degenerative neuropathies. This may be evidence of simple overlap of functional processes in the brain or suggest a more complex relationship between viral infection of the CNS and the clinicopathological states of neuropsychiatric and neurodegenerative disorders.

The other major set of pathways that were shown to be dysregulated in this investigation were those involved in the immunological response. Components of both the innate and adaptive immune response were found in all comparative analyses. The majority of immunological pathways were downregulated in the non-vaccinated exposed horses compared to the others (as well as in the thalamus) providing evidence that rather than upregulation of normal protective immune responses in the naïve host, the virus likely interacts to block induction of several responses. Apoptosis was also upregulated in WNV susceptible host undergoing grave challenge, a finding consisting observed in vitro and in the rodent models, but with limited validation in the natural host undergoing infection.

Under grave WNV challenge, specific immunological and transcriptional pathways of note included upregulation of the IL-15 production and signaling pathways, the JAK/STAT pathway, and the SOCS3 transcripts. From this data, it may be hypothesized that induction of IL-15 may be part of the immunopathogenesis of grave

WNV infection. Further, it could be hypothesized that WNV blocks induction of immunity by induction of the suppressive SOCS pathway to downregulate JAK/STAT pathway induction of the host's cytokine responses.

Specific transcripts that were significantly upregulated and downregulated were also identified that may indicate dysregulation as part of the pathogenesis of disease. Transcription genes increased in expression involved in the immune response included STAT1, IRF2, IRF3, BATF, and EOMES. Transcription genes decreased in expression included NFIA, SUB1, ASB1, and ASB5.

Individual transcripts not involved in transcription were also upregulated by a significant amount. One was PTX3 (a C reactive protein) which has been shown to be involved in the pattern recognition response to viruses and bacteria. Whether or not this is part of antigen processing and presentation by macrophages or induced by other components of the immune response such as cytokines or cellular debris is an open question. The important gene, CTNND2, from which δ-catenin is derived is important in cell adhesion and dendritic growth. Whether or not induction of this gene is cause by the virus to aid infection or represents a physiological repair response in the virally injured CNS is another issue worthy of investigating. Understanding which of these transcripts that are upregulated or downregulated during viral infection and, which, of the corresponding proteins can be detected in plasma or serum may lead identification of candidate biomarkers. This study also provides initial validation of the array which can be continued by investigation of these pathways through generation of new hypotheses and study of the array under other diseases conditions.

In summary, the microarray proved to be a useful tool to understand changes in gene expression patterns during WNV infection. Significant changes were identified in transcriptional, neurological, immunological, and apoptotic pathways with associations made between viral encephalitis and non-infectious neurological disease based on a systems biology approach. Future work will involve further data mining and validation of the array, as well as the identification of transcripts and pathways that can be targeted for therapeutics and diagnostics.

Table 4-1. Probe groups for inclusion on the microarray

Probe group	# of probes	Replicates
Important	3,883	1
Annotated	28,600	1
Annotated_minus	1,567	1
Unannotated	3,906	1
Recovered_genome	5,444	1
Control	250	1

Note: Probes were included on the array once in the 'plus' (5'-3') orientation (Annotated). Probes were individually selected to be included twice on the array (Important analyse) and included sequences involved in neurological, immunological, and transcriptional processes, as well as cell death. Probes that were determined to be correctly oriented in the 'minus' (3'-5') direction were included in Annotated_minus. Unannotated probes and probes recovered from the EqCab2 genome sequencing project were also included. 250 Agilent controls were incorporated.

Table 4-2. Samples used to obtain RNA for dye-labeling and hybridization to the array

Sample category (n)	Sample type (#)	Experiment specifics
Vaccinated/Immune + Exposed (n = 6)	Thalamus (6) Cerebrum (6)	Day 0- non control horses vaccinated[A] Day 365- challenged with WNV[B] intrathecally Day 365-386- monitored for clinical signs Day 386 (21 days PI)- euthanasia, necropsy, tissue collection
Unvaccinated/Non-immune + Exposed (n = 6)	Thalamus (6) Cerebrum (6)	Day 0- mock vaccination Day 365- challenged with WNV[B] intrathecally Day 365-374- monitored for clinical signs Day 372-374 (7-9 days PI)- euthanasia, necropsy, tissue collection
Untreated (n = 6)	Thalamus (6) Cerebrum (6)	Normal Horse

[A]Live-chimera WNV vaccine containing the prM and E proteins of WNV expressed in a YF17D vector

[B]WNV NY99 strain 10^5 pfu/mL

Note: Horses from three analyses (vaccinated/exposed to WNV, nonvaccinated/exposed to WNV, and untreated) were used in the study. RNA was extracted from the cerebrum and thalamus from each of the horses (total of 36 samples) and used to create Cy3 dye-labeled samples that were hybridized to the arrays.

Table 4-3. Samples and analyses for the array

Analysis	Samples	Tissue type	Exposed to WNV?
Exposure Status	Not vaccinated- 6 horses	Thalamus	X
	Untreated- 6 horses	Thalamus	
Survival/Immune Status	Not vaccinated- 6 horses	Thalamus	X
	Vaccinated- 6 horses	Thalamus	X
CNS Location	Not vaccinated- 6 horses	Thalamus	X
	Not vaccinated- 6 horses	Cerebrum	X

Note: A total of 12 tissues were compared for each of the analyses/questions asked. The questions included determining if there was a difference in gene expression due to exposure to WNV, recovery from WNV infection, and location in the brain.

Table 4-4. Number of significant genes for each analysis

Analyses	Samples	Before duplicate removal	After duplicate removal
Exposure Status	Nonvaccinate vs Control	12,029	9,020
Survival/Immune Status	Nonvaccinate vs Vaccinate	9,978	7,395
CNS Location	Nonvaccinate Cerebrum vs Thalamus	10,555	7,649

Note: The number of significant genes for each analyse (with and without duplicate removal) was determined. An ANOVA with interactions ($p<0.05$) was used to determine significance.

Table 4-5. Canonical pathways for all analyses

	Exposure status		Survival/Immune status		CNS location	
Canonical Pathways	-log(p-value)	Transcripts	-log(p-value)	Transcripts	-log(p-value)	Transcripts
α-Adrenergic Signaling	1.89E+00	11	2.21E+00	11	4.35E+00	14
Amyotrophic Lateral Sclerosis Signaling*	1.75E+00	12	1.64E+00	14	4.75E+00	15
Antiproliferative Role of Somatostatin Receptor 2					3.49E+00	11
Axonal Guidance Signaling*			1.84E+00	29		
β-alanine Metabolism	1.93E+00	8				
Breast Cancer Regulation by Stathmin1					4.95E+00	23
Butanoate Metabolism	1.55E+00	8				
Calcium Signaling			2.68E+00	21		
Calcium Signaling					3.45E+00	19
cAMP-mediated Signaling	1.71E+00	18	2.75E+00	18	4.04E+00	19
Cardiac β-adrenergic Signaling	1.99E+00	16	2.52E+00	16	5.05E+00	18
Caveolar-mediated Endocytosis Signaling			1.75E+00	8		
CDK5 Signaling*	1.89E+00	11	1.76E+00	9		
Corticotropin Releasing Hormone Signaling	1.55E+00	13	2.36E+00	13		
CREB Signaling in Neurons*	2.41E+00	19	2.84E+00	21	6.23E+00	24
CXCR4 Signaling^					3.71E+00	18
Dopamine Receptor Signaling*	2.41E+00	11	1.72E+00	8		
EGF Signaling					3.92E+00	9
Endothelin-1 Signaling	2.07E+00	19			4.08E+00	20
G Beta Gamma Signaling	1.78E+00	11	2.11E+00	11	4.18E+00	14
Glutamate Receptor Signaling*	1.70E+00	9	5.02E+00	15	5.77E+00	13
GNRH Signaling	1.90E+00	15				
G-Protein Coupled Receptor Signaling			3.40E+00	24	7.28E+00	29
IL-10 Signaling^	1.62E+00	8				
Leptin Signaling in Obesity			2.77E+00	11		

Table 4-5. Continued

	Exposure status		Survival/Immune status		CNS location	
Canonical Pathways	-log(p-value)	Transcripts	-log(p-value)	Transcripts	-log(p-value)	Transcripts
Leukocyte Extravasation Signaling^			1.73E+00	17	4.38E+00	22
Melatonin Signaling			2.40E+00	11		
Molecular Mechanisms of Cancer			2.88E+00	31	3.82E+00	31
Neuregulin Signaling*					5.60E+00	16
Neuropathic Pain Signaling In Dorsal Horn Neurons*			3.44E+00	17	7.30E+00	19
Phenylalanine Metabolism	1.75E+00	6				
Phospholipase C Signaling	1.57E+00	22				
PPARα/RXRα Activation	1.73E+00	17				
Protein Kinase A Signaling			1.65E+00	26		
Rac Signaling					3.60E+00	14
Relaxin Signaling			2.40E+00	15	5.39E+00	19
Renin-Angiotensin Signaling	1.75E+00	12			4.16E+00	15
Role of NFAT in Cardiac Hypertrophy					4.09E+00	21
Role of NFAT in Regulation of the Immune Response^	1.71E+00	17				
SAPK/JNK Signaling	1.78E+00	11				
Semaphorin Signaling in Neurons*			2.05E+00	7		
Sphingosine-1-phosphate Signaling			1.78E+00	11		
Synaptic Long Term Depression*	1.82E+00	18	2.84E+00	20	5.21E+00	20
Synaptic Long Term Potentiation*	1.75E+00	12	2.60E+00	16	6.03E+00	18
Thrombin Signaling	2.14E+00	22	2.28E+00	20	4.28E+00	22
Valine, Leucine and Isoleucine Degradation	1.71E+00	9				

Note: All significant canonical pathways for all analyses are listed. The * denotes pathways involved with the nervous system (11), while the ^ denotes pathways involved with the immunological response (4).

Table 4-6. Functions for all analyses

Function Category	Transcripts Exposure Status	Transcripts Survival/Immune Status	Transcripts CNS Location
Amino Acid Metabolism	61	75	178
^Antigen Presentation	2		8
*Auditory and Vestibular System Development and Function		7	
*Auditory Disease			12
*Behavior	237	195	301
Cancer	648	918	893
Carbohydrate Metabolism	61	48	4
Cardiovascular Disease	744	505	618
Cardiovascular System Development and Function	61	37	44
Cell Cycle	174	239	390
^Cell Death	1153	1082	719
Cell Morphology	214	230	326
Cell Signaling	107	60	164
^Cell-mediated Immune Response	42	42	25
Cell-To-Cell Signaling and Interaction	361	453	455
Cellular Assembly and Organization	364	319	420
Cellular Compromise	32	11	8
Cellular Development	375	270	501
Cellular Function and Maintenance	140	63	104
Cellular Growth and Proliferation	806	721	424
Cellular Movement	546	671	699
Connective Tissue Development and Function	71	31	16
Connective Tissue Disorders	562	435	506
Dermatological Diseases and Conditions	20	11	18
Developmental Disorder	22	12	14
DNA Replication, Recombination, and Repair	46	16	35
Drug Metabolism		4	2
Embryonic Development	28	22	16
Endocrine System Development and Function		5	7
Endocrine System Disorders	518	502	566
Gastrointestinal Disease	404	345	328
Gene Expression	130	404	18
Genetic Disorder	1544	1269	1498
Hair and Skin Development and Function	2	2	4
Hematological Disease	12	22	13
Hematological System Development and Function	169	318	217
Hematopoiesis	40	81	50
Hepatic System Development and Function	3	3	

Table 4-6. Continued

Function Category	Transcripts Exposure Status	Transcripts Survival/Immune Status	Transcripts CNS Location
Hepatic System Disease	13	13	
^Humoral Immune Response	20	18	29
^Hypersensitivity Response	7		
^Immune Cell Trafficking	16	6	24
^Immunological Disease	575	569	577
^Infection Mechanism	12	21	3
^Infectious Disease	164	54	58
^Inflammatory Disease	965	798	824
^Inflammatory Response	27	34	10
Lipid Metabolism	52	27	4
Lymphoid Tissue Structure and Development	7	2	
Metabolic Disease	547	524	573
Molecular Transport	176	132	239
*Nervous System Development and Function	578	670	981
*Neurological Disease	1316	1210	1626
Nucleic Acid Metabolism	59	6	16
Ophthalmic Disease	2	2	18
Organ Development	36	14	64
Organ Morphology	24	9	20
Organismal Development	2	8	2
Organismal Functions	13	15	25
Organismal Injury and Abnormalities	11	16	61
Organismal Survival	155	140	126
Post-Translational Modification	2	200	238
*Psychological Disorders	195	164	322
Renal and Urological Disease	2		19
Renal and Urological System Development and Function	7	2	
Reproductive System Development and Function	6	2	2
Reproductive System Disease	2	3	63
Respiratory Disease	2	53	6
Respiratory System Development and Function		3	
RNA Post-Transcriptional Modification	2	4	
Skeletal and Muscular Disorders	886	728	793
Skeletal and Muscular System Development and Function	92	39	14
Small Molecule Biochemistry	181	129	206
Tissue Development	102	245	234
Tissue Morphology	45	58	11
Tumor Morphology		5	18

Table 4-6. Continued

Function Category	Transcripts Exposure Status	Transcripts Survival/Immune Status	Transcripts CNS Location
Vitamin and Mineral Metabolism	24	14	64

Note: The number of transcripts for significant functions for all analyses are listed. The * denotes functions involved with the nervous system (6) while the ^ denotes functions involved with the immunological system (11).

Table 4-7. Transcriptional regulators with increased expression

Symbol	Entrez gene name	GenBank	Location	Fold change exposure status	Fold change survival/immune status	Fold change CNS location
ALX3	ALX homeobox 3	NM_006492	Nucleus	2.05		
ANKFY1	Ankyrin repeat and FYVE domain containing 1	XM_511280	Nucleus	1.329	1.508	1.017
ATF3	Activating transcription factor 3	NM_001046193	Nucleus	3.255	4.896	2.049
ATF6	Activating transcription factor 6	XM_513949	Cytoplasm		1.225	
BATF	Basic leucine zipper transcription factor, ATF-like	BC032294	Nucleus	5.086	4.364	2.596
BHLHE41	Basic helix-loop-helix family, member e41	NM_001002973	Nucleus			1.421
BLZF1	Basic leucine zipper nuclear factor 1	XM_001136772	Cytoplasm	1.103		
CSDA	Cold shock domain protein A	NM_003651	Nucleus	2.243	3.216	1.808
CTNNB1	Catenin (cadherin-associated protein), beta 1, 88kda	XM_845101	Nucleus			1.126
DDX54	DEAD (Asp-Glu-Ala-Asp) box polypeptide 54	XM_001152033	Nucleus	1.207		
ELF1	E74-like factor 1 (ets domain transcription factor)	XM_852043	Nucleus		1.163	1.872
ELK1	ELK1, member of ETS oncogene family	XM_548979	Nucleus	1.242		
ELK3	ELK3, ETS-domain protein (SRF accessory protein 2)	XM_001146216	Nucleus	1.871	1.151	1.465
EOMES	Eomesodermin homolog (Xenopus laevis)	XM_001165845	Nucleus	3.849	3.344	
ETV6	Ets variant 6	NM_001987	Nucleus		1.07	
ETV7	Ets variant 7	XM_001172937	Nucleus	5.863	6.179	2.475
FOXP2	Forkhead box P2	NM_014491	Nucleus			1.598

Table 4-7. Continued

Symbol	Entrez gene name	GenBank	Location	Fold change exposure status	Fold change survival/immune status	Fold change CNS location
GBX2	Gastrulation brain homeobox 2	XM_543300	Nucleus		1.721	3.717
GTF2E1	General transcription factor IIE, polypeptide 1, alpha 56kda	NM_001103294	Nucleus		1.51	1.872
ID4	Inhibitor of DNA binding 4, dominant negative helix-loop-helix protein	XM_001170946	Nucleus			1.363
IKZF2	IKAROS family zinc finger 2 (Helios)	NM_016260	Nucleus		1.414	
IRF2	Interferon regulatory factor 2	XM_532847	Nucleus	2.61	1.797	
IRF3	Interferon regulatory factor 3	AK292027	Nucleus	1.31	1.935	1.086
IRX1	Iroquois homeobox 1	XM_001251876	Nucleus			5.101
IRX3	Iroquois homeobox 3	NM_001104996	Nucleus			3.398
IRX4	Iroquois homeobox 4	NM_001098466	Nucleus	1.02		
ISL1	ISL LIM homeobox 1	XM_001150633	Nucleus			2.327
JUNB	Jun B proto-oncogene	NM_001075656	Nucleus	2.201	2.017	
KHDRBS1	KH domain containing, RNA binding, signal transduction associated 1	CU210913	Nucleus	1.116		
KLF6	Kruppel-like factor 6	AK151769	Nucleus		1.746	
LASS2	LAG1 homolog, ceramide synthase 2	NM_001034667	Nucleus			1.029
LBH	Limb bud and heart development homolog (mouse)	NM_001099152	Nucleus	2.376	2.11	1.208
LRRFIP1	Leucine rich repeat (in FLII) interacting protein 1	BC083492	Nucleus		1.42	1.516
MAX	MYC associated factor X	XM_847808	Nucleus	1.087	1.382	
MED21	Mediator complex subunit 21	XM_534858	Nucleus	1.056	1.001	

Table 4-7. Continued

Symbol	Entrez gene name	GenBank	Location	Fold change exposure status	Fold change survival/immune status		Fold change CNS location
MYB (includes EG:4602)	V-myb myeloblastosis viral oncogene homolog (avian)	D26147	Nucleus		1.557	1.081	
NCOA3	Nuclear receptor coactivator 3	XM_543039	Nucleus		1.112		
NFE2L2	Nuclear factor (erythroid-derived 2)-like 2	XM_857112	Nucleus			1.037	1.337
NFIC	Nuclear factor I/C (CCAAT-binding transcription factor)	XM_542179	Nucleus		1.626		
NFIL3	Nuclear factor, interleukin 3 regulated	NM_001075240	Nucleus		1.802	2.263	1.836
NFKBIE	Nuclear factor of kappa light polypeptide gene enhancer in B-cells inhibitor, epsilon	XM_583214	Nucleus			1.482	
PAX3	Paired box 3	AC118213	Nucleus		2.534		
PAX4	Paired box 4	NM_006193	Nucleus		2.674		
PRRX1	Paired related homeobox 1	NM_006902	Nucleus			1.319	1.421
PURA	Purine-rich element binding protein A	XM_001251355	Nucleus		1.225		
REL	V-rel reticuloendotheliosis viral oncogene homolog (avian)	XM_531836	Nucleus		1.124	1.88	2.204
SAP30	Sin3A-associated protein, 30kda	XM_843990	Nucleus		1.382	1.973	1.588
SFRS2	Splicing factor, arginine/serine-rich 2	XM_852679	Nucleus		1.075		
SHOX2	Short stature homeobox 2	AK145063	Nucleus				3.957
SIM2	Single-minded homolog 2 (Drosophila)	XM_001169429	Nucleus		1.408		
SOX10	SRY (sex determining region Y)-box 10	DQ896471	Nucleus				1.049
SOX2	SRY (sex determining region Y)-box 2	XM_516895	Nucleus				1.016

Table 4-7. Continued

Symbol	Entrez gene name	GenBank	Location	Fold change exposure status	Fold change survival/immune status	Fold change CNS location
SP1	Sp1 transcription factor	XM_509098	Nucleus	1.155	1.625	1.364
ST18	Suppression of tumorigenicity 18 (breast carcinoma) (zinc finger protein)	XM_001148965	Nucleus			1.307
STAT1	Signal transducer and activator of transcription 1, 91kda	BC151378	Nucleus	3.021	3.763	2.384
TARBP1 (includes EG:6894)	TAR (HIV-1) RNA binding protein 1	XM_514281	Nucleus		1.041	
TCF12	Transcription factor 12	NM_001077885	Nucleus			1.157
TEAD1	TEA domain family member 1 (SV40 transcriptional enhancer factor)	XM_001171565	Nucleus	1.786		1.319
TGIF2	TGFB-induced factor homeobox 2	NM_021809	Nucleus			1.11
TP73	Tumor protein p73	XM_593064	Nucleus	1.171		
TTF2	Transcription termination factor, RNA polymerase II	XM_513683	Nucleus	1.17	1.74	
VGLL2	Vestigial like 2 (Drosophila)	BC118622	Nucleus		2.693	
WWTR1	WW domain containing transcription regulator 1	XM_847454	Nucleus	3.107	2.939	2.33
ZFP57	Zinc finger protein 57 homolog (mouse)	NM_001109809	Nucleus			1.025
ZIC1	Zic family member 1 (odd-paired homolog, Drosophila)	XM_516806	Nucleus			1.836
ZNFX1	Zinc finger, NFX1-type containing 1	XM_534452	Nucleus	3.531	3.311	1.255

Note: Transcriptional transcripts upregulated by 1-fold or greater for all analyses.

Table 4-8. Transcriptional regulators with increased expression

Symbol	Entrez gene name	GenBank	Location	Fold change exposure status	Fold change survival/ immune status	Fold change CNS location
AFF3	AF4/FMR2 family, member 3	XM_001161010	Nucleus	-1.068		-1.474
ANKIB1	Ankyrin repeat and IBR domain containing 1	XM_844926	Nucleus	-1.194		
ANKRD54	Ankyrin repeat domain 54	XM_538382	Nucleus		-1.217	-1.074
ARID4A	AT rich interactive domain 4A (RBP1-like)	XM_859819	Nucleus	-1.76	-2.145	-2.296
ARNT2	Aryl-hydrocarbon receptor nuclear translocator 2	AC101776	Nucleus	-2.328	-1.231	-1.274
ARX	Aristaless related homeobox	XM_854885	Nucleus			-1.721
ASB1	Ankyrin repeat and SOCS box-containing 1	XM_516189	Nucleus	-2.439		-1.24
ASB5	Ankyrin repeat and SOCS box-containing 5	NM_001075744	Nucleus		-1.292	
BCL11A	B-cell CLL/lymphoma 11A (zinc finger protein)	NM_022893	Nucleus			-1.539
BCLAF1	BCL2-associated transcription factor 1	XM_855478	Nucleus	-1.121		
CAND1	Cullin-associated and neddylation-dissociated 1	XM_531667	Cytoplasm		-1.104	
CASKIN1	CASK interacting protein 1	XM_848538	Nucleus		-1.253	-1.474
CBFA2T2	Core-binding factor, runt domain, alpha subunit 2; translocated to, 2	XM_606138	Nucleus		-1.097	-1.196
CBFA2T3	Core-binding factor, runt domain, alpha subunit 2; translocated to, 3	XM_546780	Nucleus	-1.112		
CLIP2	CAP-GLY domain containing linker protein 2	XM_583422	Cytoplasm	-1.084	-1.056	-1.116
CREBL2	Camp responsive element binding protein-like 2	XM_001153386	Nucleus	-1.359		
CREG1	Cellular repressor of E1A-stimulated genes 1	NM_001075942	Nucleus	-1.883		
CRTC1	CREB regulated transcription coactivator 1	XM_866768	Nucleus		-1.268	-1.098
CUX2	Cut-like homeobox 2	BC151245	Nucleus			-2.455
EBF1	Early B-cell factor 1	CU012046	Nucleus	-1.014		
EGR4	Early growth response 4	XM_540228	Nucleus		-2.667	-3.288
ETV5	Ets variant 5	NM_004454	Nucleus		-1.36	-1.263

Table 4-8. Continued

Symbol	Entrez gene name	GenBank	Location	Fold change exposure status	Fold change survival/ immune status	Fold change CNS location
FBXW7	F-box and WD repeat domain containing 7	NM_018315	Nucleus			-2.149
FOXG1	Forkhead box G1	NM_005249	Nucleus		-3.475	-5.43
FOXO1	Forkhead box O1	NM_002015	Nucleus		-1.012	
FOXO4	Forkhead box O4	XM_529032	Nucleus	-1.942	-1.496	
GBX2	Gastrulation brain homeobox 2	XM_543300	Nucleus	-1.602		
GRLF1	Glucocorticoid receptor DNA binding factor 1	NM_004491	Nucleus			-1.153
HIVEP2	Human immunodeficiency virus type I enhancer binding protein 2	XM_518773	Nucleus			-1.097
HTATSF1	HIV-1 Tat specific factor 1	EU176345	Nucleus	-1.341		
ID4	Inhibitor of DNA binding 4, dominant negative helix-loop-helix protein	XM_001170946	Nucleus	-1.647		
JMY	Junction mediating and regulatory protein, p53 cofactor	NM_152405	Nucleus		-1.662	
KIDINS220	Kinase D-interacting substrate, 220kda	XM_532865	Nucleus	-1.676	-1.505	-1.016
LCOR	Ligand dependent nuclear receptor corepressor	XM_584325	Nucleus		-1.23	
LHX5	LIM homeobox 5	NM_001102061	Nucleus		-1.487	
MED16	Mediator complex subunit 16	XM_849586	Nucleus		-1.48	
MEF2B	Myocyte enhancer factor 2B	NM_001103231	Nucleus	-2.336		
MEIS2	Meis homeobox 2	NM_170674	Nucleus		-2.279	
MEOX2	Mesenchyme homeobox 2	NM_001098045	Nucleus		-1.714	-2.945

Table 4-8. Continued

Symbol	Entrez gene name	GenBank	Location	Fold change exposure status	Fold change survival/ immune status	Fold change CNS location
MLL2	Myeloid/lymphoid or mixed-lineage leukemia 2	XM_543684	Nucleus			-1.004
MYCN	V-myc myelocytomatosis viral related oncogene, neuroblastoma derived (avian)	XM_540091	Nucleus	-1.166	-1.441	-1.682
MYOCD	Myocardin	AL669846	Nucleus		-2.41	-1.62
MYT1L	Myelin transcription factor 1-like	NM_001093776	Nucleus			-2.568
NAB1	NGFI-A binding protein 1 (EGR1 binding protein 1)	AC006460	Nucleus	-1.929	-1.809	
NFIA	Nuclear factor I/A	XM_536691	Nucleus	-2.799	-1.243	
NFIB	Nuclear factor I/B	XM_531936	Nucleus	-1.524	-1.168	
NFIX	Nuclear factor I/X (CCAAT-binding transcription factor)	XM_862151	Nucleus	-1.043	-1.16	-1.198
NKX2-8	NK2 homeobox 8	XM_584660	Nucleus	-2.093		
NPAS4	Neuronal PAS domain protein 4	XM_540832	Nucleus		-1.881	-2.893
PBX1	Pre-B-cell leukemia homeobox 1	XM_001174513	Nucleus	-2.117	-1.794	-1.64
PIAS2	Protein inhibitor of activated STAT, 2	XM_612798	Nucleus		-1.014	
PROX1	Prospero homeobox 1	BX928753	Nucleus			-1.367
RAI14	Retinoic acid induced 14	XM_001151240	Nucleus			-1.081
RBM9	RNA binding motif protein 9	NM_001082579	Nucleus			-1.303
RERE	Arginine-glutamic acid dipeptide (RE) repeats	XM_536734	Nucleus		-1.17	
RFC1	Replication factor C (activator 1) 1, 145kda	AY600371	Nucleus	-2.124		
RNF112	Ring finger protein 112	XM_546649	Nucleus		-2.082	-1.936

Table 4-8. Continued

Symbol	Entrez gene name	GenBank	Location	Fold change exposure status	Fold change survival/ immune status	Fold change CNS location
RNF14	Ring finger protein 14	NM_001081540	Nucleus	-1.112		
SIN3B	SIN3 homolog B, transcription regulator (yeast)	XM_847635	Nucleus		-1.559	
SMAD4	SMAD family member 4	AC091551	Nucleus	-1.72	-1.399	
SMAD7	SMAD family member 7	XM_512124	Nucleus	-1.416		
SMAD9	SMAD family member 9	XM_001144071	Nucleus		-1.053	
SOX10	SRY (sex determining region Y)-box 10	DQ896471	Nucleus	-1.251		
SOX6	SRY (sex determining region Y)-box 6	AC068405	Nucleus		-1.351	
SP4	Sp4 transcription factor	XM_527679	Nucleus		-1.065	
SPEN	Spen homolog, transcriptional regulator (Drosophila)	XM_591419	Nucleus	-1.019		
SRF	Serum response factor (c-fos serum response element-binding transcription factor)	XM_847209	Nucleus		-1.177	
SRY	Sex determining region Y	AC146189	Nucleus		-1.397	
SS18L1	Synovial sarcoma translocation gene on chromosome 18-like 1	NM_001078095	Nucleus	-1.89	-1.064	-1.138
SUB1	SUB1 homolog (S. Cerevisiae)	NM_001105407	Nucleus	-3.347	-2.235	-2.353
TCEA2	Transcription elongation factor A (SII), 2	XM_001152936	Nucleus		-1.104	-1.116
TCF4	Transcription factor 4	NM_003199	Nucleus	-1.122		-1.255
TCF7L2 (includes EG:6934)	Transcription factor 7-like 2 (T-cell specific, HMG-box)	AL158212	Nucleus			-1.027
TLE2	Transducin-like enhancer of split 2 (E(sp1) homolog, Drosophila)	NM_003260	Nucleus	-1.051		-1.182

Table 4-8. Continued

Symbol	Entrez gene name	GenBank	Location	Fold change exposure status	Fold change survival/ immune status	Fold change CNS location
TSHZ1	Teashirt zinc finger homeobox 1	XM_533368	Nucleus		-1.13	
TULP4	Tubby like protein 4	BC152476	Cytoplasm			-1.67
YY1	YY1 transcription factor	XM_510162	Nucleus	-1.186	-1.383	-1.206
ZEB1	Zinc finger E-box binding homeobox 1	XM_615192	Nucleus	-1.093		
ZEB2	Zinc finger E-box binding homeobox 2	AY029472	Nucleus	-2.033	-1.285	
ZFP57	Zinc finger protein 57 homolog (mouse)	NM_001109809	Nucleus	-2.323		
ZIC1	Zic family member 1 (odd-paired homolog, Drosophila)	XM_516806	Nucleus	-2.372		
ZMYND8	Zinc finger, MYND-type containing 8	XM_866938	Nucleus			-1.082
ZNF219	Zinc finger protein 219	XM_867319	Nucleus	-1.162		
ZNF398	Zinc finger protein 398	AK290499	Nucleus		-1.446	

Note: Transcriptional genes downregulated by -1-fold or less for all analyses.

Table 4-9. Transcripts for all analyses mapped to neurological CPs

	Exposure Status		Survival/Immune Status		CNS Location	
	Decreased	Increased	Decreased	Increased	Decreased	Increased
Agrin Interactions at Neuromuscular Junction	1	4	2	2	2	4
Amyloid Processing	4	1	3	1	3	3
Amyotrophic Lateral Sclerosis Signaling	11	1	14	0	13	2
Axonal Guidance Signaling	25	6	22	7	19	10
CDK5 Signaling	11	0	9	0	10	2
Cholecystokinin/Gastrin-mediated Signaling	5	2	7	2	6	1
Circadian Rhythm Signaling	2	1	4	1	5	1
CNTF Signaling	1	2	2	1	4	3
CREB Signaling in Neurons	15	4	19	2	20	4
Docosahexaenoic Acid (DHA) Signaling			2	0	2	1
Dopamine Receptor Signaling	10	1	6	2	6	2
GABA Receptor Signaling	6	0	6	0	8	0
Glutamate Receptor Signaling	8	1	15	0	12	1
GNRH Signaling	12	3	11	1	13	2
Huntington's Disease Signaling	10	5	8	5	12	7
Melatonin Signaling	6	1	10	1	8	1
Neuregulin Signaling			6	3	10	6
Neuropathic Pain Signaling In Dorsal Horn Neurons	8	2	16	1	17	2
Neurotrophin/TRK Signaling	5	0	4	0	6	2
Reelin Signaling in Neurons	4	2	3	3	5	5

Table 4-9. Continued

	Exposure Status		Survival/Immune Status		CNS Location	
	Decreased	Increased	Decreased	Increased	Decreased	Increased
Regulation of Actin-based Motility by Rho			3	2		
Semaphorin Signaling in Neurons	6	1	5	2	2	1
Serotonin Receptor Signaling	1	1	0	2	1	1
Synaptic Long Term Depression	14	4	17	3	17	3
Synaptic Long Term Potentiation	11	1	15	1	17	1
Total	176	43	209	42	218	65

Note: This table shows the number of transcripts that mapped to each pathway for all analyses. The majority of the transcripts demonstrated a decrease in expression values. Transcripts were included if they demonstrated a fold change >1 or <-1.

Table 4-10. Transcripts in glutamate signaling pathway for all analyses

Symbol	Entrez Gene Name	GenBank	Fold change exposure status	Fold change survival/ immune status	Fold change CNS location
CAMK4	Calcium/calmodulin-dependent protein kinase IV	XM_517873		-1.976	
GLS	Glutaminase	AC005540		-1.009	
GNB1	Guanine nucleotide binding protein (G protein), beta polypeptide 1	BC004186	-1.638		
GNG5	Guanine nucleotide binding protein (G protein), gamma 5	BC003563			1.359
GRIA1	Glutamate receptor, ionotropic, AMPA 1	XM_001169416	-1.398	-1.057	-1.498
GRIA2	Glutamate receptor, ionotropic, AMPA 2	NM_000826		-1.505	-1.643
GRIA3	Glutamate receptor, ionotrophic, AMPA 3	NM_007325		-2.33	-2.719
GRIA4	Glutamate receptor, ionotrophic, AMPA 4	NM_000829	1.253		-1.039
GRID2	Glutamate receptor, ionotropic, delta 2	AC022317		-1.581	
GRIK1	Glutamate receptor, ionotropic, kainate 1	NM_000830	-1.098	-1.933	-2.626
GRIK2	Glutamate receptor, ionotropic, kainate 2	XM_866973		-1.533	
GRIN1	Glutamate receptor, ionotropic, N-methyl D-aspartate 1	AF015731		-1.949	-1.487
GRIN2A	Glutamate receptor, ionotropic, N-methyl D-aspartate 2A	XM_547132	-2.836	-1.631	-2.369
GRIN2B	Glutamate receptor, ionotropic, N-methyl D-aspartate 2B	AC007535		-1.563	-1.989
GRIN3A	Glutamate receptor, ionotropic, N-methyl-D-aspartate 3A	XM_862276			-1.032
GRIP1	Glutamate receptor interacting protein 1	XM_001162097		-1.23	
GRM8	Glutamate receptor, metabotropic 8	AC079957	-1.856		
HOMER1	Homer homolog 1 (Drosophila)	XM_001139767			-1.084
HOMER3	Homer homolog 3 (Drosophila)	XM_541929	-1.718	-1.134	

Table 4-10. Continued

Symbol	Entrez Gene Name	GenBank	Fold change exposure status	Fold change survival/ immune status	Fold change CNS location
SLC17A7	Solute carrier family 17 (sodium-dependent inorganic phosphate cotransporter), member 7	NM_001098046	-1.598	-2.652	-8.147
SLC1A2	Solute carrier family 1 (glial high affinity glutamate transporter), member 2	NM_004171	-1.639	-2.869	-2.278

Note: The transcripts significantly changed in the glutamate signaling pathway are shown for all three analyses. The transcripts were mainly glutamate receptors, although other components of the pathway, such as glutamate re-uptake receptors, are also present. Almost all transcripts are downregulated, providing evidence that glutamate excitotoxicity may be present and damaging the neurons. Transcripts were included if they demonstrated a fold change >1 or <-1.

Table 4-11. Transcripts in dopamine signaling pathways for all analyses

Symbol	Entrez Gene Name	GenBank	Fold change exposure status	Fold change survival/ immune status	Fold change CNS location
ADCY1	Adenylate cyclase 1 (brain)	NM_174229		-1.789	-1.898
ADCY2	Adenylate cyclase 2 (brain)	XM_851103	-1.683	-1.223	-2.027
ADCY5	Adenylate cyclase 5	NM_183357	-1.258	-1.379	
ADCY8	Adenylate cyclase 8 (brain)	XM_539166	-1.021		-1.954
ADCY9	Adenylate cyclase 9	BC151229			-1.46
DRD5	Dopamine receptor D5	XM_604584	-1.097		
GCH1	GTP cyclohydrolase 1	XM_846790		1.296	
IL4I1	Interleukin 4 induced 1	AY358933	3.176	3.265	1.405
PPP1R14A	Protein phosphatase 1, regulatory (inhibitor) subunit 14A	XM_867134	-2.083		
PPP1R3C	Protein phosphatase 1, regulatory (inhibitor) subunit 3C	BT030698	-2.27	-1.746	-1.686
PPP2R2B	Protein phosphatase 2 (formerly 2A), regulatory subunit B, beta isoform	XM_001159292	-2.348		1.14
PPP2R2C	Protein phosphatase 2 (formerly 2A), regulatory subunit B, gamma isoform	XM_001250700	-1.243	-1.378	-1.446
PRKACB	Protein kinase, camp-dependent, catalytic, beta	XM_862471		-2.225	
PRKAR2B	Protein kinase, camp-dependent, regulatory, type II, beta	XM_001148361	-1.627		
TH	Tyrosine hydroxylase	BC149072	-2.857		

Note: The transcripts significantly changed in the dopamine signaling pathway are shown for all three analyses. Dopamine receptors(DRD5) and downstream signaling transcripts, as well as enzymes that create dopamine (TH) were downregulated. Enzymes that degrade dopamine (MAO) were upregulated. Thus it appears that WNV infection decreases dopamine levels. Transcripts were included if they demonstrated a fold change >1 or <-1.

Table 4-12. Transcripts for all analyses mapped to immunological CPs

	Exposure Status		Survival/Immune Status		CNS Location	
	Down	Up	Down	Up	Down	Up
4-1BB Signaling in T Lymphocytes	1	1	1	1	3	1
Activation of IRF by Cytosolic Pattern Recognition Receptors	1	3	0	5		
Acute Myeloid Leukemia Signaling					4	1
Acute Phase Response Signaling	5	6	4	5	6	3
Amyloid Processing			3	1		
B Cell Activating Factor Signaling	2	2			0	2
B Cell Development					0	3
B Cell Receptor Signaling	6	4	7	3	7	5
Calcium-induced T Lymphocyte Apoptosis	4	3	2	3	2	4
Cardiac Hypertrophy Signaling			15	4	14	6
Caveolar-mediated \Endocytosis Signaling	6	1	6	2	2	3
CCR3 Signaling in Eosinophils	7	2	8	2	8	4
CCR5 Signaling in Macrophages	3	2	4	3	4	4
CD27 Signaling in Lymphocytes					2	1
CD28 Signaling in T Helper Cells	6	5	2	4	3	5
CD40 Signaling			3	1	4	1
Chemokine Signaling			8	1	7	1
Chronic Myeloid Leukemia Signaling					4	2
Clathrin-mediated Endocytosis Signaling	13	1	7	1	9	3
CNTF Signaling	1	2	2	1		
CNTF Signaling						
Complement System			0	3	0	2
CTLA4 Signaling in Cytotoxic T Lymphocytes	4	3	3	3	5	5
CXCR4 Signaling	13	3	10	4	13	5
Cytotoxic T Lymphocyte-mediated Apoptosis of Target Cells	1	1				
Dendritic Cell Maturation			3	6	4	5
Fc Epsilon RI Signaling			5	1	7	3
Fcγ Receptor-mediated Phagocytosis in Macrophages and Monocytes			4	2	6	4
FcγRIIB Signaling in B Lymphocytes			1	1	2	2
FLT3 Signaling in Hematopoietic Progenitor Cells					4	2
fMLP Signaling in Neutrophils	7	4	6	4	7	5
GM-CSF Signaling	3	2	4	1	6	2
iCOS-iCOSL Signaling in T Helper Cells	6	4	4	4	4	4
IL-1 Signaling					7	3
IL-10 Signaling	3	5	1	3		
IL-12 Signaling and Production in Macrophages			3	3	6	4
IL-15 Production	0	4	1	3	1	4
IL-15 Signaling			2	1	4	3
IL-17 Signaling					4	2

Table 4-12. Continued

	Exposure Status		Survival/Immune Status		CNS Location	
	Down	Up	Down	Up	Down	Up
IL-2 Signaling			3	0	5	2
IL-22 Signaling	0	3	1	2	1	2
IL-3 Signaling	4	2	4	2	6	4
IL-4 Signaling					2	3
IL-6 Signaling	4	2	3	2		
IL-8 Signaling	11	3	9	7	9	8
IL-9 Signaling	1	2	1	2	2	3
Interferon Signaling	0	2			0	2
Leukocyte Extravasation Signaling	6	7	8	9	8	14
LPS/IL-1 Mediated Inhibition of RXR Function	7	7				
LPS-stimulated MAPK Signaling	4	1	5	2	7	2
Macropinocytosis Signaling	4	1	3	3	4	5
Mechanisms of Viral Exit from Host Cells			3	2	5	1
MIF Regulation of Innate Immunity			2	1	2	0
Natural Killer Cell Signaling			4	4	7	5
NF-κB Activation by Viruses			4	3	5	6
NF-κB Signaling	8	3	4	4		
Oncostatin M Signaling	0	3	1	1	2	2
p38 MAPK Signaling	3	3	3	2		
Primary Immunodeficiency Signaling	1	4	1	5	0	5
Production of Nitric Oxide and Reactive Oxygen Species in Macrophages	9	4	6	6	9	7
Regulation of IL-2 Expression in Activated and Anergic T Lymphocytes					2	4
Role of Macrophages, Fibroblasts and Endothelial Cells in Rheumatoid Arthritis			11	8	9	8
Role of NFAT in Regulation of the Immune Response	10	7	7	8	7	8
Role of Pattern Recognition Receptors in Recognition of Bacteria and Viruses	1	5	2	5	3	4
Role of PKR in Interferon Induction and Antiviral Response	2	1	1	2		
Role of RIG1-like Receptors in Antiviral Innate Immunity	1	2	0	4		
T Cell Receptor Signaling	4	6	4	4	4	6
T Helper Cell Differentiation	1	2				
Toll-like Receptor Signaling	3	2				
TREM1 Signaling					2	1
Virus Entry via Endocytic Pathways			6	2	6	4
Total	176	130	215	166	266	210

Note: This table shows the number of transcripts that mapped to each pathway for all analyses. The majority of the transcripts demonstrated a decrease in expression values. Transcripts were included if they demonstrated a fold change >1 or <-1.

Table 4-13. Transcripts in IL-15 production and signaling for all analyses

Symbol	Entrez gene name	Genbank	Fold change exposure status	Fold change survival/ immune status	Fold change CNS location
IL15	Interleukin 15	AK290619	2.369	2.29	2.004
IRF3	Interferon regulatory factor 3	AK292027	1.31	1.935	1.086
JAK1	Janus kinase 1	XM_001161295			1.079
MAP2K1	Mitogen-activated protein kinase kinase 1	XM_612526			-1.4
MAPK1	Mitogen-activated protein kinase 1	NM_002745		-1.095	-1.061
MAPK1	Mitogen-activated protein kinase 1	DQ508104			
PIK3R1	Phosphoinositide-3-kinase, regulatory subunit 1 (alpha)	NM_181504	-1.062		-1.339
PIK3R2	Phosphoinositide-3-kinase, regulatory subunit 2 (beta)	XM_847313		-2.44	-2.341
PIK3R3	Phosphoinositide-3-kinase, regulatory subunit 3 (gamma)	XM_856294			1.537
PTK2B	PTK2B protein tyrosine kinase 2 beta	XM_543228		-1.029	-1.545
STAT1	Signal transducer and activator of transcription 1, 91kda	BC151378	3.021	3.763	2.384
TYK2	Tyrosine kinase 2	XM_590006	1.504		

Note: The transcripts significantly changed in the IL-15 production and signaling pathways are shown for all three analyses. Transcripts involved in IL-15 production are upregulated for all analyses (IL-15 and STAT1) while transcripts involved in signaling are downregulated. Transcripts were included if they demonstrated a fold change >1 or <-1.

Table 4-14. Transcripts in IL-9, IL-22, and JAK/STAT signaling for all analyses

Symbol	Entrez gene name	Genbank	Fold change exposure status	Fold change survival/ immune status	Fold change CNS location
JAK1	Janus kinase 1	XM_001161295			1.079
MAP2K1	Mitogen-activated protein kinase kinase 1	XM_612526			-1.4
MAPK1	Mitogen-activated protein kinase 1	NM_002745		-1.095	-1.061
PIAS2	Protein inhibitor of activated STAT, 2	XM_612798		-1.014	
PIK3R1	Phosphoinositide-3-kinase, regulatory subunit 1 (alpha)	NM_181504	-1.062		-1.339
PIK3R2	Phosphoinositide-3-kinase, regulatory subunit 2 (beta)	XM_847313		-2.44	-2.341
PIK3R3	Phosphoinositide-3-kinase, regulatory subunit 3 (gamma)	XM_856294			1.537
SOCS3	Suppressor of cytokine signaling 3	NM_174466	1.535	1.809	
STAT1	Signal transducer and activator of transcription 1, 91kda	BC151378	3.021	3.763	2.384
TYK2	Tyrosine kinase 2	XM_590006	1.504		

Note: The transcripts significantly changed in the IL-9, IL-22, and JAK/STAT signaling pathways are shown for all three analyses. Transcripts involved in the upregulation of the innate immune response are increased (JAK1, TYK2, STAT1) while transcripts involved in inhibiting the innate immune response are also upregulated (SOCS3). Therefore there appears to be an induction of the innate immune response during viral infection that is counteracted in naïve horses by an inhibition of the innate immune response. Transcripts were included if they demonstrated a fold change >1 or <-1.

Table 4-15. Functions for genes common to all groups

Category	# Transcripts	p-value
Cell Death	646	0.007846
Genetic Disorder	629	0.006721
Neurological Disease	479	0.004563
Cancer	436	0.003866
Cellular Growth and Proliferation	409	0.015065
Cell Cycle	394	0.009029
Cellular Movement	388	0.00561
Inflammatory Disease	312	0.006328
Metabolic Disease	263	0.005236
Cell-To-Cell Signaling and Interaction	256	0.007265
Endocrine System Disorders	253	0.003244
Immunological Disease	238	0.005106
Hematological System Development and Function	217	0.012534
Skeletal and Muscular Disorders	203	0.003841
Cardiovascular Disease	172	0.01405
Cellular Assembly and Organization	165	0.007591
Gastrointestinal Disease	164	0.006634
Tissue Development	161	0.008721
Nervous System Development and Function	142	0.011708
Cell Morphology	109	0.010085
Cellular Development	94	0.017048
Tissue Morphology	92	0.012873
Cellular Function and Maintenance	74	0.01076
Psychological Disorders	68	0.015
Post-Translational Modification	65	0.011553
Small Molecule Biochemistry	61	0.012521
Cardiovascular System Development and Function	58	0.015677
Carbohydrate Metabolism	52	0.007987
Hematological Disease	46	0.019348
Reproductive System Disease	44	0.017469
Cell Signaling	43	0.006106
Hematopoiesis	38	0.012244
Molecular Transport	38	0.010292
Infectious Disease	38	0.015653
Connective Tissue Development and Function	36	0.011979
DNA Replication, Recombination, and Repair	36	0.009334
Gene Expression	27	0.011831
Respiratory Disease	27	0.009232
Humoral Immune Response	24	0.010206
Skeletal and Muscular System Development and Function	24	0.02575
Embryonic Development	22	0.0234
Vitamin and Mineral Metabolism	21	0.008228
Cell-mediated Immune Response	21	0.009502
Inflammatory Response	20	0.015859
Infection Mechanism	19	0.016993
Behavior	18	0.010367
Amino Acid Metabolism	18	0.006076
Immune Cell Trafficking	18	0.016015

Table 4-15. Continued

Category	# Transcripts	p-value
Cellular Compromise	16	0.020284
Organismal Development	16	0.023265
Lymphoid Tissue Structure and Development	14	0.021864
Developmental Disorder	13	0.010329
Lipid Metabolism	12	0.012967
Nucleic Acid Metabolism	11	0.020762
Antigen Presentation	9	0.020867
Connective Tissue Disorders	8	0.00695
Organ Morphology	8	0.016938
Organismal Injury and Abnormalities	8	0.016113
Renal and Urological Disease	8	0.026863
Organ Development	6	0.018
Tumor Morphology	5	0.01772
Reproductive System Development and Function	5	0.02464
Organismal Survival	4	0.00931
Endocrine System Development and Function	3	0.012347
Dermatological Diseases and Conditions	3	0.0166
Organismal Functions	2	0.0023
Hepatic System Development and Function	2	0.0196
Protein Synthesis	2	0.0196
Hair and Skin Development and Function	2	0.028
Digestive System Development and Function	1	0.028
Drug Metabolism	1	0.028
Hepatic System Disease	1	0.028
Renal and Urological System Development and Function	1	0.028
Visual System Development and Function	1	0.028

Note: The majority of functions were classified under cell death, genetic disorder, and neurological disease. However, the most significant classifications occurred in the neurological disease category which had the lowest p-value.

Table 4-16. Validation of the array

	Nonvaccinate average relative expression QPCR	Vaccinate average relative expression QPCR	Average expression nonvaccinate: vaccinate QPCR	Nonvaccinate: vaccinate array expression
2'5'OAS	+1.689667	-0.71533	+2.4050	+6.539663
Complement Component 1 r	+2.0895	-0.2185	+2.3080	+1.886843
DEADBox60	+1.7625	-0.895	+2.6575	+5.651655
Defensin B4	+0.365333	-1.907	+2.2723	+6.99401
IL-6	+1.342833	-0.56933	+1.9122	+5.97945
TNF	+0.649	-0.90583	+1.5548	+3.471118

Note: Comparison of the relative expression levels between the nonvaccinate and vaccinate thalamus and QPCR to array platforms.

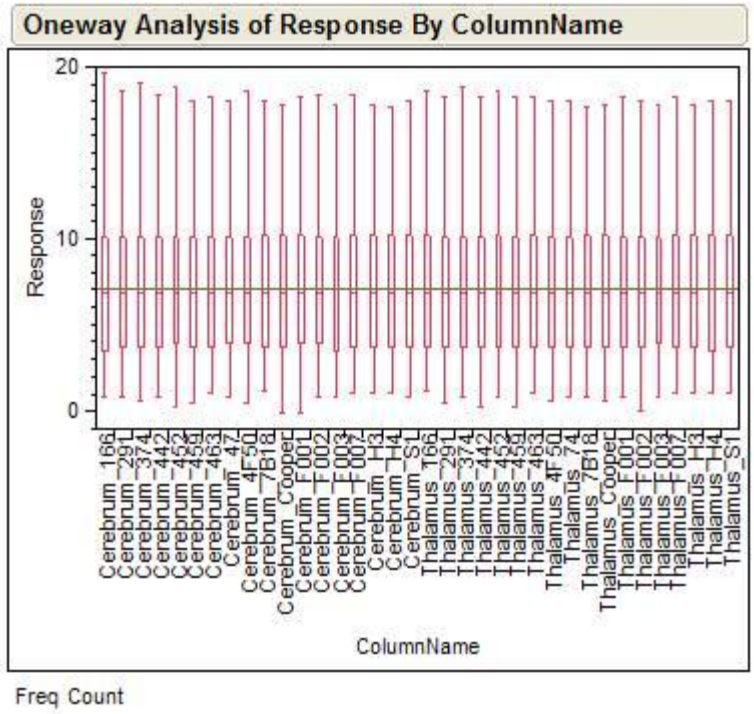

Figure 4-1. Box plots for Loess normalization. The green line indicates the mean of all arrays after normalization, while the red boxes indicate the range of response, the red lines in the boxes the median of each array, and the extended red lines standard deviations. All arrays normalized correctly.

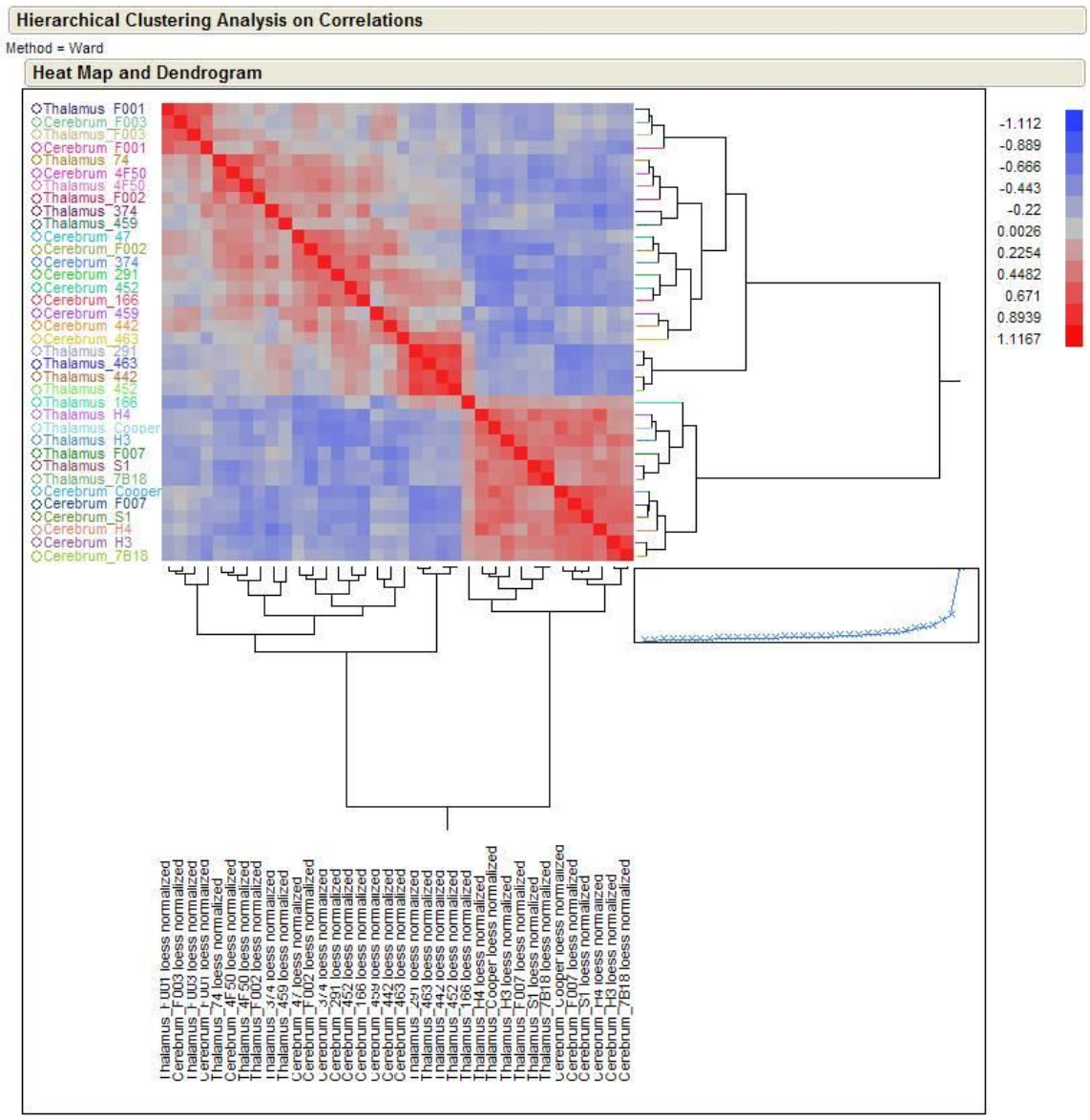

Figure 4-2. Heat map and dendrogram of all arrays demonstrating similarity in gene expression. Dark red indicates a high degree of similarity, while blue indicates a low degree of similarity.

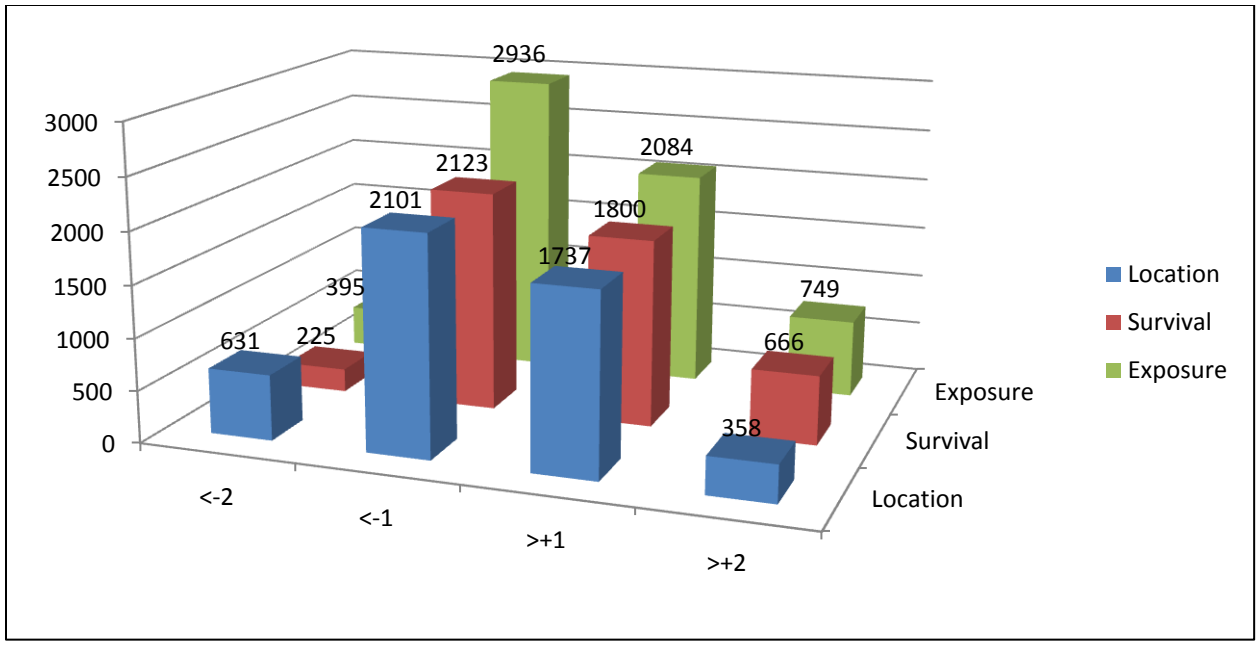

Figure 4-3. Fold change analysis of signficant genes ($p<0.05$). Transcripts that increased by greater than 1 fold and less than -1 fold were counted for all three analyses. For the purposes of this study, 'exposure' represents the difference in gene expression between the nonvaccinated/exposed-normal, 'survival' represents the difference in gene expression between the nonvaccinated/exposed-vaccinated/exposed, and 'location' represents the difference in gene expression between the thalamus and cerebrum of the nonvaccinated/exposed.

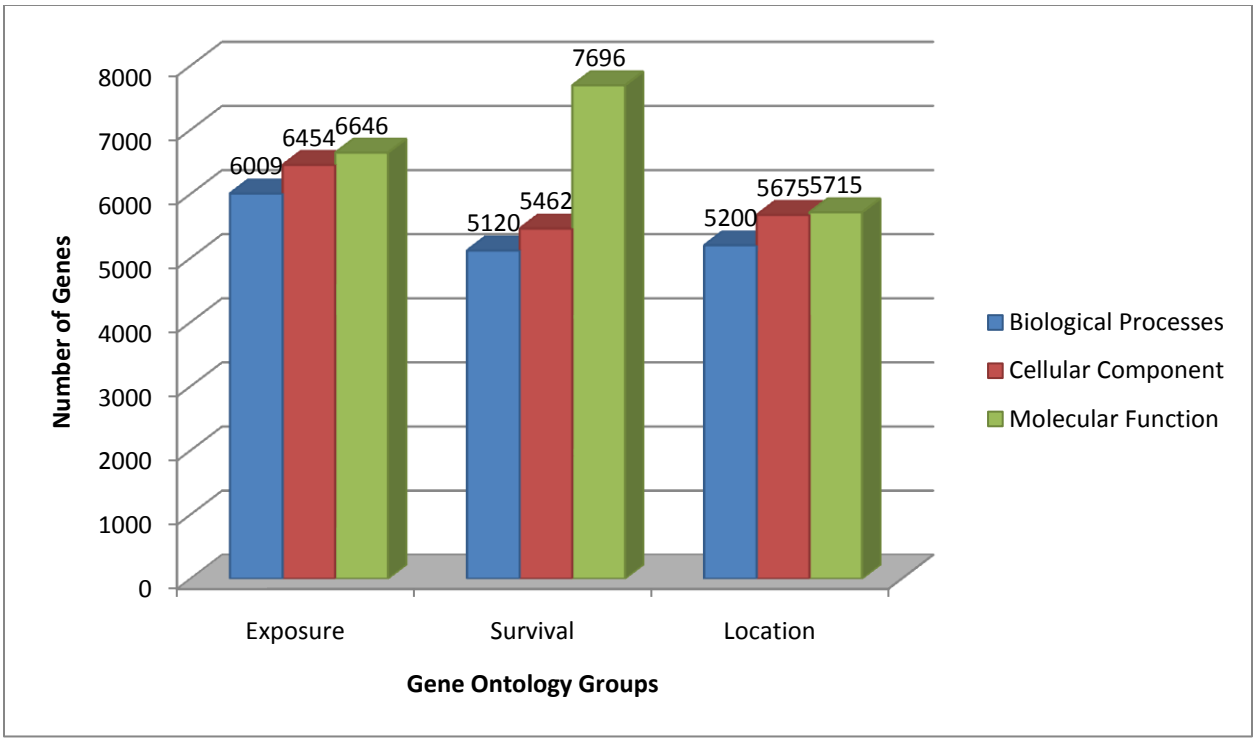

Figure 4-4. Number of genes that mapped to GO categories for all analyses. The distribution of genes is relatively even, with slightly more genes overall in the exposure analysis compared to the nonsurvival and location analysis. For the purposes of this study, 'exposure' represents the difference in gene expression between the nonvaccinated/exposed-normal, 'survival' represents the difference in gene expression between the nonvaccinated/exposed-vaccinated/exposed, and 'location' represents the difference in gene expression between the thalamus and cerebrum of the nonvaccinated/exposed.

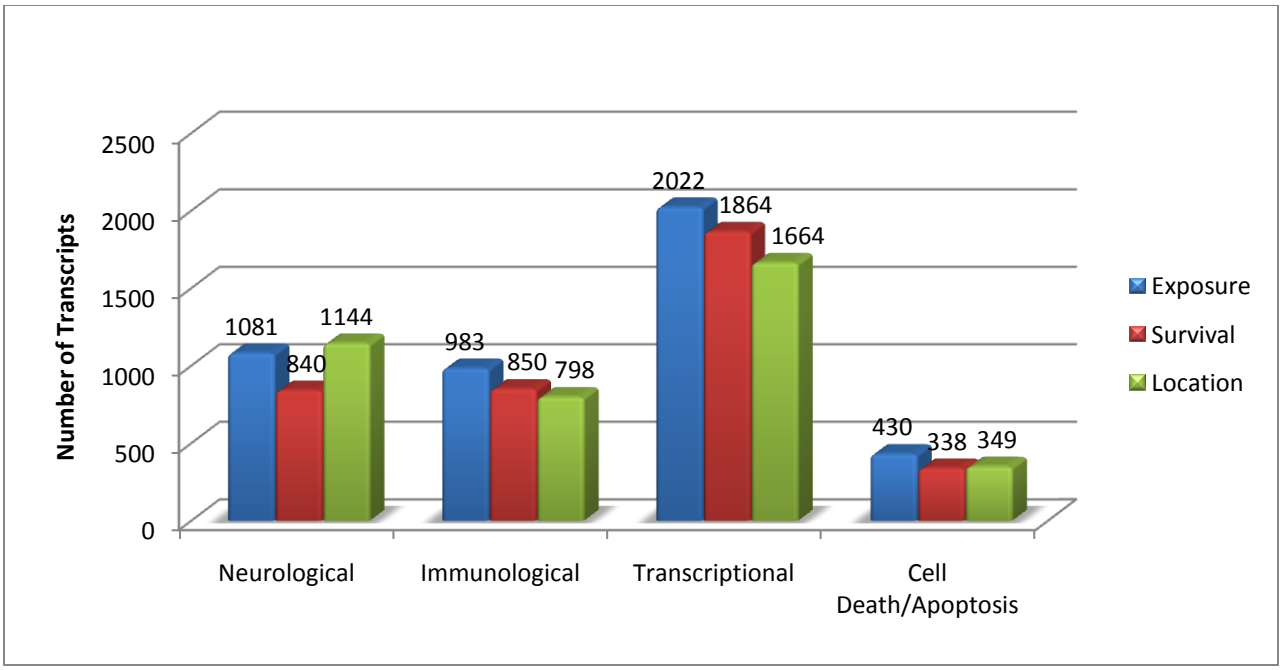

Figure 4-5. Distribution of genes among GO categories. Most genes for all analyses were classified under transcriptional categories, with neurological categories containing the second highest number of genes. For the purposes of this study, 'exposure' represents the difference in gene expression between the nonvaccinated/exposed-normal, 'survival' represents the difference in gene expression between the nonvaccinated/exposed-vaccinated/exposed, and 'location' represents the difference in gene expression between the thalamus and cerebrum of the nonvaccinated/exposed.

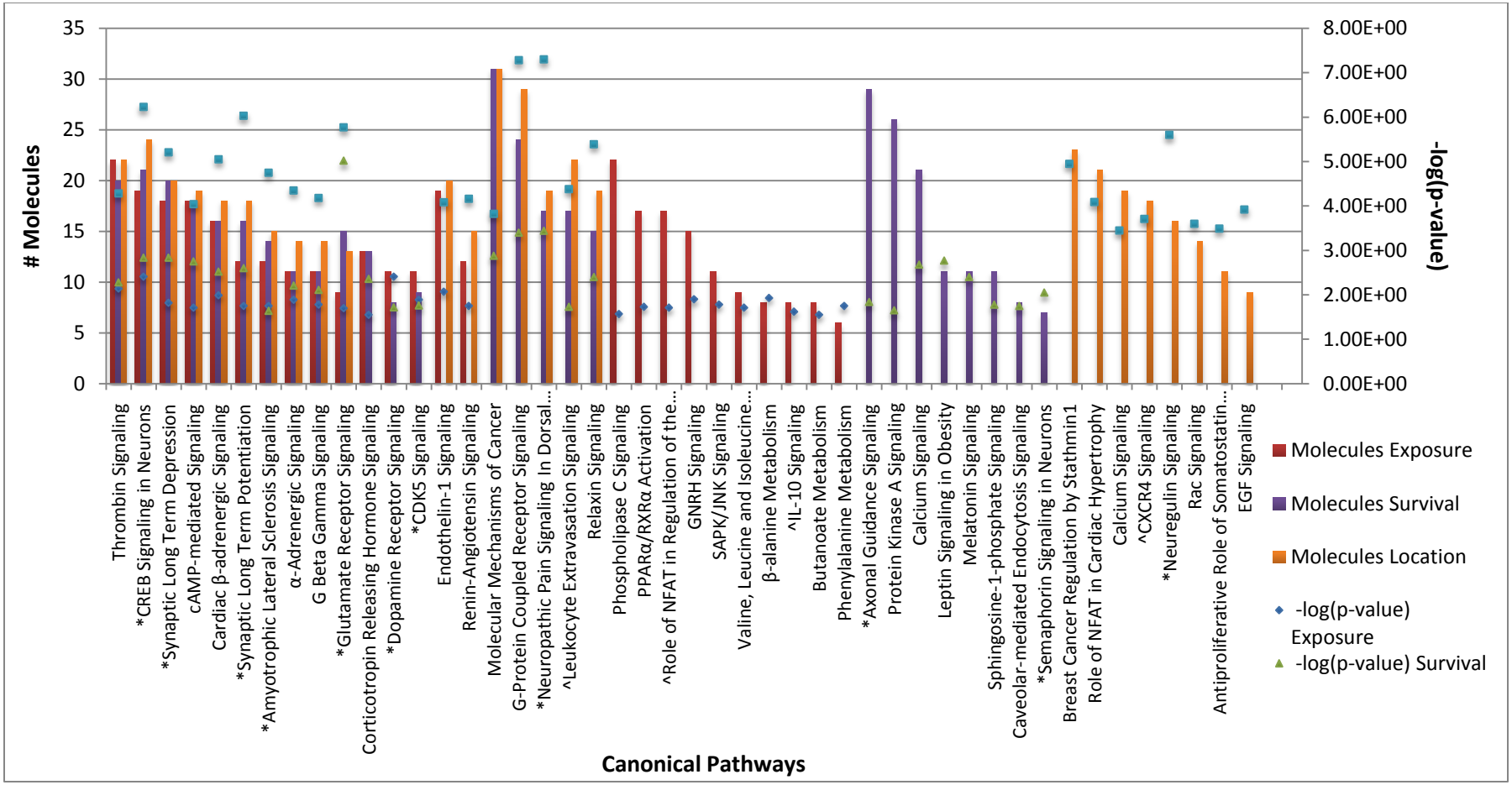

Figure 4-6. Top 25 canonical pathways for all analyses. The number of transcripts in the top 25 canonical pathways for exposure, survival, and location are graphed out. Neurological pathways are marked with an * while immunological pathways are marked with a ^. The majority of pathways are involved with signaling, then with neurological functions. For the purposes of this study, 'exposure' represents the difference in gene expression between the nonvaccinated/exposed-normal, 'survival' represents the difference in gene expression between the nonvaccinated/exposed-vaccinated/exposed, and 'location' represents the difference in gene expression between the thalamus and cerebrum of the nonvaccinated/exposed.

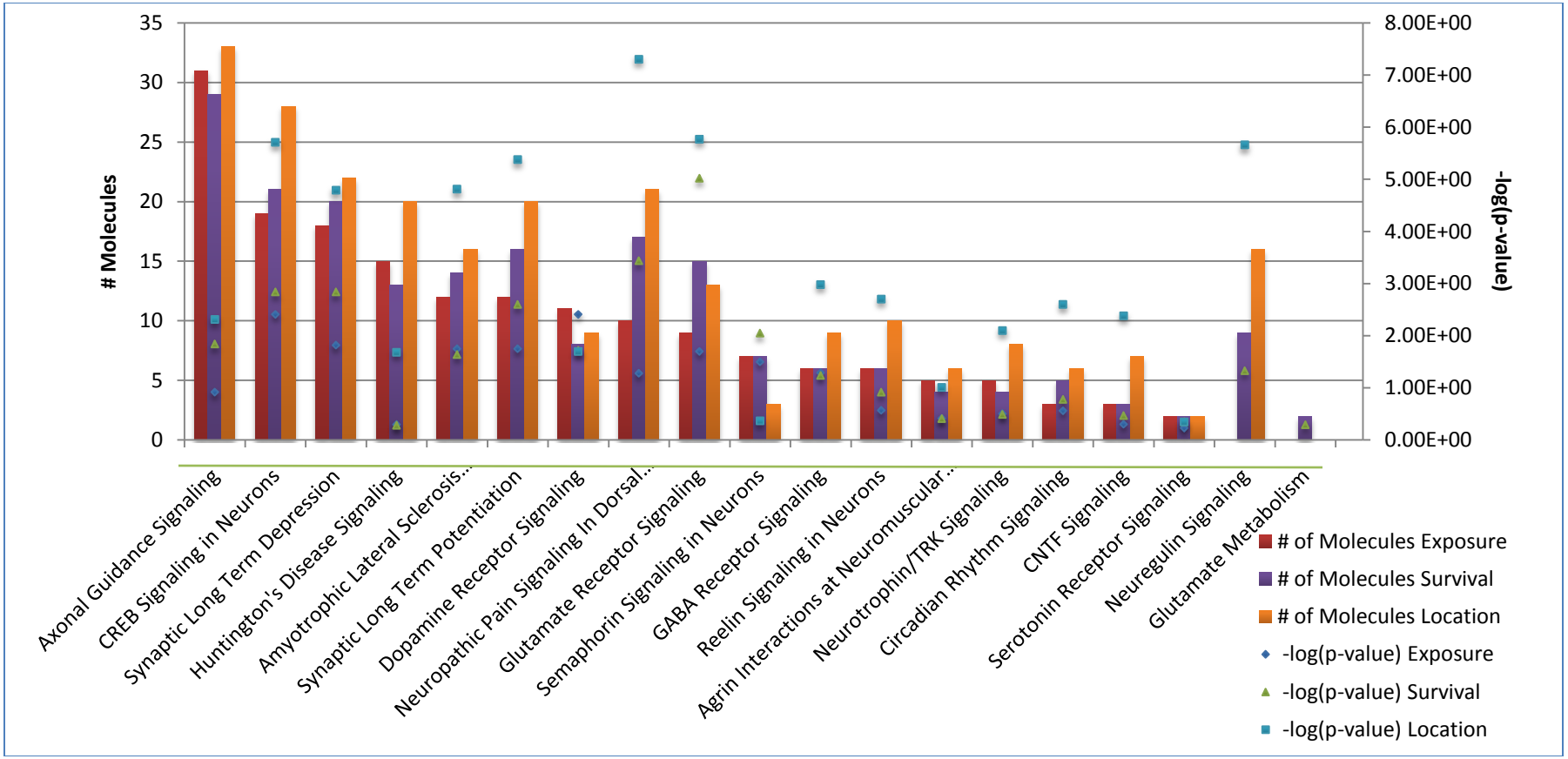

Figure 4-7. Neurological canonical pathways for all analyses. Canonical pathways identified as significant for each analyses were selected. There was a high degree of overlap between all three analyses in neurological pathways. The location analysis contained transcripts that mapped to the most neurological pathways. The green line represents significance. For the purposes of this study, 'exposure' represents the difference in gene expression between the nonvaccinated/exposed-normal, 'survival' represents the difference in gene expression between the nonvaccinated/exposed-vaccinated/exposed, and 'location' represents the difference in gene expression between the thalamus and cerebrum of the nonvaccinated/exposed.

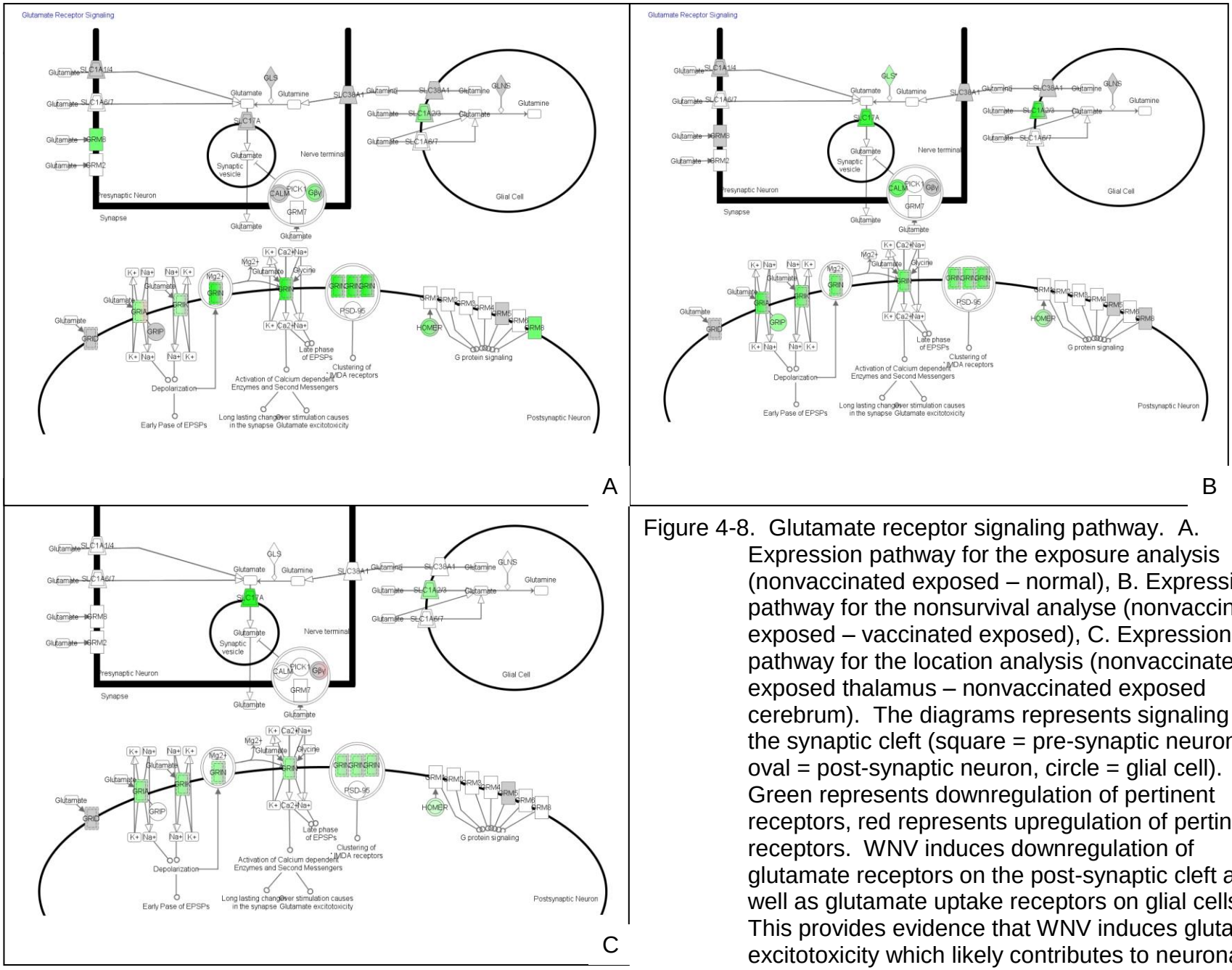

Figure 4-8. Glutamate receptor signaling pathway. A. Expression pathway for the exposure analysis (nonvaccinated exposed – normal), B. Expression pathway for the nonsurvival analyse (nonvaccinated exposed – vaccinated exposed), C. Expression pathway for the location analysis (nonvaccinated exposed thalamus – nonvaccinated exposed cerebrum). The diagrams represents signaling in the synaptic cleft (square = pre-synaptic neuron, oval = post-synaptic neuron, circle = glial cell). Green represents downregulation of pertinent receptors, red represents upregulation of pertinent receptors. WNV induces downregulation of glutamate receptors on the post-synaptic cleft as well as glutamate uptake receptors on glial cells. This provides evidence that WNV induces glutamate excitotoxicity which likely contributes to neuronal pathology.

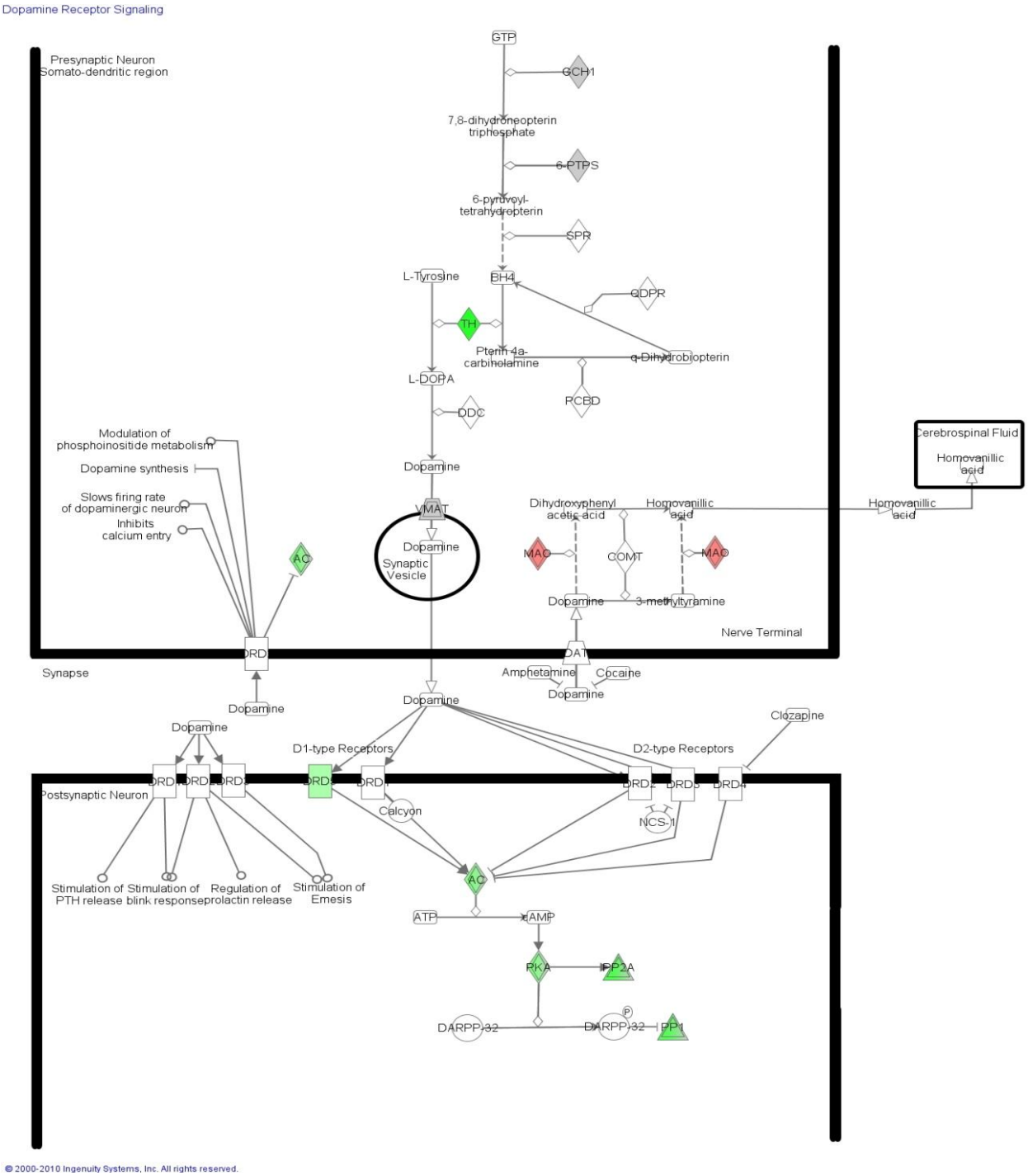

Figure 4-9. Dopamine receptor signaling pathway. The graphic shown is for the exposure analysis, but was similar in all analyses (see table 4-9). Green represents down-regulation of transcripts, red represents upregulation. Dopamine receptors (DRD5) and downstream signaling pathways as well as enzymes that create dopamine (TH) were downregulated, while MAO (enzyme that degrades dopamine) was upregulated. Thus it appears that WNV infection induces a decrease in the levels of dopamine.

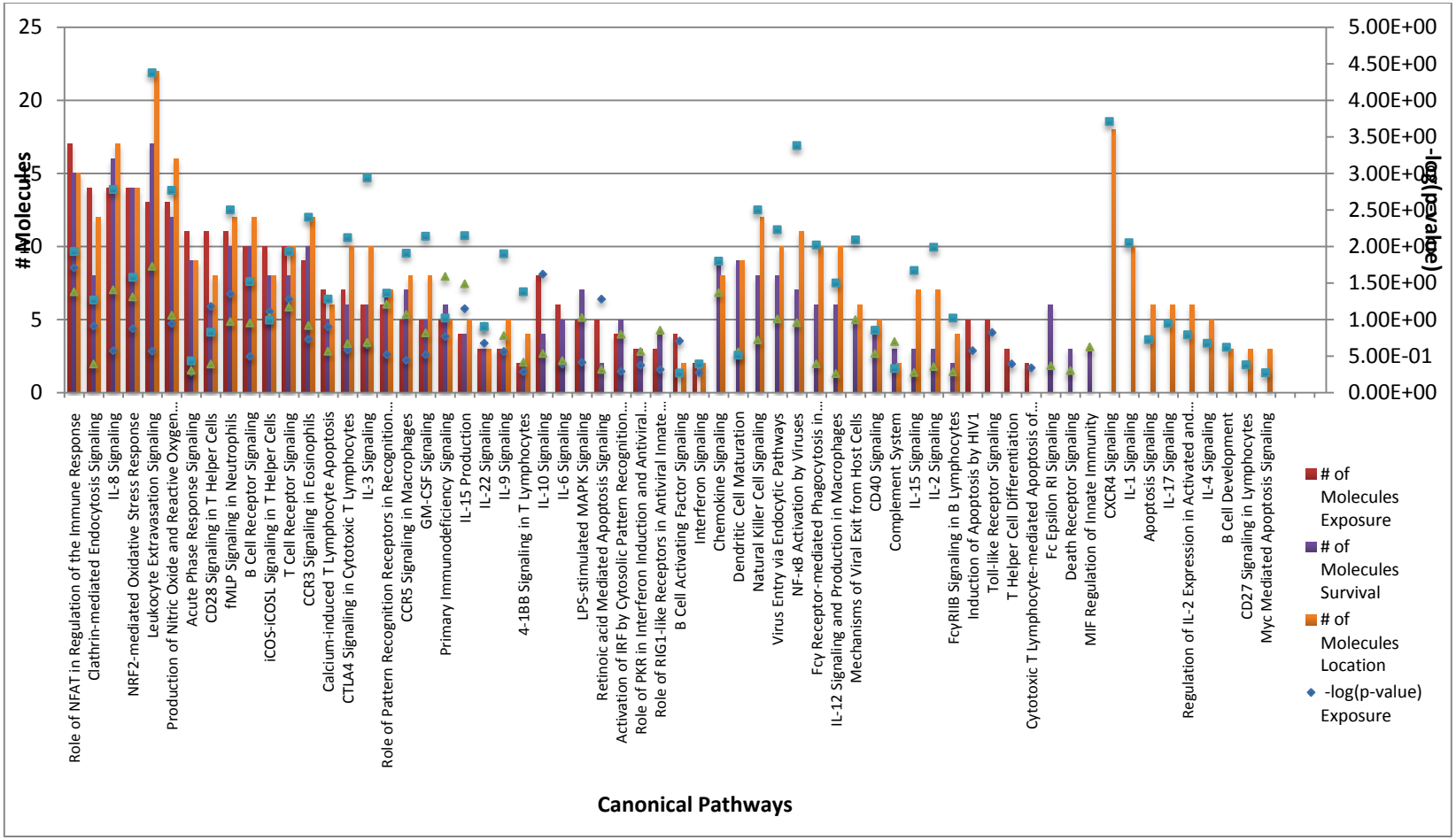

Figure 4-10. Immunological canonical pathways for all analyses. The location analysis contained transcripts that mapped to the most immunological pathways. The green line indicates significance. For the purposes of this study, 'exposure' represents the difference in gene expression between the nonvaccinated/exposed-normal, 'survival' represents the difference in gene expression between the nonvaccinated/exposed-vaccinated/exposed, and 'location' represents the difference in gene expression between the thalamus and cerebrum of the nonvaccinated/exposed.

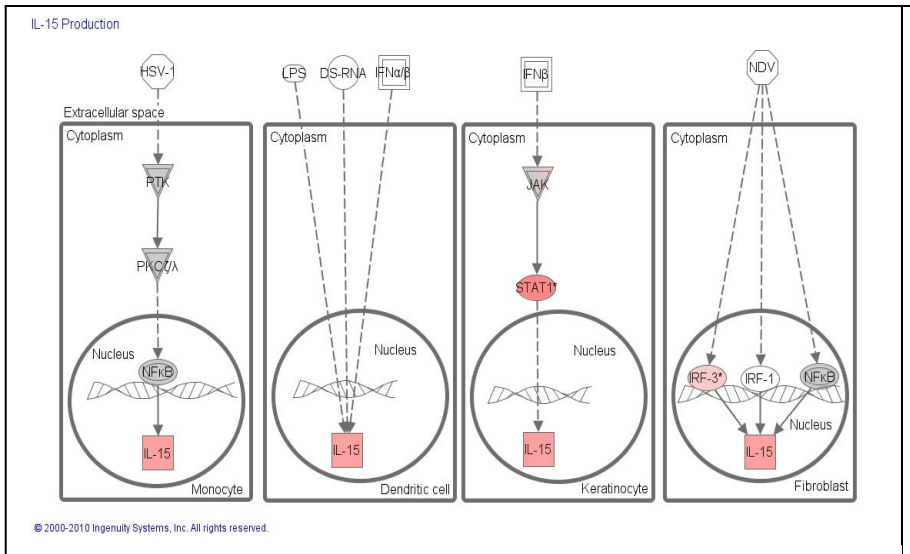

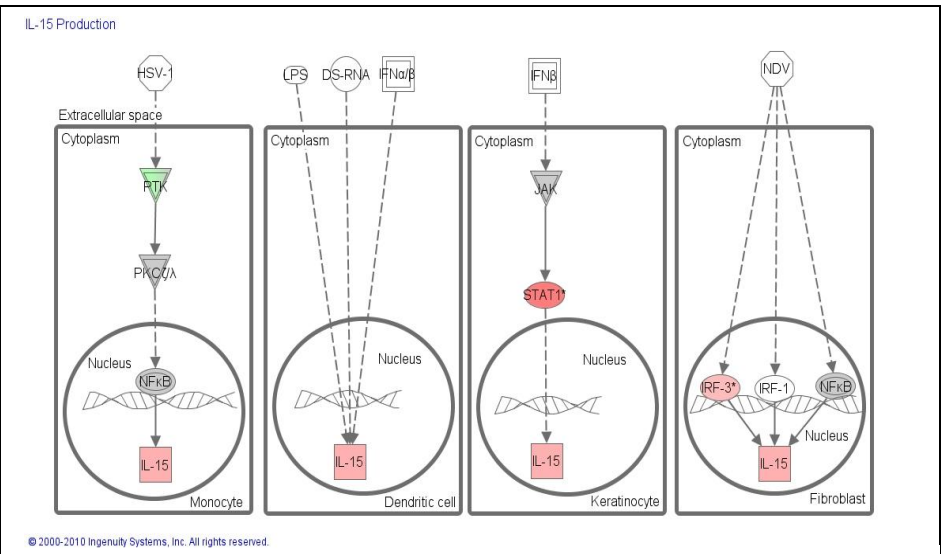

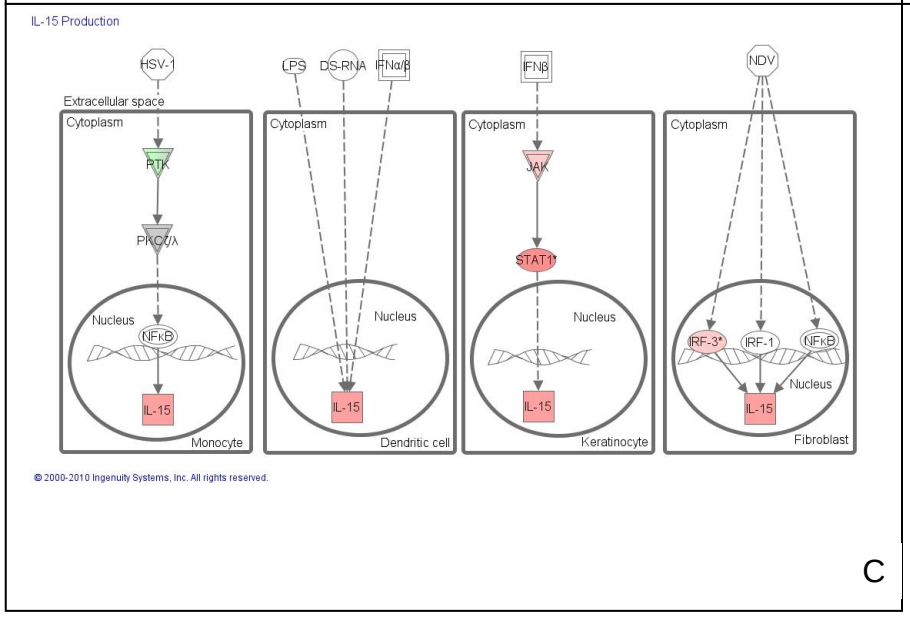

Figure 4-11. IL-15 production pathway. A. Expression pathway for the exposure analysis (nonvaccinated exposed – untreated), B. Expression pathway for the nonsurvival analysis (nonvaccinated exposed – vaccinated exposed), C. Expression pathway for the location analyse (nonvaccinated exposed thalamus – nonvaccinated exposed cerebrum). The diagrams represent the different methods of IL-15 production. Green represents downregulation of pertinent molecules, red represents upregulation of pertinent molecules. WNV induces upregulation of the production of IL-15. This likely contributes to the immune response against WNV.

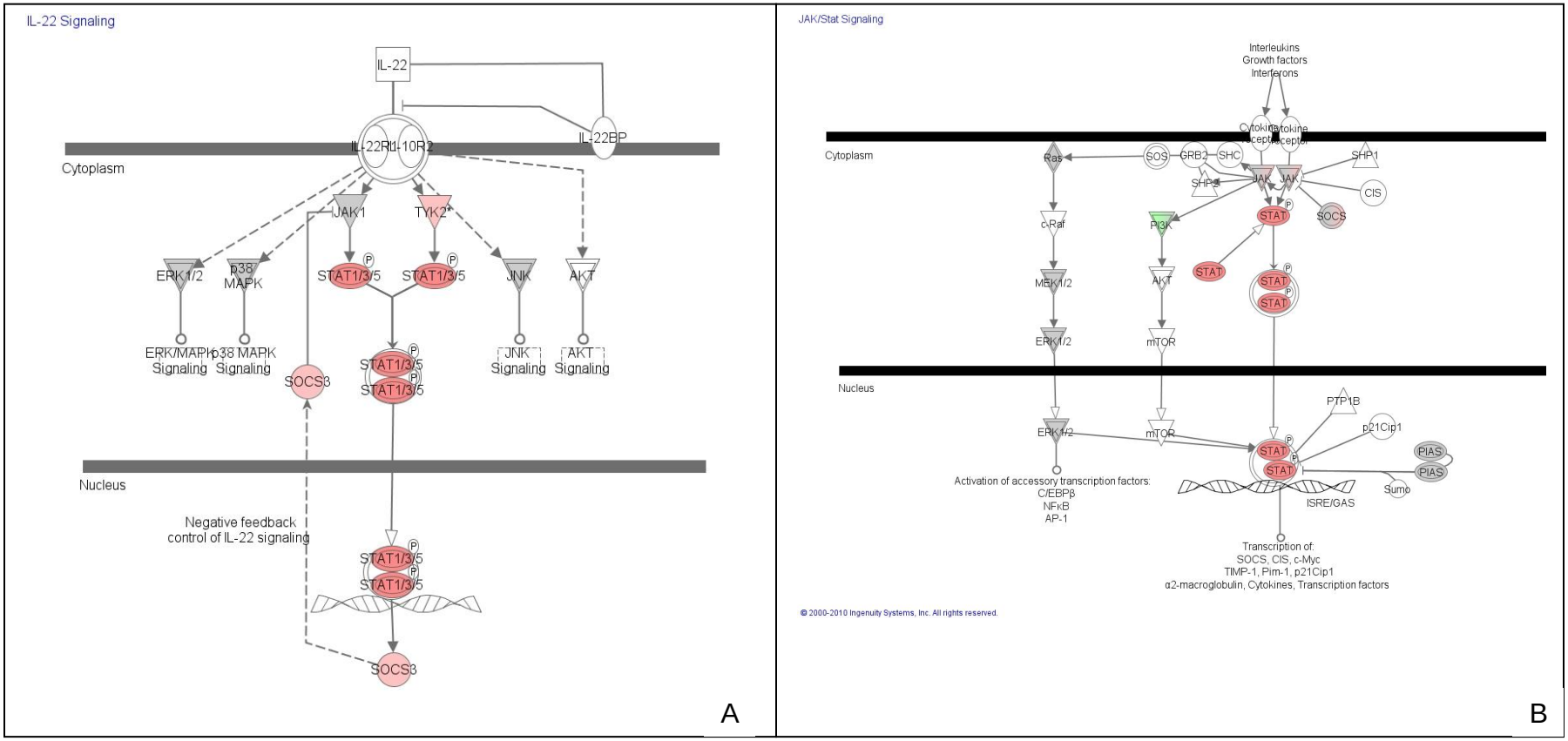

Figure 4-12. IL-22 and JAK/STAT pathways for exposure. A. IL-22 signaling pathway and B. JAK/STAT signaling pathway comparing expression levels between non-vaccinated/exposed horses and vaccinated/exposed horses (exposure analysis). Red represents upregulation of gene expression, green represents down-regulation of gene expression. The JAK/STAT pathway is upregulated during viral infection, demonstrating an innate immune response. However, the SOCS3 molecule is also upregulated, indicating that infection with the virus may lead to subsequent suppression of the JAK/STAT pathway and evasion of the innate immune response. The pathways and levels of expression were similar for the nonsurvival analysis. The location analysis did not demonstrate upregulation of SOCS3.

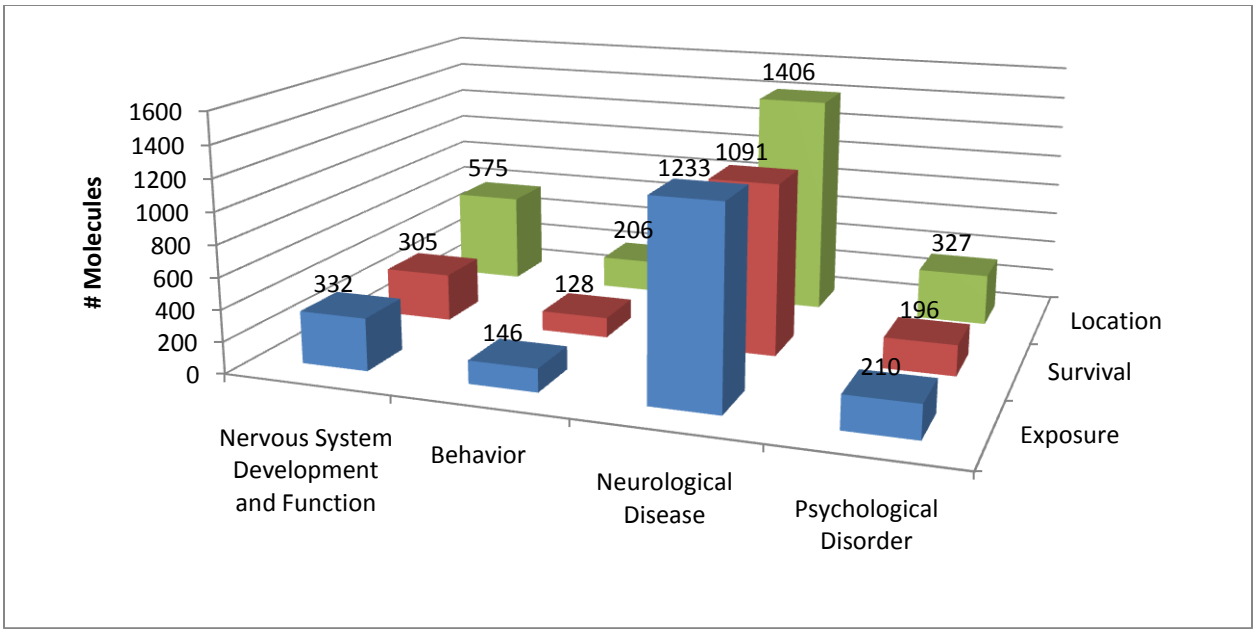

Figure 4-13. Neurological functions by category for all analyses. As can be seen for all analyses, the majority of transcripts were classified under neurological disease. For the purposes of this study, 'exposure' represents the difference in gene expression between the nonvaccinated/exposed-normal, 'survival' represents the difference in gene expression between the nonvaccinated/exposed-vaccinated/exposed, and 'location' represents the difference in gene expression between the thalamus and cerebrum of the nonvaccinated/exposed.

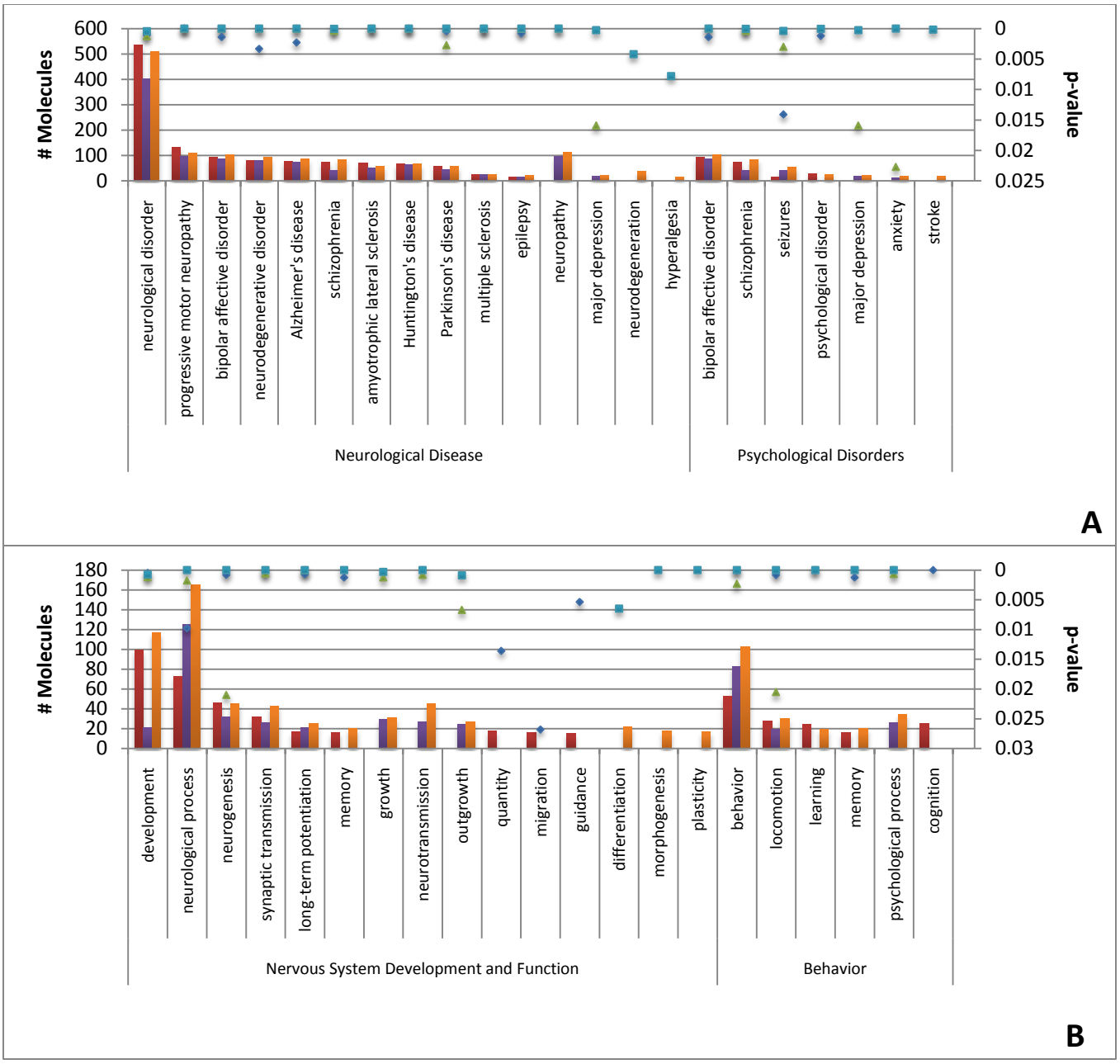

Figure 4-14. Neurological functions all analyses. A. Neurological disease and psychological disorders categories, and B. Nervous system development and function and behavior categories. The majority of transcripts mapped to neurological disease. The red bars represent the exposure analysis, the purple bars the survival analysis, and the orange bars the location analysis. The diamonds represent the p-value for exposure, the triangles the p-value for nonsurvival, and the squares the p-value for location. For the purposes of this study, 'exposure' represents the difference in gene expression between the nonvaccinated/exposed-normal, 'survival' represents the difference in gene expression between the nonvaccinated/exposed-vaccinated/exposed, and 'location' represents the difference in gene expression between the thalamus and cerebrum of the nonvaccinated/exposed.

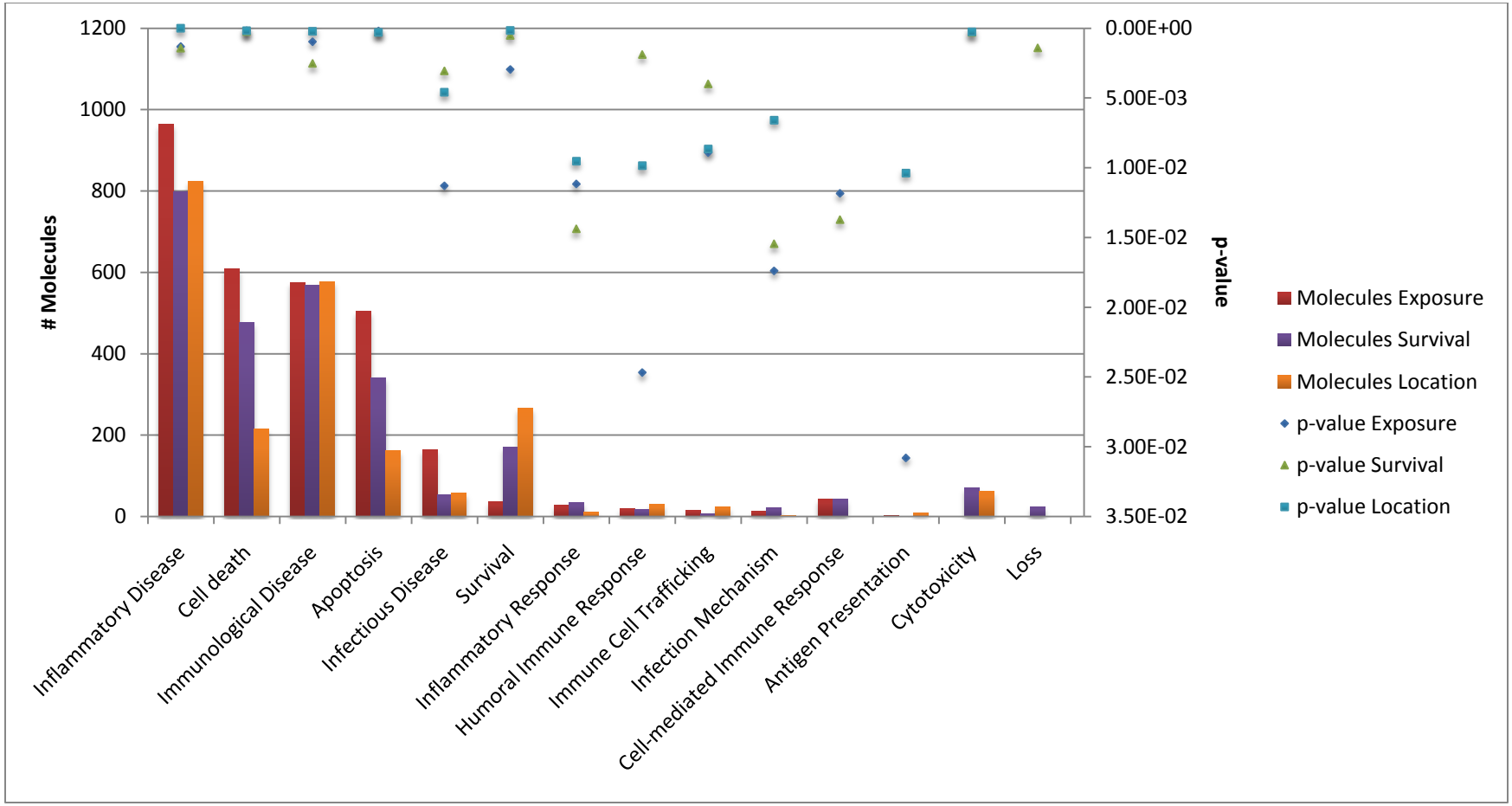

Figure 4-15. Immunological and cell death/apoptosis functions for all analyses. The majority of all transcripts mapped to the exposure analysis. Both innate and adaptive immune categories are present, as well as both cell death and apoptosis. For the purposes of this study, 'exposure' represents the difference in gene expression between the nonvaccinated/exposed-normal, 'survival' represents the difference in gene expression between the nonvaccinated/exposed-vaccinated/exposed, and 'location' represents the difference in gene expression between the thalamus and cerebrum of the nonvaccinated/exposed.

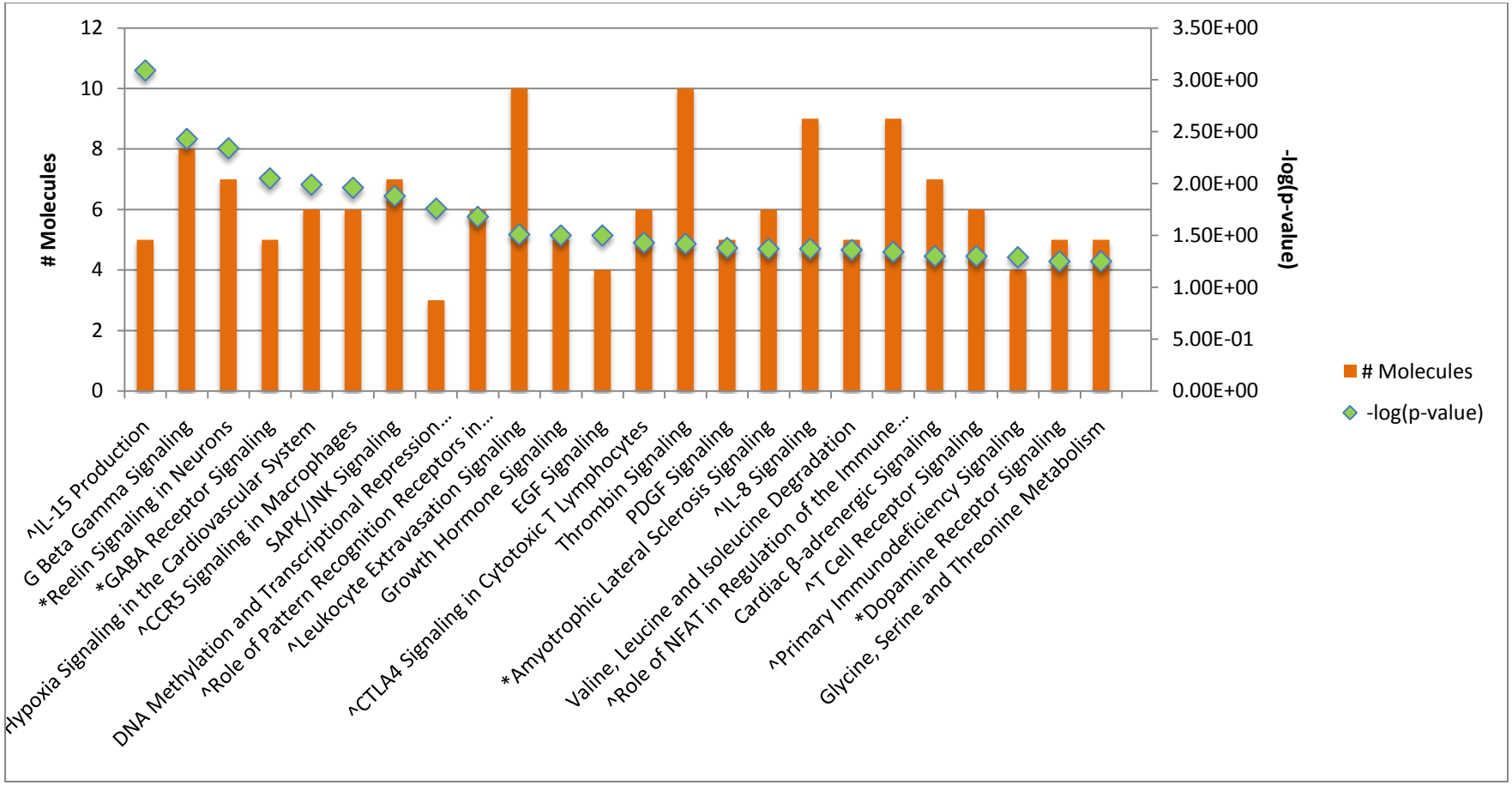

Figure 4-16. Canonical pathways for significant genes common to all analyses. The * represents neurological pathways, while the ^ represents immunological pathways. A large number of genes mapped to both neurological and immunological categories. For the purposes of this study, 'exposure' represents the difference in gene expression between the nonvaccinated/exposed-normal, 'survival' represents the difference in gene expression between the nonvaccinated/exposed-vaccinated/exposed, and 'location' represents the difference in gene expression between the thalamus and cerebrum of the nonvaccinated/exposed.

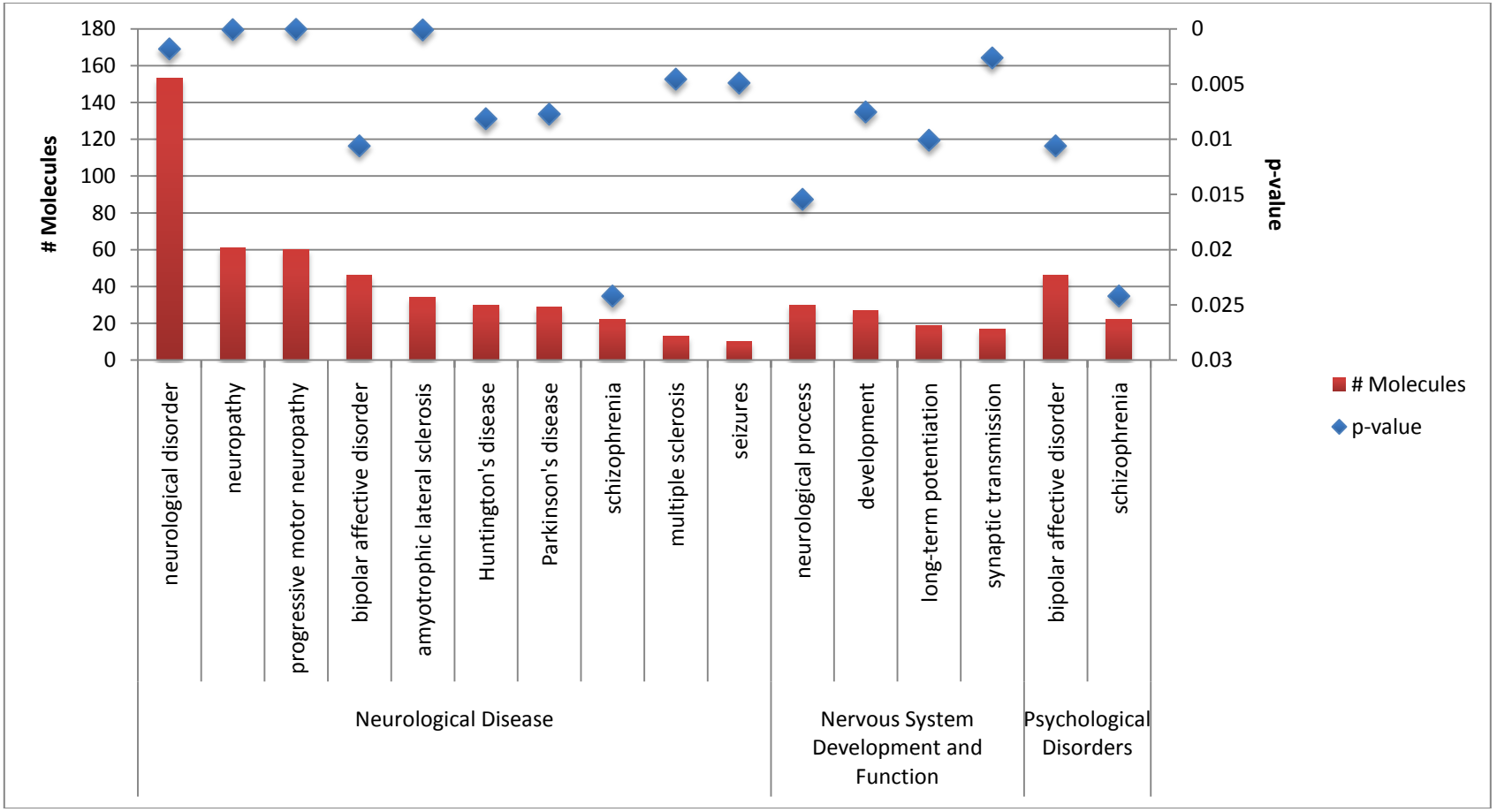

Figure 4-17. Neurological functions for significant genes common to all analyses. The functions identified include those involved with mental disorders and neurodegenerative disorders. For the purposes of this study, 'exposure' represents the difference in gene expression between the nonvaccinated/exposed-normal, 'survival' represents the difference in gene expression between the nonvaccinated/exposed-vaccinated/exposed, and 'location' represents the difference in gene expression between the thalamus and cerebrum of the nonvaccinated/exposed.

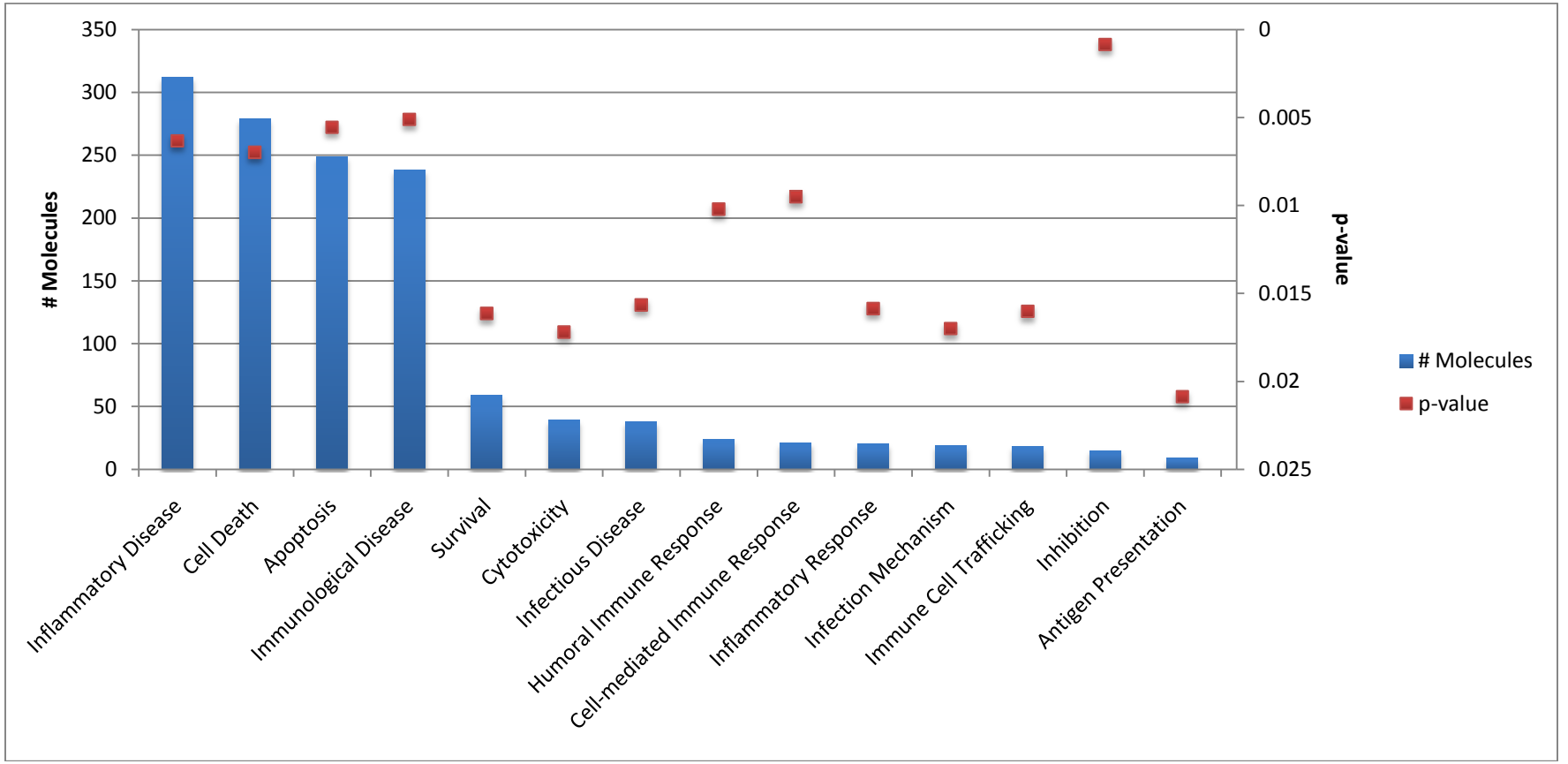

Figure 4-18. Immunological functions for significant genes common to all analyses. A large number of immunological genes are common between all analyses, as well as genes classified to cell death and apoptosis. For the purposes of this study, 'exposure' represents the difference in gene expression between the nonvaccinated/exposed-normal, 'survival' represents the difference in gene expression between the nonvaccinated/exposed-vaccinated/exposed, and 'location' represents the difference in gene expression between the thalamus and cerebrum of the nonvaccinated/exposed.

CHAPTER 5
CONCLUSIONS

Many novel findings were made during the course of this project that will further our understanding of both equine genetics and viral encephalitis/neuropathology. In the first portion of this project, pyrosequencing technology was used to sequence the transcriptome of the central nervous system of horses. In total, 41,040 sequences were identified by BLAST analysis in 5 sequence databases. Over 27,000 of these sequences grouped under Gene Ontology classifications. Analysis of these sequences revealed that they were enriched for those genes involved with the nervous system. Of the 41,040 sequences, 9,504 sequences were identified that were missed by equine predicted databases, and 1,280 genes were identified that were completely novel to the equine genome project. Biomarker analysis was performed on all of the sequences and 3,227 recognized potential biomarkers were identified (496 of these involved in neurological disease, 11 in the novel genes category). These will be important targets for system biology strategies utilizing genomic and proteomic techniques. Many of the biomarkers that were identified are accessible in easily accessible clinical samples (urine, blood, plasma, CSF). Thus this project identified many genes that are specific to the neurological system, are completely novel to the horse, and have potential applications as biomarkers. Finally, the equine transcriptome sequenced in this project was compared to the human EST project and demonstrated high sequence homology (69-80%) between the ESTs of the two species. This provides evidence that data generated from equine studies can be directly applicable to human studies. This portion of the project demonstrated that gene expression studies are necessary to supplement the limitations of current sequence databases. This is the first report of the use of

pyrosequencing to analyze the transcriptome of the equine with contribution of genes novel to the equine genome project.

In the second portion of the project, the 41,040 sequences generated from the equine transcriptome were used to create a 4x44,000 custom oligonucleotide microarray. This array was used to analyze gene expression in the brain of non-vaccinated horses exposed to WNV, vaccinated horses exposed to WNV, and untreated horses. Specifically, three questions were asked- was there was a difference in gene expression due to 1. Exposure to WNV (comparing the nonvaccinated/exposed horses to normal horses), 2. Survival from WNV infection (comparing the nonvaccinated/exposed horses to vaccinated/exposed horses), and 3. Location in the brain during WNV infection (comparing the thalamus of nonvaccinated/exposed horses to the cerebrum from the same horses). Statistical analysis was performed on the data using an ANOVA with interactions ($p<0.05$) to identify genes that were significantly up or down regulated. This data was then fed into IPA software to identify pathways, functions, and networks to map out the data.

A large number of genes were identified as significant when looking at the three different analyses (9,020 for exposure, 7,395 for survival, and 7,649 for location). GO analysis was performed on the data from all three analyses. Most genes mapped to transcription/RNA processing (5,550) with the second most genes mapping to neurological categories (3,065) for all analyses. A large number of genes also mapped to immunological categories (2,631) and cell death/apoptosis (1,117).

The GO data corresponded to the IPA analysis, which found that the most genes mapped to signaling pathways, many of which were involved with transcription. The

second most number of genes mapped to neurological pathways and disease functions. Detailed analysis revealed that components of both the glutamate and dopamine pathways were down-regulated in the WNV infected brain, providing evidence of glutamate excitotoxicity and pathology associated with a lack of dopamine. In addition, many of the transcripts mapped to non-infectious neurological disease functions, including mental disorders (bipolar affective disorder, Alzheimer's, schizophrenia, and depression) and degenerative neuropathies (progressive motor neuropathy, Huntington's disease, Parkinson's disease, neurodegeneration, amytrophic lateral sclerosis, and multiple sclerosis). This study showed that WNV has an effect on the central nervous system of affected hosts by dysregulating pathways involved with neurotransmission and downstream signaling. This corresponds with clinical signs of disease in affected hosts, and also suggests a correlate between the neuropathology induced by viral infection of the CNS and the neuropathology seen in non-infectious neurological disease.

The other major set of pathways that were shown to be dysregulated by IPA analysis were those involved in the immunological response. Pathways involving both the innate and adaptive immune response were demonstrated in all analyses. The majority of immunological pathways were downregulated in the non-vaccinated exposed horses compared to the others (as well as in the thalamus) providing evidence that a balanced immune response is present in recovery from disease. Detailed analyses of the pathways revealed an increase in IL-15 production but a decrease in IL-15 downstream signaling in the WNV infected brain, providing evidence that IL-15 is part of a balanced immune response important in recovery from WNV infection. Another

detailed analysis of the pathways revealed that WNV is likely able to evade innate immunity in naïve horses by upregulating the production of the SOCS3 molecule which itself functions to block the JAK/STAT pathway and subsequent innate immune stimulation. Apoptosis was found to be upregulated in the non-vaccinated exposed analysis, providing expression level evidence of neuropathology due to viral infection.

Individual transcripts that were significantly upregulated and downregulated were also identified. For all analyses, transcription regulators were both increased and decreased in expression. Transcription transcripts increased in expression involved in both the innate and adaptive immune response included STAT1, IRF2, IRF3, BATF, and EOMES. Transcription genes decreased in expression included NFIA, SUB1, ASB1, and ASB5. ASB1 and ASB5 function to suppress the SOCS transcripts. Thus the transcriptional immune response coincides with the findings downstream mentioned above. Other transcriptional genes, including those associated with the nervous system, were also affected. Individual transcripts not involved in transcription upregulated by a significant amount including PTX3, involved in the pattern recognition response to viruses and bacteria, and CTNND2, involved with the connection between neuron cytoskeleton and signaling. Understanding which transcripts are upregulated or downregulated during viral infection will be useful for the future identification of candidate biomarkers and important genes. Finally, the array was validated with real time reverse transcription PCR on six sets of primers.

In summary, this was the first project to sequence the equine brain transcriptome. This data was used to create a microarray platform that successfully analyzed gene expression during WNV disease, infection, and recovery. Novel

pathways were revealed to be involved in the pathology of and defense against WNV infection. A link was made between infectious and non-infectious neurological disease. A balanced immune response was shown to be important in recovery from WNV infection. This data will continue to be analyzed and will be used in the future to discover potential therapeutics and diagnostic options for viral encephalitis. The information gained from this project has furthered our knowledge of the neuropathology and neuroimmunology of viral encephalitis, and will continue to do so for years to come.

APPENDIX A
RNA QUALITY DATA ANALYSIS

The isolation of high quality RNA is difficult, due to the fast rate of degradation of RNA transcripts and the presence of RNases. Because of this, before any RNA is used during an experiment, the quality of the RNA must be assessed. Previous work has demonstrated that RNA of low quality demonstrates up to a 7-fold difference in relative gene expression using Q-PCR[173], and that RNA of low quality demonstrates different levels of gene expression and hierachical clustering when analyzed by microarray analysis.[174]

Traditionally, to assess the RNA quality before its use, the 28S:18S rRNA ratio is used. This technique relies on the fact that rRNA comprises over 80% of the cellular rRNA, and therefore the quality of the rRNA will reflect the quality of the cellular RNA. The sample is run on a gel and two bands (corresponding to a 28S band and a 18S band) are visualized using either traditional measurement techniques for gel bands or the Agilent 2100 bioanalyzer. The ratio of these two bands is then measured to determine the degree of RNA degradation. The ideal ratio is 2.7:1 (since 28S rRNA is approximately 5kb in size and 18S rRNA is approximately 2kb in size), but a ratio of 2:1 is considered the standard. However, there are problems with using this technique, especially when it is used to determine the quality of mRNA. rRNA quality does not necessarily reflect mRNA quality, as mRNA is smaller (less degradation) and has a faster turn-over rate. Previous work has also shown there to be a large amount of variability in the assessment method[173, 175], and that the technique is affected by sample dilution.

A new technique, called the RNA integrity number (RIN), was created to standardize the process of RNA integrity interpretation. This technique uses the Agilent 2100 bioanalyzer, a micro-fluidics based platform for the analysis of RNA. Small amounts of RNA are incubated with dye, the samples separated on microfabricated chips via gel electrophoresis (molecular weight separation), and a laser used to induce fluorescence. A computer captures the fluorescence images corresponding to the bands of RNA. If RNA degradation is present, a decrease in the 18S and 28S band ratio develops with a corresponding increase in the baseline signal between the two peaks. A RIN is generated, which evaluates the entire electrophoretic trace using a software algorithm. This includes the 28S:18S ratio, degradation of RNA (baseline), contamination of samples, etc. This allows for the evaluation of the integrity of all of the RNA. Samples with a RIN of > 6-7 is the standard for high quality RNA, and high scoring samples demonstrate expected values.[176] In addition, the RIN has been shown to have less variability than other standardization methods,[173, 175] and ensures repeatability and reliability between experiments. This project only used RNA samples with a RIN >7. An example of an electropherogram trace for all samples can be seen in figure 3-1. Table A-1 shows the individual RIN numbers for the samples used to create the cDNA library.

Table A-1. RNA quality data for all samples used to create the cDNA library

Sample	Tissue	Concentration (ng/uL)	RNA Integrity Number	260/280 Ratio
Uninfected	Cerebrum	298	8	1.8
	Cerebellum	596	7.8	1.9
	Cervical SC	152	6.6	1.98
	Lumbar SC	334	6	1.97
	Cervical SC	524.5	7.2	1.97
	Spleen	311.5	7.5	2.08
	Midbrain	424.88	6.7	2.04
	Hindbrain	652.13	7.2	1.94
Vaccinates	Cerebrum	1551	8.2	1.95
	Cerebellum	996.35	8.2	2.05
	Cerv. SC	602.43	6.7	1.87
	Lum. SC	369.45	7.7	1.96
	Spleen	424	7	1.93
	Hindbrain	456	6.9	2.02
	Thalamus	848.48	6.7	2.03
	Cerebrum	1042.72	8	2.05
	Cerebellum	1404	7.8	1.99
	Cerv. SC	323	7.4	1.95
	Lum. SC	520.12	6.8	1.98
	Thalamus	555.75	8.4	2.06
	Spleen	122	7.8	1.92
	Midbrain	1515.72	6.8	2.02
	Hindbrain	1712.28	6.7	2.03
Non-Vaccinates	Cerebrum	700.59	7.7	1.99
	Cerv. SC	256.12	6.9	1.99
	Thalamus	316.38	7.7	1.99
	Spleen	501.5	8.3	1.96
	Midbrain	217.73	7.4	1.94
	Hindbrain	236.08	7.4	1.97
	Cerebellum	399	8	1.9
	Lum. SC	236	6.7	1.9
	Cerebrum	886	7.9	2.01
	Cerebellum	968	8.4	1.96
	Cerv. SC	152	7.1	2.01
	Lum. SC	279	6.7	1.75
	Thalamus	618	7.5	1.91
	Spleen	468	8.4	1.95
	Midbrain	425	7.6	1.97
	Hindbrain	365	7.6	2.04

Samples used to create the cDNA library were assessed using the Agilent 2100 Bioanalyzer. Only samples with a RIN>6.5 were used in the library.

APPENDIX B
LIST OF HIGHLY UPREGULATED TRANSCRIPTS RECOGNIZED BY IPA

Table B-1. Transcripts increased in expression recognized by IPA

Symbol	Entrez gene name	GenBank	Location	Type(s)	Fold change exposure	Fold change survival	Fold change location
ABCA1	ATP-binding cassette, sub-family A (ABC1), member 1	NM_005502	Plasma Membrane	Transporter	1.095		
ABCC9	ATP-binding cassette, sub-family C (CFTR/MRP), member 9	NM_020297	Plasma Membrane	Ion channel	1.395		
ACN9	ACN9 homolog (S. Cerevisiae)	NM_001080352	Cytoplasm	Other			1.964
ACSL5	Acyl-coa synthetase long-chain family member 5	XM_859627	Cytoplasm	Enzyme	1.541	2.592	1.615
ACTN1	Actinin, alpha 1	DQ496098	Cytoplasm	Other	1.733		
ADAM17	ADAM metallopeptidase domain 17	XM_515293	Plasma Membrane	Peptidase		1.237	
ADAM9	ADAM metallopeptidase domain 9 (meltrin gamma)	XM_614306	Plasma Membrane	Peptidase			1.005
ADAMTS7	ADAM metallopeptidase with thrombospondin type 1 motif, 7	AY327122	Extracellular Space	Peptidase	1.646		
ADAMTSL1	ADAMTS-like 1	NM_001040272	Extracellular Space	Other	2.247		
ADAMTSL3	ADAMTS-like 3	CR926461	unknown	Other			1.616
ADI1	Acireductone dioxygenase 1	XM_001153173	Nucleus	Enzyme		1.021	
AGBL1	ATP/GTP binding protein-like 1	AC022817	unknown	Other			1.863
AGFG1 (includes EG:3267)	Arfgap with FG repeats 1	XM_516132	Nucleus	Other		1.049	1.113
AGPS	Alkylglycerone phosphate synthase	XM_001154263	Cytoplasm	Enzyme			1.328
AIM2	Absent in melanoma 2	XM_513914	Cytoplasm	Other	2.316	2.376	1.469
AK3	Adenylate kinase 3	D10376	Cytoplasm	Kinase			1.321
AK7	Adenylate kinase 7	XM_537550	unknown	Kinase			5.023
ALDH3A1	Aldehyde dehydrogenase 3 family, membera1	NM_001082420	Cytoplasm	Enzyme	1.294		
ALPK1	Alpha-kinase 1	XM_545029	unknown	Kinase	1.586	1.828	1.818
ALPK2	Alpha-kinase 2	NM_052947	unknown	Kinase	1.285		
ALX3	ALX homeobox 3	NM_006492	Nucleus	Transcription regulator	2.05		
AMD1	Adenosylmethionine decarboxylase 1	BX640599	unknown	Enzyme	1.439		
ANKFY1	Ankyrin repeat and FYVE domain containing 1	XM_511280	Nucleus	Transcription regulator	1.329	1.508	1.017
ANLN	Anillin, actin binding protein	XM_596461	Cytoplasm	Other			1.249
AOX1	Aldehyde oxidase 1	BC105265	Cytoplasm	Enzyme	1.034	1.653	1.22
APLP2	Amyloid beta (A4) precursor-like protein 2	XM_001155586	Extracellular Space	Other	1.521		
ARHGAP15	Rho gtpase activating protein 15	AC092652	unknown	Other	1.894	1.066	1.492

Table B-1. Continued

Symbol	Entrez gene name	GenBank	Location	Type(s)	Fold change exposure	Fold change survival	Fold change location
ARHGEF12	Rho guanine nucleotide exchange factor (GEF) 12	XM_508820	Cytoplasm	Other	1.235	1.008	
ARHGEF5	Rho guanine nucleotide exchange factor (GEF) 5	NM_001110075	Cytoplasm	Other			1.018
ARHGEF6	Rac/Cdc42 guanine nucleotide exchange factor (GEF) 6	XM_865157	Cytoplasm	Other	1.011	1.167	1.303
ASAP3	Arfgap with SH3 domain, ankyrin repeat and PH domain 3	NM_001083446	unknown	Other	1.774		
ASXL2	Additional sex combs like 2 (Drosophila)	XM_515337	unknown	Other	1.211	1.186	1.18
ATF3	Activating transcription factor 3	NM_001046193	Nucleus	Transcription regulator	3.255	4.896	2.049
ATF6	Activating transcription factor 6	XM_513949	Cytoplasm	Transcription regulator		1.225	
ATG16L2	ATG16 autophagy related 16-like 2 (S. Cerevisiae)	BC146660	unknown	Other	1.547		
ATP11B	Atpase, class VI, type 11B	AC069431	Plasma Membrane	Transporter	1.173		
ATP6V0A2	Atpase, H+ transporting, lysosomal V0 subunit a2	AK289391	Cytoplasm	Transporter	1.263	1.479	1.31
ATP6V0E1	Atpase, H+ transporting, lysosomal 9kda, V0 subunit e1	AF343440	Cytoplasm	Transporter			1.096
ATP8B1	Atpase, class I, type 8B, member 1	XM_533394	Plasma Membrane	Transporter		1.261	
ATP8B3	Atpase, class I, type 8B, member 3	XM_849983	Cytoplasm	Transporter	1.652		
ATPAF1	ATP synthase mitochondrial F1 complex assembly factor 1	NM_001042546	unknown	Other			1.059
ATXN1	Ataxin 1	BC011026	Nucleus	Other		1.019	
ATXN7L1	Ataxin 7-like 1	XM_001162005	unknown	Other	1.497	1.225	
AVEN	Apoptosis, caspase activation inhibitor	XM_510277	Cytoplasm	Ion channel	1.118		
B3GNT2	UDP-glcnac:betagal beta-1,3-N-acetylglucosaminyltransferase 2	NM_001102497	Cytoplasm	Enzyme	1.16		
B3GNT6	UDP-glcnac:betagal beta-1,3-N-acetylglucosaminyltransferase 6 (core 3 synthase)	NM_001103307	Cytoplasm	Enzyme	1.573		
BAG3	BCL2-associated athanogene 3	XM_544046	Cytoplasm	Other	1.184	2.262	1.611
BAT2	HLA-B associated transcript 2	XM_581077	Cytoplasm	Other		1.003	
BATF	Basic leucine zipper transcription factor, ATF-like	BC032294	Nucleus	Transcription regulator	5.086	4.364	2.596
BCHE	Butyrylcholinesterase	AC009811	Plasma Membrane	Enzyme			1.412
BHLHE41	Basic helix-loop-helix family, member e41	NM_001002973	Nucleus	Transcription regulator			1.421
BIRC5	Baculoviral IAP repeat-containing 5	NM_001001855	Cytoplasm	Other	1.626	2.123	1.736
BLNK	B-cell linker	XM_001159213	Cytoplasm	Other		1.021	1.583
BLZF1	Basic leucine zipper nuclear factor 1	XM_001136772	Cytoplasm	Transcription regulator	1.103		
BTN3A2	Butyrophilin, subfamily 3, member A2	BC002832	unknown	Other	2.562	4.179	2.671

Table B-1. Continued

Symbol	Entrez gene name	GenBank	Location	Type(s)	Fold change exposure	Fold change survival	Fold change location
BTN3A3	Butyrophilin, subfamily 3, member A3	AK291722	unknown	Other	2.897	2.54	1.684
C12ORF26	Chromosome 12 open reading frame 26	AC089998	unknown	Other		1.042	
C12ORF63	Chromosome 12 open reading frame 63	XM_849752	unknown	Other	1.645		1.855
C13ORF31	Chromosome 13 open reading frame 31	XM_509657	unknown	Other			1.271
C14ORF147	Chromosome 14 open reading frame 147	NM_138288	unknown	Other			1.382
C14ORF159	Chromosome 14 open reading frame 159	NM_001102368	Cytoplasm	Other	1.449		
C14ORF80	Chromosome 14 open reading frame 80	XM_850440	unknown	Other	1.449		
C15ORF41	Chromosome 15 open reading frame 41	AC007429	unknown	Other	1.33		
C15ORF48	Chromosome 15 open reading frame 48	BC142379	Nucleus	Other	2.988	3.454	2.32
C17ORF76	Chromosome 17 open reading frame 76	XM_001170539	unknown	Other		1.32	
C18ORF54	Chromosome 18 open reading frame 54	XM_001156992	Extracellular Space	Other	1.153		1.785
C1ORF141	Chromosome 1 open reading frame 141	XM_001163680	unknown	Other	1.292	1.535	1.105
C1ORF58	Chromosome 1 open reading frame 58	XM_600599	Cytoplasm	Other			1.145
C1QA	Complement component 1, q subcomponent, A chain	XM_535367	Extracellular Space	Other	1.602	1.985	
C1R	Complement component 1, r subcomponent	XM_862090	Extracellular Space	Peptidase	3.745	3.937	1.435
C4ORF22	Chromosome 4 open reading frame 22	XM_845542	unknown	Other			1.899
C6ORF167	Chromosome 6 open reading frame 167	XM_612135	unknown	Other			1.923
C6ORF72	Chromosome 6 open reading frame 72	XM_001173165	unknown	Other	1.178		2.057
C7ORF57	Chromosome 7 open reading frame 57	NM_001079785	unknown	Other			3.883
C8ORF37	Chromosome 8 open reading frame 37	XM_866332	unknown	Other		1.162	
CACNA1H	Calcium channel, voltage-dependent, T type, alpha 1H subunit	XM_537016	Plasma Membrane	Ion channel		1.305	
CALB1	Calbindin 1, 28kda	NM_001076195	Cytoplasm	Other			2.684
CALCOCO2	Calcium binding and coiled-coil domain 2	XM_537667	Nucleus	Other			1.251
CAPN2	Calpain 2, (m/II) large subunit	NM_001748	Cytoplasm	Peptidase			1.115
CASP4	Caspase 4, apoptosis-related cysteine peptidase	EF636667	Cytoplasm	Peptidase	3.771	4.336	2.227
CCDC50	Coiled-coil domain containing 50	NM_001038147	unknown	Other	1.115	1.962	1.385
CCDC60	Coiled-coil domain containing 60	XM_865397	unknown	Other			1.553
CCDC68	Coiled-coil domain containing 68	XM_001135637	unknown	Other			1.274
CCL1	Chemokine (C-C motif) ligand 1	NM_001005252	Extracellular Space	Cytokine	1.332		
CCNL1	Cyclin L1	XM_875093	Nucleus	Other	1.033		
CD244	CD244 molecule, natural killer cell receptor 2B4	BC041607	Plasma Membrane	Other		1.026	
CD38	CD38 molecule	XM_001160533	Plasma M	Enzyme	2.073	3.989	2.73

Table B-1. Continued

Symbol	Entrez gene name	GenBank	Location	Type(s)	Fold change exposure	Fold change survival	Fold change location
CD3E	CD3e molecule, epsilon (CD3-TCR complex)	NM_001003379	Plasma Membrane	Transmembrane receptor	1.68	2.895	1.533
CD44	CD44 molecule (Indian blood analyse)	XM_001151212	Plasma Membrane	Other	1.166	2.443	1.773
CD46	CD46 molecule, complement regulatory protein	NM_010778	Plasma Membrane	Other		1.392	1.952
CD47	CD47 molecule	AK050387	Plasma Membrane	Other	1.045		
CD5L	CD5 molecule-like	XM_513905	Plasma Membrane	Transmembrane receptor	2.874	4.599	
CD8A	CD8a molecule	BC151259	Plasma Membrane	Other	3.548	3.691	2.581
CDC7	Cell division cycle 7 homolog (S. Cerevisiae)	AY585721	Nucleus	Kinase	1.7		
CDH16	Cadherin 16, KSP-cadherin	XM_546890	Plasma Membrane	Enzyme	2.226	1.086	
CDK5R2	Cyclin-dependent kinase 5, regulatory subunit 2 (p39)	XM_848027	Nucleus	Other	1.264		
CDX2	Caudal type homeobox 2	XM_522747	Nucleus	Transcription regulator	1.514		
CEACAM1	Carcinoembryonic antigen-related cell adhesion molecule 1 (biliary glycoprotein)	DQ989182	Plasma Membrane	Transmembrane receptor	2.647	3.391	3.295
CHIT1	Chitinase 1 (chitotriosidase)	XM_514112	Extracellular Space	Enzyme	2.153	2.046	1.383
CHORDC1	Cysteine and histidine-rich domain (CHORD)-containing 1	NM_001045912	unknown	Other	1.046		
CLCF1	Cardiotrophin-like cytokine factor 1	XM_540818	Extracellular Space	Cytokine	1.818		
CLDN10	Claudin 10	XM_509702	Plasma Membrane	Other		1.065	1.342
CLIC1	Chloride intracellular channel 1	BC102103	Nucleus	Ion channel			1.863
CLIC4	Chloride intracellular channel 4	XM_001168510	Cytoplasm	Ion channel			1.354
CMPK2	Cytidine monophosphate (UMP-CMP) kinase 2, mitochondrial	NM_001108017	Cytoplasm	Kinase	2.476	3.001	2.022
CMTM7	CKLF-like MARVEL transmembrane domain containing 7	AK055554	Extracellular Space	Cytokine		1.862	
CNRIP1	Cannabinoid receptor interacting protein 1	XM_419337	unknown	Other	1.256		
CNTN4	Contactin 4	AC026882	Plasma Membrane	Enzyme	1.218		
COBLL1	COBL-like 1	NM_014900	unknown	Other			1.494
CPEB3	Cytoplasmic polyadenylation element binding protein 3	NM_014912	unknown	Other		1.338	
CPNE3	Copine III	XM_544163	Cytoplasm	Kinase	1.002		
CPNE5	Copine V	XM_518438	unknown	Other	1.743		
CRTAM	Cytotoxic and regulatory T cell molecule	XM_001136009	Plasma Membrane	Other		1.253	1.317
CRYBG3	Beta-gamma crystallin domain containing 3	XM_594681	unknown	Other			1.972
CSDA	Cold shock domain protein A	NM_003651	Nucleus	Transcription regulator	2.243	3.216	1.808

Table B-1. Continued

Symbol	Entrez gene name	GenBank	Location	Type(s)	Fold change exposure	Fold change survival	Fold change location
CSMD3 (includes EG:114788)	CUB and Sushi multiple domains 3	AC104380	unknown	Enzyme	1.069		
CSNK1A1	Casein kinase 1, alpha 1	XM_001163993	Cytoplasm	Kinase			1.048
CSNK1D	Casein kinase 1, delta	NM_001102080	Cytoplasm	Kinase	1.244	1.184	
CTDSPL2	CTD (carboxy-terminal domain, RNA polymerase II, polypeptide A) small phosphatase like 2	XM_001161626	unknown	Other			1.422
CTNNA3	Catenin (cadherin-associated protein), alpha 3	AC018979	Plasma Membrane	Other			1.636
CTNNB1	Catenin (cadherin-associated protein), beta 1, 88kda	XM_845101	Nucleus	Transcription regulator			1.126
CTNND1	Catenin (cadherin-associated protein), delta 1	XM_853917	Nucleus	Other	1.319	1.25	1.033
CTNND2	Catenin (cadherin-associated protein), delta 2 (neural plakophilin-related arm-repeat protein)	AC003954	Plasma Membrane	Other	5.619	5.741	2.321
CTTN	Cortactin	NM_005231	Plasma Membrane	Other	1.671		
CUGBP2	CUG triplet repeat, RNA binding protein 2	XM_507653	Nucleus	Other	1.236	1.197	
CX3CL1	Chemokine (C-X3-C motif) ligand 1	XM_544391	Extracellular Space	Cytokine	1.151		
CXCR6 (includes EG:10663)	Chemokine (C-X-C motif) receptor 6	XM_846798	Plasma Membrane	G-protein coupled receptor	1.062		
CYBB	Cytochrome b-245, beta polypeptide	XM_001136243	Cytoplasm	Enzyme		1.303	1.351
CYBRD1	Cytochrome b reductase 1	XM_001142821	Cytoplasm	Enzyme		1.154	
CYP4F22	Cytochrome P450, family 4, subfamily F, polypeptide 22	XM_541984	unknown	Enzyme	1.166		
CYTIP	Cytohesin 1 interacting protein	NM_001102243	Cytoplasm	Other	2.434	3.185	2.773
DAGLB	Diacylglycerol lipase, beta	XM_536885	unknown	Enzyme	1.295	1.213	1.072
DCAF7	DDB1 and CUL4 associated factor 7	XM_511593	Cytoplasm	Other	1.522		1.068
DDX54	DEAD (Asp-Glu-Ala-Asp) box polypeptide 54	XM_001152033	Nucleus	Transcription regulator	1.207		
DDX58	DEAD (Asp-Glu-Ala-Asp) box polypeptide 58	NM_014314	Cytoplasm	Enzyme	5.135	5.684	2.393
DDX60	DEAD (Asp-Glu-Ala-Asp) box polypeptide 60	XM_532716	unknown	Enzyme	5.189		
DENND1B	DENN/MADD domain containing 1B	AK091207	unknown	Other		1.071	
DGKH	Diacylglycerol kinase, eta	XM_534133	Cytoplasm	Kinase	1.292		
DGKI	Diacylglycerol kinase, iota	XM_539825	Cytoplasm	Kinase	1.332		
DHX15	DEAH (Asp-Glu-Ala-His) box polypeptide 15	AC102739	Nucleus	Enzyme	1.453		
DIO2	Deiodinase, iodothyronine, type II	NM_001007023	Cytoplasm	Enzyme		1.908	
DNAH10	Dynein, axonemal, heavy chain 10	NM_001083900	unknown	Other	1.382		
DNAH11	Dynein, axonemal, heavy chain 11	XM_539463	Cytoplasm	Enzyme	1.555		1.768

Table B-1. Continued

Symbol	Entrez gene name	GenBank	Location	Type(s)	Fold change exposure	Fold change survival	Fold change location
DNAH6	Dynein, axonemal, heavy chain 6	XM_532984	unknown	Other			3.114
DNAJA1	Dnaj (Hsp40) homolog, subfamily A, member 1	XM_860318	Nucleus	Other	1.195	1.182	
DNAJB1	Dnaj (Hsp40) homolog, subfamily B, member 1	XM_847807	Nucleus	Other	1.173	1.126	
DNAJC13	Dnaj (Hsp40) homolog, subfamily C, member 13	AC026374	unknown	Other	2.391		
DOT1L	DOT1-like, histone H3 methyltransferase (S. Cerevisiae)	XM_542191	Nucleus	Phosphatase		1.027	
DPCR1	Diffuse panbronchiolitis critical region 1	NM_080870	unknown	Other	2.376		
DUOXA1	Dual oxidase maturation factor 1	XM_544660	unknown	Other	1.564		
DYNLT1	Dynein, light chain, Tctex-type 1	XM_001147088	Cytoplasm	Other			1.008
DYRK4	Dual-specificity tyrosine-(Y)-phosphorylation regulated kinase 4	XM_534917	Nucleus	Kinase	1.331		
EDNRB	Endothelin receptor type B	XM_001141717	Plasma Membrane	G-protein coupled receptor			1.473
EFEMP1	EGF-containing fibulin-like extracellular matrix protein 1	NM_001081717	Extracellular Space	Other	2.501		1.322
EIF2C2	Eukaryotic translation initiation factor 2C, 2	XM_532338	Cytoplasm	Translation regulator	1.112		
EIF2S3	Eukaryotic translation initiation factor 2, subunit 3 gamma, 52kda	XM_001149353	Cytoplasm	Translation regulator		1.326	
EIF5	Eukaryotic translation initiation factor 5	XM_863525	Cytoplasm	Translation regulator	1.063		
ELF1	E74-like factor 1 (ets domain transcription factor)	XM_852043	Nucleus	Transcription regulator		1.163	1.872
ELK1	ELK1, member of ETS oncogene family	XM_548979	Nucleus	Transcription regulator	1.242		
ELK3	ELK3, ETS-domain protein (SRF accessory protein 2)	XM_001146216	Nucleus	Transcription regulator	1.871	1.151	1.465
EMILIN2	Elastin microfibril interfacer 2	XM_592120	Extracellular Space	Other	3.313	3.091	1.685
EML6	Echinoderm microtubule associated protein like 6	NM_146016	unknown	Other		1.035	
ENPP2	Ectonucleotide pyrophosphatase/phospho diesterase 2	XM_856150	Plasma Membrane	Enzyme			1.185
ENPP4	Ectonucleotide pyrophosphatase/phospho diesterase 4 (putative function)	NM_001081535	unknown	Enzyme		1.468	2.123
EOMES	Eomesodermin homolog (Xenopus laevis)	XM_001165845	Nucleus	Transcription regulator	3.849	3.344	
EPHA10	EPH receptor A10	XM_539588	Extracellular Space	Kinase	1.764		
ERBB3	V-erb-b2 erythroblastic leukemia viral oncogene homolog 3 (avian)	NM_001103105	Plasma Membrane	Kinase			1.359
ERI1	Exoribonuclease 1	XM_539997	unknown	Enzyme		1.042	
ERMN	Ermin, ERM-like protein	NM_001009959	Extracellular Space	Other			1.421
ETHE1	Ethylmalonic encephalopathy 1	XM_850148	Cytoplasm	Other		1.582	

Table B-1. Continued

Symbol	Entrez gene name	GenBank	Location	Type(s)	Fold change exposure	Fold change survival	Fold change location
ETV6	Ets variant 6	NM_001987	Nucleus	Transcription regulator		1.07	
ETV7	Ets variant 7	XM_001172937	Nucleus	Transcription regulator	5.863	6.179	2.475
EYA3	Eyes absent homolog 3 (Drosophila)	NM_001990	Nucleus	Phosphatase	1.465	1.617	
F10	Coagulation factor X	XM_534191	Extracellular Space	Peptidase	1.867	2.495	1.283
F12	Coagulation factor XII (Hageman factor)	XM_546206	Extracellular Space	Peptidase	3.041	2.435	1.489
F3	Coagulation factor III (thromboplastin, tissue factor)	XM_001252442	Plasma Membrane	Transmembrane receptor	1.301	1.561	1.025
FAM107A	Family with sequence similarity 107, member A	XM_844019	Nucleus	Other	1.823		
FAM107B	Family with sequence similarity 107, member B	NM_031453	unknown	Other		1.24	1.561
FAM126A	Family with sequence similarity 126, member A	XM_532489	Cytoplasm	Other			1.307
FAM129B	Family with sequence similarity 129, member B	XM_864533	unknown	Other	1.187		
FAM92B	Family with sequence similarity 92, member B	BC111944	unknown	Other			1.689
FCGR3A	Fc fragment of igg, low affinity iiia, receptor (CD16a)	XM_001174057	Plasma Membrane	Transmembrane receptor	4.213	5.193	2.557
FGFRL1	Fibroblast growth factor receptor-like 1	XM_610839	Plasma Membrane	Transmembrane receptor	1.245		
FKBP5	FK506 binding protein 5	XM_518427	Nucleus	Enzyme	1.982	2.208	
FLJ32810	Rho-type gtpase-activating protein FLJ32810	XM_001127597	unknown	Other	1.482		
FMN1	Formin 1	XM_535422	Nucleus	Transporter	1.218		
FMN2	Formin 2	XM_001155137	unknown	Other	1.279	1.806	
FOXP2	Forkhead box P2	NM_014491	Nucleus	Transcription regulator			1.598
FRMD4B	FERM domain containing 4B	NM_001102099	Cytoplasm	Other			1.332
FRY	Furry homolog (Drosophila)	XM_001477828	unknown	Other			1.187
FUSIP1	Splicing factor, arginine/serine-rich 13A	XM_001166490	Nucleus	Other		1.043	
FYB	FYN binding protein (FYB-120/130)	NM_001105414	Nucleus	Other			1.522
GAB1	GRB2-associated binding protein 1	NM_002039	Cytoplasm	Other			1.541
GADD45A	Growth arrest and DNA-damage-inducible, alpha	NM_001924	Nucleus	Other	1.792	1.407	1.324
GALNT13	UDP-N-acetyl-alpha-D-galactosamine:polypeptide N-acetylgalactosaminyltransferase 13 (galnac-T13)	AC009227	Cytoplasm	Enzyme	1.543		
GALNT7	UDP-N-acetyl-alpha-D-galactosamine:polypeptide N-acetylgalactosaminyltransferase 7 (galnac-T7)	NM_017423	Cytoplasm	Enzyme			1.187
GALNT8	UDP-N-acetyl-alpha-D-galactosamine:polypeptide N-acetylgalactosaminyltransf	NM_017417	Cytoplasm	Enzyme	3.1	4.034	2.983

Table B-1. Continued

Symbol	Entrez gene name	GenBank	Location	Type(s)	Fold change exposure	Fold change survival	Fold change location
	erase 8 (galnac-T8)						
GBP1 (includes EG:2633)	Guanylate binding protein 1, interferon-inducible, 67kda	XM_590008	Cytoplasm	Enzyme	3.061	4.381	2.033
GBP5	Guanylate binding protein 5	NM_001075746	Plasma Membrane	Enzyme	3.2	3.467	2.283
GBP6	Guanylate binding protein family, member 6	XM_617067	unknown	Enzyme	3.829	4.739	
GBX2	Gastrulation brain homeobox 2	XM_543300	Nucleus	Transcription regulator		1.721	3.717
GCH1	GTP cyclohydrolase 1	XM_846790	Cytoplasm	Enzyme		1.296	
GFPT1	Glutamine-fructose-6-phosphate transaminase 1	XM_515528	Cytoplasm	Enzyme	1.124	1.212	
GFRA4	GDNF family receptor alpha 4	XM_846396	Plasma Membrane	Transmembrane receptor	1.134		
GHR	Growth hormone receptor	XM_526938	Plasma Membrane	Transmembrane receptor	1.171		1.025
GHRHR	Growth hormone releasing hormone receptor	NM_000823	Plasma Membrane	G-protein coupled receptor	2.169		
GLDC	Glycine dehydrogenase (decarboxylating)	XM_538655	Cytoplasm	Enzyme	1.621	1.326	
GLDN	Gliomedin	XM_510405	Cytoplasm	Other		2.456	
GLRA3	Glycine receptor, alpha 3	AC093868	Plasma Membrane	Ion channel			1.04
GNG12	Guanine nucleotide binding protein (G protein), gamma 12	NM_018841	Plasma Membrane	Enzyme	1.789	1.925	2.023
GNG5	Guanine nucleotide binding protein (G protein), gamma 5	BC003563	Plasma Membrane	Enzyme			1.359
GRIA4	Glutamate receptor, ionotrophic, AMPA 4	AP001561	Plasma Membrane	Ion channel	1.253		
GTF2E1	General transcription factor IIE, polypeptide 1, alpha 56kda	NM_001103294	Nucleus	Transcription regulator		1.51	1.872
GUCY1A3	Guanylate cyclase 1, soluble, alpha 3	BX649180	Cytoplasm	Enzyme	1.55	1.024	
HAVCR2	Hepatitis A virus cellular receptor 2	NM_001077105	Plasma Membrane	Transmembrane receptor	1.367	1.647	1.574
HBEGF	Heparin-binding EGF-like growth factor	XM_001137119	Extracellular Space	Growth factor	2.064	2.899	2.64
HELB	Helicase (DNA) B	XM_866120	Nucleus	Enzyme	3.483	2.251	
HLA-DQA1	Major histocompatibility complex, class II, DQ alpha 1	BC125044	Plasma Membrane	Transmembrane receptor	1.767	3.555	2.095
HMMR	Hyaluronan-mediated motility receptor (RHAMM)	XM_849558	Plasma Membrane	Other	3.501	4.141	3.2
HN1	Hematological and neurological expressed 1	NM_001002032	Nucleus	Other	1.181	1.039	
HN1L	Hematological and neurological expressed 1-like	NM_001081546	Cytoplasm	Other		1.548	1.276
HNRNPA3	Heterogeneous nuclear ribonucleoprotein A3	XM_857035	Nucleus	Other			1.169
HRASLS5	HRAS-like suppressor family, member 5	NM_054108	unknown	Other	1.587		
HRH2	Histamine receptor H2	AY136744	Plasma Membrane	G-protein coupled	1.793	1.418	

Table B-1. Continued

Symbol	Entrez gene name	GenBank	Location	Type(s)	Fold change exposure	Fold change survival	Fold change location
				receptor			
HSPBAP1	HSPB (heat shock 27kda) associated protein 1	NM_001014911	unknown	Other		2.137	
HSPG2 (includes EG:3339)	Heparan sulfate proteoglycan 2	M85289	Plasma Membrane	Other	1.658	1.116	
ICK	Intestinal cell (MAK-like) kinase	NM_016513	Cytoplasm	Kinase	1.125		
ID4	Inhibitor of DNA binding 4, dominant negative helix-loop-helix protein	XM_001170946	Nucleus	Transcription regulator			1.363
IFIT5	Interferon-induced protein with tetratricopeptide repeats 5	XM_521554	unknown	Other		4.908	
IGJ	Immunoglobulin J polypeptide, linker protein for immunoglobulin alpha and mu polypeptides	XM_532398	Extracellular Space	Other	1.838	2.228	2.031
IGSF9	Immunoglobulin superfamily, member 9	AB037776	Plasma Membrane	Other	1.509		
IKZF2	IKAROS family zinc finger 2 (Helios)	NM_016260	Nucleus	Transcription regulator		1.414	
IL10RA	Interleukin 10 receptor, alpha	XM_591164	Plasma Membrane	Transmembrane receptor	1.358		
IL15	Interleukin 15	AK290619	Extracellular Space	Cytokine	2.369	2.29	2.004
IL1RAP	Interleukin 1 receptor accessory protein	XM_001161189	Plasma Membrane	Transmembrane receptor		1.618	
IL4I1	Interleukin 4 induced 1	AY358933	Cytoplasm	Enzyme	3.176	3.265	1.405
IL7	Interleukin 7	X64540	Extracellular Space	Cytokine	2.952	2.844	3.148
IMPACT	Impact homolog (mouse)	NM_018439	unknown	Other			1.436
INADL	Inad-like (Drosophila)	NM_176877	Plasma Membrane	Other			2.169
INPPL1	Inositol polyphosphate phosphatase-like 1	XM_001251422	Cytoplasm	Phosphatase	1.312		
IRF2	Interferon regulatory factor 2	XM_532847	Nucleus	Transcription regulator	2.61	1.797	
IRF3	Interferon regulatory factor 3	AK292027	Nucleus	Transcription regulator	1.31	1.935	1.086
IRX1	Iroquois homeobox 1	XM_001251876	Nucleus	Transcription regulator			5.101
IRX3	Iroquois homeobox 3	NM_001104996	Nucleus	Transcription regulator			3.398
IRX4	Iroquois homeobox 4	NM_001098466	Nucleus	Transcription regulator	1.02		
ISL1	ISL LIM homeobox 1	XM_001150633	Nucleus	Transcription regulator			2.327
ITGAD	Integrin, alpha D	XM_547050	Plasma Membrane	Other	1.457	1.697	
ITGAV	Integrin, alpha V (vitronectin receptor, alpha polypeptide, antigen CD51)	XM_545559	Plasma Membrane	Other			1.132
ITGB1	Integrin, beta 1 (fibronectin receptor, beta polypeptide, antigen CD29 includes MDF2, MSK12)	XM_507735	Plasma Membrane	Transmembrane receptor			1.569
ITGB2	Integrin, beta 2 (complement component 3 receptor 3 and 4 subunit)	NM_000211	Plasma Membrane	Other		2.26	1.71

Table B-1. Continued

Symbol	Entrez gene name	GenBank	Location	Type(s)	Fold change exposure	Fold change survival	Fold change location
ITIH2	Inter-alpha (globulin) inhibitor H2	XM_535195	Extracellular Space	Other	1.026		
ITPR1	Inositol 1,4,5-triphosphate receptor, type 1	NM_001099952	Cytoplasm	Ion channel	1.31		
ITSN2	Intersectin 2	NM_006277	Cytoplasm	Other	1.327		
JAK1	Janus kinase 1	XM_001161295	Cytoplasm	Kinase			1.079
JUNB	Jun B proto-oncogene	NM_001075656	Nucleus	Transcription regulator	2.201	2.017	
KANK2	KN motif and ankyrin repeat domains 2	AY639929	Nucleus	Transcription regulator	1.115		
KCNA4	Potassium voltage-gated channel, shaker-related subfamily, member 4	AC124657	Plasma Membrane	Ion channel	3.018	2.528	1.645
KHDRBS1	KH domain containing, RNA binding, signal transduction associated 1	CU210913	Nucleus	Transcription regulator	1.116		
KIAA0101	Kiaa0101	AK290748	Nucleus	Other	2.014	1.988	1.464
KIAA0174	Kiaa0174	XM_857726	unknown	Other		1.017	
KIAA0494	Kiaa0494	XM_524573	unknown	Other			1.435
KIAA1244	Kiaa1244	XM_518767	unknown	Other	1.108		
KIAA1486	Kiaa1486	NM_020864	unknown	Other			1.631
KLF6	Kruppel-like factor 6	AK151769	Nucleus	Transcription regulator		1.746	
KPTN	Kaptin (actin binding protein)	XM_849863	Cytoplasm	Other	1.627		
LAMP2	Lysosomal-associated membrane protein 2	XM_859449	Plasma Membrane	Enzyme			2.575
LASS2	LAG1 homolog, ceramide synthase 2	NM_001034667	Nucleus	Transcription regulator			1.029
LBH	Limb bud and heart development homolog (mouse)	NM_001099152	Nucleus	Transcription regulator	2.376	2.11	1.208
LCP1	Lymphocyte cytosolic protein 1 (L-plastin)	XM_001157284	Cytoplasm	Other	1.791	2.476	1.668
LHFP	Lipoma HMGIC fusion partner	XM_001147653	unknown	Other	2.318	3.616	1.866
LHFPL2	Lipoma HMGIC fusion partner-like 2	NM_001099151	unknown	Enzyme	1.432	2.356	
LMNB2	Lamin B2	XM_542188	Nucleus	Other		1.496	
LRCH1	Leucine-rich repeats and calponin homology (CH) domain containing 1	BC117472	unknown	Other	1.011		
LRRC16A	Leucine rich repeat containing 16A	NM_017640	unknown	Enzyme	1.008	1.111	
LRRFIP1	Leucine rich repeat (in FLII) interacting protein 1	BC083492	Nucleus	Transcription regulator		1.42	1.516
LSP1	Lymphocyte-specific protein 1	NM_001075374	Cytoplasm	Other	1.954	3.078	2.579
LYPD1	LY6/PLAUR domain containing 1	AC153655	Plasma Membrane	G-protein coupled receptor	1.645		
MACF1	Microtubule-actin crosslinking factor 1	XM_001476185	Cytoplasm	Other		1.048	
MAN1A1	Mannosidase, alpha, class 1A, member 1	AK154820	Cytoplasm	Enzyme	1.243		
MAP3K1	Mitogen-activated protein kinase kinase kinase 1	NM_005921	Cytoplasm	Kinase	1.335		1.281
MAX	MYC associated factor X	XM_847808	Nucleus	Transcription regulator	1.087	1.382	

Table B-1. Continued

Symbol	Entrez gene name	GenBank	Location	Type(s)	Fold change exposure	Fold change survival	Fold change location
MCL1	Myeloid cell leukemia sequence 1 (BCL2-related)	NM_001003016	Cytoplasm	Transporter		1.113	
MCM6	Minichromosome maintenance complex component 6	NM_001046234	Nucleus	Enzyme		1.129	
MED12L	Mediator complex subunit 12-like	NM_053002	unknown	Other	1.118		
MED21	Mediator complex subunit 21	XM_534858	Nucleus	Transcription regulator	1.056	1.001	
METTL8	Methyltransferase like 8	XM_001142517	unknown	Enzyme			1.317
MFAP3L	Microfibrillar-associated protein 3-like	XM_001154389	unknown	Other	1.458	1.521	1.889
MFNG	MFNG O-fucosylpeptide 3-beta-N-acetylglucosaminyltransferase	NM_001101051	Cytoplasm	Enzyme	1.104		
MGAT5B	Mannosyl (alpha-1,6-)-glycoprotein beta-1,6-N-acetyl-glucosaminyltransferase, isozyme B	XM_843834	unknown	Other	2.844		
MGST2	Microsomal glutathione S-transferase 2	NM_001076382	Cytoplasm	Enzyme			1.311
MLLT4	Myeloid/lymphoid or mixed-lineage leukemia (trithorax homolog, Drosophila); translocated to, 4	XM_581038	Nucleus	Other		1.426	
MMP19	Matrix metallopeptidase 19	NM_001075983	Extracellular Space	Peptidase	3.448	2.549	3.85
MNDA	Myeloid cell nuclear differentiation antigen	AK290392	Nucleus	Other	1.392	1.928	1.541
MOXD1	Monooxygenase, DBH-like 1	XM_864684	Cytoplasm	Enzyme	1.051		
MSI1	Musashi homolog 1 (Drosophila)	XM_849159	Cytoplasm	Other	1.205		
MSN	Moesin	EF076770	Plasma Membrane	Other	1.13	2.026	1.291
MTR	5-methyltetrahydrofolate-homocysteine methyltransferase	BC130616	Cytoplasm	Enzyme	1.023		1.312
MUC3A (includes EG:4584)	Mucin 3A, cell surface associated	BC142358	Extracellular Space	Other	1.988	1.055	
MYB (includes EG:4602)	V-myb myeloblastosis viral oncogene homolog (avian)	D26147	Nucleus	Transcription regulator	1.557	1.081	
MYBPC1	Myosin binding protein C, slow type	XM_001076591	Cytoplasm	Other	1.948	1.754	
MYL2	Myosin, light chain 2, regulatory, cardiac, slow	DQ896055	Cytoplasm	Other		1.898	2.435
MYO1F	Myosin IF	XM_542129	unknown	Other	1.051		
MYST3	MYST histone acetyltransferase (monocytic leukemia) 3	NM_001099413	Nucleus	Enzyme	1.431		1.297
NAAA	N-acylethanolamine acid amidase	XM_001152628	Cytoplasm	Enzyme		1.294	1.537
NCOA3	Nuclear receptor coactivator 3	XM_543039	Nucleus	Transcription regulator	1.112		
NEB	Nebulin	NM_004543	Cytoplasm	Other		1.253	2.486
NECAP2	NECAP endocytosis associated 2	BC109915	Cytoplasm	Other		1.494	1.16

Table B-1. Continued

Symbol	Entrez gene name	GenBank	Location	Type(s)	Fold change exposure	Fold change survival	Fold change location
NEK7	NIMA (never in mitosis gene a)-related kinase 7	XM_001139810	Nucleus	Kinase	1.379		
NELL2	NEL-like 2 (chicken)	AC163991	Extracellular Space	Other	1.715		
NEXN	Nexilin (F actin binding protein)	XM_547323	Plasma Membrane	Other			3.083
NFATC2IP	Nuclear factor of activated T-cells, cytoplasmic, calcineurin-dependent 2 interacting protein	XM_844795	Nucleus	Other	1.331		
NFE2L2	Nuclear factor (erythroid-derived 2)-like 2	XM_857112	Nucleus	Transcription regulator		1.037	1.337
NFIC	Nuclear factor I/C (CCAAT-binding transcription factor)	XM_542179	Nucleus	Transcription regulator	1.626		
NFIL3	Nuclear factor, interleukin 3 regulated	NM_001075240	Nucleus	Transcription regulator	1.802	2.263	1.836
NFKBIE	Nuclear factor of kappa light polypeptide gene enhancer in B-cells inhibitor, epsilon	XM_583214	Nucleus	Transcription regulator		1.482	
NHSL1	NHS-like 1	AK025347	unknown	Other	1.172		
NIACR2	G protein-coupled receptor 109B	NM_006018	Plasma Membrane	G-protein coupled receptor	1.41	1.956	
NKTR	Natural killer-tumor recognition sequence	NM_005385	Plasma Membrane	Other	1.02	1.619	
NMUR2	Neuromedin U receptor 2	XM_546288	Plasma Membrane	G-protein coupled receptor	2.206	1.656	
NOC3L	Nucleolar complex associated 3 homolog (S. Cerevisiae)	XM_534972	Nucleus	Other			1.432
NOL10	Nucleolar protein 10	AK290680	Nucleus	Other		1.012	
NOX1	NADPH oxidase 1	XM_549136	Cytoplasm	Ion channel	1.142		
NPBWR1	Neuropeptides B/W receptor 1	XM_544078	Plasma Membrane	G-protein coupled receptor	1.472		
NRG2 (includes EG:9542)	Neuregulin 2	XM_843380	Extracellular Space	Growth factor	1.874		
NRG3	Neuregulin 3	AL096706	Extracellular Space	Growth factor	1.348		
NRK	Nik related kinase	NM_198465	unknown	Kinase	2.136		1.275
NTS	Neurotensin	XM_849385	Extracellular Space	Other			8.55
NUFIP2	Nuclear fragile X mental retardation protein interacting protein 2	XM_001250302	unknown	Other		1.028	
NUP62CL (includes EG:54830)	Nucleoporin 62kda C-terminal like	BC016327	unknown	Other			1.005
NUP98	Nucleoporin 98kda	XM_856693	Nucleus	Transporter	1.597	1.476	
NXT2	Nuclear transport factor 2-like export factor 2	NM_001100353	Nucleus	Transporter			1.451
OGFR	Opioid growth factor receptor	XM_543089	Plasma Membrane	Other	1.153	1.271	
OSBPL3	Oxysterol binding protein-like 3	AY008372	Cytoplasm	Other	1.154		
OTUD4	OTU domain containing 4	NM_001102653	unknown	Other			1.392

Table B-1. Continued

Symbol	Entrez gene name	GenBank	Location	Type(s)	Fold change exposure	Fold change survival	Fold change location
OTUD7B	OTU domain containing 7B	XM_603932	Cytoplasm	Peptidase		1.477	1.396
P2RY1	Purinergic receptor P2Y, G-protein coupled, 1	U34041	Plasma Membrane	G-protein coupled receptor	1.112		2.513
PARP10	Poly (ADP-ribose) polymerase family, member 10	NM_032789	Nucleus	Other	1.783	2.145	
PARP14	Poly (ADP-ribose) polymerase family, member 14	NM_017554	Cytoplasm	Other	4.851	5.43	2.281
PAX3	Paired box 3	AC118213	Nucleus	Transcription regulator	2.534		
PAX4	Paired box 4	NM_006193	Nucleus	Transcription regulator	2.674		
PCDHB11 (includes EG:56125)	Protocadherin beta 11	XM_844111	Plasma Membrane	Other	1.052		
PCGF5	Polycomb analyse ring finger 5	NM_032373	unknown	Other	1.937		1.547
PCP4	Purkinje cell protein 4	AK289964	Cytoplasm	Other			2.807
PDE10A	Phosphodiesterase 10A	XM_518849	Cytoplasm	Enzyme	1.442		1.071
PDE4B	Phosphodiesterase 4B, camp-specific (phosphodiesterase E4 dunce homolog, Drosophila)	AL109926	Cytoplasm	Enzyme		1.917	1.022
PDE4D	Phosphodiesterase 4D, camp-specific (phosphodiesterase E3 dunce homolog, Drosophila)	AC008829	Cytoplasm	Enzyme			1.166
PDHA2	Pyruvate dehydrogenase (lipoamide) alpha 2	AC100752	Cytoplasm	Enzyme	1.408		
PDK4	Pyruvate dehydrogenase kinase, isozyme 4	NM_001101883	Cytoplasm	Kinase	2.442	5.548	4.063
PDPN	Podoplanin	XM_513046	Plasma Membrane	Transporter	2.336	2.807	2.742
PGGT1B	Protein geranylgeranyltransferase type I, beta subunit	XM_526978	Cytoplasm	Enzyme	1.826		1.127
PHC3	Polyhomeotic homolog 3 (Drosophila)	XM_545282	Nucleus	Other	1.557		
PIK3R3	Phosphoinositide-3-kinase, regulatory subunit 3 (gamma)	XM_856294	Cytoplasm	Kinase	1.537		
PLA2R1	Phospholipase A2 receptor 1, 180kda	XM_545489	Plasma Membrane	Transmembrane receptor	1.328	1.125	2.103
PLK2	Polo-like kinase 2 (Drosophila)	XM_587229	Nucleus	Kinase	1.022		
PLN	Phospholamban	NM_001003332	Cytoplasm	Other	1.618	1.2	1.615
PLOD1	Procollagen-lysine 1, 2-oxoglutarate 5-dioxygenase 1	BT025353	Cytoplasm	Enzyme		1.133	
POMC	Proopiomelanocortin	XM_515334	Extracellular Space	Other		1.168	
PPIA (includes EG:5478)	Peptidylprolyl isomerase A (cyclophilin A)	XM_001252497	Cytoplasm	Enzyme		1.694	
PPP1R1C	Protein phosphatase 1, regulatory (inhibitor) subunit 1C	AC064837	Cytoplasm	Phosphatase		1.133	1.293

Table B-1. Continued

Symbol	Entrez gene name	GenBank	Location	Type(s)	Fold change exposure	Fold change survival	Fold change location
PPP1R2	Protein phosphatase 1, regulatory (inhibitor) subunit 2	NM_001035392	Cytoplasm	Phosphatase			1.239
PPP2R2B	Protein phosphatase 2 (formerly 2A), regulatory subunit B, beta isoform	XM_001159292	Cytoplasm	Phosphatase			1.14
PPPDE2	PPPDE peptidase domain containing 2	XM_847031	unknown	Other		1.07	
PRAM1	PML-RARA regulated adaptor molecule 1	XM_849317	unknown	Other	1.38	1.818	
PREX2 (includes EG:80243)	Phosphatidylinositol-3,4,5-trisphosphate-dependent Rac exchange factor 2	XM_544113	unknown	Other	1.026		
PRKCH	Protein kinase C, eta	NM_006255	Cytoplasm	Kinase			4.052
PRKCH	Protein kinase C, eta	NM_006255	Cytoplasm	Kinase		1.49	
PRMT3	Protein arginine methyltransferase 3	NM_005788	Nucleus	Enzyme			1.257
PRRG1	Proline rich Gla (G-carboxyglutamic acid) 1	NM_001105640	Plasma Membrane	Other			1.229
PRRX1	Paired related homeobox 1	NM_006902	Nucleus	Transcription regulator		1.319	1.421
PRTFDC1	Phosphoribosyl transferase domain containing 1	XM_001156975	unknown	Enzyme		1.133	1.725
PRTN3	Proteinase 3	BC096186	Extracellular Space	Peptidase	1.732		
PRUNE2	Prune homolog 2 (Drosophila)	AC147026	unknown	Other	1.306	1.568	1.125
PSEN1	Presenilin 1	BC151458	Plasma Membrane	Peptidase	1.271		
PSTPIP2	Proline-serine-threonine phosphatase interacting protein 2	NM_001101112	Cytoplasm	Other	2.616	2.166	1.336
PTGFRN	Prostaglandin F2 receptor negative regulator	BC152454	Plasma Membrane	Other	2.266	1.653	1.657
PTPN22	Protein tyrosine phosphatase, non-receptor type 22 (lymphoid)	XM_597200	Cytoplasm	Phosphatase	1.713	2.03	1.957
PTPRC	Protein tyrosine phosphatase, receptor type, C	XM_547374	Plasma Membrane	Phosphatase	2.333	3.479	2.52
PTPRJ	Protein tyrosine phosphatase, receptor type, J	NM_002843	Plasma Membrane	Phosphatase		1.089	
PTX3	Pentraxin-related gene, rapidly induced by IL-1 beta	DQ207368	Extracellular Space	Other	9.021	7.746	4.277
PURA	Purine-rich element binding protein A	XM_001251355	Nucleus	Transcription regulator	1.225		
PXK	PX domain containing serine/threonine kinase	NM_001099132	Cytoplasm	Kinase		1.223	1.162
QKI	Quaking homolog, KH domain RNA binding (mouse)	AK055085	Nucleus	Other			1.08
QRICH2	Glutamine rich 2	XM_533125	unknown	Other	1.205		
RAB11FIP1	RAB11 family interacting protein 1 (class I)	XM_852408	Cytoplasm	Other	2.075	2.035	1.231
RARB	Retinoic acid receptor, beta	X04014	Nucleus	Ligand-dependent nuclear receptor	1.357		

Table B-1. Continued

Symbol	Entrez gene name	GenBank	Location	Type(s)	Fold change exposure	Fold change survival	Fold change location
RBBP6 (includes EG:5930)	Retinoblastoma binding protein 6	BC029649	Nucleus	Other	1.084	1.089	1.155
RBMS1	RNA binding motif, single stranded interacting protein 1	CR591760	Nucleus	Other	1.39		
RCAN1	Regulator of calcineurin 1	XM_844202	Nucleus	Transcription regulator	1.378	1.506	
RDX	Radixin	BC149864	Cytoplasm	Other	1.068		
REL	V-rel reticuloendotheliosis viral oncogene homolog (avian)	XM_531836	Nucleus	Transcription regulator	1.124	1.88	2.204
REV1	REV1 homolog (S. Cerevisiae)	XM_001160176	Nucleus	Enzyme	1.07		
RFFL	Ring finger and FYVE-like domain containing 1	XM_867129	Cytoplasm	Enzyme	1.175		
RGL3	Ral guanine nucleotide dissociation stimulator-like 3	XM_542058	Cytoplasm	Other	1.478		
RGS16	Regulator of G-protein signaling 16	NM_002928	Cytoplasm	Other		2.038	2.282
RGS18	Regulator of G-protein signaling 18	NM_130782	Cytoplasm	Other	1.669	1.971	
RHOG	Ras homolog gene family, member G (rho G)	XM_542335	Cytoplasm	Enzyme		1.048	
RIMS1	Regulating synaptic membrane exocytosis 1	AL445256	Cytoplasm	Enzyme	1.515		
RIT1	Ras-like without CAAX 1	NM_006912	Plasma Membrane	Enzyme		1.611	1.659
RNASE4	Ribonuclease, rnase A family, 4	BC102072	Extracellular Space	Enzyme	1.04		
RNF152	Ring finger protein 152	AC105183	unknown	Other	1.165		
RNF213	Ring finger protein 213	XM_590465	unknown	Other	2.08	2.057	1.228
ROPN1L	Ropporin 1-like	NM_001075717	unknown	Kinase	1.293		
RORA	RAR-related orphan receptor A	AC012404	Nucleus	Ligand-dependent nuclear receptor	1.435		
RP13-102H20.1	Hypothetical protein FLJ30058	XM_549258	unknown	Other			2.879
RPGR (includes EG:6103)	Retinitis pigmentosa gtpase regulator	NM_001003126	Cytoplasm	Other			1.128
RXRA	Retinoid X receptor, alpha	XM_881943	Nucleus	Ligand-dependent nuclear receptor	1.199		
RYR3	Ryanodine receptor 3	NM_001036	Plasma Membrane	Ion channel	1.288		
S100A3	S100 calcium binding protein A3	BC012893	unknown	Transporter			1.76
SAP30	Sin3A-associated protein, 30kda	XM_843990	Nucleus	Transcription regulator	1.382	1.973	1.588
SASS6	Spindle assembly 6 homolog (C. Elegans)	XM_001159651	Cytoplasm	Other			1.064
SBNO2	Strawberry notch homolog 2 (Drosophila)	XM_542207	unknown	Other	1.756	1.141	
SC5DL	Sterol-C5-desaturase (ERG3 delta-5-desaturase homolog, S. Cerevisiae)-like	XM_001167254	Cytoplasm	Enzyme		1.005	1.416

Table B-1. Continued

Symbol	Entrez gene name	GenBank	Location	Type(s)	Fold change exposure	Fold change survival	Fold change location
SCN7A	Sodium channel, voltage-gated, type VII, alpha	AC092583	Plasma Membrane	Ion channel	6.334	6.37	3.151
SDCBP	Syndecan binding protein (syntenin)	AK128645	Plasma Membrane	Enzyme		2.306	1.202
SEMA3B	Sema domain, immunoglobulin domain (Ig), short basic domain, secreted, (semaphorin) 3B	XM_590757	Extracellular Space	Other	1.309		
SEMA5A	Sema domain, seven thrombospondin repeats (type 1 and type 1-like), transmembrane domain (TM) and short cytoplasmic domain, (semaphorin) 5A	NM_003966	Plasma Membrane	Transmembrane receptor	1.663		
SEPP1	Selenoprotein P, plasma, 1	XM_530812	Extracellular Space	Other			1.463
SFRS18	Splicing factor, arginine/serine-rich 18	XM_863061	Nucleus	Other			1.012
SFRS2	Splicing factor, arginine/serine-rich 2	XM_852679	Nucleus	Transcription regulator	1.075		
SFRS3	Splicing factor, arginine/serine-rich 3	XM_532124	Nucleus	Other			1.178
SFRS6	Splicing factor, arginine/serine-rich 6	NM_001035272	Nucleus	Other		1.26	
SH2D1B	SH2 domain containing 1B	NM_053282	unknown	Other			1.23
SHISA5	Shisa homolog 5 (Xenopus laevis)	XM_846245	Nucleus	Other	1.856		
SHISA5	Shisa homolog 5 (Xenopus laevis)	XM_846245	Nucleus	Other		1.604	
SHOX2	Short stature homeobox 2	AK145063	Nucleus	Transcription regulator			3.957
SHROOM3	Shroom family member 3	XM_844910	Cytoplasm	Other			2.249
SIM2	Single-minded homolog 2 (Drosophila)	XM_001169429	Nucleus	Transcription regulator	1.408		
SLAIN1	SLAIN motif family, member 1	NM_001040153	unknown	Other			1.149
SLC11A2	Solute carrier family 11 (proton-coupled divalent metal ion transporters), member 2	XM_509061	Plasma Membrane	Transporter	1.663		
SLC16A9	Solute carrier family 16, member 9 (monocarboxylic acid transporter 9)	XM_507806	unknown	Other		1.194	1.08
SLC24A4	Solute carrier family 24 (sodium/potassium/calcium exchanger), member 4	AC130838	unknown	Transporter	1.51		
SLC26A5	Solute carrier family 26, member 5 (prestin)	XM_616468	Plasma Membrane	Transporter		1.651	1.288
SLC2A9	Solute carrier family 2 (facilitated glucose transporter), member 9	XM_536240	Plasma Membrane	Transporter		1.01	1.525
SLC35F1	Solute carrier family 35, member F1	Z95326	unknown	Other	1.878	1.644	
SLC38A2	Solute carrier family 38, member 2	XM_543722	Plasma Membrane	Transporter			1.173
SLC39A1	Solute carrier family 39 (zinc transporter), member 1	NM_001035381	Plasma Membrane	Transporter		1.013	
SLC44A3	Solute carrier family 44, member 3	NM_001098900	unknown	Other	1.844		1.377

Table B-1. Continued

Symbol	Entrez gene name	GenBank	Location	Type(s)	Fold change exposure	Fold change survival	Fold change location
SLC8A1	Solute carrier family 8 (sodium/calcium exchanger), member 1	AC007281	Plasma Membrane	Transporter	1.393		
SLC9A3R1	Solute carrier family 9 (sodium/hydrogen exchanger), member 3 regulator 1	XM_540418	Plasma Membrane	Other	1.171		
SLC9A7	Solute carrier family 9 (sodium/hydrogen exchanger), member 7	XM_857172	Cytoplasm	Transporter	1.569		
SLK	STE20-like kinase (yeast)	XM_858785	Nucleus	Kinase	1.004		
SLMO2	Slowmo homolog 2 (Drosophila)	NM_016045	unknown	Other			1.285
SMPD3	Sphingomyelin phosphodiesterase 3, neutral membrane (neutral sphingomyelinase II)	XM_546863	Cytoplasm	Enzyme	1.304		
SMPX	Small muscle protein, X-linked	NM_001037626	unknown	Other		2.377	
SOCS3	Suppressor of cytokine signaling 3	NM_174466	Cytoplasm	Other	1.535	1.809	
SORBS1	Sorbin and SH3 domain containing 1	XM_001154001	Plasma Membrane	Other	2.506	1.88	1.515
SOX10	SRY (sex determining region Y)-box 10	DQ896471	Nucleus	Transcription regulator			1.049
SOX2	SRY (sex determining region Y)-box 2	XM_516895	Nucleus	Transcription regulator			1.016
SP1	Sp1 transcription factor	XM_509098	Nucleus	Transcription regulator	1.155	1.625	1.364
SPAG1	Sperm associated antigen 1	XM_843637	Cytoplasm	Other			1.64
SPATA13	Spermatogenesis associated 13	XM_001152608	unknown	Other			1.075
SPCS3	Signal peptidase complex subunit 3 homolog (S. Cerevisiae)	NM_021928	Cytoplasm	Peptidase			1.047
SPOCK3	Sparc/osteonectin, cwcv and kazal-like domains proteoglycan (testican) 3	XM_517526	Extracellular Space	Other			1.102
SSPO	SCO-spondin homolog (Bos taurus)	NM_174706	unknown	Other		1.333	
ST18	Suppression of tumorigenicity 18 (breast carcinoma) (zinc finger protein)	XM_001148965	Nucleus	Transcription regulator			1.307
ST8SIA4	ST8 alpha-N-acetyl-neuraminide alpha-2,8-sialyltransferase 4	NM_005668	Cytoplasm	Enzyme	1.025		
STARD13	Star-related lipid transfer (START) domain containing 13	NM_178006	Cytoplasm	Other	1.78	2.285	1.776
STAT1	Signal transducer and activator of transcription 1, 91kda	BC151378	Nucleus	Transcription regulator	3.021	3.763	2.384
STK38	Serine/threonine kinase 38	NM_007271	Cytoplasm	Kinase		1.193	
STRA8	Stimulated by retinoic acid gene 8 homolog (mouse)	XM_847727	unknown	Other			2.39
STRN	Striatin, calmodulin binding protein	XM_525732	Cytoplasm	Other			1.118
SUDS3	Suppressor of defective silencing 3 homolog (S. Cerevisiae)	XM_509415	Nucleus	Other	1.026		

Table B-1. Continued

Symbol	Entrez gene name	GenBank	Location	Type(s)	Fold change exposure	Fold change survival	Fold change location
SUDS3	Suppressor of defective silencing 3 homolog (S. Cerevisiae)	XM_509415	Nucleus	Other		1.142	1.109
SYNPO	Synaptopodin	AM393443	Cytoplasm	Other	1.201		
SYNRG	Synergin, gamma	XM_001173273	Cytoplasm	Other		1.134	
SYPL1	Synaptophysin-like 1	XM_533096	Plasma Membrane	Transporter			1.263
TARBP1 (includes EG:6894)	TAR (HIV-1) RNA binding protein 1	XM_514281	Nucleus	Transcription regulator		1.041	
TAX1BP1	Tax1 (human T-cell leukemia virus type I) binding protein 1	XM_859846	unknown	Other			1.046
TBK1	TANK-binding kinase 1	XM_538266	Cytoplasm	Kinase		1.427	
TCF12	Transcription factor 12	NM_001077885	Nucleus	Transcription regulator			1.157
TCIRG1	T-cell, immune regulator 1, atpase, H+ transporting, lysosomal V0 subunit A3	XM_540812	Plasma Membrane	Enzyme	1.44	1.781	
TEAD1	TEA domain family member 1 (SV40 transcriptional enhancer factor)	XM_001171565	Nucleus	Transcription regulator	1.786		1.319
TEP1	Telomerase-associated protein 1	XM_582150	Nucleus	Enzyme	1.602		
TGFBR1	Transforming growth factor, beta receptor 1	XM_001159150	Plasma Membrane	Kinase			1.071
TGIF2	TGFB-induced factor homeobox 2	NM_021809	Nucleus	Transcription regulator			1.11
THEMIS	Thymocyte selection associated	XM_541237	unknown	Other	3.534	3.277	2.199
TIAM2 (includes EG:26230)	T-cell lymphoma invasion and metastasis 2	NM_012454	Cytoplasm	Enzyme	1.225		
TICAM2	Toll-like receptor adaptor molecule 2	NM_021649	Plasma Membrane	Other		1.951	1.394
TINAG	Tubulointerstitial nephritis antigen	XM_518550	Extracellular Space	Peptidase			1.653
TJP2	Tight junction protein 2 (zona occludens 2)	NM_001003204	Plasma Membrane	Kinase		1.098	
TLL1	Tolloid-like 1	AC097502	Extracellular Space	Peptidase	2.082		
TMBIM1	Transmembrane BAX inhibitor motif containing 1	BC142530	unknown	Other		1.19	1.115
TMEM123	Transmembrane protein 123	XM_001152796	Plasma Membrane	Other			1.409
TMEM27	Transmembrane protein 27	NM_020665	Plasma Membrane	Other			1.549
TMEM43	Transmembrane protein 43	NM_001102480	Nucleus	Other			1.126
TMOD4	Tropomodulin 4 (muscle)	XM_540312	unknown	Other		1.449	
TMTC3	Transmembrane and tetratricopeptide repeat containing 3	XM_532644	unknown	Other	1.154		1.561
TMX1	Thioredoxin-related transmembrane protein 1	XM_848339	Cytoplasm	Enzyme		1.077	
TNFAIP8	Tumor necrosis factor, alpha-induced protein 8	XM_001152429	Cytoplasm	Other	1.015		1.897
TNFRSF11B	Tumor necrosis factor receptor superfamily, member 11b	NM_001098056	Plasma Membrane	Transmembrane receptor	1.832	1.25	

Table B-1. Continued

Symbol	Entrez gene name	GenBank	Location	Type(s)	Fold change exposure	Fold change survival	Fold change location
TNFRSF17	Tumor necrosis factor receptor superfamily, member 17	BC058291	Plasma Membrane	Other			1.217
TNFRSF25	Tumor necrosis factor receptor superfamily, member 25	XM_546752	Plasma Membrane	Transmembrane receptor	1.636	1.26	1.454
TNPO1	Transportin 1	NM_002270	Nucleus	Transporter		1.053	1.25
TOX	Thymocyte selection-associated high mobility group box	AC105150	Nucleus	Other	1.27		1.419
TP73	Tumor protein p73	XM_593064	Nucleus	Transcription regulator	1.171		
TRIB2	Tribbles homolog 2 (Drosophila)	XM_001161050	Plasma Membrane	Kinase	1.166		
TRIP6	Thyroid hormone receptor interactor 6	NM_001035469	Extracellular Space	Cytokine		1.109	
TRPC3	Transient receptor potential cation channel, subfamily C, member 3	XM_540964	Plasma Membrane	Ion channel			1.943
TRPV2	Transient receptor potential cation channel, subfamily V, member 2	XM_546641	Plasma Membrane	Ion channel		1.619	
TSPAN2	Tetraspanin 2	NM_005725	unknown	Other		1.31	
TSPAN8	Tetraspanin 8	XM_531678	Plasma Membrane	Other			2.49
TTC9C	Tetratricopeptide repeat domain 9C	NM_001083792	unknown	Other		1.169	
TTF2	Transcription termination factor, RNA polymerase II	XM_513683	Nucleus	Transcription regulator	1.17	1.74	
TYK2	Tyrosine kinase 2	XM_590006	Plasma Membrane	Kinase	1.504		
UBA6	Ubiquitin-like modifier activating enzyme 6	NM_018227	Cytoplasm	Enzyme	1.302	1.461	1.327
UBE2C	Ubiquitin-conjugating enzyme E2C	NM_007019	Cytoplasm	Enzyme	3.688	2.958	2.15
UBE2G1	Ubiquitin-conjugating enzyme E2G 1 (UBC7 homolog, yeast)	XM_001174528	Cytoplasm	Enzyme		1.004	1.464
UBE2L3	Ubiquitin-conjugating enzyme E2L 3	XM_855294	Cytoplasm	Enzyme	1.188		
UBR1	Ubiquitin protein ligase E3 component n-recognin 1	XM_510341	Cytoplasm	Enzyme	1.061		
UHMK1	U2AF homology motif (UHM) kinase 1	AL359699	Nucleus	Kinase			1.383
UNC119B	Unc-119 homolog B (C. Elegans)	XM_849209	unknown	Other		1.343	
UNC13A	Unc-13 homolog A (C. Elegans)	NM_001080421	Plasma Membrane	Other	1.44		
USP13 (includes EG:8975)	Ubiquitin specific peptidase 13 (isopeptidase T-3)	XM_535813	unknown	Peptidase		1.272	
USP15	Ubiquitin specific peptidase 15	XM_001166186	Cytoplasm	Peptidase	1.399		
USP25	Ubiquitin specific peptidase 25	BS000022	unknown	Peptidase	1.331		1.324
USP43	Ubiquitin specific peptidase 43	XM_511843	unknown	Peptidase		1.134	
USP53	Ubiquitin specific peptidase 53	XM_545046	unknown	Enzyme	2.099	2.066	1.8
VAT1L	Vesicle amine transport protein 1 homolog (T. Californica)-like	XM_001139539	unknown	Enzyme			1.367
VGLL2	Vestigial like 2	BC118622	Nucleus	Transcription		2.693	

Table B-1. Continued

Symbol	Entrez gene name	GenBank	Location	Type(s)	Fold change exposure	Fold change survival	Fold change location
	(Drosophila)			regulator			
VRK2	Vaccinia related kinase 2	AC073215	Nucleus	Kinase	1.755		
WDR33	WD repeat domain 33	NM_001006623	Nucleus	Other	1.14		
WIPF1	WAS/WASL interacting protein family, member 1	NM_001076923	Cytoplasm	Other			1.753
WISP3	WNT1 inducible signaling pathway protein 3	BC105941	Extracellular Space	Growth factor		1.354	1.421
WWTR1	WW domain containing transcription regulator 1	XM_847454	Nucleus	Transcription regulator	3.107	2.939	2.33
XRN1	5'-3' exoribonuclease 1	XM_847344	Cytoplasm	Enzyme	1.002		
ZAP70	Zeta-chain (TCR) associated protein kinase 70kda	BC142505	Plasma Membrane	Kinase	4.244	2.8	1.177
ZFP57	Zinc finger protein 57 homolog (mouse)	NM_001109809	Nucleus	Transcription regulator			1.025
ZIC1	Zic family member 1 (odd-paired homolog, Drosophila)	XM_516806	Nucleus	Transcription regulator			1.836
ZNF185	Zinc finger protein 185 (LIM domain)	XM_549348	Nucleus	Other	1.092		
ZNF503	Zinc finger protein 503	XM_001256479	Nucleus	Other	1.454		
ZNFX1	Zinc finger, NFX1-type containing 1	XM_534452	Nucleus	Transcription regulator	3.531	3.311	1.255

APPENDIX C
LIST OF HIGHLY DOWNREGULATED TRANSCRIPTS RECOGNIZED BY IPA

Table C-1. Transcripts decreased in expression recognized by IPA

Symbol	Entrez gene name	GenBank	Location	Type(s)	Fold change exposure	Fold change survival	Fold change location
AASDHPPT	Aminoadipate-semialdehyde dehydrogenase-phosphopantetheinyl transferase	XM_508734	Cytoplasm	Enzyme	-1.423		
ABCA2	ATP-binding cassette, sub-family A (ABC1), member 2	NM_001606	Plasma Membrane	Transporter	-2.244	-2.019	
ABCA2	ATP-binding cassette, sub-family A (ABC1), member 2	NM_001606	Plasma Membrane	Transporter			
ABCB7	ATP-binding cassette, sub-family B (MDR/TAP), member 7	AL359545	Cytoplasm	Transporter	-1.402		
ABCD2	ATP-binding cassette, sub-family D (ALD), member 2	XM_001168647	Cytoplasm	Transporter		-1.286	
ABCD3	ATP-binding cassette, sub-family D (ALD), member 3	NM_001105396	Cytoplasm	Transporter	-1.917		
ABI2	Abl-interactor 2	XM_001173163	Cytoplasm	Other			-1.132
ABL1	C-abl oncogene 1, receptor tyrosine kinase	NM_005157	Nucleus	Kinase		-1.181	
ABLIM1	Actin binding LIM protein 1	XM_535022	Cytoplasm	Other		-1.463	
ABLIM2	Actin binding LIM protein family, member 2	XM_847882	Cytoplasm	Other		-1.632	
ACADS	Acyl-Coenzyme A dehydrogenase, C-2 to C-3 short chain	XM_534712	Cytoplasm	Enzyme	-1.033		
ACCN1	Amiloride-sensitive cation channel 1, neuronal	XM_548270	Plasma Membrane	Ion channel	-2.229	-2.002	-2.603
ACCN2	Amiloride-sensitive cation channel 2, neuronal	XM_001155207	Plasma Membrane	Ion channel			-1.194
ACER3	Alkaline ceramidase 3	NM_001102285	Cytoplasm	Enzyme	-1.388		
ACSBG1	Acyl-coa synthetase bubblegum family member 1	XM_510525	Cytoplasm	Enzyme	-1.886		
ACSL3	Acyl-coa synthetase long-chain family member 3	XM_516118	Cytoplasm	Enzyme			-1.027
ACSS2	Acyl-coa synthetase short-chain family member 2	NM_001076552	Cytoplasm	Enzyme	-1.169		
ACTR1A	ARP1 actin-related protein 1 homolog A, centractin alpha (yeast)	NM_001003164	Cytoplasm	Other	-1.031		
ADAM22	ADAM metallopeptidase domain 22	XM_001164160	Plasma Membrane	Peptidase	-1.062		-1.138
ADAMTS2	ADAM metallopeptidase with thrombospondin type 1 motif, 2	XM_538574	Extracellular Space	Peptidase		-1.031	
ADCK1	Aarf domain containing kinase 1	XM_547933	unknown	Kinase		-1.443	
ADCY1	Adenylate cyclase 1 (brain)	NM_174229	Plasma Membrane	Enzyme		-1.789	-1.898
ADCY2	Adenylate cyclase 2 (brain)	XM_851103	Plasma Membrane	Enzyme	-1.683		
ADCY2	Adenylate cyclase 2 (brain)	XM_535798	Plasma Membrane	Enzyme		-1.223	-2.027
ADCY5	Adenylate cyclase 5	NM_183357	Plasma Membrane	Enzyme	-1.258	-1.379	
ADCY8	Adenylate cyclase 8 (brain)	XM_539166	Plasma Membrane	Enzyme	-1.021		-1.954
ADCY9	Adenylate cyclase 9	BC151229	Plasma Membrane	Enzyme			-1.46
ADHFE1	Alcohol dehydrogenase, iron containing, 1	XM_844355	unknown	Enzyme	-1.32	-1.415	
ADORA3	Adenosine A3 receptor	BC029831	Plasma Membrane	G-protein coupled receptor	-1.966		

Table C-1. Continued

Symbol	Entrez gene name	GenBank	Location	Type(s)	Fold change exposure	Fold change survival	Fold change location
ADRA1B	Adrenergic, alpha-1B-, receptor	XM_001250068	Plasma Membrane	G-protein coupled receptor			-1.222
ADRA2A	Adrenergic, alpha-2A-, receptor	BC035047	Plasma Membrane	G-protein coupled receptor			-1.285
ADRBK2	Adrenergic, beta, receptor kinase 2	NM_005160	Cytoplasm	Kinase	-1.806	-1.882	-1.792
AFF3	AF4/FMR2 family, member 3	XM_001161010	Nucleus	Transcription regulator	-1.068		-1.474
AFG3L2	AFG3 atpase family gene 3-like 2 (yeast)	XM_547682	Cytoplasm	Peptidase	-1.007		
AGAP2	Arfgap with gtpase domain, ankyrin repeat and PH domain 2	XM_581013	Nucleus	Enzyme		-1.881	-1.544
AGPAT4	1-acylglycerol-3-phosphate O-acyltransferase 4 (lysophosphatidic acid acyltransferase, delta)	XM_001153359	Cytoplasm	Enzyme	-1.087		
AHI1	Abelson helper integration site 1	BC151742	unknown	Other		-2.099	-1.644
AHNAK	AHNAK nucleoprotein	NM_024060	Nucleus	Other	-1.841	-1.088	
AK5	Adenylate kinase 5	XM_547325	Cytoplasm	Kinase	-1.29	-1.044	-2.248
AKAP11	A kinase (PRKA) anchor protein 11	XM_001151850	Cytoplasm	Other		-1.148	-1.084
ALDH4A1	Aldehyde dehydrogenase 4 family, member A1	XM_850179	Cytoplasm	Enzyme	-1.27		
ALDH6A1	Aldehyde dehydrogenase 6 family, member A1	XM_001152670	Cytoplasm	Enzyme	-1.852	-1.52	
ALOX15B	Arachidonate 15-lipoxygenase, type B	XM_588924	Cytoplasm	Enzyme	-1.511		-1.032
ALOX5	Arachidonate 5-lipoxygenase	XM_613515	Cytoplasm	Enzyme	-1.761	-1.274	
ALOX5AP	Arachidonate 5-lipoxygenase-activating protein	XM_534516	Plasma Membrane	Other	-2.782	-1.019	
ALS2	Amyotrophic lateral sclerosis 2 (juvenile)	NM_001079920	Cytoplasm	Other		-1.074	-1.067
AMT (includes EG:275)	Aminomethyltransferase	NM_001033993	Cytoplasm	Enzyme	-2.11	-1.193	-1.126
AMY2A	Amylase, alpha 2A (pancreatic)	NM_001035016	Extracellular Space	Enzyme	-1.2	-1.429	
ANKH	Ankylosis, progressive homolog (mouse)	NM_001109793	Plasma Membrane	Transporter	-1.75	-1.213	-1.383
ANKIB1	Ankyrin repeat and IBR domain containing 1	XM_844926	Nucleus	Transcription regulator	-1.194		
ANKRD11	Ankyrin repeat domain 11	XM_546778	Nucleus	Other	-1.235		
ANKRD54	Ankyrin repeat domain 54	XM_538382	Nucleus	Transcription regulator		-1.217	-1.074
ANKS1B	Ankyrin repeat and sterile alpha motif domain containing 1B	AC084374	Nucleus	Other		-2.279	
ANTXR1	Anthrax toxin receptor 1	AF090095	Plasma Membrane	Other	-1.132		
ANTXR2	Anthrax toxin receptor 2	AC109518	Plasma Membrane	Other		-1.881	
ANXA3	Annexin A3	XM_535624	Cytoplasm	Enzyme	-1.341		
ANXA9	Annexin A9	NM_001035373	Plasma Membrane	Transmembrane receptor	-2.76		
AP2B1	Adaptor-related protein complex 2, beta 1 subunit	XM_001174101	Cytoplasm	Transporter		-1.024	-1.219
AP2S1	Adaptor-related protein complex 2, sigma 1 subunit	XM_533634	Cytoplasm	Transporter	-1.137		
AP3M2	Adaptor-related protein complex 3, mu 2 subunit	XM_877825	Cytoplasm	Transporter	-2.167	-2.199	-1.352
APBA2	Amyloid beta (A4) precursor protein-binding, family A, member 2	XM_843605	Cytoplasm	Transporter	-1.356		-1.543

Table C-1. Continued

Symbol	Entrez gene name	GenBank	Location	Type(s)	Fold change exposure	Fold change survival	Fold change location
APH1B	Anterior pharynx defective 1 homolog B (C. Elegans)	XM_001173827	Plasma Membrane	Peptidase	-1.106		
APLNR	Apelin receptor	AK097232	Plasma Membrane	G-protein coupled receptor	-2.857	-2.059	-2.364
APOLD1	Apolipoprotein L domain containing 1	BC126435	unknown	Other	-2.369		-1.406
APPL2	Adaptor protein, phosphotyrosine interaction, PH domain and leucine zipper containing 2	AY113704	Cytoplasm	Other	-1.205		
ARF2	ADP-ribosylation factor 2	XM_537606	Cytoplasm	Transporter	-1.591		
ARF3	ADP-ribosylation factor 3	BC007647	Cytoplasm	Enzyme		-1.333	-1.284
ARHGAP22	Rho gtpase activating protein 22	NM_021226	Cytoplasm	Other		-1.124	-1.139
ARHGAP6	Rho gtpase activating protein 6	XM_548858	Cytoplasm	Other		-1.058	
ARHGDIG	Rho GDP dissociation inhibitor (GDI) gamma	XM_849221	Cytoplasm	Other			-1.27
ARHGEF2	Rho/Rac guanine nucleotide exchange factor (GEF) 2	BC020567	Cytoplasm	Other	-1.13		
ARID4A	AT rich interactive domain 4A (RBP1-like)	XM_859819	Nucleus	Transcription regulator	-1.76	-2.145	-2.296
ARL4C	ADP-ribosylation factor-like 4C	NM_001102348	Nucleus	Enzyme	-1.246		
ARL5A	ADP-ribosylation factor-like 5A	XM_001136344	unknown	Enzyme		-1.576	
ARL5B	ADP-ribosylation factor-like 5B	XM_843199	unknown	Enzyme		-1.099	
ARMCX2	Armadillo repeat containing, X-linked 2	AK291342	unknown	Other	-1.529		
ARNT2	Aryl-hydrocarbon receptor nuclear translocator 2	AC101776	Nucleus	Transcription regulator	-2.328	-1.231	-1.274
ARX	Aristaless related homeobox	XM_854885	Nucleus	Transcription regulator			-1.721
AS3MT	Arsenic (+3 oxidation state) methyltransferase	AY817668	Cytoplasm	Enzyme		-1.253	
ASB1	Ankyrin repeat and SOCS box-containing 1	XM_516189	Nucleus	Transcription regulator	-2.439		-1.24
ASB13	Ankyrin repeat and SOCS box-containing 13	XM_001145055	unknown	Other	-1.765		
ASB5	Ankyrin repeat and SOCS box-containing 5	NM_001075744	Nucleus	Transcription regulator		-1.292	
ASPA	Aspartoacylase (Canavan disease)	XM_849422	unknown	Enzyme	-2.156		
ASTN2 (includes EG:23245)	Astrotactin 2	NM_014010	unknown	Other			-1.039
ATMIN	ATM interactor	XM_001249565	Nucleus	Other	-1.835		
ATP1A2	Atpase, Na+/K+ transporting, alpha 2 (+) polypeptide	XM_513921	Plasma Membrane	Transporter	-1.752		
ATP2B2	Atpase, Ca++ transporting, plasma membrane 2	NM_001001331	Plasma Membrane	Transporter		-1.796	-1.967
ATP2B3	Atpase, Ca++ transporting, plasma membrane 3	XM_001251087	Plasma Membrane	Transporter		-1.379	-1.784
ATP8A1 (includes EG:10396)	Atpase, aminophospholipid transporter (APLT), class I, type 8A, member 1	XM_517167	Cytoplasm	Transporter		-1.641	-1.144
ATP9B	Atpase, class II, type 9B	NM_198531	Cytoplasm	Transporter		-1.098	
ATRNL1	Attractin-like 1	NM_207303	unknown	Other			-1.085
ATXN1	Ataxin 1	NM_000332	Nucleus	Other			-1.01
AUH	AU RNA binding protein/enoyl-Coenzyme A hydratase	XM_533549	Cytoplasm	Enzyme	-1.123		
AVP	Arginine vasopressin	BC102897	Extracellular Space	Other	-2.246		

Table C-1. Continued

Symbol	Entrez gene name	GenBank	Location	Type(s)	Fold change exposure	Fold change survival	Fold change location
AVPR1A	Arginine vasopressin receptor 1A	NM_000706	Plasma Membrane	G-protein coupled receptor		-2.362	-3.53
AXIN2	Axin 2	XM_001163124	Cytoplasm	Other	-2.657	-1.554	
B3GALNT1	Beta-1,3-N-acetylgalactosaminyltransferase 1 (globoside blood group)	NM_001076963	Cytoplasm	Enzyme	-1.157		
B3GALT2	UDP-Gal:betaglcnac beta 1,3-galactosyltransferase, polypeptide 2	NM_001076188	Cytoplasm	Enzyme			-1.823
B3GAT1	Beta-1,3-glucuronyltransferase 1 (glucuronosyltransferase P)	NM_054025	Cytoplasm	Enzyme	-1.507	-1.53	-1.451
B3GAT2	Beta-1,3-glucuronyltransferase 2 (glucuronosyltransferase S)	BC113995	Cytoplasm	Enzyme	-1.777		
B3GNT1	UDP-glcnac:betagal beta-1,3-N-acetylglucosaminyltransferase 1	XM_533222	Cytoplasm	Enzyme		-1.121	
B4GALT6	UDP-Gal:betaglcnac beta 1,4-galactosyltransferase, polypeptide 6	XM_523901	Cytoplasm	Enzyme		-1.323	
BAALC	Brain and acute leukemia, cytoplasmic	AK093819	Cytoplasm	Other	-2.305	-1.263	-1.561
BACE1	Beta-site APP-cleaving enzyme 1	XM_001158264	Cytoplasm	Peptidase	-1.546		
BAG4	BCL2-associated athanogene 4	XM_519710	Cytoplasm	Other		-1.167	
BAG5	BCL2-associated athanogene 5	NM_001015049	unknown	Other		-1.278	
BASP1	Brain abundant, membrane attached signal protein 1	XM_001175409	Plasma Membrane	Other			-1.276
BAT2L	HLA-B associated transcript 2-like	XM_520327	unknown	Other		-1.331	
BBOX1	Butyrobetaine (gamma), 2-oxoglutarate dioxygenase (gamma-butyrobetaine hydroxylase) 1	BC011034	Cytoplasm	Enzyme	-2.586	-2.935	-2.068
BCHE	Butyrylcholinesterase	AC009811	Plasma Membrane	Enzyme	-1.653		
BCL11A	B-cell CLL/lymphoma 11A (zinc finger protein)	NM_022893	Nucleus	Transcription regulator			-1.539
BCLAF1	BCL2-associated transcription factor 1	XM_855478	Nucleus	Transcription regulator	-1.121		
BICD1	Bicaudal D homolog 1 (Drosophila)	AC087245	Cytoplasm	Other		-1.079	
BLOC1S3	Biogenesis of lysosomal organelles complex-1, subunit 3	NM_001099086	Cytoplasm	Other	-2.57		
BMP2K (includes EG:55589)	BMP2 inducible kinase	XM_843801	Nucleus	Kinase	-1.151		
BMP3	Bone morphogenetic protein 3	XM_001144027	Extracellular Space	Growth factor	-1.048	-1.662	-1.235
BNIP3L	BCL2/adenovirus E1B 19kda interacting protein 3-like	XM_001162226	Cytoplasm	Other	-1.032		
BRP44	Brain protein 44	Z97876	Plasma Membrane	Other	-1.134		
BRUNOL4	Bruno-like 4, RNA binding protein (Drosophila)	NM_001099068	Nucleus	Translation regulator		-1.272	-1.335
BSN	Bassoon (presynaptic cytomatrix protein)	NM_003458	Plasma Membrane	Other	-1.911	-1.478	-2.518
C10ORF10	Chromosome 10 open reading frame 10	XM_534951	Cytoplasm	Other			-2.06
C10ORF72	Chromosome 10 open reading frame 72	NM_001031746	unknown	Other	-1.385		
C11ORF41	Chromosome 11 open reading frame 41	NM_012194	unknown	Other			-1.967
C12ORF51	Chromosome 12 open reading frame 51	NM_001109662	unknown	Other	-1.229	-1.086	
C17ORF28	Chromosome 17 open reading frame 28	AK074401	unknown	Other	-1.713	-1.894	-1.452

Table C-1. Continued

Symbol	Entrez gene name	GenBank	Location	Type(s)	Fold change exposure	Fold change survival	Fold change location
C17ORF46	Chromosome 17 open reading frame 46	XM_843189	unknown	Other			-1.173
C18ORF1	Chromosome 18 open reading frame 1	NM_001003675	unknown	Other		-1.499	-1.305
C1ORF96	Chromosome 1 open reading frame 96	XM_611981	unknown	Other	-1.797		
C1QL3	Complement component 1, q subcomponent-like 3	XM_865369	Extracellular Space	Other			-3.055
C1QTNF4	C1q and tumor necrosis factor related protein 4	XM_540740	Extracellular Space	Other			-1.766
C20ORF103	Chromosome 20 open reading frame 103	XM_845541	Cytoplasm	Other		-2.458	-3.139
C20ORF194	Chromosome 20 open reading frame 194	NM_001009984	Nucleus	Other		-1.099	
C21ORF33	Chromosome 21 open reading frame 33	NM_198155	Cytoplasm	Other	-1.718		
C2CD2L	C2CD2-like	BC022219	unknown	Other			-1.032
C3ORF10	Chromosome 3 open reading frame 10	XM_591430	unknown	Other	-1.267		
C5ORF44	Chromosome 5 open reading frame 44	XM_001163559	unknown	Other			-1.141
C6ORF142	Chromosome 6 open reading frame 142	NM_138569	unknown	Other			-2.615
C6ORF168	Chromosome 6 open reading frame 168	AK055101	unknown	Other			-1.148
C6ORF222	Chromosome 6 open reading frame 222	XM_845363	unknown	Other	-1.041		
C7ORF42	Chromosome 7 open reading frame 42	XM_536835	unknown	Other	-1.586		
C8ORF46	Chromosome 8 open reading frame 46	NM_001076475	unknown	Other			-1.568
C8ORF79	Chromosome 8 open reading frame 79	NM_001099677	unknown	Other	-1.119	-2.078	-1.123
C9ORF93	Chromosome 9 open reading frame 93	XM_531940	unknown	Other	-1.367	-1.215	
CA14	Carbonic anhydrase XIV	XM_001167925	Plasma Membrane	Enzyme	-1.655	-1.654	
CA5B	Carbonic anhydrase VB, mitochondrial	XM_001139130	Cytoplasm	Enzyme	-1.757	-1.393	
CA7	Carbonic anhydrase VII	XM_598644	Cytoplasm	Enzyme			-2.335
CA8	Carbonic anhydrase VIII	NM_001083690	Cytoplasm	Enzyme	-1.453		
CAB39	Calcium binding protein 39	NM_001046087	Cytoplasm	Other	-1.115		
CACNA1B	Calcium channel, voltage-dependent, N type, alpha 1B subunit	BC033060	Plasma Membrane	Ion channel			-1.579
CACNA1E	Calcium channel, voltage-dependent, R type, alpha 1E subunit	L27745	Plasma Membrane	Ion channel		-1.778	
CACNA1G	Calcium channel, voltage-dependent, T type, alpha 1G subunit	XM_001252666	Plasma Membrane	Ion channel	-1.257		
CACNG2	Calcium channel, voltage-dependent, gamma subunit 2	NM_007583	Plasma Membrane	Ion channel			-1.513
CADPS2	Ca++-dependent secretion activator 2	NM_001102055	Plasma Membrane	Other			-3.008
CALB1	Calbindin 1, 28kda	NM_001076195	Cytoplasm	Other		-1.27	
CALCRL	Calcitonin receptor-like	NM_005795	Plasma Membrane	G-protein coupled receptor	-1.833		
CALN1	Calneuron 1	NM_001017440	unknown	Other		-1.579	-1.806
CAMK2A	Calcium/calmodulin-dependent protein kinase II alpha	NM_001075938	Cytoplasm	Kinase		-1.408	-3.062

Table C-1. Continued

Symbol	Entrez gene name	GenBank	Location	Type(s)	Fold change exposure	Fold change survival	Fold change location
CAMK2G	Calcium/calmodulin-dependent protein kinase II gamma	XM_846444	Cytoplasm	Kinase	-2.489	-1.146	-1.625
CAMK2N1	Calcium/calmodulin-dependent protein kinase II inhibitor 1	BC151544	Plasma Membrane	Kinase		-1.096	-1.297
CAMK4	Calcium/calmodulin-dependent protein kinase IV	XM_517873	Nucleus	Kinase		-1.976	
CAMKK2	Calcium/calmodulin-dependent protein kinase kinase 2, beta	NM_172214	Cytoplasm	Kinase		-1.087	-1.495
CAMTA1 (includes EG:23261)	Calmodulin binding transcription activator 1	BC151835	unknown	Other		-1.335	-1.397
CAND1	Cullin-associated and neddylation-dissociated 1	XM_531667	Cytoplasm	Transcription regulator		-1.104	
CAPN2	Calpain 2, (m/II) large subunit	NM_001748	Cytoplasm	Peptidase	-1.194		
CASK	Calcium/calmodulin-dependent serine protein kinase (MAGUK family)	BC029936	Plasma Membrane	Kinase			-1.144
CASKIN1	CASK interacting protein 1	XM_848538	Nucleus	Transcription regulator		-1.253	-1.474
CAST	Calpastatin	BC148894	Cytoplasm	Peptidase	-1.055		
CBFA2T2	Core-binding factor, runt domain, alpha subunit 2; translocated to, 2	XM_606138	Nucleus	Transcription regulator		-1.097	-1.196
CBFA2T3	Core-binding factor, runt domain, alpha subunit 2; translocated to, 3	XM_546780	Nucleus	Transcription regulator	-1.112		
CBLC	Cas-Br-M (murine) ecotropic retroviral transforming sequence c	NM_001101248	Nucleus	Enzyme	-1.145		
CBLN1	Cerebellin 1 precursor	XM_001163762	Cytoplasm	Other	-2.19		
CCDC132	Coiled-coil domain containing 132	AC027655	unknown	Other	-1.062		
CCND2	Cyclin D2	XM_849493	Nucleus	Other		-1.035	-1.658
CD109	CD109 molecule	NM_133493	Plasma Membrane	Other	-2.211		
CD163L1 (includes EG:283316)	CD163 molecule-like 1	NM_174941	Plasma Membrane	Transmembrane receptor			-1.024
CDH10	Cadherin 10, type 2 (T2-cadherin)	NM_006727	Plasma Membrane	Other			-2.094
CDH4 (includes EG:1002)	Cadherin 4, type 1, R-cadherin (retinal)	NM_001794	Plasma Membrane	Other		-1.934	
CDH9	Cadherin 9, type 2 (T1-cadherin)	XM_001135234	Plasma Membrane	Other		-1.244	-1.892
CDK5R1	Cyclin-dependent kinase 5, regulatory subunit 1 (p35)	NM_003885	Nucleus	Kinase			-1.567
CDR2L	Cerebellar degeneration-related protein 2-like	XM_540425	unknown	Other	-1.774		
CENPB	Centromere protein B, 80kda	NM_001810	Nucleus	Other	-1.027		
CEP170	Centrosomal protein 170kda	XM_537218	Nucleus	Other	-1.239		
CETN2	Centrin, EF-hand protein, 2	NM_001038515	Nucleus	Enzyme	-1.679		
CHD3	Chromodomain helicase DNA binding protein 3	NM_005852	Nucleus	Enzyme	-1.367	-1.852	-1.585
CHGB	Chromogranin B (secretogranin 1)	XM_534354	Extracellular Space	Other	-1.184		-1.449
CHN1 (includes EG:1123)	Chimerin (chimaerin) 1	XM_856276	Cytoplasm	Other		-1.943	-2.319
CHN2	Chimerin (chimaerin) 2	NM_001045963	Cytoplasm	Other		-1.174	
CHP	Calcium binding protein P22	BT030715	Cytoplasm	Transporter	-1.276		
CHP2	Calcineurin B homologous protein 2	XM_547089	Cytoplasm	Other	-1.921		

Table C-1. Continued

Symbol	Entrez gene name	GenBank	Location	Type(s)	Fold change exposure	Fold change survival	Fold change location
CHRNA4	Cholinergic receptor, nicotinic, alpha 4	XM_543097	Plasma Membrane	Transmembrane receptor	-2.705		
CHRNB4	Cholinergic receptor, nicotinic, beta 4	NM_174517	Plasma Membrane	Transmembrane receptor	-1.908		
CLASP2	Cytoplasmic linker associated protein 2	XM_609911	Cytoplasm	Other	-1.072		
CLCN3	Chloride channel 3	XM_001154165	Plasma Membrane	Ion channel	-1.767		
CLCN4	Chloride channel 4	NM_001830	Plasma Membrane	Ion channel		-1.249	
CLIP2	CAP-GLY domain containing linker protein 2	XM_583422	Cytoplasm	Transcription regulator	-1.084	-1.056	-1.116
CLIP4	CAP-GLY domain containing linker protein family, member 4	XM_001162138	unknown	Other		-1.274	
CLTB	Clathrin, light chain (Lcb)	XM_546220	Plasma Membrane	Other			-1.069
CMTM4	CKLF-like MARVEL transmembrane domain containing 4	CR933620	Extracellular Space	Cytokine		-1.37	-1.28
CNP	2',3'-cyclic nucleotide 3' phosphodiesterase	XM_511496	Cytoplasm	Enzyme	-1.785		
CNTN1	Contactin 1	XM_001168019	Plasma Membrane	Enzyme	-1.716	-1.624	
CNTN2	Contactin 2 (axonal)	X67734	Plasma Membrane	Other	-1.453		
CNTN4	Contactin 4	AC026882	Plasma Membrane	Enzyme		-1.608	
COBRA1	Cofactor of BRCA1	BC114764	Nucleus	Other	-1.374	-1.247	
COCH	Coagulation factor C homolog, cochlin (Limulus polyphemus)	XM_509886	Extracellular Space	Other			-2.996
COL13A1	Collagen, type XIII, alpha 1	XM_001170115	Plasma Membrane	Other	-1.322	-2.04	
COL5A1	Collagen, type V, alpha 1	NM_000093	Extracellular Space	Other		-1.01	
COL5A2	Collagen, type V, alpha 2	AC064833	Extracellular Space	Other	-1.02	-1.038	
COL6A6	Collagen, type VI, alpha 6	NM_001102608	unknown	Other	-2.26		-5.583
COPG2	Coatomer protein complex, subunit gamma 2	AC144863	Cytoplasm	Transporter	-2.578	-2.591	-1.047
CORO6	Coronin 6	XM_001137660	unknown	Other			-1.23
CORO7	Coronin 7	NM_001075903	Cytoplasm	Other	-1.715	-1.899	
COX6B1	Cytochrome c oxidase subunit Vib polypeptide 1 (ubiquitous)	XM_850376	Cytoplasm	Enzyme	-1.349		
COX7A2	Cytochrome c oxidase subunit viia polypeptide 2 (liver)	XM_848778	Cytoplasm	Enzyme	-1.382		
COX7C (includes EG:1350)	Cytochrome c oxidase subunit viic	AC108110	Cytoplasm	Enzyme	-1.447	-1.366	
CPEB1	Cytoplasmic polyadenylation element binding protein 1	AF329402	Cytoplasm	Other			-1.013
CRAT	Carnitine acetyltransferase	BT030711	Cytoplasm	Enzyme	-1.258	-1.009	
CREBL2	Camp responsive element binding protein-like 2	XM_001153386	Nucleus	Transcription regulator	-1.359		
CREG1	Cellular repressor of E1A-stimulated genes 1	NM_001075942	Nucleus	Transcription regulator	-1.883		
CRLF1	Cytokine receptor-like factor 1	XM_588353	Extracellular	Other	-2.126	-1.456	

Table C-1. Continued

Symbol	Entrez gene name	GenBank	Location	Type(s)	Fold change exposure	Fold change survival	Fold change location
			Space				
CRTC1	CREB regulated transcription coactivator 1	XM_866768	Nucleus	Transcription regulator		-1.268	-1.098
CRTC3	CREB regulated transcription coactivator 3	NM_173863	unknown	Other	-1.561		
CRYZ	Crystallin, zeta (quinone reductase)	AK128794	Cytoplasm	Enzyme	-1.422		
CSMD1	CUB and Sushi multiple domains 1	AC087367	Plasma Membrane	Other	-1.6	-2.328	-2.461
CSMD3 (includes EG:114788)	CUB and Sushi multiple domains 3	AK095111	unknown	Enzyme		-1.334	
CSNK1A1	Casein kinase 1, alpha 1	XM_862545	Cytoplasm	Kinase		-1.211	
CSRP1	Cysteine and glycine-rich protein 1	XM_843516	Nucleus	Other	-1.226		
CTDSPL	CTD (carboxy-terminal domain, RNA polymerase II, polypeptide A) small phosphatase-like	XM_001170981	Nucleus	Other			-1.15
CTNNA3	Catenin (cadherin-associated protein), alpha 3	AC018979	Plasma Membrane	Other		-1.221	
CUX2	Cut-like homeobox 2	BC151245	Nucleus	Transcription regulator			-2.455
CX3CL1	Chemokine (C-X3-C motif) ligand 1	XM_544391	Extracellular Space	Cytokine			-1.015
CYB5B	Cytochrome b5 type B (outer mitochondrial membrane)	XM_582806	Cytoplasm	Enzyme	-2.232	-1.636	-1.143
CYFIP2 (includes EG:26999)	Cytoplasmic FMR1 interacting protein 2	XM_597034	Cytoplasm	Other	-1.441	-1.381	-1.25
CYTSB	Cytospin B	AC004702	Nucleus	Other			-1.156
DAB1	Disabled homolog 1 (Drosophila)	XM_847827	Cytoplasm	Other		-1.181	-1.156
DAP3	Death associated protein 3	XM_580421	Cytoplasm	Other	-1.526		
DARC	Duffy blood group, chemokine receptor	XM_001170629	Plasma Membrane	G-protein coupled receptor			-1.009
DCAF7	DDB1 and CUL4 associated factor 7	XM_511593	Cytoplasm	Other		-2.092	
DCLK1	Doublecortin-like kinase 1	NM_004734	Cytoplasm	Kinase		-1.902	-3.317
DCN	Decorin	AK291309	Extracellular Space	Other	-1.224	-1.917	-3.633
DDAH1	Dimethylarginine dimethylaminohydrolase 1	NM_001102201	Cytoplasm	Enzyme	-2.404		
DDO	D-aspartate oxidase	BC103184	Cytoplasm	Enzyme	-1.003		
DDX17	DEAD (Asp-Glu-Ala-Asp) box polypeptide 17	XM_855709	Nucleus	Enzyme	-1.44	-1.557	
DEPDC6 (includes EG:64798)	DEP domain containing 6	AC091563	unknown	Other	-1.699	-1.14	
DFFA	DNA fragmentation factor, 45kda, alpha polypeptide	NM_001075342	Nucleus	Enzyme	-1.811		
DGKG	Diacylglycerol kinase, gamma 90kda	NM_001080745	Cytoplasm	Kinase	-1.447	-1.309	-1.244
DGKQ	Diacylglycerol kinase, theta 110kda	XM_872918	Cytoplasm	Kinase	-2.06	-1.188	
DHCR24	24-dehydrocholesterol reductase	XM_001153810	Cytoplasm	Enzyme	-1.463		
DIP2B	DIP2 disco-interacting protein 2 homolog B (Drosophila)	NM_173602	unknown	Other	-1.847		
DIRAS1	DIRAS family, GTP-binding RAS-like 1	XM_542186	Plasma Membrane	Enzyme	-1.889	-1.41	-1.262
DIRAS2	DIRAS family, GTP-binding RAS-like 2	XM_001142598	Plasma Membrane	Enzyme		-1.116	-1.501
DIXDC1	DIX domain containing 1	NM_033425	unknown	Other	-1.909	-1.299	

Table C-1. Continued

Symbol	Entrez gene name	GenBank	Location	Type(s)	Fold change exposure	Fold change survival	Fold change location
DLAT	Dihydrolipoamide S-acetyltransferase	XM_590291	Cytoplasm	Enzyme	-1.106		
DLC1	Deleted in liver cancer 1	XM_001139043	Cytoplasm	Other	-1.422		
DLG3	Discs, large homolog 3 (Drosophila)	NM_021120	Plasma Membrane	Kinase		-1.19	-1.423
DLGAP1	Discs, large (Drosophila) homolog-associated protein 1	XM_852594	Plasma Membrane	Other			-2.262
DLK1	Delta-like 1 homolog (Drosophila)	XM_547982	Extracellular Space	Other	-2.824		
DMXL2	Dmx-like 2	NM_015263	Cytoplasm	Other			-1.096
DNAH8	Dynein, axonemal, heavy chain 8	XM_001173791	Cytoplasm	Enzyme	-1.418	-1.052	
DNAJA4	Dnaj (Hsp40) homolog, subfamily A, member 4	XM_510526	Nucleus	Other	-1.42	-1.668	
DNAJB14	Dnaj (Hsp40) homolog, subfamily B, member 14	XM_001167856	unknown	Enzyme		-1.04	
DNAJC10	Dnaj (Hsp40) homolog, subfamily C, member 10	XM_001159760	Cytoplasm	Enzyme	-1.308		
DNAJC9	Dnaj (Hsp40) homolog, subfamily C, member 9	XM_588123	unknown	Other	-1.206	-1.27	-1.515
DNASE1L1	Deoxyribonuclease I-like 1	XM_862570	Extracellular Space	Enzyme	-1.076		
DNM3	Dynamin 3	NM_015569	Cytoplasm	Enzyme	-1.073		
DOCK3	Dedicator of cytokinesis 3	XM_533813	Cytoplasm	Other	-1.078	-1.671	-1.025
DPEP3	Dipeptidase 3	XM_546868	unknown	Peptidase	-1.448		
DPP6	Dipeptidyl-peptidase 6	BC150304	Plasma Membrane	Peptidase	-1.502	-1.325	
DPT	Dermatopontin	XM_547476	Extracellular Space	Other	-2.949		-2.518
DPYS	Dihydropyrimidinase	BC034395	Cytoplasm	Enzyme	-1.202		
DPYSL2	Dihydropyrimidinase-like 2	XM_519672	Cytoplasm	Enzyme	-1.717	-1.062	
DPYSL3	Dihydropyrimidinase-like 3	NM_001387	Cytoplasm	Enzyme	-1.045	-1.434	
DRD5	Dopamine receptor D5	XM_604584	Plasma Membrane	G-protein coupled receptor	-1.097		
DSCAML1	Down syndrome cell adhesion molecule like 1	XM_508782	Plasma Membrane	Other	-1.199		
DSPP	Dentin sialophosphoprotein	XM_544971	Extracellular Space	Other	-2.079		
DTNA	Dystrobrevin, alpha	NM_001392	Plasma Membrane	Other	-1.35		
DUSP3	Dual specificity phosphatase 3	BC151264	Cytoplasm	Phosphatase	-1.252		
DUSP8	Dual specificity phosphatase 8	NM_004420	Nucleus	Phosphatase		-1.453	-1.534
DUSP9	Dual specificity phosphatase 9	XM_549360	Nucleus	Phosphatase		-1.112	
DYNLT3	Dynein, light chain, Tctex-type 3	XM_001136823	Cytoplasm	Other	-1.069		
DYRK2	Dual-specificity tyrosine-(Y)-phosphorylation regulated kinase 2	XM_538273	Cytoplasm	Kinase		-1.065	-1.139
DYSF	Dysferlin, limb girdle muscular dystrophy 2B (autosomal recessive)	NM_001102490	Plasma Membrane	Other	-1.322		
EBF1	Early B-cell factor 1	CU012046	Nucleus	Transcription regulator	-1.014		
ECE2	Endothelin converting enzyme 2	NM_177956	Plasma Membrane	Peptidase	-1.443		
EDIL3	EGF-like repeats and discoidin I-like domains 3	XM_001146613	Extracellular	Other	-1.12		

Table C-1. Continued

Symbol	Entrez gene name	GenBank	Location	Type(s)	Fold change exposure	Fold change survival	Fold change location
			Space				
EDN1	Endothelin 1	AC154635	Extracellular Space	Other	-2.635		
EDNRB	Endothelin receptor type B	XM_001141717	Plasma Membrane	G-protein coupled receptor	-2.271		
EEF1A2	Eukaryotic translation elongation factor 1 alpha 2	NM_001037464	Cytoplasm	Translation regulator	-1.356	-1.323	-1.533
EFCAB2	EF-hand calcium binding domain 2	NM_001101247	unknown	Other	-1.19		
EFHD1	EF-hand domain family, member D1	NM_001109310	unknown	Other	-1.794		
EFNA5	Ephrin-A5	AK025909	Plasma Membrane	Kinase			-1.457
EGF	Epidermal growth factor (beta-urogastrone)	NM_001003094	Extracellular Space	Growth factor	-1.06		
EGLN3	Egl nine homolog 3 (C. Elegans)	NM_001101164	Cytoplasm	Enzyme	-1.805		
EGR4	Early growth response 4	XM_540228	Nucleus	Transcription regulator		-2.667	-3.288
EHD3	EH-domain containing 3	NM_014600	Cytoplasm	Other	-1.178	-1.638	-2.038
EIF2AK3	Eukaryotic translation initiation factor 2-alpha kinase 3	AF110146	Cytoplasm	Kinase	-1.16		
ELOVL2	Elongation of very long chain fatty acids (FEN1/Elo2, SUR4/Elo3, yeast)-like 2	XM_001175069	Cytoplasm	Enzyme	-1.877	-1.846	
ELOVL6	ELOVL family member 6, elongation of long chain fatty acids (FEN1/Elo2, SUR4/Elo3-like, yeast)	XM_545023	Cytoplasm	Enzyme	-2.336		
ELP3 (includes EG:55140)	Elongation protein 3 homolog (S. Cerevisiae)	NM_018091	Nucleus	Enzyme	-1.606		
EMID1	EMI domain containing 1	AJ416090	Extracellular Space	Other		-2.515	
ENAH	Enabled homolog (Drosophila)	NM_018212	Cytoplasm	Other	-1.983		-1.337
ENC1	Ectodermal-neural cortex (with BTB-like domain)	NM_001078067	Nucleus	Peptidase	-1.978		-3.011
ENDOD1	Endonuclease domain containing 1	NM_001102519	Extracellular Space	Enzyme	-1.924		-1.053
ENPEP	Glutamyl aminopeptidase (aminopeptidase A)	AC113992	Plasma Membrane	Peptidase	-2.44		
ENPP7	Ectonucleotide pyrophosphatase/phosphodiesterase 7	XM_845707	unknown	Enzyme			-2.059
EPB41L3	Erythrocyte membrane protein band 4.1-like 3	XM_853634	Plasma Membrane	Other	-1.6		
EPDR1	Ependymin related protein 1 (zebrafish)	NM_001102288	Nucleus	Other	-1.674		
EPHA4	EPH receptor A4	NM_004438	Plasma Membrane	Kinase			-1.129
EPHA7	EPH receptor A7	AL354857	Plasma Membrane	Kinase		-1.455	-1.297
EPHB1	EPH receptor B1	AC109247	Plasma Membrane	Kinase		-1.482	
EPM2A (includes EG:7957)	Epilepsy, progressive myoclonus type 2A, Lafora disease (laforin)	NM_001099709	Cytoplasm	Phosphatase	-1.149		
EPN1	Epsin 1	AK022454	Plasma Membrane	Other			-1.124
ERMN	Ermin, ERM-like protein			Other	-1.138		

Table C-1. Continued

Symbol	Entrez gene name	GenBank	Location	Type(s)	Fold change exposure	Fold change survival	Fold change location
		XM_001144090	Extracellular Space				
ETV5	Ets variant 5	NM_004454	Nucleus	Transcription regulator		-1.36	-1.263
EVI5L	Ecotropic viral integration site 5-like	NM_145245	unknown	Other		-1.276	
EVL	Enah/Vasp-like	AK289720	Cytoplasm	Other	-2.224		
EXOC2	Exocyst complex component 2	NM_018303	Cytoplasm	Transporter	-1.46		
EXTL2	Exostoses (multiple)-like 2	NM_001076224	Cytoplasm	Enzyme		-1.161	
FA2H	Fatty acid 2-hydroxylase	XM_847921	unknown	Enzyme	-2.089	-1.133	
FAAH	Fatty acid amide hydrolase	XM_539627	Plasma Membrane	Enzyme		-1.022	-1.287
FABP7	Fatty acid binding protein 7, brain	XM_533484	Cytoplasm	Transporter	-1.647		
FADS1	Fatty acid desaturase 1	NM_013402	Plasma Membrane	Enzyme		-1.027	
FAF2	Fas associated factor family member 2	NM_014613	unknown	Other	-1.999		
FAM117B	Family with sequence similarity 117, member B	XM_516038	unknown	Other		-1.004	
FAM120C	Family with sequence similarity 120C	NM_017848	unknown	Other		-1.147	
FAM135A	Family with sequence similarity 135, member A	XM_848166	unknown	Enzyme		-1.166	
FAM135B	Family with sequence similarity 135, member B	AC103777	unknown	Enzyme	-1.06		
FAM158A	Family with sequence similarity 158, member A	XM_586913	Plasma Membrane	Other			-1.257
FAM162A	Family with sequence similarity 162, member A	XM_526284	Cytoplasm	Other	-1.245		
FAM168A	Family with sequence similarity 168, member A	XM_508631	unknown	Other		-1.408	
FAM171A1	Family with sequence similarity 171, member A1	NM_001102180	unknown	Other	-1.924	-1.712	
FAM190B	Family with sequence similarity 190, member B	XM_001155519	unknown	Other	-1.157	-1.113	
FAM198B	Family with sequence similarity 198, member B	AK095474	Cytoplasm	Other	-1.14		
FAM19A5	Family with sequence similarity 19 (chemokine (C-C motif)-like), member A5	Z83837	Extracellular Space	Other	-2.342	-2.147	-1.615
FAM5C	Family with sequence similarity 5, member C	XM_536117	Cytoplasm	Other		-1.373	
FAM81A	Family with sequence similarity 81, member A	NM_152450	unknown	Other	-1.415	-2.4	-1.966
FANCM	Fanconi anemia, complementation group M	XM_537429	Nucleus	Enzyme	-1.674		
FARP1	FERM, rhogef (ARHGEF) and pleckstrin domain protein 1 (chondrocyte-derived)	AF339817	unknown	Other	-1.778	-1.011	-1.698
FAT3	FAT tumor suppressor homolog 3 (Drosophila)	NM_001008781	unknown	Other			-1.244
FBN2 (includes EG:2201)	Fibrillin 2	NM_001999	Extracellular Space	Other			-1.283
FBXL16	F-box and leucine-rich repeat protein 16	XM_547211	unknown	Other		-1.637	
FBXL17	F-box and leucine-rich repeat protein 17	BC018548	unknown	Other	-1.427	-1.36	
FBXO34	F-box protein 34	XM_509963	unknown	Other			-1.456
FBXW7	F-box and WD repeat domain containing 7	NM_018315	Nucleus	Transcription regulator			-2.149
FCGBP	Fc fragment of igg binding protein	NM_003890	Extracellular	Other		-1.656	

Table C-1. Continued

Symbol	Entrez gene name	GenBank	Location	Type(s)	Fold change exposure	Fold change survival	Fold change location
			Space				
FCHO1	FCH domain only 1	AK291410	unknown	Other	-1.365	-1.063	-1.09
FDX1	Ferredoxin 1	XM_508877	Cytoplasm	Transporter	-1.339		
FEZF1	FEZ family zinc finger 1	BC127714	unknown	Other	-2.104		
FGD4	FYVE, rhogef and PH domain containing 4	XM_001135948	Cytoplasm	Other		-1.466	
FGFR1	Fibroblast growth factor receptor 1	XM_001171010	Plasma Membrane	Kinase	-1.24		
FGGY	FGGY carbohydrate kinase domain containing	AC093424	unknown	Other			-1.037
FHL1	Four and a half LIM domains 1	AK122708	Cytoplasm	Other	-1.341		
FHOD3 (includes EG:80206)	Formin homology 2 domain containing 3	XM_537280	unknown	Other			-1.134
FITM2	Fat storage-inducing transmembrane protein 2	BC029662	unknown	Other		-1.216	
FLJ10357	Hypothetical protein FLJ10357	XM_605753	unknown	Other		-1.261	
FNDC3B	Fibronectin type III domain containing 3B	AC069259	unknown	Other		-1.37	
FOXG1	Forkhead box G1	NM_005249	Nucleus	Transcription regulator		-3.475	-5.43
FOXO1	Forkhead box O1	NM_002015	Nucleus	Transcription regulator		-1.012	
FOXO4	Forkhead box O4	XM_529032	Nucleus	Transcription regulator	-1.942	-1.496	
FRMD5	FERM domain containing 5	AC090513	unknown	Other	-1.239	-1.482	
FRMPD3	FERM and PDZ domain containing 3	XM_937007	unknown	Other		-1.165	
FRS2	Fibroblast growth factor receptor substrate 2	NM_001042555	Plasma Membrane	Other	-1.015		
FSTL5	Follistatin-like 5	XM_001147682	Extracellular Space	Other	-1.283		
FUT9	Fucosyltransferase 9 (alpha (1,3) fucosyltransferase)	NM_006581	Cytoplasm	Enzyme	-2.355	-1.387	-1.928
FYB	FYN binding protein (FYB-120/130)	NM_001465	Nucleus	Other	-1.493		
FZD2	Frizzled homolog 2 (Drosophila)	XM_580783	Plasma Membrane	G-protein coupled receptor		-1.248	
G3BP1	Gtpase activating protein (SH3 domain) binding protein 1	XM_001168937	Nucleus	Enzyme	-1.666		
GAB1	GRB2-associated binding protein 1	AK022142	Cytoplasm	Other	-2.077		
GABBR1	Gamma-aminobutyric acid (GABA) B receptor, 1	BC149396	Plasma Membrane	G-protein coupled receptor	-1.653	-1.642	-1.479
GABBR2	Gamma-aminobutyric acid (GABA) B receptor, 2	XM_538749	Plasma Membrane	G-protein coupled receptor	-2.458	-1.167	-2.305
GABRA1	Gamma-aminobutyric acid (GABA) A receptor, alpha 1	XM_001145178	Plasma Membrane	Ion channel			-1.625
GABRA2	Gamma-aminobutyric acid (GABA) A receptor, alpha 2	AC104072	Plasma Membrane	Ion channel		-1.807	
GABRB1	Gamma-aminobutyric acid (GABA) A receptor, beta 1	AC097712	Plasma Membrane	Ion channel	-1.985	-2.339	-1.995
GABRB2	Gamma-aminobutyric acid (GABA) A receptor, beta 2	XM_518078	Plasma Membrane	Ion channel			-1.213
GABRG2	Gamma-aminobutyric acid (GABA) A receptor, gamma 2	NM_198904	Plasma Membrane	Ion channel			-1.043
GALNTL6 (includes EG:442117)	UDP-N-acetyl-alpha-D-galactosamine:polypeptide N-acetylgalactosaminyltransferase-like 6	NM_001034845	unknown	Other			-1.05

Table C-1. Continued

Symbol	Entrez gene name	GenBank	Location	Type(s)	Fold change exposure	Fold change survival	Fold change location
GARNL1	Ral gtpase activating protein, alpha subunit 1 (catalytic)	XM_001140817	Cytoplasm	Other		-1.848	
GBE1	Glucan (1,4-alpha-), branching enzyme 1	AC099049	Cytoplasm	Enzyme	-1.06		
GBX2	Gastrulation brain homeobox 2	XM_543300	Nucleus	Transcription regulator	-1.602		
GCNT4 (includes EG:51301)	Glucosaminyl (N-acetyl) transferase 4, core 2 (beta-1,6-N-acetylglucosaminyltransferase)	XM_546063	unknown	Enzyme			-1.239
GCSH	Glycine cleavage system protein H (aminomethyl carrier)	BC009065	Cytoplasm	Enzyme	-1.08		
GDF6	Growth differentiation factor 6	XM_867875	Extracellular Space	Growth factor		-1.271	
GFRA1	GDNF family receptor alpha 1	AC102457	Plasma Membrane	Transmembrane receptor	-2.657	-1.53	
GFRA2	GDNF family receptor alpha 2	XM_846385	Plasma Membrane	Transmembrane receptor	-1.235	-1.738	-2.787
GINS3	GINS complex subunit 3 (Psf3 homolog)	XM_001152113	unknown	Other	-1.757		
GJB6	Gap junction protein, beta 6, 30kda	NM_001110219	Plasma Membrane	Transporter	-1.841	-1.465	-1.21
GLRA3	Glycine receptor, alpha 3	AC093868	Plasma Membrane	Ion channel	-2.423		
GLS	Glutaminase	AC005540	Cytoplasm	Enzyme		-1.009	
GNA11	Guanine nucleotide binding protein (G protein), alpha 11 (Gq class)	NM_174322	Plasma Membrane	Enzyme			-1.216
GNAI1	Guanine nucleotide binding protein (G protein), alpha inhibiting activity polypeptide 1	BC105419	Plasma Membrane	Enzyme	-1.304	-1.367	-1.388
GNAO1	Guanine nucleotide binding protein (G protein), alpha activating activity polypeptide O	AK056008	Plasma Membrane	Enzyme	-1.715	-1.372	-1.254
GNAS	GNAS complex locus	BC149250	Plasma Membrane	Enzyme	-1.751		
GNB1	Guanine nucleotide binding protein (G protein), beta polypeptide 1	BC004186	Plasma Membrane	Enzyme	-1.638		
GNPTAB	N-acetylglucosamine-1-phosphate transferase, alpha and beta subunits	NM_024312	unknown	Enzyme	-1.252		
GNS	Glucosamine (N-acetyl)-6-sulfatase	NM_001075562	Cytoplasm	Enzyme	-1.292		
GORASP1	Golgi reassembly stacking protein 1, 65kda	XM_542713	Cytoplasm	Other	-1.954		
GOSR1	Golgi SNAP receptor complex member 1	NM_001007025	Cytoplasm	Transporter	-1.219		
GPC2	Glypican 2	XM_870336	Plasma Membrane	Other			-1.128
GPC5	Glypican 5	NM_001102070	Plasma Membrane	Other	-1.345		
GPR12	G protein-coupled receptor 12	XM_001157564	Plasma Membrane	G-protein coupled receptor		-1.429	
GPR126	G protein-coupled receptor 126	XM_518772	Plasma Membrane	G-protein coupled receptor			-1.017
GPR22	G protein-coupled receptor 22	XM_843786	Plasma Membrane	G-protein coupled receptor			-2.962
GPR98	G protein-coupled receptor 98	AC034215	Plasma Membrane	G-protein coupled receptor	-1.539		
GPRASP1	G protein-coupled receptor associated sorting protein 1	XM_538117	Cytoplasm	Transporter	-1.475	-1.244	

Table C-1. Continued

Symbol	Entrez gene name	GenBank	Location	Type(s)	Fold change exposure	Fold change survival	Fold change location
GRASP	GRP1 (general receptor for phosphoinositides 1)-associated scaffold protein	XM_583750	Plasma Membrane	Other		-1.999	-1.645
GRIA1	Glutamate receptor, ionotropic, AMPA 1	AB209094	Plasma Membrane	Ion channel	-1.398	-1.057	-1.498
GRIA2	Glutamate receptor, ionotropic, AMPA 2	NM_000826	Plasma Membrane	Ion channel		-1.505	-1.643
GRIA3	Glutamate receptor, ionotrophic, AMPA 3	NM_007325	Plasma Membrane	Ion channel		-2.33	-2.719
GRIA4	Glutamate receptor, ionotrophic, AMPA 4	NM_000829	Plasma Membrane	Ion channel			-1.039
GRID2	Glutamate receptor, ionotropic, delta 2	AC022317	Plasma Membrane	Ion channel		-1.581	
GRIK1	Glutamate receptor, ionotropic, kainate 1	XM_544843	Plasma Membrane	Ion channel	-1.098	-1.933	-2.626
GRIK2	Glutamate receptor, ionotropic, kainate 2	XM_866973	Plasma Membrane	Ion channel		-1.533	
GRIN1	Glutamate receptor, ionotropic, N-methyl D-aspartate 1	AF015731	Plasma Membrane	Ion channel		-1.949	-1.487
GRIN2A	Glutamate receptor, ionotropic, N-methyl D-aspartate 2A	NM_001034189	Plasma Membrane	Ion channel	-2.836	-1.631	-2.369
GRIN2B	Glutamate receptor, ionotropic, N-methyl D-aspartate 2B	AC007535	Plasma Membrane	Ion channel		-1.563	-1.989
GRIN3A	Glutamate receptor, ionotropic, N-methyl-D-aspartate 3A	XM_862276	Plasma Membrane	Ion channel			-1.032
GRIP1	Glutamate receptor interacting protein 1	XM_001162097	Plasma Membrane	Other		-1.23	
GRLF1	Glucocorticoid receptor DNA binding factor 1	NM_004491	Nucleus	Transcription regulator			-1.153
GRM8	Glutamate receptor, metabotropic 8	AC079957	Plasma Membrane	G-protein coupled receptor	-1.856		
GSTT3	Glutathione S-transferase, theta 3	XM_534750	unknown	Enzyme		-1.067	
GYG2	Glycogenin 2	XM_548837	unknown	Enzyme	-1.267		
HAP1	Huntingtin-associated protein 1	XM_844535	Cytoplasm	Other	-1.373		
HCN1	Hyperpolarization activated cyclic nucleotide-gated potassium channel 1	NM_021072	Plasma Membrane	Ion channel		-1.318	-2.128
HDLBP	High density lipoprotein binding protein	NM_005336	Nucleus	Transporter		-1.026	
HECW2	HECT, C2 and WW domain containing E3 ubiquitin protein ligase 2	AC020571	unknown	Enzyme			-1.121
HERC1	Hect (homologous to the E6-AP (UBE3A) carboxyl terminus) domain and RCC1 (CHC1)-like domain (RLD) 1	XM_001477062	Cytoplasm	Other	-1.862		
HGSNAT	Heparan-alpha-glucosaminide N-acetyltransferase	XM_519741	unknown	Other	-1.504	-1.405	
HISPPD2A	Histidine acid phosphatase domain containing 2A	AF502588	Nucleus	Phosphatase	-1.29		
HIVEP2	Human immunodeficiency virus type I enhancer binding protein 2	XM_518773	Nucleus	Transcription regulator			-1.097
HMGB1 (includes EG:3146)	High-mobility group box 1	AK291494	Nucleus	Other	-1.432		
HNRPDL	Heterogeneous nuclear ribonucleoprotein D-like	BC105386	Nucleus	Other	-1.519		
HOMER1	Homer homolog 1 (Drosophila)	XM_001139767	Plasma Membrane	Other			-1.084
HOMER3	Homer homolog 3 (Drosophila)	XM_541929	Plasma Membrane	Other	-1.718	-1.134	
HSPA12A	Heat shock 70kda protein 12A	NM_025015	unknown	Other		-1.821	-1.305

Table C-1. Continued

Symbol	Entrez gene name	GenBank	Location	Type(s)	Fold change exposure	Fold change survival	Fold change location
HTATSF1	HIV-1 Tat specific factor 1	EU176345	Nucleus	Transcription regulator	-1.341		
HTR5B	5-hydroxytryptamine (serotonin) receptor 5B	XM_601784	Plasma Membrane	G-protein coupled receptor	-1.877		-2.428
ICAM5	Intercellular adhesion molecule 5, telencephalin	NM_003259	Plasma Membrane	Other			-4.261
ID4	Inhibitor of DNA binding 4, dominant negative helix-loop-helix protein	XM_001170946	Nucleus	Transcription regulator	-1.647		
IDS	Iduronate 2-sulfatase	NM_000202	Cytoplasm	Enzyme		-1.173	
IGBP1	Immunoglobulin (CD79A) binding protein 1	XM_843517	Cytoplasm	Phosphatase	-1.027		
IGF1R	Insulin-like growth factor 1 receptor	NM_000875	Plasma Membrane	Transmembrane receptor		-1.173	
IKBKB	Inhibitor of kappa light polypeptide gene enhancer in B-cells, kinase beta	NM_174353	Cytoplasm	Kinase	-1.558		
IL25	Interleukin 25	XM_605190	Extracellular Space	Cytokine	-1.135		
IL31	Interleukin 31	BC132998	unknown	Other		-1.503	
IL33	Interleukin 33	NM_001075297	Extracellular Space	Cytokine		-1.848	
INA	Internexin neuronal intermediate filament protein, alpha	NM_001075958	Cytoplasm	Other	-1.367		
INSR	Insulin receptor	XM_590552	Plasma Membrane	Kinase	-1.359	-1.259	
IPCEF1	Interaction protein for cytohesin exchange factors 1	XM_527543	Cytoplasm	Enzyme			-1.696
IPP	Intracisternal A particle-promoted polypeptide	XM_001252535	Cytoplasm	Other	-2.089		
IPPK	Inositol 1,3,4,5,6-pentakisphosphate 2-kinase	BC026154	Cytoplasm	Kinase	-1.6		
IQCE	IQ motif containing E	XM_547007	unknown	Other			-1.219
IQSEC1	IQ motif and Sec7 domain 1	XM_516294	Cytoplasm	Other		-1.129	-1.328
ITFG1	Integrin alpha FG-GAP repeat containing 1	XM_846378	Plasma Membrane	Other		-1.022	
ITGAM	Integrin, alpha M (complement component 3 receptor 3 subunit)	XM_510949	Plasma Membrane	Other	-2.852	-1.789	
ITGB5	Integrin, beta 5	XM_516706	Plasma Membrane	Other	-2.332	-1.676	
ITIH2	Inter-alpha (globulin) inhibitor H2	XM_535195	Extracellular Space	Other		-1.605	
ITPKA	Inositol 1,4,5-trisphosphate 3-kinase A	XM_544631	Cytoplasm	Kinase		-1.889	-2.504
ITPR3	Inositol 1,4,5-triphosphate receptor, type 3	NM_174370	Cytoplasm	Ion channel	-1.639		
JMY	Junction mediating and regulatory protein, p53 cofactor	NM_152405	Nucleus	Transcription regulator		-1.662	
JPH4	Junctophilin 4	XM_547737	Cytoplasm	Other			-1.069
KAL1	Kallmann syndrome 1 sequence	NM_000216	Extracellular Space	Other		-1.371	-1.349
KBTBD7	Kelch repeat and BTB (POZ) domain containing 7	XM_522666	unknown	Other	-1.284		
KCNH1	Potassium voltage-gated channel, subfamily H (eag-related), member 1	AC158791	Plasma Membrane	Ion channel	-1.576		
KCNH4	Potassium voltage-gated channel, subfamily H (eag-related), member 4	XM_844412	Plasma Membrane	Ion channel		-1.552	-1.097
KCNJ3	Potassium inwardly-rectifying		Plasma	Ion channel	-2.406		-2.02

Table C-1. Continued

Symbol	Entrez gene name	GenBank	Location	Type(s)	Fold change exposure	Fold change survival	Fold change location
	channel, subfamily J, member 3	XM_001141809	Membrane				
KCNJ4	Potassium inwardly-rectifying channel, subfamily J, member 4	XM_538374	Plasma Membrane	Ion channel		-1.962	-2.195
KCNK1	Potassium channel, subfamily K, member 1	XM_525096	Plasma Membrane	Ion channel			-1.675
KCNK9	Potassium channel, subfamily K, member 9	XM_519977	Plasma Membrane	Ion channel			-1.535
KCNMA1	Potassium large conductance calcium-activated channel, subfamily M, alpha member 1	U09383	Plasma Membrane	Ion channel		-1.102	-1.832
KCNN1	Potassium intermediate/small conductance calcium-activated channel, subfamily N, member 1	XM_541945	Plasma Membrane	Ion channel		-1.008	-1.317
KCNQ3	Potassium voltage-gated channel, KQT-like subfamily, member 3	NM_031597	Plasma Membrane	Ion channel			-1.775
KCNS3	Potassium voltage-gated channel, delayed-rectifier, subfamily S, member 3	XM_001137103	Plasma Membrane	Ion channel		-1.547	-3.49
KDM6A	Lysine (K)-specific demethylase 6A	XM_548964	Nucleus	Other		-1.153	
KIAA0319	Kiaa0319	NM_014809	unknown	Other	-1.877		
KIAA0494	Kiaa0494	XM_524573	unknown	Other	-1.579		
KIAA1045	Kiaa1045	NM_015297	unknown	Other			-1.745
KIAA1543	Kiaa1543	XM_869459	unknown	Other			-1.801
KIAA1671	Kiaa1671	XM_531255	unknown	Other			-1.229
KIDINS220	Kinase D-interacting substrate, 220kda	XM_532865	Nucleus	Transcription regulator	-1.676	-1.505	-1.016
KIF13B	Kinesin family member 13B	AC105979	Cytoplasm	Other		-1.633	
KIF1A	Kinesin family member 1A	NM_004321	Cytoplasm	Other		-1.039	-1.237
KIF1B	Kinesin family member 1B	NM_015074	Cytoplasm	Transporter	-1.322	-1.254	
KIF26A	Kinesin family member 26A	NM_015656	unknown	Other	-1.574		-1.207
KIF26B	Kinesin family member 26B	NM_018012	unknown	Other	-1.065	-1.014	
KIF5A	Kinesin family member 5A	XM_531648	Cytoplasm	Transporter			-1.793
KIF5C	Kinesin family member 5C	AK126689	Cytoplasm	Other	-1.666		
KIF5C	Kinesin family member 5C	AK126689	Cytoplasm	Other			-1.282
KIFC2	Kinesin family member C2	XM_532358	Cytoplasm	Other		-1.694	
KLHDC5	Kelch domain containing 5	XM_520814	unknown	Other	-1.046		
KLHL35	Kelch-like 35 (Drosophila)	BC132710	unknown	Other		-1.574	-1.116
KRT72	Keratin 72	XM_522393	unknown	Other	-1.414		-1.017
KSR2	Kinase suppressor of ras 2	NM_173598	Cytoplasm	Kinase	-1.602		
LAMB3	Laminin, beta 3	NM_000228	Extracellular Space	Transporter			-1.07
LANCL1	Lanc lantibiotic synthetase component C-like 1 (bacterial)	NM_001076227	Plasma Membrane	Other	-1.406		
LARP1	La ribonucleoprotein domain family, member 1	XM_582017	unknown	Other			-1.019
LCOR	Ligand dependent nuclear receptor corepressor	XM_584325	Nucleus	Transcription regulator		-1.23	
LENG8	Leukocyte receptor cluster (LRC) member 8	NM_052925	unknown	Other	-1.299		
LHX5	LIM homeobox 5	NM_001102061	Nucleus	Transcription regulator		-1.487	
LIMCH1	LIM and calponin homology domains 1	CR936664	unknown	Other	-1.574		
LMBR1	Limb region 1 homolog (mouse)	NM_022458	Plasma Membrane	Transmembrane receptor	-1.04	-1.047	

Table C-1. Continued

Symbol	Entrez gene name	GenBank	Location	Type(s)	Fold change exposure	Fold change survival	Fold change location
LMO3	LIM domain only 3 (rhombotin-like 2)	XM_520773	Nucleus	Other		-2.642	
LMTK2	Lemur tyrosine kinase 2	XM_846103	unknown	Kinase		-1.011	
LOC285696	Hypothetical LOC285696	AC026790	unknown	Other			-1.036
LOR	Loricrin	NM_000427	Cytoplasm	Other			-1.795
LOXL1	Lysyl oxidase-like 1	BC126600	Extracellular Space	Enzyme			-2.189
LPAR1	Lysophosphatidic acid receptor 1	XM_001146627	Plasma Membrane	G-protein coupled receptor	-1.117		
LPAR3	Lysophosphatidic acid receptor 3	XM_612024	Plasma Membrane	G-protein coupled receptor	-1.942		
LPHN1	Latrophilin 1	XM_001254045	Plasma Membrane	G-protein coupled receptor	-1.799	-2.19	-1.402
LPHN2	Latrophilin 2	AC113949	Plasma Membrane	G-protein coupled receptor			-1.081
LPHN3	Latrophilin 3	BC039452	Plasma Membrane	G-protein coupled receptor		-1.375	-1.136
LRPPRC	Leucine-rich PPR-motif containing	XM_531800	Cytoplasm	Other	-1.242		
LTBP3	Latent transforming growth factor beta binding protein 3	XM_611940	Extracellular Space	Other	-2.047	-2.524	-2.134
LUZP2	Leucine zipper protein 2	BC151234	unknown	Other	-2.011		
MACF1	Microtubule-actin crosslinking factor 1	XM_583217	Cytoplasm	Other	-2.19		
MACROD1	MACRO domain containing 1	NM_001046509	Cytoplasm	Other	-1.489	-1.547	-1.158
MADD	MAP-kinase activating death domain	XM_855777	Cytoplasm	Other		-1.092	-1.507
MAL2	Mal, T-cell differentiation protein 2	NM_001081719	Plasma Membrane	Transporter		-1.391	-1.662
MAP1B	Microtubule-associated protein 1B	XM_857079	Cytoplasm	Other		-1.636	-1.067
MAP2	Microtubule-associated protein 2	XM_001144480	Cytoplasm	Other		-1.233	-1.369
MAP2K1	Mitogen-activated protein kinase kinase 1	XM_612526	Cytoplasm	Kinase			-1.4
MAP2K6	Mitogen-activated protein kinase kinase 6	AC002546	Cytoplasm	Kinase	-1.534	-1.134	
MAP3K5 (includes EG:4217)	Mitogen-activated protein kinase kinase kinase 5	XM_001171211	Cytoplasm	Kinase			-1.842
MAP4	Microtubule-associated protein 4	BC051843	Cytoplasm	Other			-1.24
MAP4K3	Mitogen-activated protein kinase kinase kinase kinase 3	AC007684	unknown	Kinase	-1.849		
MAP4K4	Mitogen-activated protein kinase kinase kinase kinase 4	XM_515665	Cytoplasm	Kinase	-1.041		
MAP4K5	Mitogen-activated protein kinase kinase kinase kinase 5	NM_198794	Cytoplasm	Kinase	-2.021		
MAP7	Microtubule-associated protein 7	NM_001101874	Cytoplasm	Other	-1.091		
MAP7D1	MAP7 domain containing 1	NM_018067	unknown	Other			-1.006
MAPK1	Mitogen-activated protein kinase 1	NM_002745	Cytoplasm	Kinase		-1.095	-1.061
MAPK1IP1L	Mitogen-activated protein kinase 1 interacting protein 1-like	XM_001148351	Nucleus	Other	-1.056		
MAPK4	Mitogen-activated protein kinase 4	NM_002747	Cytoplasm	Kinase		-1.941	-1.391

Table C-1. Continued

Symbol	Entrez gene name	GenBank	Location	Type(s)	Fold change exposure	Fold change survival	Fold change location
MAPK8IP1	Mitogen-activated protein kinase 8 interacting protein 1	XM_540760	Cytoplasm	Other	-1.322	-1.528	-1.173
MAPRE2	Microtubule-associated protein, RP/EB family, member 2	XM_512089	Cytoplasm	Other	-1.349		-1.004
MATK	Megakaryocyte-associated tyrosine kinase	XM_849722	Cytoplasm	Kinase		-1.207	-2.265
MBOAT1	Membrane bound O-acyltransferase domain containing 1	AL450321	unknown	Other			-1.178
MBP	Myelin basic protein	AK122594	Extracellular Space	Other	-1.927		
MCAM	Melanoma cell adhesion molecule	AK291571	Plasma Membrane	Other	-1.919		
MDGA1	MAM domain containing glycosylphosphatidylinositol anchor 1	XM_616613	Plasma Membrane	Other		-1.117	-2.233
MDGA2	MAM domain containing glycosylphosphatidylinositol anchor 2	AL079306	unknown	Other		-1.739	
MED16	Mediator complex subunit 16	XM_849586	Nucleus	Transcription regulator		-1.48	
MEF2B	Myocyte enhancer factor 2B	NM_001103231	Nucleus	Transcription regulator	-2.336		
MEGF10	Multiple EGF-like-domains 10	AK021631	unknown	Other	-1.34	-1.139	
MEIS2	Meis homeobox 2	NM_170674	Nucleus	Transcription regulator		-2.279	
MELK	Maternal embryonic leucine zipper kinase	AL354932	Cytoplasm	Kinase		-1.049	
MEOX2	Mesenchyme homeobox 2	NM_001098045	Nucleus	Transcription regulator		-1.714	-2.945
METTL8	Methyltransferase like 8	XM_001142517	unknown	Enzyme	-1.23		
MFHAS1	Malignant fibrous histiocytoma amplified sequence 1	AC090567	Cytoplasm	Other			-1.742
MGST2	Microsomal glutathione S-transferase 2	NM_001076382	Cytoplasm	Enzyme	-1.811		
MID1IP1	MID1 interacting protein 1 (gastrulation specific G12 homolog (zebrafish))	XM_001137047	Cytoplasm	Other	-1.515		
MINK1	Misshapen-like kinase 1 (zebrafish)	NM_170663	Cytoplasm	Kinase			-1.204
MKX	Mohawk homeobox	NM_177595	unknown	Other			-2.207
MLL2	Myeloid/lymphoid or mixed-lineage leukemia 2	XM_543684	Nucleus	Transcription regulator			-1.004
MMAA	Methylmalonic aciduria (cobalamin deficiency) cbla type	NM_001105112	Cytoplasm	Other	-1.33		
MMD	Monocyte to macrophage differentiation-associated	NM_012329	Plasma Membrane	Other		-1.911	-2.287
MMP11	Matrix metallopeptidase 11 (stromelysin 3)	XM_584877	Extracellular Space	Peptidase	-1.211		
MMP28	Matrix metallopeptidase 28	NM_024302	Extracellular Space	Peptidase			-1.229
MOBKL1A	MOB1, Mps One Binder kinase activator-like 1A (yeast)	XM_001159188	Cytoplasm	Other		-1.417	
MOBP	Myelin-associated oligodendrocyte basic protein	XM_845077	Cytoplasm	Other	-2.232		
MPP2	Membrane protein, palmitoylated 2 (MAGUK p55 subfamily member 2)	XM_867199	Plasma Membrane	Kinase	-1.029	-1.439	-1.138
MPRIP	Myosin phosphatase Rho interacting protein	XM_536669	Cytoplasm	Other		-1.983	-1.545
MRC2	Mannose receptor, C type 2	XM_607489	Plasma Membrane	Transmembrane receptor	-3.218	-2.436	-2.226

Table C-1. Continued

Symbol	Entrez gene name	GenBank	Location	Type(s)	Fold change exposure	Fold change survival	Fold change location
MTCH2	Mitochondrial carrier homolog 2 (C. Elegans)	BC150080	Cytoplasm	Other	-1.623		
MTM1	Myotubularin 1	BC030779	Cytoplasm	Phosphatase	-1.773		
MTMR10	Myotubularin related protein 10	XM_867245	unknown	Other	-1.146		
MTMR6	Myotubularin related protein 6	NM_004685	Cytoplasm	Phosphatase	-1.432		
MTSS1L	Metastasis suppressor 1-like	XM_600126	unknown	Other		-1.22	
MTUS1	Microtubule associated tumor suppressor 1	BC142971	unknown	Other	-1.392		
MTUS2	Microtubule associated tumor suppressor candidate 2	NM_015233	unknown	Other			-1.172
MYBPC1	Myosin binding protein C, slow type	XM_861573	Cytoplasm	Other			-1.849
MYCN	V-myc myelocytomatosis viral related oncogene, neuroblastoma derived (avian)	XM_540091	Nucleus	Transcription regulator	-1.166	-1.441	-1.682
MYH11	Myosin, heavy chain 11, smooth muscle	XM_845671	Cytoplasm	Other	-1.213		-1.542
MYL2	Myosin, light chain 2, regulatory, cardiac, slow	DQ896055	Cytoplasm	Other	-1.441		
MYLK	Myosin light chain kinase	NM_053027	Cytoplasm	Kinase		-1.224	
MYO10	Myosin X	XM_001175408	Cytoplasm	Other	-1.679	-2.012	-1.365
MYO6	Myosin VI	XM_001145098	Cytoplasm	Other	-1.29		
MYOCD	Myocardin	AL669846	Nucleus	Transcription regulator		-2.41	-1.62
MYT1L	Myelin transcription factor 1-like	NM_001093776	Nucleus	Transcription regulator			-2.568
NAB1	NGFI-A binding protein 1 (EGR1 binding protein 1)	AC006460	Nucleus	Transcription regulator	-1.929	-1.809	
NAP1L5	Nucleosome assembly protein 1-like 5	XM_845030	unknown	Other	-2.09		
NAPB	N-ethylmaleimide-sensitive factor attachment protein, beta	AK124876	Cytoplasm	Transporter	-1.12		-1.318
NBEA (includes EG:26960)	Neurobeachin	XM_844120	Cytoplasm	Other		-1.321	
NCALD	Neurocalcin delta	NM_001040630	Cytoplasm	Other	-2.335		-1.635
NCAN	Neurocan	BC154393	Extracellular Space	Other	-1.586	-2.117	-1.601
NCKIPSD	NCK interacting protein with SH3 domain	XM_595101	Nucleus	Other		-1.177	-1.164
NDFIP2	Nedd4 family interacting protein 2	XM_522688	Cytoplasm	Other		-1.312	-2.57
NDST3	N-deacetylase/N-sulfotransferase (heparan glucosaminyl) 3	XM_001147455	Cytoplasm	Enzyme		-1.231	
NDUFB5	NADH dehydrogenase (ubiquinone) 1 beta subcomplex, 5, 16kda	NM_002492	Cytoplasm	Enzyme	-1.964		
NEBL	Nebulette	AL157398	Cytoplasm	Other	-2.473		
NEDD4L	Neural precursor cell expressed, developmentally down-regulated 4-like	XM_001140823	Cytoplasm	Enzyme		-1.112	-1.83
NEFH	Neurofilament, heavy polypeptide	NM_001003352	Cytoplasm	Other	-2.788	-1.045	
NEFL	Neurofilament, light polypeptide	XM_534572	Cytoplasm	Other	-1.744		
NEFM	Neurofilament, medium polypeptide	XM_543237	Cytoplasm	Other	-1.092		
NEGR1	Neuronal growth regulator 1	XM_001167096	Extracellular Space	Other		-1.409	
NELF	Nasal embryonic LHRH factor	XM_868817	Extracellular	Other	-1.805	-1.816	-1.999

Table C-1. Continued

Symbol	Entrez gene name	GenBank	Location	Type(s)	Fold change exposure	Fold change survival	Fold change location
			Space				
NETO1	Neuropilin (NRP) and tolloid (TLL)-like 1	NM_138966	Extracellular Space	Other		-1.529	-1.668
NFIA	Nuclear factor I/A	XM_536691	Nucleus	Transcription regulator	-2.799	-1.243	
NFIB	Nuclear factor I/B	XM_531936	Nucleus	Transcription regulator	-1.524	-1.168	
NFIX	Nuclear factor I/X (CCAAT-binding transcription factor)	XM_862151	Nucleus	Transcription regulator	-1.043	-1.16	-1.198
NGFR	Nerve growth factor receptor (TNFR superfamily, member 16)	XM_511950	Plasma Membrane	Transmembrane receptor	-1.625		
NGRN	Neugrin, neurite outgrowth associated	XM_001168693	unknown	Other	-1.416		
NHEJ1	Nonhomologous end-joining factor 1	XM_848099	Nucleus	Other	-1.338		
NIPA1	Non imprinted in Prader-Willi/Angelman syndrome 1	NM_144599	Plasma Membrane	Other	-1.666	-1.112	
NKAIN2	Na+/K+ transporting atpase interacting 2	AL109842	unknown	Other	-2.393		
NKAIN3	Na+/K+ transporting atpase interacting 3	AC023095	unknown	Other	-1.271	-1.272	
NKX2-8	NK2 homeobox 8	XM_584660	Nucleus	Transcription regulator	-2.093		
NLRP10	NLR family, pyrin domain containing 10	XM_848981	unknown	Other			-1.895
NLRP5	NLR family, pyrin domain containing 5	XM_533576	Cytoplasm	Other			-3.204
NMNAT3 (includes EG:349565)	Nicotinamide nucleotide adenylyltransferase 3	XM_534286	Cytoplasm	Enzyme	-1.717	-1.746	
NMT2	N-myristoyltransferase 2	NM_174456	Cytoplasm	Enzyme	-1.566	-1.287	
NNAT	Neuronatin	XM_530290	Plasma Membrane	Transporter		-1.941	
NOV	Nephroblastoma overexpressed gene	NM_001102382	Extracellular Space	Growth factor		-1.495	-3.622
NOVA2	Neuro-oncological ventral antigen 2	XM_849950	Nucleus	Other		-1.792	-2.137
NPAS3	Neuronal PAS domain protein 3	XM_509895	Nucleus	Other	-1.44		
NPAS4	Neuronal PAS domain protein 4	XM_540832	Nucleus	Transcription regulator		-1.881	-2.893
NPHS1	Nephrosis 1, congenital, Finnish type (nephrin)	XM_597931	Plasma Membrane	Other	-1.704	-1.269	-2.549
NPL	N-acetylneuraminate pyruvate lyase (dihydrodipicolinate synthase)	XM_001161861	unknown	Enzyme		-1.6	
NPR1	Natriuretic peptide receptor A/guanylate cyclase A (atrionatriuretic peptide receptor A)	XM_612318	Plasma Membrane	Enzyme	-1.661	-2.209	-1.886
NPTX1	Neuronal pentraxin I	NM_002522	Extracellular Space	Other		-2.131	-4.515
NPY	Neuropeptide Y	NM_001014845	Extracellular Space	Other		-2.532	-3.728
NR1D2	Nuclear receptor subfamily 1, group D, member 2	XM_857692	Nucleus	Ligand-dependent nuclear receptor	-1.232		
NR2F1	Nuclear receptor subfamily 2, group F, member 1	XM_852342	Nucleus	Ligand-dependent nuclear receptor			-1.395
NRG3	Neuregulin 3	DQ857894	Extracellular Space	Growth factor		-1.069	-1.582

Table C-1. Continued

Symbol	Entrez gene name	GenBank	Location	Type(s)	Fold change exposure	Fold change survival	Fold change location
NRGN	Neurogranin (protein kinase C substrate, RC3)	NM_006176	Cytoplasm	Other		-1.731	-3.458
NRIP3	Nuclear receptor interacting protein 3	NM_001102218	unknown	Other			-1.276
NRXN1	Neurexin 1	NM_174404	Plasma Membrane	Transporter	-1.387	-2.591	-1.66
NRXN3	Neurexin 3	XM_001165759	Plasma Membrane	Transporter		-1.128	-1.279
NT5C1A	5'-nucleotidase, cytosolic IA	XM_580585	Cytoplasm	Phosphatase		-2.508	-1.501
NTM	Neurotrimin	NM_017354	Plasma Membrane	Other		-1.137	-1.218
NTN3	Netrin 3	XM_537003	Extracellular Space	Other	-1.243	-1.624	
NTN4	Netrin 4	XM_532655	Extracellular Space	Other			-1.041
NTNG2	Netrin G2	AB058760	Plasma Membrane	Enzyme		-2.318	-1.377
NTRK2	Neurotrophic tyrosine kinase, receptor, type 2	AL445532	Plasma Membrane	Kinase		-1.354	-1.559
NXT2	Nuclear transport factor 2-like export factor 2	NM_001100353	Nucleus	Transporter	-1.003		
OBSCN (includes EG:84033)	Obscurin, cytoskeletal calmodulin and titin-interacting rhogef	NM_001098623	Cytoplasm	Kinase		-2.173	-1.772
OCIAD1	OCIA domain containing 1	AC079927	unknown	Other		-1.737	
OGN	Osteoglycin	NM_008760	Extracellular Space	Growth factor	-2.024	-1.648	
OLFM1	Olfactomedin 1	BC008763	Cytoplasm	Other		-1.222	-1.931
OPCML	Opioid binding protein/cell adhesion molecule-like	AC154803	Plasma Membrane	Transmembrane receptor	-1.682	-1.929	-1.373
OPN3	Opsin 3	NM_014322	Plasma Membrane	G-protein coupled receptor			-2.557
OSBPL3	Oxysterol binding protein-like 3	AY008372	Cytoplasm	Other			-1.06
OTUD3	OTU domain containing 3	NM_015207	unknown	Other	-2.618		
OXA1L	Oxidase (cytochrome c) assembly 1-like	XM_537362	Cytoplasm	Enzyme	-1.845		
OXR1	Oxidation resistance 1	XM_539119	Cytoplasm	Other	-1.341		
P2RY12	Purinergic receptor P2Y, G-protein coupled, 12	NM_001003365	Plasma Membrane	G-protein coupled receptor	-3.352	-2.293	
P2RY2	Purinergic receptor P2Y, G-protein coupled, 2	XM_001174775	Plasma Membrane	G-protein coupled receptor	-1.147		
PADI2	Peptidyl arginine deiminase, type II	NM_007365	Cytoplasm	Enzyme	-1.742	-1.282	
PAFAH1B1	Platelet-activating factor acetylhydrolase, isoform Ib, subunit 1 (45kda)	NM_174663	Cytoplasm	Enzyme	-1.015		
PAK1	P21 protein (Cdc42/Rac)-activated kinase 1	XM_844558	Cytoplasm	Kinase	-1.661		
PANK1	Pantothenate kinase 1	XM_001143021	Cytoplasm	Kinase	-2.432	-1.305	
PBX1	Pre-B-cell leukemia homeobox 1	XM_001174513	Nucleus	Transcription regulator	-2.117	-1.794	-1.64
PCDH10	Protocadherin 10	AC105383	Plasma Membrane	Other		-1.482	
PCDH11X	Protocadherin 11 X-linked	AF332219	Plasma Membrane	Other	-1.567		

Table C-1. Continued

Symbol	Entrez gene name	GenBank	Location	Type(s)	Fold change exposure	Fold change survival	Fold change location
PCDH19	Protocadherin 19	XM_602429	unknown	Other		-1.52	
PCDH20	Protocadherin 20	AL833830	unknown	Other			-1.153
PCDH7	Protocadherin 7	XM_001134665	Plasma Membrane	Other	-1.365	-1.553	-1.393
PCDH8	Protocadherin 8	XM_542588	Plasma Membrane	Other			-2.661
PCDH9	Protocadherin 9	AL160254	Plasma Membrane	Other	-2.885	-2.025	
PCDHA1	Protocadherin alpha 1	XM_843778	Plasma Membrane	Other	-1.075	-1.124	-1.359
PCDHA3	Protocadherin alpha 3	XM_843795	Plasma Membrane	Other	-1.272	-1.362	-1.593
PCDHAC2	Protocadherin alpha subfamily C, 2	XM_852697	Plasma Membrane	Other		-1.584	-1.687
PCLO	Piccolo (presynaptic cytomatrix protein)	XM_001160582	Cytoplasm	Transporter		-1.339	-1.355
PCM1	Pericentriolar material 1	NM_006197	Cytoplasm	Other		-1.416	
PCNX	Pecanex homolog (Drosophila)	NM_014982	Plasma Membrane	Other	-1.302	-1.071	-1.128
PCSK1	Proprotein convertase subtilisin/kexin type 1	XM_001134900	Extracellular Space	Peptidase			-2.352
PCYT1B	Phosphate cytidylyltransferase 1, choline, beta	EU181262	Cytoplasm	Enzyme		-1.4	-1.787
PDE10A	Phosphodiesterase 10A	XM_518849	Cytoplasm	Enzyme		-1.989	
PDE1A	Phosphodiesterase 1A, calmodulin-dependent	AL110263	Cytoplasm	Enzyme	-1.095	-1.456	-3.065
PDE4DIP	Phosphodiesterase 4D interacting protein	NM_014644	Cytoplasm	Enzyme	-1.322		
PDXDC1	Pyridoxal-dependent decarboxylase domain containing 1	NM_001101859	unknown	Other	-1.57		
PEA15	Phosphoprotein enriched in astrocytes 15	AK095879	Cytoplasm	Transporter	-1.639	-1.297	
PERP	PERP, TP53 apoptosis effector	AK097958	Plasma Membrane	Other	-2.971		
PFKFB2	6-phosphofructo-2-kinase/fructose-2,6-biphosphatase 2	BC147889	Cytoplasm	Kinase		-1.072	
PFN2	Profilin 2	AK132651	Cytoplasm	Other		-1.042	-1.153
PGM2L1	Phosphoglucomutase 2-like 1	XM_508639	unknown	Enzyme			-1.213
PGM5	Phosphoglucomutase 5	NM_001102335	Cytoplasm	Enzyme	-1.13	-1.166	
PHACTR2	Phosphatase and actin regulator 2	NM_014721	unknown	Other		-1.593	
PHYHIPL	Phytanoyl-coa 2-hydroxylase interacting protein-like	XM_001164280	Cytoplasm	Other	-2.107	-2.399	
PIAS2	Protein inhibitor of activated STAT, 2	XM_612798	Nucleus	Transcription regulator		-1.014	
PIK3IP1	Phosphoinositide-3-kinase interacting protein 1	XM_543490	unknown	Other	-2.794	-1.663	
PIK3R1	Phosphoinositide-3-kinase, regulatory subunit 1 (alpha)	NM_181504	Cytoplasm	Kinase	-1.062		-1.339
PIK3R2	Phosphoinositide-3-kinase, regulatory subunit 2 (beta)	XM_847313	Cytoplasm	Kinase		-2.44	-2.341
PIP4K2A	Phosphatidylinositol-5-phosphate 4-kinase, type II, alpha	XM_845439	Cytoplasm	Kinase	-1.595		
PITPNM1	Phosphatidylinositol transfer protein, membrane-associated 1	XM_846736	Cytoplasm	Transporter		-1.378	-1.211
PKM2	Pyruvate kinase, muscle	BT030503	Cytoplasm	Kinase			-1.005
PKP2	Plakophilin 2	NM_004572	Plasma Membrane	Other	-1.098	-1.273	
PLA2G12A	Phospholipase A2, group XIIA	CR591422	Extracellular Space	Enzyme	-1.523	-1.233	-1.13

Table C-1. Continued

Symbol	Entrez gene name	GenBank	Location	Type(s)	Fold change exposure	Fold change survival	Fold change location
PLCB2	Phospholipase C, beta 2	XM_510305	Cytoplasm	Enzyme		-1.285	
PLCL1	Phospholipase C-like 1	XM_001169525	Cytoplasm	Enzyme	-2.849		
PLEKHG3	Pleckstrin homology domain containing, family G (with rhogef domain) member 3	BC129953	unknown	Other	-1.488		
PLEKHG3	Pleckstrin homology domain containing, family G (with rhogef domain) member 3	BC129953	unknown	Other		-1.085	
PLEKHG5	Pleckstrin homology domain containing, family G (with rhogef domain) member 5	NM_001042665	Cytoplasm	Other			-1.939
PLK1	Polo-like kinase 1 (Drosophila)	XM_510879	Nucleus	Kinase			-1.285
PLK2	Polo-like kinase 2 (Drosophila)	XM_587229	Nucleus	Kinase		-1.33	-2.329
PLSCR4	Phospholipid scramblase 4	AK128442	Plasma Membrane	Enzyme	-1.202	-1.316	
PLXNB1	Plexin B1	XM_533841	Plasma Membrane	Transmembrane receptor	-2.001	-1.596	-1.201
PLXNB3	Plexin B3	NM_005393	Plasma Membrane	Other	-1.395		
PODXL2	Podocalyxin-like 2	DQ202369	Plasma Membrane	Other	-1.109	-1.014	-1.46
POGK	Pogo transposable element with KRAB domain	NM_001099100	Nucleus	Other	-1.665		
POLE	Polymerase (DNA directed), epsilon	XM_543348	Nucleus	Enzyme	-1.374		
POLE3	Polymerase (DNA directed), epsilon 3 (p17 subunit)	BT030577	Nucleus	Enzyme	-2.567		
PPAP2B	Phosphatidic acid phosphatase type 2B	XM_536696	Plasma Membrane	Phosphatase	-2.486	-2.111	-1.577
PPFIA2	Protein tyrosine phosphatase, receptor type, f polypeptide (PTPRF), interacting protein (liprin), alpha 2	AB210009	Plasma Membrane	Phosphatase			-1.129
PPFIA3 (includes EG:8541)	Protein tyrosine phosphatase, receptor type, f polypeptide (PTPRF), interacting protein (liprin), alpha 3	AK289757	Plasma Membrane	Phosphatase		-2.359	-2.532
PPP1R12C	Protein phosphatase 1, regulatory (inhibitor) subunit 12C	BC010628	Cytoplasm	Phosphatase	-1.656		
PPP1R14A	Protein phosphatase 1, regulatory (inhibitor) subunit 14A	XM_867134	Cytoplasm	Other	-2.083		
PPP1R3C	Protein phosphatase 1, regulatory (inhibitor) subunit 3C	BT030698	Cytoplasm	Phosphatase	-2.27	-1.746	-1.686
PPP1R3F	Protein phosphatase 1, regulatory (inhibitor) subunit 3F	XM_548997	unknown	Other			-1.243
PPP1R9A	Protein phosphatase 1, regulatory (inhibitor) subunit 9A	XM_001169436	Cytoplasm	Other		-1.279	
PPP2R2B	Protein phosphatase 2 (formerly 2A), regulatory subunit B, beta isoform	XM_001159292	Cytoplasm	Phosphatase	-2.348		
PPP2R2C	Protein phosphatase 2 (formerly 2A), regulatory subunit B, gamma isoform	XM_001250700	unknown	Phosphatase	-1.243	-1.378	-1.446
PPP3CB	Protein phosphatase 3 (formerly 2B), catalytic subunit, beta isoform	XM_857434	unknown	Phosphatase	-1.636		
PRDX2	Peroxiredoxin 2	AK289485	Cytoplasm	Enzyme	-1.059		
PRICKLE2	Prickle homolog 2 (Drosophila)	NM_198859	Nucleus	Other	-1.497		
PRKAA2	Protein kinase, AMP-activated, alpha 2 catalytic subunit	NM_006252	Cytoplasm	Kinase		-1.591	-1.394
PRKACB	Protein kinase, camp-dependent, catalytic, beta	XM_862471	Cytoplasm	Kinase		-2.225	
PRKAR2B	Protein kinase, camp-dependent,		Cytoplasm	Kinase	-1.627		

Table C-1. Continued

Symbol	Entrez gene name	GenBank	Location	Type(s)	Fold change exposure	Fold change survival	Fold change location
	regulatory, type II, beta	XM_001148361					
PRKCA	Protein kinase C, alpha	BC071767	Cytoplasm	Kinase		-1.002	-1.513
PRKCE	Protein kinase C, epsilon	XM_583587	Cytoplasm	Kinase			-1.979
PRKG2	Protein kinase, cgmp-dependent, type II	NM_006259	Cytoplasm	Kinase	-1.047		
PRKRA	Protein kinase, interferon-inducible double stranded RNA dependent activator	AK290601	Cytoplasm	Other	-1.093	-1.031	
PRMT3	Protein arginine methyltransferase 3	NM_005788	Nucleus	Enzyme	-1.166		
PROX1	Prospero homeobox 1	BX928753	Nucleus	Transcription regulator			-1.367
PRR5	Proline rich 5 (renal)	NM_001101305	unknown	Other		-1.063	-1.099
PRRT1	Proline-rich transmembrane protein 1	NM_030651	unknown	Other		-1.024	-1.364
PRRT2 (includes EG:112476)	Proline-rich transmembrane protein 2	NM_145239	unknown	Other		-1.559	-2.515
PRUNE	Prune homolog (Drosophila)	BC142289	Nucleus	Enzyme	-1.759		
PSAT1	Phosphoserine aminotransferase 1	NM_001102150	Cytoplasm	Enzyme	-3.321	-1.734	
PSD	Pleckstrin and Sec7 domain containing	XM_543989	unknown	Other		-2.275	-2.953
PSD3	Pleckstrin and Sec7 domain containing 3	NM_015310	unknown	Other	-1.527	-1.851	-1.444
PTGS1	Prostaglandin-endoperoxide synthase 1 (prostaglandin G/H synthase and cyclooxygenase)	XM_001136739	Cytoplasm	Enzyme	-2.728	-1.491	
PTK2B	PTK2B protein tyrosine kinase 2 beta	XM_543228	Cytoplasm	Kinase		-1.029	-1.545
PTP4A1	Protein tyrosine phosphatase type IVA, member 1	NM_003463	Nucleus	Phosphatase	-1.484		
PTPRD	Protein tyrosine phosphatase, receptor type, D	AL135790	Plasma Membrane	Phosphatase	-1.668		
PTPRF	Protein tyrosine phosphatase, receptor type, F	NM_001101079	Plasma Membrane	Phosphatase	-1.019	-1.611	-2.088
PTPRG	Protein tyrosine phosphatase, receptor type, G	XM_001174413	Plasma Membrane	Phosphatase		-1.045	
PTPRK	Protein tyrosine phosphatase, receptor type, K	XM_001167645	Plasma Membrane	Phosphatase	-1.074		-1.07
PTPRN	Protein tyrosine phosphatase, receptor type, N	XM_536080	Plasma Membrane	Phosphatase	-1.123	-1.582	
PTPRN2	Protein tyrosine phosphatase, receptor type, N polypeptide 2	AC159625	Plasma Membrane	Phosphatase	-2.299		
PTPRO	Protein tyrosine phosphatase, receptor type, O	NM_030667	Plasma Membrane	Phosphatase			-1.829
PTPRT	Protein tyrosine phosphatase, receptor type, T	XM_543002	Plasma Membrane	Phosphatase		-1.352	-1.488
PVALB	Parvalbumin	NM_001076114	Cytoplasm	Other	-1.515		-1.932
PVRL3	Poliovirus receptor-related 3	AC133477	Plasma Membrane	Other		-1.281	
PXMP3	Peroxisomal membrane protein 3, 35kda	NM_001079867	Cytoplasm	Other	-1.621		
QKI	Quaking homolog, KH domain RNA binding (mouse)	NM_206853	Nucleus	Other	-1.717		
RAB4A	RAB4A, member RAS oncogene family	AY585832	Cytoplasm	Enzyme	-1.107		
RAB5B	RAB5B, member RAS oncogene family	XM_866612	Cytoplasm	Enzyme	-1.903		
RAB6B	RAB6B, member RAS oncogene family	XM_001147918	Cytoplasm	Enzyme	-1.869	-1.013	-1.345
RABEP1	Rabaptin, RAB gtpase binding	XM_869715	Cytoplasm	Transporter	-2.06		

Table C-1. Continued

Symbol	Entrez gene name	GenBank	Location	Type(s)	Fold change exposure	Fold change survival	Fold change location
	effector protein 1						
RAI14	Retinoic acid induced 14	XM_001151240	Nucleus	Transcription regulator			-1.081
RALGPS1	Ral GEF with PH domain and SH3 binding motif 1	NM_014636	Cytoplasm	Other	-1.174		
RANBP3L	RAN binding protein 3-like	XM_546345	unknown	Other		-1.594	
RAP1GAP2	RAP1 gtpase activating protein 2	NM_001100398	unknown	Other	-1.16	-1.45	-1.834
RAP2A	RAP2A, member of RAS oncogene family	XM_509705	Cytoplasm	Enzyme		-1.03	
RAPGEF5	Rap guanine nucleotide exchange factor (GEF) 5	NM_012294	Nucleus	Other	-1.285		
RASAL1	RAS protein activator like 1 (GAP1 like)	XM_590469	unknown	Other			-1.957
RASGRF1	Ras protein-specific guanine nucleotide-releasing factor 1	XM_510534	Cytoplasm	Other	-1.177	-1.272	-2.325
RASGRF2	Ras protein-specific guanine nucleotide-releasing factor 2	BC041953	Cytoplasm	Other			-1.341
RASGRP2	RAS guanyl releasing protein 2 (calcium and DAG-regulated)	XM_508531	Cytoplasm	Other		-1.236	
RASL10A	RAS-like, family 10, member A	XM_001173334	Nucleus	Enzyme		-3.098	-5.486
RAVER2	Ribonucleoprotein, PTB-binding 2	XM_546676	Nucleus	Other	-1.333		
RBM9	RNA binding motif protein 9	NM_001082579	Nucleus	Transcription regulator			-1.303
RECK	Reversion-inducing-cysteine-rich protein with kazal motifs	XM_001168411	Plasma Membrane	Other		-1.225	
RECQL5	Recq protein-like 5	XM_540436	Nucleus	Enzyme		-1.368	
RELT	RELT tumor necrosis factor receptor	XM_542318	Plasma Membrane	Transmembrane receptor	-1.496		
RERE	Arginine-glutamic acid dipeptide (RE) repeats	XM_536734	Nucleus	Transcription regulator		-1.17	
RFC1	Replication factor C (activator 1) 1, 145kda	AY600371	Nucleus	Transcription regulator	-2.124		
RFFL	Ring finger and FYVE-like domain containing 1	XM_867129	Cytoplasm	Enzyme	-1.233		
RG9MTD3	RNA (guanine-9-) methyltransferase domain containing 3	NM_001076859	unknown	Other	-1.279		
RGNEF	Rho-guanine nucleotide exchange factor	NM_012026	unknown	Other			-1.22
RGS12	Regulator of G-protein signaling 12	XM_845461	Nucleus	Other	-1.489	-1.676	-2.104
RGS4	Regulator of G-protein signaling 4	XM_001174415	Cytoplasm	Other			-1
RGS5	Regulator of G-protein signaling 5	XM_001174428	Plasma Membrane	Other	-1.569	-1.617	
RHOBTB3	Rho-related BTB domain containing 3	NM_014899	unknown	Enzyme	-1.27	-1.054	
RHOU	Ras homolog gene family, member U	DQ384425	Cytoplasm	Enzyme	-1.815	-1.937	
RICS	Rho gtpase-activating protein	XM_546401	Cytoplasm	Other		-1.15	-1.345
RIMKLB	Ribosomal modification protein rimk-like family member B	BC015879	unknown	Other	-1.203		
RIMS1	Regulating synaptic membrane exocytosis 1	NM_014989	Cytoplasm	Enzyme			-1.497
RIN2	Ras and Rab interactor 2	XM_843542	Cytoplasm	Other	-1.513		
RLTPR	RGD motif, leucine rich repeats, tropomodulin domain and proline-rich containing	BC115830	unknown	Other			-2.351
RND2	Rho family gtpase 2	XM_587874	Cytoplasm	Enzyme	-1.537		
RNF112	Ring finger protein 112	XM_546649	Nucleus	Transcription regulator		-2.082	-1.936

Table C-1. Continued

Symbol	Entrez gene name	GenBank	Location	Type(s)	Fold change exposure	Fold change survival	Fold change location
RNF125	Ring finger protein 125	NM_017831	unknown	Other	-1.845		
RNF14	Ring finger protein 14	NM_001081540	Nucleus	Transcription regulator	-1.112		
RNF144A	Ring finger protein 144A	NM_014746	Nucleus	Other		-1.198	
RNF165	Ring finger protein 165	XM_547590	unknown	Other	-1.702	-1.622	
RNF220	Ring finger protein 220	XM_845722	unknown	Other	-1.524	-1.186	
RNLS	Renalase, FAD-dependent amine oxidase	AL353149	Extracellular Space	Other	-1.041		
ROBO3	Roundabout, axon guidance receptor, homolog 3 (Drosophila)	XM_546425	Plasma Membrane	Other	-1.068		
ROPN1L	Ropporin 1-like	NM_001075717	unknown	Kinase		-1.473	
RP11-307F22.3	Notch 5-like	XM_001126083	unknown	Other			-2.403
RPH3A	Rabphilin 3A homolog (mouse)	BC150131	Plasma Membrane	Transporter		-1.354	-2.134
RTN1	Reticulon 1	NM_001075966	Cytoplasm	Other	-1.152		
RYK	RYK receptor-like tyrosine kinase	NM_002958	Plasma Membrane	Kinase	-1.22		
RYR2	Ryanodine receptor 2 (cardiac)	XM_514296	Plasma Membrane	Ion channel		-2.312	-3.405
RYR3	Ryanodine receptor 3	NM_001036	Plasma Membrane	Ion channel		-1.367	
S100B	S100 calcium binding protein B	NM_009115	Cytoplasm	Other	-1.647		
SAMD11	Sterile alpha motif domain containing 11	XM_536715	Nucleus	Other		-1.395	
SAR1B	SAR1 homolog B (S. Cerevisiae)	XM_001167398	Cytoplasm	Enzyme	-1.405	-1.184	
SBF1	SET binding factor 1	NM_002972	Plasma Membrane	Phosphatase			-1.349
SBF2	SET binding factor 2	XM_534052	Cytoplasm	Other		-1.248	
SC5DL	Sterol-C5-desaturase (ERG3 delta-5-desaturase homolog, S. Cerevisiae)-like	XM_001167254	Cytoplasm	Enzyme	-1.592		
SCARA5	Scavenger receptor class A, member 5 (putative)	XM_543223	Cytoplasm	Other			-1.807
SCARB2	Scavenger receptor class B, member 2	NM_001102153	Plasma Membrane	Other	-1.229		
SCD	Stearoyl-coa desaturase (delta-9-desaturase)	XM_543968	Cytoplasm	Enzyme	-1.392		
SCD	Stearoyl-coa desaturase (delta-9-desaturase)	XM_543968	Cytoplasm	Enzyme		-1.148	
SCN2B	Sodium channel, voltage-gated, type II, beta	XM_522196	Plasma Membrane	Ion channel			-1.206
SCN3B	Sodium channel, voltage-gated, type III, beta	BC126265	Plasma Membrane	Ion channel		-1.389	-2.12
SCN8A	Sodium channel, voltage gated, type VIII, alpha subunit	XM_845041	Plasma Membrane	Ion channel		-1.934	-2.209
SCNN1D	Sodium channel, nonvoltage-gated 1, delta	XM_546718	Plasma Membrane	Ion channel	-1.243		
SCRIB	Scribbled homolog (Drosophila)	BC146321	Cytoplasm	Other	-1.129		
SDHD	Succinate dehydrogenase complex, subunit D, integral membrane protein	XM_536573	Cytoplasm	Enzyme	-1.579		
SEL1L	Sel-1 suppressor of lin-12-like (C. Elegans)	BC040498	Cytoplasm	Other	-1.254		
SEMA3B	Sema domain, immunoglobulin domain (Ig), short basic domain, secreted, (semaphorin) 3B	XM_590757	Extracellular Space	Other		-1.167	
SEMA3C	Sema domain, immunoglobulin domain (Ig), short basic domain,	XM_001159821	Extracellular	Other	-1.167		

Table C-1. Continued

Symbol	Entrez gene name	GenBank	Location	Type(s)	Fold change exposure	Fold change survival	Fold change location
	secreted, (semaphorin) 3C		Space				
SEMA6A	Sema domain, transmembrane domain (TM), and cytoplasmic domain, (semaphorin) 6A	NM_020796	Plasma Membrane	Other	-1.135		
SEMA6D	Sema domain, transmembrane domain (TM), and cytoplasmic domain, (semaphorin) 6D	AC018900	Plasma Membrane	Other	-2.368	-1.326	
SENP5 (includes EG:205564)	SUMO1/sentrin specific peptidase 5	NM_152699	unknown	Peptidase	-1.617		
SEPT7	Septin 7	AK290545	Cytoplasm	Other	-1.239	-1.19	-1.07
SEPW1	Selenoprotein W, 1	NM_003009	Cytoplasm	Enzyme	-2.598		
SERP1	Stress-associated endoplasmic reticulum protein 1	XM_606511	Cytoplasm	Other	-1.714		
SERTAD4	SERTA domain containing 4	AK021425	unknown	Other	-2.597		-2.669
SESTD1	SEC14 and spectrin domains 1	BC061918	unknown	Other	-1.213		
SEZ6	Seizure related 6 homolog (mouse)	NM_001098635	unknown	Other	-1.353		
SEZ6L	Seizure related 6 homolog (mouse)-like	XM_515042	Plasma Membrane	Other	-2.079		-1.91
SFXN5	Sideroflexin 5	NM_001075914	Cytoplasm	Transporter		-1.632	
SGCB	Sarcoglycan, beta (43kda dystrophin-associated glycoprotein)	NM_000232	Plasma Membrane	Other	-1.433		
SGCD	Sarcoglycan, delta (35kda dystrophin-associated glycoprotein)	XM_001134904	Cytoplasm	Other	-1.205		
SGK1	Serum/glucocorticoid regulated kinase 1	AL135839	Cytoplasm	Kinase	-1.643		
SGSM2	Small G protein signaling modulator 2	NM_014853	unknown	Other		-1.652	
SGTB	Small glutamine-rich tetratricopeptide repeat (TPR)-containing, beta	XM_535258	unknown	Other		-1.313	-1.655
SH3BP5	SH3-domain binding protein 5 (BTK-associated)	XM_542777	Cytoplasm	Other		-1.467	
SH3GL2	SH3-domain GRB2-like 2	XM_848878	Plasma Membrane	Enzyme			-1.154
SH3GL3	SH3-domain GRB2-like 3	XM_847205	Cytoplasm	Other	-1.587	-1.328	-1.459
SH3GLB2 (includes EG:56904)	SH3-domain GRB2-like endophilin B2	NM_020145	Cytoplasm	Other	-1.133	-1.45	-2.083
SHANK1	SH3 and multiple ankyrin repeat domains 1	AF102855	Cytoplasm	Other		-2.026	-1.564
SHANK2	SH3 and multiple ankyrin repeat domains 2	XM_522093	Cytoplasm	Other	-1.379		
SHB	Src homology 2 domain containing adaptor protein B	XM_538741	unknown	Other	-1.093	-1.159	
SHF	Src homology 2 domain containing F	XM_590296	unknown	Other		-1.219	
SHROOM2	Shroom family member 2	NM_001649	Plasma Membrane	Ion channel	-2.02		-1.381
SIN3B	SIN3 homolog B, transcription regulator (yeast)	XM_847635	Nucleus	Transcription regulator		-1.559	
SIPA1L2	Signal-induced proliferation-associated 1 like 2	XM_867577	unknown	Other	-1.882		
SLC12A5	Solute carrier family 12 (potassium-chloride transporter), member 5	BC154376	Plasma Membrane	Transporter		-1.032	-1.303
SLC16A12	Solute carrier family 16, member 12 (monocarboxylic acid transporter 12)	XM_543918	unknown	Other		-1.678	
SLC17A7	Solute carrier family 17 (sodium-dependent inorganic phosphate cotransporter), member 7	NM_001098046	Plasma Membrane	Transporter	-1.598	-2.652	-8.147
SLC19A3	Solute carrier family 19, member 3		Plasma	Transporter	-1.365	-1.436	

Table C-1. Continued

Symbol	Entrez gene name	GenBank	Location	Type(s)	Fold change exposure	Fold change survival	Fold change location
		NM_001102198	Membrane				
SLC1A2	Solute carrier family 1 (glial high affinity glutamate transporter), member 2	NM_004171	Plasma Membrane	Transporter	-1.639	-2.869	-2.278
SLC24A2	Solute carrier family 24 (sodium/potassium/calcium exchanger), member 2	AL133281	Plasma Membrane	Transporter	-1.047		
SLC25A23	Solute carrier family 25 (mitochondrial carrier; phosphate carrier), member 23	XM_542138	unknown	Transporter		-1.718	
SLC25A36	Solute carrier family 25, member 36	XM_001159385	unknown	Transporter		-1.247	
SLC25A46	Solute carrier family 25, member 46	AC008650	unknown	Other	-1.247		
SLC25A5	Solute carrier family 25 (mitochondrial carrier; adenine nucleotide translocator), member 5	BC102950	Cytoplasm	Transporter	-1.274		
SLC27A1	Solute carrier family 27 (fatty acid transporter), member 1	NM_001033625	Plasma Membrane	Transporter	-1.125		
SLC2A12	Solute carrier family 2 (facilitated glucose transporter), member 12	XM_527510	unknown	Transporter	-1.736		
SLC30A7	Solute carrier family 30 (zinc transporter), member 7	XM_001136030	Cytoplasm	Transporter	-1.311		-1.098
SLC35F1	Solute carrier family 35, member F1	XM_527490	unknown	Other			-1.532
SLC38A2	Solute carrier family 38, member 2	XM_543722	Plasma Membrane	Transporter	-1.416		
SLC39A10	Solute carrier family 39 (zinc transporter), member 10	XM_599261	unknown	Transporter		-1.197	
SLC39A3	Solute carrier family 39 (zinc transporter), member 3	XM_849855	Plasma Membrane	Transporter		-1.728	-1.39
SLC44A5	Solute carrier family 44, member 5	AC093156	unknown	Other		-2.683	-1.762
SLC4A4	Solute carrier family 4, sodium bicarbonate cotransporter, member 4	NM_003759	Plasma Membrane	Transporter	-1.063		
SLC6A1	Solute carrier family 6 (neurotransmitter transporter, GABA), member 1	XM_001152302	Plasma Membrane	Transporter	-1.367	-1.04	-1.192
SLC6A11	Solute carrier family 6 (neurotransmitter transporter, GABA), member 11	XM_533741	Plasma Membrane	Transporter	-1.122		
SLC6A7	Solute carrier family 6 (neurotransmitter transporter, L-proline), member 7	AK096607	Plasma Membrane	Transporter			-1.184
SLC6A9	Solute carrier family 6 (neurotransmitter transporter, glycine), member 9	NM_006934	Plasma Membrane	Transporter	-2.471	-1.459	
SLC7A11	Solute carrier family 7, (cationic amino acid transporter, y+ system) member 11	XM_001136486	Plasma Membrane	Transporter	-1.882	-2.607	-1.082
SLC8A2	Solute carrier family 8 (sodium/calcium exchanger), member 2	XM_615995	Cytoplasm	Transporter		-1.366	-1.958
SLC9A9 (includes EG:285195)	Solute carrier family 9 (sodium/hydrogen exchanger), member 9	XM_001162839	Cytoplasm	Other	-2.054		
SLIT1	Slit homolog 1 (Drosophila)	BC146761	Extracellular Space	Other	-1.656	-3.085	-4.752
SLIT3	Slit homolog 3 (Drosophila)	AY358884	Extracellular Space	Other			-1.558
SLITRK4	SLIT and NTRK-like family, member 4	XM_609417	unknown	Other		-2.469	-1.725
SLITRK5	SLIT and NTRK-like family, member 5	XM_542632	unknown	Other		-1.107	-1.654

Table C-1. Continued

Symbol	Entrez gene name	GenBank	Location	Type(s)	Fold change exposure	Fold change survival	Fold change location
SMAD4	SMAD family member 4	AC091551	Nucleus	Transcription regulator	-1.72	-1.399	
SMAD7	SMAD family member 7	XM_512124	Nucleus	Transcription regulator	-1.416		
SMAD9	SMAD family member 9	XM_001144071	Nucleus	Transcription regulator		-1.053	
SMARCAD1	SWI/SNF-related, matrix-associated actin-dependent regulator of chromatin, subfamily a, containing DEAD/H box 1	NM_020159	Nucleus	Enzyme	-2.057		
SNED1	Sushi, nidogen and EGF-like domains 1	NM_001080437	Plasma Membrane	Other	-2.091	-1.477	
SNIP	SNAP25-interacting protein	XM_869703	Cytoplasm	Other			-1.497
SNIP1	Smad nuclear interacting protein 1	XM_532557	Nucleus	Other	-1.082		
SNTG1	Syntrophin, gamma 1	XM_001066932	Nucleus	Other	-1.157		
SNX30	Sorting nexin family member 30	NM_001012994	unknown	Other	-1.57		-1.186
SNX6	Sorting nexin 6	AL445883	Cytoplasm	Transporter	-1.062		
SNX9 (includes EG:51429)	Sorting nexin 9	XM_582637	Cytoplasm	Transporter	-2.203		
SOBP	Sine oculis binding protein homolog (Drosophila)	NM_001101170	unknown	Other	-1.544		-1.551
SOCS7	Suppressor of cytokine signaling 7	AC124789	Cytoplasm	Other	-1.705		
SORBS2	Sorbin and SH3 domain containing 2	AC108472	Nucleus	Other			-1.519
SOX10	SRY (sex determining region Y)-box 10	DQ896471	Nucleus	Transcription regulator	-1.251		
SOX6	SRY (sex determining region Y)-box 6	AC068405	Nucleus	Transcription regulator		-1.351	
SP4	Sp4 transcription factor	XM_527679	Nucleus	Transcription regulator		-1.065	
SPAG9	Sperm associated antigen 9	AC005920	Plasma Membrane	Other	-1.319	-1.19	
SPAM1 (includes EG:6677)	Sperm adhesion molecule 1 (PH-20 hyaluronidase, zona pellucida binding)	AC127559	Plasma Membrane	Enzyme	-2.199		
SPEN	Spen homolog, transcriptional regulator (Drosophila)	XM_591419	Nucleus	Transcription regulator	-1.019		
SPHKAP	SPHK1 interactor, AKAP domain containing	XM_001137938	unknown	Other			-1.692
SPOCK1	Sparc/osteonectin, cwcv and kazal-like domains proteoglycan (testican) 1	XM_517947	Extracellular Space	Other			-1.111
SPON1	Spondin 1, extracellular matrix protein	NM_174743	Extracellular Space	Other	-1.116		
SPRYD3	SPRY domain containing 3	AK074694	unknown	Other			-1.392
SPTBN2	Spectrin, beta, non-erythrocytic 2	XM_540827	Cytoplasm	Other		-2.253	-2.573
SPTBN4	Spectrin, beta, non-erythrocytic 4	XM_541613	Cytoplasm	Other	-1.656	-1.955	-2.401
SRF	Serum response factor (c-fos serum response element-binding transcription factor)	XM_847209	Nucleus	Transcription regulator		-1.177	
SRY	Sex determining region Y	AC146189	Nucleus	Transcription regulator		-1.397	
SS18L1	Synovial sarcoma translocation gene on chromosome 18-like 1	NM_001078095	Nucleus	Transcription regulator	-1.89	-1.064	-1.138
SSX2IP	Synovial sarcoma, X breakpoint 2 interacting protein	XM_001139311	Plasma Membrane	Other		-1.042	-1.951
ST3GAL3	ST3 beta-galactoside alpha-2,3-sialyltransferase 3	NM_001037299	Cytoplasm	Enzyme	-1.254		

Table C-1. Continued

Symbol	Entrez gene name	GenBank	Location	Type(s)	Fold change exposure	Fold change survival	Fold change location
ST6GAL2	ST6 beta-galactosamide alpha-2,6-sialyltranferase 2	AK095049	Cytoplasm	Enzyme	-1.572	-1.146	-1.669
STAU2	Staufen, RNA binding protein, homolog 2 (Drosophila)	XM_001165689	Cytoplasm	Other	-1.346		
STIM1	Stromal interaction molecule 1	BC021300	Plasma Membrane	Other	-1.471		
STMN1	Stathmin 1	XM_535349	Cytoplasm	Other	-1.944		
STON2	Stonin 2	AK094799	Cytoplasm	Other		-1.631	-1.239
STRA6	Stimulated by retinoic acid gene 6 homolog (mouse)	BC142342	Plasma Membrane	Other			-1.78
STX2	Syntaxin 2	NM_001980	Cytoplasm	Transporter	-1.394		
STXBP3	Syntaxin binding protein 3	NM_001083415	Plasma Membrane	Transporter	-1.081		
STXBP5	Syntaxin binding protein 5 (tomosyn)	BC113382	Plasma Membrane	Other			-1.241
STXBP6	Syntaxin binding protein 6 (amisyn)	AL834346	Cytoplasm	Other	-2.01		
SUB1	SUB1 homolog (S. Cerevisiae)	NM_001105407	Nucleus	Transcription regulator	-3.347	-2.235	-2.353
SV2B	Synaptic vesicle glycoprotein 2B	AC123784	Plasma Membrane	Transporter			-2.218
SVEP1	Sushi, von Willebrand factor type A, EGF and pentraxin domain containing 1	XM_532030	unknown	Other		-1.282	
SVOP	SV2 related protein homolog (rat)	BC033587	Cytoplasm	Transporter	-1.608	-2.243	-2.577
SYN1	Synapsin I	BC149033	Plasma Membrane	Transporter			-1.824
SYN2	Synapsin II	XM_001171832	Plasma Membrane	Other	-1.876		-1.99
SYNC	Syncoilin, intermediate filament protein	XM_544429	Cytoplasm	Other	-1.294		
SYNPR	Synaptoporin	XM_516566	Plasma Membrane	Transporter		-1.126	
SYNRG	Synergin, gamma	XM_001173273	Cytoplasm	Other	-1.478		
SYT11	Synaptotagmin XI	NM_001099171	Cytoplasm	Transporter	-1.698		
SYT13	Synaptotagmin XIII	NM_001098115	unknown	Transporter	-1.613		-1.25
SYT14	Synaptotagmin XIV	AL513263	unknown	Transporter		-1.028	
SYT9	Synaptotagmin IX	XM_521824	Plasma Membrane	Transporter	-1.964		
TADA1L	Transcriptional adaptor 1	AK291922	unknown	Other	-1.309		
TBC1D30	TBC1 domain family, member 30	XM_939476	Cytoplasm	Other			-1.293
TCEA2	Transcription elongation factor A (SII), 2	XM_001152936	Nucleus	Transcription regulator		-1.104	-1.116
TCF4	Transcription factor 4	NM_003199	Nucleus	Transcription regulator	-1.122		-1.255
TCF7L2 (includes EG:6934)	Transcription factor 7-like 2 (T-cell specific, HMG-box)	AL158212	Nucleus	Transcription regulator			-1.027
TEKT5	Tektin 5	XM_536976	unknown	Other	-1.154		
TEX15	Testis expressed 15	NM_031271	unknown	Other			-1.731
TFRC	Transferrin receptor (p90, CD71)	XM_580860	Plasma Membrane	Transporter		-1.619	
TGOLN2 (includes EG:10618)	Trans-golgi network protein 2	XM_001165520	Cytoplasm	Other	-1.354		
TH	Tyrosine hydroxylase	BC149072	Cytoplasm	Enzyme	-2.857		
THADA	Thyroid adenoma associated	AC092838	unknown	Other		-2.026	-2.126
THRB	Thyroid hormone receptor, beta (erythroblastic leukemia viral (v-erb-	XM_001163770	Nucleus	Ligand-dependent		-1.657	-2.777

Table C-1. Continued

Symbol	Entrez gene name	GenBank	Location	Type(s)	Fold change exposure	Fold change survival	Fold change location
	a) oncogene homolog 2, avian)			nuclear receptor			
TIPRL	TIP41, TOR signaling pathway regulator-like (S. Cerevisiae)	NM_152902	unknown	Other		-1.029	
TLE2	Transducin-like enhancer of split 2 (E(sp1) homolog, Drosophila)	NM_003260	Nucleus	Transcription regulator	-1.051		-1.182
TM6SF1	Transmembrane 6 superfamily member 1	NM_001102295	Plasma Membrane	Other		-1.315	
TMEM106C	Transmembrane protein 106C	XM_509025	unknown	Other	-1.397		
TMEM116	Transmembrane protein 116	XM_509382	unknown	Other	-1.917	-1.589	
TMEM132A	Transmembrane protein 132A	XM_001142704	Cytoplasm	Other	-1.942	-1.514	
TMEM132C (includes EG:92293)	Transmembrane protein 132C	XM_522557	unknown	Other			-1.572
TMEM178	Transmembrane protein 178	AY358773	unknown	Other			-2.685
TMEM35	Transmembrane protein 35	BC122649	unknown	Other	-2.458		-1.131
TMEM47	Transmembrane protein 47	NM_001003045	Plasma Membrane	Other	-1.427		
TMEM8B	Transmembrane protein 8B	NM_001042589	Plasma Membrane	Other			-1.665
TMOD2	Tropomodulin 2 (neuronal)	XM_001169950	Cytoplasm	Other	-1.26	-1.542	-1.483
TMX1	Thioredoxin-related transmembrane protein 1	DQ786761	Cytoplasm	Enzyme	-1.343		
TNFRSF17	Tumor necrosis factor receptor superfamily, member 17	BC058291	Plasma Membrane	Other	-1.274		
TNIK	TRAF2 and NCK interacting kinase	XM_001164224	Cytoplasm	Kinase	-1.794		
TNNC2	Troponin C type 2 (fast)	AK291323	unknown	Other	-1.719		
TNR	Tenascin R (restrictin, janusin)	Z94057	Plasma Membrane	Other	-1.864	-1.734	-1.426
TNRC6B	Trinucleotide repeat containing 6B	NM_015088	unknown	Other			-1.231
TNS1	Tensin 1	AC116419	Plasma Membrane	Other	-1.667		
TOR1AIP1	Torsin A interacting protein 1	AL050126	Nucleus	Other	-1.013		
TRAK1	Trafficking protein, kinesin binding 1	NM_001042646	Nucleus	Other		-1.216	-1.274
TRAK2	Trafficking protein, kinesin binding 2	AB038964	Plasma Membrane	Transporter	-1.985		
TRAPPC10	Trafficking protein particle complex 10	XM_544914	Cytoplasm	Transporter		-1.903	-1.3
TRIM15	Tripartite motif-containing 15	XM_591350	unknown	Other	-1.34		
TRIM44	Tripartite motif-containing 44	XM_508888	Cytoplasm	Other	-1.067		
TRIM72	Tripartite motif-containing 72	XM_547047	unknown	Other	-1.166		
TRIM9	Tripartite motif-containing 9	XM_001156808	Cytoplasm	Other			-1.251
TRPM3	Transient receptor potential cation channel, subfamily M, member 3	AL442645	Plasma Membrane	Ion channel	-1.229	-1.814	
TSHZ1	Teashirt zinc finger homeobox 1	XM_533368	Nucleus	Transcription regulator		-1.13	
TSNARE1	T-SNARE domain containing 1	XM_539185	unknown	Other		-1.362	
TSPAN5	Tetraspanin 5	XM_001165628	Plasma Membrane	Other	-1.341		
TTC13	Tetratricopeptide repeat domain 13	AL591292	unknown	Other		-1.299	
TTC22	Tetratricopeptide repeat domain 22	NM_001098055	unknown	Other	-1.762		
TTC9	Tetratricopeptide repeat domain 9	NM_015351	unknown	Other			-1.621
TTLL7	Tubulin tyrosine ligase-like family, member 7	XM_001134864	Plasma Membrane	Other	-1.022	-1.266	

Table C-1. Continued

Symbol	Entrez gene name	GenBank	Location	Type(s)	Fold change exposure	Fold change survival	Fold change location
TUBA1B	Tubulin, alpha 1b	BC146060	Cytoplasm	Other	-1.856		
TULP3	Tubby like protein 3	NM_011657	unknown	Other	-1.195		
TULP4	Tubby like protein 4	BC152476	Cytoplasm	Transcription regulator			-1.67
TUSC3	Tumor suppressor candidate 3	AC091559	Extracellular Space	Enzyme		-1.788	
TYROBP	TYRO protein tyrosine kinase binding protein	XM_533687	Plasma Membrane	Other		-1.177	-1.413
UBE4B	Ubiquitination factor E4B (UFD2 homolog, yeast)	XM_854670	Cytoplasm	Enzyme	-1.009		
UBOX5	U-box domain containing 5	XM_001160362	Nucleus	Enzyme		-1.206	
UGT8	UDP glycosyltransferase 8	NM_001083635	Cytoplasm	Enzyme	-1.905		
ULK2	Unc-51-like kinase 2 (C. Elegans)	NM_014683	Cytoplasm	Kinase	-2.093	-1.14	
UNC119B	Unc-119 homolog B (C. Elegans)	XM_870226	unknown	Other	-1.593		
UNC50	Unc-50 homolog (C. Elegans)	BC103305	Cytoplasm	Other		-1.546	
UNC5B	Unc-5 homolog B (C. Elegans)	XM_856306	Plasma Membrane	Transmembrane receptor	-1.511		
UNG	Uracil-DNA glycosylase	XM_543441	Nucleus	Enzyme	-1.301	-1.062	
UNQ1887	Signal peptide peptidase 3	XM_543427	Plasma Membrane	Peptidase	-1.315		
USHBP1	Usher syndrome 1C binding protein 1	NM_001077137	unknown	Other	-1.583		
USP31	Ubiquitin specific peptidase 31	NM_020718	unknown	Peptidase	-1.077		
USP46	Ubiquitin specific peptidase 46	XM_001148401	unknown	Peptidase		-1.019	
USP5	Ubiquitin specific peptidase 5 (isopeptidase T)	NM_001098536	Cytoplasm	Peptidase	-1.152	-1.021	
VAMP1	Vesicle-associated membrane protein 1 (synaptobrevin 1)	NM_199245	Plasma Membrane	Transporter	-1.406		
VCL	Vinculin	XM_507854	Plasma Membrane	Enzyme	-1.08		
VDAC3	Voltage-dependent anion channel 3	XM_001138480	Cytoplasm	Ion channel	-1.637		
VHL	Von Hippel-Lindau tumor suppressor	NM_001008552	Nucleus	Other	-1.063		
VIP	Vasoactive intestinal peptide	NM_173970	Extracellular Space	Other		-2.367	-6.831
VSTM2L	V-set and transmembrane domain containing 2 like	NM_080607	unknown	Other		-2.516	-1.966
WAC	WW domain containing adaptor with coiled-coil	XM_611722	unknown	Other	-1.305		
WAPAL	Wings apart-like homolog (Drosophila)	XM_846909	Nucleus	Other	-1.021		
WDR66	WD repeat domain 66	XM_854906	unknown	Other		-1.615	-1.384
WIPF3	WAS/WASL interacting protein family, member 3	XM_001254241	Plasma Membrane	Other			-2.291
WNK2	WNK lysine deficient protein kinase 2	XM_582977	unknown	Kinase		-1.442	-1.508
XIST	X (inactive)-specific transcript (non-protein coding)	AK054860	Nucleus	Other	-1.669		
XYLT1	Xylosyltransferase I	AC122836	Cytoplasm	Enzyme		-1.334	-2.381
YY1	YY1 transcription factor	XM_510162	Nucleus	Transcription regulator	-1.186	-1.383	-1.206
ZAK	Sterile alpha motif and leucine zipper containing kinase AZK	AF480462	Cytoplasm	Kinase	-1.618	-1.052	
ZCCHC24	Zinc finger, CCHC domain containing 24	XM_507867	unknown	Other	-1.097		

Table C-1. Continued

Symbol	Entrez gene name	GenBank	Location	Type(s)	Fold change exposure	Fold change survival	Fold change location
ZDHHC20	Zinc finger, DHHC-type containing 20	XM_509571	unknown	Other	-1.399		
ZEB1	Zinc finger E-box binding homeobox 1	XM_615192	Nucleus	Transcription regulator	-1.093		
ZEB2	Zinc finger E-box binding homeobox 2	AY029472	Nucleus	Transcription regulator	-2.033	-1.285	
ZFP161	Zinc finger protein 161 homolog (mouse)	XM_512037	Nucleus	Other		-1.234	
ZFP57	Zinc finger protein 57 homolog (mouse)	NM_001109809	Nucleus	Transcription regulator	-2.323		
ZFYVE26	Zinc finger, FYVE domain containing 26	AK055455	unknown	Other	-1.093		
ZIC1	Zic family member 1 (odd-paired homolog, Drosophila)	XM_516806	Nucleus	Transcription regulator	-2.372		
ZIC5	Zic family member 5 (odd-paired homolog, Drosophila)	NM_033132	Nucleus	Other	-1.412		
ZMIZ1	Zinc finger, MIZ-type containing 1	NM_020338	Nucleus	Other	-1.105		
ZMYM2	Zinc finger, MYM-type 2	NM_003453	Nucleus	Other	-1.582		
ZMYND8	Zinc finger, MYND-type containing 8	XM_866938	Nucleus	Transcription regulator			-1.082
ZNF219	Zinc finger protein 219	XM_867319	Nucleus	Transcription regulator	-1.162		
ZNF267	Zinc finger protein 267	AC165088	Nucleus	Other	-1.397	-1.126	
ZNF331	Zinc finger protein 331	NM_001103251	Nucleus	Other	-2.17		
ZNF395	Zinc finger protein 395	NM_018660	Cytoplasm	Other	-2.826		
ZNF398	Zinc finger protein 398	AK290499	Nucleus	Transcription regulator		-1.446	
ZNF407	Zinc finger protein 407	XM_533370	Nucleus	Other	-1.084		
ZNF451	Zinc finger protein 451	XM_518562	Nucleus	Other	-1.01		
ZNF532	Zinc finger protein 532	XM_613386	unknown	Other	-1.099		
ZNF594	Zinc finger protein 594	NM_032530	unknown	Other		-1.853	
ZNF653	Zinc finger protein 653	XM_848511	unknown	Other		-1.163	
ZNF664	Zinc finger protein 664	AK023009	Nucleus	Other	-1.331		
ZNF827	Zinc finger protein 827	XM_862289	unknown	Other		-1.346	
ZYG11B	Zyg-11 homolog B (C. Elegans)	XM_001139134	unknown	Other		-1.009	
ZZEF1	Zinc finger, ZZ-type with EF-hand domain 1	AC067815	unknown	Other	-1.162		

LIST OF REFERENCES

1. [<http://www.aphis.usda.gov/vs/nahss/equine/wnv/wnv_distribution_maps.htm>]

2. Centers for Disease Control and Prevention WNS: 2010.

3. Farajollahi A, Crans WJ, Bryant P, Wolf B, Burkhalter KL, Godsey MS, Aspen SE, Nasci RS: **Detection of West Nile viral RNA from an overwintering pool of Culex pipens pipiens (Diptera: Culicidae) in New Jersey, 2003**. *J Med Entomol* 2005, **42**(3):490-494.

4. Girard YA, Klingler KA, Higgs S: **West Nile virus dissemination and tissue tropisms in orally infected Culex pipiens quinquefasciatus**. *Vector Borne Zoonotic Dis* 2004, **4**(2):109-122.

5. CDC: **Outbreak of West Nile-like viral encephalitis--New York, 1999**. *MMWR Morb Mortal Wkly Rep* 1999, **48**(38):845-849.

6. Lanciotti RS, Roehrig JT, Deubel V, Smith J, Parker M, Steele K, Crise B, Volpe KE, Crabtree MB, Scherret JH *et al*: **Origin of the West Nile virus responsible for an outbreak of encephalitis in the northeastern United States**. *Science* 1999, **286**(5448):2333-2337.

7. Beasley DW, Whiteman MC, Zhang S, Huang CY, Schneider BS, Smith DR, Gromowski GD, Higgs S, Kinney RM, Barrett AD: **Envelope protein glycosylation status influences mouse neuroinvasion phenotype of genetic lineage 1 West Nile virus strains**. *J Virol* 2005, **79**(13):8339-8347.

8. Botha EM, Markotter W, Wolfaardt M, Paweska JT, Swanepoel R, Palacios G, Nel LH, Venter M: **Genetic determinants of virulence in pathogenic lineage 2 West Nile virus strains**. *Emerg Infect Dis* 2008, **14**(2):222-230.

9. Brault AC, Powers AM, Holmes EC, Woelk CH, Weaver SC: **Positively charged amino acid substitutions in the e2 envelope glycoprotein are associated with the emergence of venezuelan equine encephalitis virus**. *J Virol* 2002, **76**(4):1718-1730.

10. Long MT: **Equine Infectious Diseases**. In: *Equine Infectious Diseases.* Edited by Sellon DCL, M.T. St. Louis, MO: Elsevier; 2007: 198-206.

11. Nasci RS, Savage HM, White DJ, Miller JR, Cropp BC, Godsey MS, Kerst AJ, Bennett P, Gottfried K, Lanciotti RS: **West Nile virus in overwintering Culex mosquitoes, New York City, 2000**. *Emerg Infect Dis* 2001, **7**(4):742-744.

12. Reisen W, Brault AC: **West Nile virus in North America: perspectives on epidemiology and intervention**. *Pest Manag Sci* 2007, **63**(7):641-646.

13. Sardelis MR, Turell MJ, Dohm DJ, O'Guinn ML: **Vector competence of selected North American Culex and Coquillettidia mosquitoes for West Nile virus**. *Emerg Infect Dis* 2001, **7**(6):1018-1022.

14. Turell MJ, Dohm DJ, Sardelis MR, Oguinn ML, Andreadis TG, Blow JA: **An update on the potential of north American mosquitoes (Diptera: Culicidae) to transmit West Nile Virus**. *J Med Entomol* 2005, **42**(1):57-62.

15. Turell MJ, O'Guinn ML, Dohm DJ, Jones JW: **Vector competence of North American mosquitoes (Diptera: Culicidae) for West Nile virus**. *J Med Entomol* 2001, **38**(2):130-134.

16. Turell MJ, Sardelis MR, Dohm DJ, O'Guinn ML: **Potential North American vectors of West Nile virus**. *Ann N Y Acad Sci* 2001, **951**:317-324.

17. Tesh RB, Parsons R, Siirin M, Randle Y, Sargent C, Guzman H, Wuithiranyagool T, Higgs S, Vanlandingham DL, Bala AA *et al*: **Year-round West Nile virus activity, Gulf Coast region, Texas and Louisiana**. *Emerg Infect Dis* 2004, **10**(9):1649-1652.

18. Reisen WK, Fang Y, Martinez VM: **Avian host and mosquito (Diptera: Culicidae) vector competence determine the efficiency of West Nile and St. Louis encephalitis virus transmission**. *J Med Entomol* 2005, **42**(3):367-375.

19. Savage HM, Aggarwal D, Apperson CS, Katholi CR, Gordon E, Hassan HK, Anderson M, Charnetzky D, McMillen L, Unnasch EA *et al*: **Host choice and West Nile virus infection rates in blood-fed mosquitoes, including members of the Culex pipiens complex, from Memphis and Shelby County, Tennessee, 2002-2003**. *Vector Borne Zoonotic Dis* 2007, **7**(3):365-386.

20. Sardelis MR, Turell MJ, O'Guinn ML, Andre RG, Roberts DR: **Vector competence of three North American strains of Aedes albopictus for West Nile virus**. *J Am Mosq Control Assoc* 2002, **18**(4):284-289.

21. Goddard LB, Roth AE, Reisen WK, Scott TW: **Vertical transmission of West Nile Virus by three California Culex (Diptera: Culicidae) species**. *J Med Entomol* 2003, **40**(6):743-746.

22. Hayes EB, Komar N, Nasci RS, Montgomery SP, O'Leary DR, Campbell GL: **Epidemiology and transmission dynamics of West Nile virus disease**. *Emerg Infect Dis* 2005, **11**(8):1167-1173.

23. Weingartl HM, Neufeld JL, Copps J, Marszal P: **Experimental West Nile virus infection in blue jays (Cyanocitta cristata) and crows (Corvus brachyrhynchos)**. *Vet Pathol* 2004, **41**(4):362-370.

24. Komar N, Langevin S, Hinten S, Nemeth N, Edwards E, Hettler D, Davis B, Bowen R, Bunning M: **Experimental infection of North American birds with the New York 1999 strain of West Nile virus**. *Emerg Infect Dis* 2003, **9**(3):311-322.

25. Kilpatrick AM, Daszak P, Jones MJ, Marra PP, Kramer LD: **Host heterogeneity dominates West Nile virus transmission**. *Proc Biol Sci* 2006, **273**(1599):2327-2333.

26. McLean RG, Francy DB, Campos EG: **Experimental studies of St. Louis encephalitis virus in vertebrates**. *J Wildl Dis* 1985, **21**(2):85-93.

27. McLean RG, Kirk LJ, Shriner RB, Townsend M: **Avian hosts of St. Louis encephalitis virus in Pine Bluff, Arkansas, 1991**. *Am J Trop Med Hyg* 1993, **49**(1):46-52.

28. Austgen LE, Bowen RA, Bunning ML, Davis BS, Mitchell CJ, Chang GJ: **Experimental infection of cats and dogs with West Nile virus**. *Emerg Infect Dis* 2004, **10**(1):82-86.

29. Davis A, Bunning M, Gordy P, Panella N, Blitvich B, Bowen R: **Experimental and natural infection of North American bats with West Nile virus**. *Am J Trop Med Hyg* 2005, **73**(2):467-469.

30. Teehee ML, Bunning ML, Stevens S, Bowen RA: **Experimental infection of pigs with West Nile virus**. *Arch Virol* 2005, **150**(6):1249-1256.

31. Platt KB, Tucker BJ, Halbur PG, Blitvich BJ, Fabiosa FG, Mullin K, Parikh GR, Kitikoon P, Bartholomay LC, Rowley WA: **Fox Squirrels (Sciurus niger) Develop West Nile Virus Viremias Sufficient for Infecting Select Mosquito Species**. *Vector Borne Zoonotic Dis* 2008.

32. Platt KB, Tucker BJ, Halbur PG, Tiawsirisup S, Blitvich BJ, Fabiosa FG, Bartholomay LC, Rowley WA: **West Nile virus viremia in eastern chipmunks (Tamias striatus) sufficient for infecting different mosquitoes**. *Emerg Infect Dis* 2007, **13**(6):831-837.

33. Klenk K, Snow J, Morgan K, Bowen R, Stephens M, Foster F, Gordy P, Beckett S, Komar N, Gubler D *et al*: **Alligators as West Nile virus amplifiers**. *Emerg Infect Dis* 2004, **10**(12):2150-2155.

34. Jacobson ER, Ginn PE, Troutman JM, Farina L, Stark L, Klenk K, Burkhalter KL, Komar N: **West Nile virus infection in farmed American alligators (Alligator mississippiensis) in Florida**. *J Wildl Dis* 2005, **41**(1):96-106.

35. Beasley DW, Davis CT, Whiteman M, Granwehr B, Kinney RM, Barrett AD: **Molecular determinants of virulence of West Nile virus in North America**. *Arch Virol Suppl* 2004(18):35-41.

36. Chambers TJ, Halevy M, Nestorowicz A, Rice CM, Lustig S: **West Nile virus envelope proteins: nucleotide sequence analysis of strains differing in mouse neuroinvasiveness**. *J Gen Virol* 1998, **79 (Pt 10)**:2375-2380.

37. Beasley DW, Davis CT, Estrada-Franco J, Navarro-Lopez R, Campomanes-Cortes A, Tesh RB, Weaver SC, Barrett AD: **Genome sequence and attenuating mutations in West Nile virus isolate from Mexico**. *Emerg Infect Dis* 2004, **10**(12):2221-2224.

38. Beasley DW, Davis CT, Guzman H, Vanlandingham DL, Travassos da Rosa AP, Parsons RE, Higgs S, Tesh RB, Barrett AD: **Limited evolution of West Nile virus has occurred during its southwesterly spread in the United States**. *Virology* 2003, **309**(2):190-195.

39. Davis CT, Li L, May FJ, Bueno R, Jr., Dennett JA, Bala AA, Guzman H, Quiroga-Elizondo D, Tesh RB, Barrett AD: **Genetic stasis of dominant West Nile virus genotype, Houston, Texas**. *Emerg Infect Dis* 2007, **13**(4):601-604.

40. Davis CT, Beasley DW, Guzman H, Siirin M, Parsons RE, Tesh RB, Barrett AD: **Emergence of attenuated West Nile virus variants in Texas, 2003**. *Virology* 2004, **330**(1):342-350.

41. Beasley DW: **Recent advances in the molecular biology of west nile virus**. *Curr Mol Med* 2005, **5**(8):835-850.

42. Yuan F, Lou Z, Li X, Chen YW, Bell JI, Rao Z, Gao GF: **Refolding, crystallization and preliminary X-ray structural studies of the West Nile virus envelope (E) protein domain III**. *Acta Crystallogr Sect F Struct Biol Cryst Commun* 2005, **61**(Pt 4):421-423.

43. Zhou H, Singh NJ, Kim KS: **Homology modeling and molecular dynamics study of West Nile virus NS3 protease: a molecular basis for the catalytic activity increased by the NS2B cofactor**. *Proteins* 2006, **65**(3):692-701.

44. Chernov AV, Shiryaev SA, Aleshin AE, Ratnikov BI, Smith JW, Liddington RC, Strongin AY: **The two-component NS2B-NS3 proteinase represses DNA unwinding activity of the West Nile virus NS3 helicase**. *J Biol Chem* 2008, **283**(25):17270-17278.

45. Tilgner M, Shi PY: **Structure and function of the 3' terminal six nucleotides of the west nile virus genome in viral replication**. *J Virol* 2004, **78**(15):8159-8171.

46. Li W, Brinton MA: **The 3' stem loop of the West Nile virus genomic RNA can suppress translation of chimeric mRNAs**. *Virology* 2001, **287**(1):49-61.

47. Shiryaev SA, Chernov AV, Aleshin AE, Shiryaeva TN, Strongin AY: **NS4A regulates the ATPase activity of the NS3 helicase: a novel cofactor role of the non-structural protein NS4A from West Nile virus**. *J Gen Virol* 2009, **90**(Pt 9):2081-2085.

48. Yu L, Nomaguchi M, Padmanabhan R, Markoff L: **Specific requirements for elements of the 5' and 3' terminal regions in flavivirus RNA synthesis and viral replication**. *Virology* 2008, **374**(1):170-185.

49. Li XF, Jiang T, Yu XD, Deng YQ, Zhao H, Zhu QY, Qin ED, Qin CF: **RNA elements within the 5' UTR of West Nile virus genome are critical for RNA synthesis and viral replication**. *J Gen Virol* 2009.

50. Davis WG, Blackwell JL, Shi PY, Brinton MA: **Interaction between the cellular protein eEF1A and the 3'-terminal stem-loop of West Nile virus genomic RNA facilitates viral minus-strand RNA synthesis**. *J Virol* 2007, **81**(18):10172-10187.

51. Ray D, Shah A, Tilgner M, Guo Y, Zhao Y, Dong H, Deas TS, Zhou Y, Li H, Shi PY: **West Nile virus 5'-cap structure is formed by sequential guanine N-7 and ribose 2'-O methylations by nonstructural protein 5**. *J Virol* 2006, **80**(17):8362-8370.

52. Leung JY, Pijlman GP, Kondratieva N, Hyde J, Mackenzie JM, Khromykh AA: **Role of nonstructural protein NS2A in flavivirus assembly**. *J Virol* 2008, **82**(10):4731-4741.

53. Brinton MA: **The molecular biology of West Nile Virus: a new invader of the western hemisphere**. *Annu Rev Microbiol* 2002, **56**:371-402.

54. Bunning ML, Bowen RA, Cropp CB, Sullivan KG, Davis BS, Komar N, Godsey MS, Baker D, Hettler DL, Holmes DA *et al*: **Experimental infection of horses with West Nile virus**. *Emerg Infect Dis* 2002, **8**(4):380-386.

55. Nemeth N, Gould D, Bowen R, Komar N: **Natural and experimental West Nile virus infection in five raptor species**. *J Wildl Dis* 2006, **42**(1):1-13.

56. Tesh RB, Siirin M, Guzman H, Travassos da Rosa AP, Wu X, Duan T, Lei H, Nunes MR, Xiao SY: **Persistent West Nile virus infection in the golden hamster: studies on its mechanism and possible implications for other flavivirus infections**. *J Infect Dis* 2005, **192**(2):287-295.

57. Styer LM, Bernard KA, Kramer LD: **Enhanced early West Nile virus infection in young chickens infected by mosquito bite: effect of viral dose**. *Am J Trop Med Hyg* 2006, **75**(2):337-345.

58. Long MT, Gibbs EP, Mellencamp MW, Bowen RA, Seino KK, Zhang S, Beachboard SE, Humphrey PP: **Efficacy, duration, and onset of immunogenicity of a West Nile virus vaccine, live Flavivirus chimera, in horses with a clinical disease challenge model**. *Equine Vet J* 2007, **39**(6):491-497.

59. Seino KK, Long, M.T., Gibbs, E.P.J., Abbott, J.R., Beachboard, S.E., Bourgeois, M.A., Fanta, D.K.: **Protective Immune Responses to West Nile Virus (WNV) of 28 Day Vaccinated Horses**. In.; 2008.

60. Osorio JE, Godsey MS, Defoliart GR, Yuill TM: **La Crosse viremias in white-tailed deer and chipmunks exposed by injection or mosquito bite**. *Am J Trop Med Hyg* 1996, **54**(4):338-342.

61. Nemeth NM, Bowen RA: **Dynamics of passive immunity to West Nile virus in domestic chickens (Gallus gallus domesticus)**. *Am J Trop Med Hyg* 2007, **76**(2):310-317.

62. Phipps LP, Gough RE, Ceeraz V, Cox WJ, Brown IH: **Detection of West Nile virus in the tissues of specific pathogen free chickens and serological response to laboratory infection: a comparative study**. *Avian Pathol* 2007, **36**(4):301-305.

63. Joyner PH, Kelly S, Shreve AA, Snead SE, Sleeman JM, Pettit DA: **West Nile virus in raptors from Virginia during 2003: clinical, diagnostic, and epidemiologic findings**. *J Wildl Dis* 2006, **42**(2):335-344.

64. Mashimo T, Lucas M, Simon-Chazottes D, Frenkiel MP, Montagutelli X, Ceccaldi PE, Deubel V, Guenet JL, Despres P: **A nonsense mutation in the gene encoding 2'-5'-oligoadenylate synthetase/L1 isoform is associated with West Nile virus susceptibility in laboratory mice**. *Proc Natl Acad Sci U S A* 2002, **99**(17):11311-11316.

65. Lucas M, Mashimo T, Frenkiel MP, Simon-Chazottes D, Montagutelli X, Ceccaldi PE, Guenet JL, Despres P: **Infection of mouse neurones by West Nile virus is modulated by the interferon-inducible 2'-5' oligoadenylate synthetase 1b protein**. *Immunol Cell Biol* 2003, **81**(3):230-236.

66. Perelygin AA, Scherbik SV, Zhulin IB, Stockman BM, Li Y, Brinton MA: **Positional cloning of the murine flavivirus resistance gene**. *Proc Natl Acad Sci U S A* 2002, **99**(14):9322-9327.

67. Bunning ML, Bowen RA, Cropp B, Sullivan K, Davis B, Komar N, Godsey M, Baker D, Hettler D, Holmes D *et al*: **Experimental infection of horses with West Nile virus and their potential to infect mosquitoes and serve as amplifying hosts**. *Ann N Y Acad Sci* 2001, **951**:338-339.

68. Minke JM, Siger L, Karaca K, Austgen L, Gordy P, Bowen R, Renshaw RW, Loosmore S, Audonnet JC, Nordgren B: **Recombinant canarypoxvirus vaccine carrying the prM/E genes of West Nile virus protects horses against a West Nile virus-mosquito challenge**. *Arch Virol Suppl* 2004(18):221-230.

69. Snook CS, Hyman SS, Del Piero F, Palmer JE, Ostlund EN, Barr BS, Desrochers AM, Reilly LK: **West Nile virus encephalomyelitis in eight horses**. *J Am Vet Med Assoc* 2001, **218**(10):1576-1579.

70. Porter MB, Long MT, Getman LM, Giguere S, MacKay RJ, Lester GD, Alleman AR, Wamsley HL, Franklin RP, Jacks S *et al*: **West Nile virus encephalomyelitis in horses: 46 cases (2001)**. *J Am Vet Med Assoc* 2003, **222**(9):1241-1247.

71. IG M: **Large Animal Neurology**: In: Lea & Febiger; 1989.

72. Hayes EB, O'Leary DR: **West Nile virus infection: a pediatric perspective**. *Pediatrics* 2004, **113**(5):1375-1381.

73. Kramer LD, Li J, Shi PY: **West Nile virus**. *Lancet Neurol* 2007, **6**(2):171-181.

74. Wang T, Town T, Alexopoulou L, Anderson JF, Fikrig E, Flavell RA: **Toll-like receptor 3 mediates West Nile virus entry into the brain causing lethal encephalitis**. *Nat Med* 2004, **10**(12):1366-1373.

75. Daffis S, Samuel MA, Suthar MS, Gale M, Jr., Diamond MS: **Toll-like receptor 3 has a protective role against West Nile virus infection**. *J Virol* 2008, **82**(21):10349-10358.

76. Shrestha B, Samuel MA, Diamond MS: **CD8+ T cells require perforin to clear West Nile virus from infected neurons**. *J Virol* 2006, **80**(1):119-129.

77. Shrestha B, Diamond MS: **Role of CD8+ T cells in control of West Nile virus infection**. *J Virol* 2004, **78**(15):8312-8321.

78. Diamond MS, Shrestha B, Mehlhop E, Sitati E, Engle M: **Innate and adaptive immune responses determine protection against disseminated infection by West Nile encephalitis virus**. *Viral Immunol* 2003, **16**(3):259-278.

79. Kesson AM, Cheng Y, King NJ: **Regulation of immune recognition molecules by flavivirus, West Nile**. *Viral Immunol* 2002, **15**(2):273-283.

80. Samuel MA, Diamond MS: **Pathogenesis of West Nile Virus infection: a balance between virulence, innate and adaptive immunity, and viral evasion**. *J Virol* 2006, **80**(19):9349-9360.

81. Wang T, Fikrig E: **Immunity to West Nile virus**. *Curr Opin Immunol* 2004, **16**(4):519-523.

82. Diamond MS, Sitati EM, Friend LD, Higgs S, Shrestha B, Engle M: **A critical role for induced IgM in the protection against West Nile virus infection**. *J Exp Med* 2003, **198**(12):1853-1862.

83. Engle MJ, Diamond MS: **Antibody prophylaxis and therapy against West Nile virus infection in wild-type and immunodeficient mice**. *J Virol* 2003, **77**(24):12941-12949.

84. Fredericksen BL, Keller BC, Fornek J, Katze MG, Gale M, Jr.: **Establishment and maintenance of the innate antiviral response to West Nile Virus involves both RIG-I and MDA5 signaling through IPS-1**. *J Virol* 2008, **82**(2):609-616.

85. Fredericksen BL, Smith M, Katze MG, Shi PY, Gale M, Jr.: **The host response to West Nile Virus infection limits viral spread through the activation of the interferon regulatory factor 3 pathway**. *J Virol* 2004, **78**(14):7737-7747.

86. Town T, Jeng D, Alexopoulou L, Tan J, Flavell RA: **Microglia recognize double-stranded RNA via TLR3**. *J Immunol* 2006, **176**(6):3804-3812.

87. Samuel MA, Diamond MS: **Alpha/beta interferon protects against lethal West Nile virus infection by restricting cellular tropism and enhancing neuronal survival**. *J Virol* 2005, **79**(21):13350-13361.

88. Scherbik SV, Paranjape JM, Stockman BM, Silverman RH, Brinton MA: **RNase L plays a role in the antiviral response to West Nile virus**. *J Virol* 2006, **80**(6):2987-2999.

89. Ghoshal A, Das S, Ghosh S, Mishra MK, Sharma V, Koli P, Sen E, Basu A: **Proinflammatory mediators released by activated microglia induces neuronal death in Japanese encephalitis**. *Glia* 2007, **55**(5):483-496.

90. Klein RS, Lin E, Zhang B, Luster AD, Tollett J, Samuel MA, Engle M, Diamond MS: **Neuronal CXCL10 directs CD8+ T-cell recruitment and control of West Nile virus encephalitis**. *J Virol* 2005, **79**(17):11457-11466.

91. Wang Y, Lobigs M, Lee E, Mullbacher A: **CD8+ T cells mediate recovery and immunopathology in West Nile virus encephalitis**. *J Virol* 2003, **77**(24):13323-13334.

92. Erdmann NB, Whitney NP, Zheng J: **Potentiation of Excitotoxicity in HIV-1 Associated Dementia and the Significance of Glutaminase**. *Clin Neurosci Res* 2006, **6**(5):315-328.

93. Kaul M: **HIV's double strike at the brain: neuronal toxicity and compromised neurogenesis**. *Front Biosci* 2008, **13**:2484-2494.

94. Kaul M, Lipton SA: **Mechanisms of neuronal injury and death in HIV-1 associated dementia**. *Curr HIV Res* 2006, **4**(3):307-318.

95. Kaul M, Lipton SA: **Mechanisms of neuroimmunity and neurodegeneration associated with HIV-1 infection and AIDS**. *J Neuroimmune Pharmacol* 2006, **1**(2):138-151.

96. Darman J, Backovic S, Dike S, Maragakis NJ, Krishnan C, Rothstein JD, Irani DN, Kerr DA: **Viral-induced spinal motor neuron death is non-cell-autonomous and involves glutamate excitotoxicity**. *J Neurosci* 2004, **24**(34):7566-7575.

97. Mark LP, Prost RW, Ulmer JL, Smith MM, Daniels DL, Strottmann JM, Brown WD, Hacein-Bey L: **Pictorial review of glutamate excitotoxicity: fundamental concepts for neuroimaging**. *AJNR Am J Neuroradiol* 2001, **22**(10):1813-1824.

98. Blakely PK, Kleinschmidt-DeMasters BK, Tyler KL, Irani DN: **Disrupted glutamate transporter expression in the spinal cord with acute flaccid paralysis caused by West Nile virus infection**. *J Neuropathol Exp Neurol* 2009, **68**(10):1061-1072.

99. Davis LE, DeBiasi R, Goade DE, Haaland KY, Harrington JA, Harnar JB, Pergam SA, King MK, DeMasters BK, Tyler KL: **West Nile virus neuroinvasive disease**. *Ann Neurol* 2006, **60**(3):286-300.

100. Zhang JS, Zhang PH, Si BY, Yang H, Cao WC: **[Comparison and discrimination of the biological characteristics between West Nile virus and Japanese encephalitis virus]**. *Zhonghua Shi Yan He Lin Chuang Bing Du Xue Za Zhi* 2005, **19**(4):340-343.

101. Cao NJ, Ranganathan C, Kupsky WJ, Li J: **Recovery and prognosticators of paralysis in West Nile virus infection**. *J Neurol Sci* 2005, **236**(1-2):73-80.

102. Petzold A, Groves M, Leis AA, Scaravilli F, Stokic DS: **Neuronal and glial cerebrospinal fluid protein biomarkers are elevated after West Nile virus infection**. *Muscle Nerve*, **41**(1):42-49.

103. Porter MB, Long M, Gosche DG, Schott HM, 2nd, Hines MT, Rossano M, Sellon DC: **Immunoglobulin M-capture enzyme-linked immunosorbent assay testing of cerebrospinal fluid and serum from horses exposed to west nile virus by vaccination or natural infection**. *J Vet Intern Med* 2004, **18**(6):866-870.

104. Cernescu C, Ruta SM, Tardei G, Grancea C, Moldoveanu L, Spulbar E, Tsai T: **A high number of severe neurologic clinical forms during an epidemic of West Nile virus infection**. *Rom J Virol* 1997, **48**(1-4):13-25.

105. Wamsley HL, Alleman AR, Porter MB, Long MT: **Findings in cerebrospinal fluids of horses infected with West Nile virus: 30 cases (2001)**. *J Am Vet Med Assoc* 2002, **221**(9):1303-1305.

106. Jeha LE, Sila CA, Lederman RJ, Prayson RA, Isada CM, Gordon SM: **West Nile virus infection: a new acute paralytic illness**. *Neurology* 2003, **61**(1):55-59.

107. Ostlund EN, Andresen JE, Andresen M: **West Nile encephalitis**. *Vet Clin North Am Equine Pract* 2000, **16**(3):427-441.

108. Ostlund EN, Crom RL, Pedersen DD, Johnson DJ, Williams WO, Schmitt BJ: **Equine West Nile encephalitis, United States**. *Emerg Infect Dis* 2001, **7**(4):665-669.

109. Tewari D, Kim H, Feria W, Russo B, Acland H: **Detection of West Nile virus using formalin fixed paraffin embedded tissues in crows and horses: quantification of viral transcripts by real-time RT-PCR**. *J Clin Virol* 2004, **30**(4):320-325.

110. Ng T, Hathaway D, Jennings N, Champ D, Chiang YW, Chu HJ: **Equine vaccine for West Nile virus**. *Dev Biol (Basel)* 2003, **114**:221-227.

111. Tesh RB, Arroyo J, Travassos Da Rosa AP, Guzman H, Xiao SY, Monath TP: **Efficacy of killed virus vaccine, live attenuated chimeric virus vaccine, and passive immunization for prevention of West Nile virus encephalitis in hamster model**. *Emerg Infect Dis* 2002, **8**(12):1392-1397.

112. Epp T, Waldner C, Townsend HG: **A case-control study of factors associated with development of clinical disease due to West Nile virus, Saskatchewan 2003**. *Equine Vet J* 2007, **39**(6):498-503.

113. Davidson AH, Traub-Dargatz JL, Rodeheaver RM, Ostlund EN, Pedersen DD, Moorhead RG, Stricklin JB, Dewell RD, Roach SD, Long RE *et al*: **Immunologic responses to West Nile virus in vaccinated and clinically affected horses**. *J Am Vet Med Assoc* 2005, **226**(2):240-245.

114. [http://www.aaep.org/vaccination_guidelines.htm]

115. Siger L, Bowen RA, Karaca K, Murray MJ, Gordy PW, Loosmore SM, Audonnet JC, Nordgren RM, Minke JM: **Assessment of the efficacy of a single dose of a recombinant vaccine against West Nile virus in response to natural challenge with West Nile virus-infected mosquitoes in horses**. *Am J Vet Res* 2004, **65**(11):1459-1462.

116. Arroyo J, Miller CA, Catalan J, Monath TP: **Yellow fever vector live-virus vaccines: West Nile virus vaccine development**. *Trends Mol Med* 2001, **7**(8):350-354.

117. Long MT, Gibbs EP, Mellencamp MW, Zhang S, Barnett DC, Seino KK, Beachboard SE, Humphrey PP: **Safety of an attenuated West Nile virus vaccine, live Flavivirus chimera in horses**. *Equine Vet J* 2007, **39**(6):486-490.

118. Mao C, Evans C, Jensen RV, Sobral BW: **Identification of new genes in Sinorhizobium meliloti using the Genome Sequencer FLX system**. *BMC Microbiol* 2008, **8**:72.

119. Vera JC, Wheat CW, Fescemyer HW, Frilander MJ, Crawford DL, Hanski I, Marden JH: **Rapid transcriptome characterization for a nonmodel organism using 454 pyrosequencing**. *Mol Ecol* 2008, **17**(7):1636-1647.

120. Chung W, Kwabi-Addo B, Ittmann M, Jelinek J, Shen L, Yu Y, Issa JP: **Identification of novel tumor markers in prostate, colon and breast cancer by unbiased methylation profiling**. *PLoS ONE* 2008, **3**(4):e2079.

121. Tang H, Goldberg E: **Homo Sapiens Lactate Dehydrogenase c (Ldhc) Gene Expression in Cancer Cells is Regulated by Transcription Factor Sp1, CREB and CpG Island Methylation**. *J Androl* 2008.

122. Feng W, Marquez RT, Lu Z, Liu J, Lu KH, Issa JP, Fishman DM, Yu Y, Bast RC, Jr.: **Imprinted tumor suppressor genes ARHI and PEG3 are the most frequently down-regulated in human ovarian cancers by loss of heterozygosity and promoter methylation**. *Cancer* 2008, **112**(7):1489-1502.

123. Tshuikina M, Jernberg-Wiklund H, Nilsson K, Oberg F: **Epigenetic silencing of the interferon regulatory factor ICSBP/IRF8 in human multiple myeloma**. *Exp Hematol* 2008.

124. Yu Y, Zhang H, Tian F, Bacon L, Zhang Y, Zhang W, Song J: **Quantitative evaluation of DNA methylation patterns for ALVE and TVB genes in a neoplastic disease susceptible and resistant chicken model**. *PLoS ONE* 2008, **3**(3):e1731.

125. Bordoni R, Bonnal R, Rizzi E, Carrera P, Benedetti S, Cremonesi L, Stenirri S, Colombo A, Montrasio C, Bonalumi S *et al*: **Evaluation of human gene variant detection in amplicon pools by the GS-FLX parallel Pyrosequencer**. *BMC Genomics* 2008, **9**:464.

126. Guo DC, Qi Y, He R, Gupta P, Milewicz DM: **High throughput detection of small genomic insertions or deletions by Pyrosequencing**. *Biotechnol Lett* 2003, **25**(20):1703-1707.

127. Ronaghi M, Elahi E: **Discovery of single nucleotide polymorphisms and mutations by pyrosequencing**. *Comp Funct Genomics* 2002, **3**(1):51-56.

128. Morin RD, Aksay G, Dolgosheina E, Ebhardt HA, Magrini V, Mardis ER, Sahinalp SC, Unrau PJ: **Comparative analysis of the small RNA transcriptomes of Pinus contorta and Oryza sativa**. *Genome Res* 2008, **18**(4):571-584.

129. Heisel SE, Zhang Y, Allen E, Guo L, Reynolds TL, Yang X, Kovalic D, Roberts JK: **Characterization of unique small RNA populations from rice grain**. *PLoS ONE* 2008, **3**(8):e2871.

130. Moxon S, Jing R, Szittya G, Schwach F, Rusholme Pilcher RL, Moulton V, Dalmay T: **Deep sequencing of tomato short RNAs identifies microRNAs targeting genes involved in fruit ripening**. *Genome Res* 2008, **18**(10):1602-1609.

131. Sunkar R, Zhou X, Zheng Y, Zhang W, Zhu JK: **Identification of novel and candidate miRNAs in rice by high throughput sequencing**. *BMC Plant Biol* 2008, **8**:25.

132. Shin H, Hirst M, Bainbridge MN, Magrini V, Mardis E, Moerman DG, Marra MA, Baillie DL, Jones SJ: **Transcriptome analysis for Caenorhabditis elegans based on novel expressed sequence tags**. *BMC Biol* 2008, **6**:30.

133. Weber AP, Weber KL, Carr K, Wilkerson C, Ohlrogge JB: **Sampling the Arabidopsis transcriptome with massively parallel pyrosequencing**. *Plant Physiol* 2007, **144**(1):32-42.

134. Sun A, Ge J, Siffert W, Frey UH: **Quantification of allele-specific G-protein beta3 subunit mRNA transcripts in different human cells and tissues by Pyrosequencing**. *Eur J Hum Genet* 2005, **13**(3):361-369.

135. Zou Z, Najar F, Wang Y, Roe B, Jiang H: **Pyrosequence analysis of expressed sequence tags for Manduca sexta hemolymph proteins involved in immune responses**. *Insect Biochem Mol Biol* 2008, **38**(6):677-682.

136. [http://www.nih.gov/news/pr/feb2007/nhgri-07.htm]

137. Metzgar D, Myers CA, Russell KL, Faix D, Blair PJ, Brown J, Vo S, Swayne DE, Thomas C, Stenger DA *et al*: **Single assay for simultaneous detection and differential identification of human and avian influenza virus types, subtypes, and emergent variants**. *PLoS One*, **5**(2):e8995.

138. Sip M, Bystricka D, Kmoch S, Noskova L, Hartmannova H, Dedic P: **Detection of viral infections by an oligonucleotide microarray**. *J Virol Methods*.

139. Guo J, Dong Q, Fang Z, Chen X, Lu H, Wang K, Yin Y, Cai X, Zhao N, Chen J *et al*: **Identification of miRNAs that are associated with tumor metastasis in neuroblastoma**. *Cancer Biol Ther*, **9**(6).

140. Zhou X, Ren Y, Han L, Mei M, Xu P, Zhang CZ, Wang GX, Jia ZF, Pu PY, Kang CS: **Role of the AKT pathway in microRNA expression of human U251 glioblastoma cells**. *Int J Oncol*, **36**(3):665-672.

141. Qu K, Yesnik AM, Ortoleva PJ: **Alternative splicing regulatory network reconstruction from exon array data**. *J Theor Biol*.

142. de la Grange P, Gratadou L, Delord M, Dutertre M, Auboeuf D: **Splicing factor and exon profiling across human tissues**. *Nucleic Acids Res*.

143. Dutertre M, Lacroix-Triki M, Driouch K, de la Grange P, Gratadou L, Beck S, Millevoi S, Tazi J, Lidereau R, Vagner S *et al*: **Exon-based clustering of murine breast tumor transcriptomes reveals alternative exons whose expression is associated with metastasis**. *Cancer Res*, **70**(3):896-905.

144. Li J, Yu YJ, Feng L, Cai XB, Tang HB, Sun SK, Zhang HY, Liang JJ, Luo TR: **Global transcriptional profiles in peripheral blood mononuclear cell during classical swine fever virus infection**. *Virus Res*, **148**(1-2):60-70.

145. Conceicao TM, El-Bacha T, Villas-Boas CS, Coello G, Ramirez J, Montero-Lomeli M, Da Poian AT: **Gene expression analysis during dengue virus infection in HepG2 cells reveals virus control of innate immune response**. *J Infect*, **60**(1):65-75.

146. Xiao WW, Ma WL, Ma XD, Mao XM, Zheng WL: **[Bioinformatic analysis of dengue virus cDNAs and design of oligonucleotide probes for microarray detection of the virus]**. *Di Yi Jun Yi Da Xue Xue Bao* 2003, **23**(9):905-907.

147. Korimbocus J, Scaramozzino N, Lacroix B, Crance JM, Garin D, Vernet G: **DNA probe array for the simultaneous identification of herpesviruses, enteroviruses, and flaviviruses**. *J Clin Microbiol* 2005, **43**(8):3779-3787.

148. Nordstrom H, Falk KI, Lindegren G, Mouzavi-Jazi M, Walden A, Elgh F, Nilsson P, Lundkvist A: **DNA microarray technique for detection and identification of seven flaviviruses pathogenic for man**. *J Med Virol* 2005, **77**(4):528-540.

149. Grinev A, Daniel S, Laassri M, Chumakov K, Chizhikov V, Rios M: **Microarray-based assay for the detection of genetic variations of structural genes of West Nile virus**. *J Virol Methods* 2008, **154**(1-2):27-40.

150. Gupta N, Santhosh SR, Babu JP, Parida MM, Rao PV: **Chemokine profiling of Japanese encephalitis virus-infected mouse neuroblastoma cells by microarray and real-time RT-PCR: implication in neuropathogenesis**. *Virus Res*, **147**(1):107-112.

151. Nasirudeen AM, Liu DX: **Gene expression profiling by microarray analysis reveals an important role for caspase-1 in dengue virus-induced p53-mediated apoptosis**. *J Med Virol* 2009, **81**(6):1069-1081.

152. Ubol S, Masrinoul P, Chaijaruwanich J, Kalayanarooj S, Charoensirisuthikul T, Kasisith J: **Differences in global gene expression in peripheral blood mononuclear cells indicate a significant role of the innate responses in progression of dengue fever but not dengue hemorrhagic fever**. *J Infect Dis* 2008, **197**(10):1459-1467.

153. Lefeuvre A, Contamin H, Decelle T, Fournier C, Lang J, Deubel V, Marianneau P: **Host-cell interaction of attenuated and wild-type strains of yellow fever virus can be differentiated at early stages of hepatocyte infection**. *Microbes Infect* 2006, **8**(6):1530-1538.

154. Liew KJ, Chow VT: **Microarray and real-time RT-PCR analyses of a novel set of differentially expressed human genes in ECV304 endothelial-like cells infected with dengue virus type 2**. *J Virol Methods* 2006, **131**(1):47-57.

155. Moreno-Altamirano MM, Romano M, Legorreta-Herrera M, Sanchez-Garcia FJ, Colston MJ: **Gene expression in human macrophages infected with dengue virus serotype-2**. *Scand J Immunol* 2004, **60**(6):631-638.

156. Venter M, Myers TG, Wilson MA, Kindt TJ, Paweska JT, Burt FJ, Leman PA, Swanepoel R: **Gene expression in mice infected with West Nile virus strains of different neurovirulence**. *Virology* 2005, **342**(1):119-140.

157. **GenBank** [http://www.ncbi.nlm.nih.gov/sites/entrez?db=nucleotide]

158. Bene R, Antic S, Budisic M, Lisak M, Trkanjec Z, Demarin V, Podobnik-Sarkanji S: **Parkinson's disease**. *Acta Clin Croat* 2009, **48**(3):377-380.

159. Boyman O, Letourneau S, Krieg C, Sprent J: **Homeostatic proliferation and survival of naive and memory T cells**. *Eur J Immunol* 2009, **39**(8):2088-2094.

160. van Leeuwen EM, Sprent J, Surh CD: **Generation and maintenance of memory CD4(+) T Cells**. *Curr Opin Immunol* 2009, **21**(2):167-172.

161. Rodrigues L, Nandakumar S, Bonorino C, Rouse BT, Kumaraguru U: **IL-21 and IL-15 cytokine DNA augments HSV specific effector and memory CD8+ T cell response**. *Mol Immunol* 2009, **46**(7):1494-1504.

162. Rodrigues L, Bonorino C: **Role of IL-15 and IL-21 in viral immunity: applications for vaccines and therapies**. *Expert Rev Vaccines* 2009, **8**(2):167-177.

163. Yoneyama M, Fujita T: **Recognition of viral nucleic acids in innate immunity**. *Rev Med Virol*, **20**(1):4-22.

164. Baker BJ, Akhtar LN, Benveniste EN: **SOCS1 and SOCS3 in the control of CNS immunity**. *Trends Immunol* 2009, **30**(8):392-400.

165. Koeberlein B, zur Hausen A, Bektas N, Zentgraf H, Chin R, Nguyen LT, Kandolf R, Torresi J, Bock CT: **Hepatitis B virus overexpresses suppressor of cytokine signaling-3 (SOCS3) thereby contributing to severity of inflammation in the liver**. *Virus Res*, **148**(1-2):51-59.

166. Hashimoto K, Ishibashi K, Ishioka K, Zhao D, Sato M, Ohara S, Abe Y, Kawasaki Y, Sato Y, Yokota S *et al*: **RSV replication is attenuated by counteracting expression of the suppressor of cytokine signaling (SOCS) molecules**. *Virology* 2009, **391**(2):162-170.

167. Schraml BU, Hildner K, Ise W, Lee WL, Smith WA, Solomon B, Sahota G, Sim J, Mukasa R, Cemerski S *et al*: **The AP-1 transcription factor Batf controls T(H)17 differentiation**. *Nature* 2009, **460**(7253):405-409.

168. Pipkin ME, Sacks JA, Cruz-Guilloty F, Lichtenheld MG, Bevan MJ, Rao A: **Interleukin-2 and inflammation induce distinct transcriptional programs that promote the differentiation of effector cytolytic T cells**. *Immunity*, **32**(1):79-90.

169. Wek RC, Jiang HY, Anthony TG: **Coping with stress: eIF2 kinases and translational control**. *Biochem Soc Trans* 2006, **34**(Pt 1):7-11.

170. Bozza S, Bistoni F, Gaziano R, Pitzurra L, Zelante T, Bonifazi P, Perruccio K, Bellocchio S, Neri M, Iorio AM *et al*: **Pentraxin 3 protects from MCMV infection and reactivation through TLR sensing pathways leading to IRF3 activation**. *Blood* 2006, **108**(10):3387-3396.

171. Reading PC, Bozza S, Gilbertson B, Tate M, Moretti S, Job ER, Crouch EC, Brooks AG, Brown LE, Bottazzi B *et al*: **Antiviral activity of the long chain pentraxin PTX3 against influenza viruses**. *J Immunol* 2008, **180**(5):3391-3398.

172. Matter C, Pribadi M, Liu X, Trachtenberg JT: **Delta-catenin is required for the maintenance of neural structure and function in mature cortex in vivo**. *Neuron* 2009, **64**(3):320-327.

173. Imbeaud S, Graudens E, Boulanger V, Barlet X, Zaborski P, Eveno E, Mueller O, Schroeder A, Auffray C: **Towards standardization of RNA quality assessment using user-independent classifiers of microcapillary electrophoresis traces**. *Nucleic Acids Res* 2005, **33**(6):e56.

174. Catts VS, Catts SV, Fernandez HR, Taylor JM, Coulson EJ, Lutze-Mann LH: **A microarray study of post-mortem mRNA degradation in mouse brain tissue**. *Brain Res Mol Brain Res* 2005, **138**(2):164-177.

175. Copois V, Bibeau F, Bascoul-Mollevi C, Salvetat N, Chalbos P, Bareil C, Candeil L, Fraslon C, Conseiller E, Granci V *et al*: **Impact of RNA degradation on gene expression profiles: assessment of different methods to reliably determine RNA quality**. *J Biotechnol* 2007, **127**(4):549-559.

176. Strand C, Enell J, Hedenfalk I, Ferno M: **RNA quality in frozen breast cancer samples and the influence on gene expression analysis--a comparison of three evaluation methods using microcapillary electrophoresis traces**. *BMC Mol Biol* 2007, **8**:38.

BIOGRAPHICAL SKETCH

Melissa Bourgeois was born in Millington, Tennessee to Robert and Pamela Bourgeois. The youngest of two children, she spent most of her childhood in St. Albans, Maine and Ft. Myers, Florida. She graduated from the University of Florida with her Bachelor of Science in zoology in 2002. She began veterinary school at the University of Florida that same year and enrolled during her second year of veterinary school into a combined DVM/PhD program. She graduated with her Doctorate in Veterinary Medicine from the Unversity of Florida in 2007. In 2010, she received her Doctor of Philosophy in veterinary medicine. Upon completion of her PhD, she began work at the Centers for Disease Control and Prevention in Atlanta focusing on influenza research.